AD NUMBER
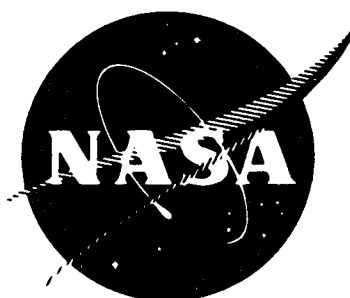
ADB211394

NEW LIMITATION CHANGE

TO

Approved for public release, distribution unlimited

FROM

Distribution authorized to U.S. Gov't. agencies and their contractors; Administrative/Operational Use; 31 MAR 1971. Other requests shall be referred to National Aeronautics and Space Administration, Washington, DC 20546.

AUTHORITY

NASA TR Server Website

NASA CR-72797

FINAL REPORT
LOW THERMAL FLUX GLASS-FIBER TUBING
FOR CRYOGENIC SERVICE

by

C. A. Hall, T. J. Pharo, J. M. Phillips, and J. P. Gille

MARTIN MARIETTA CORPORATION

Prepared for
NATIONAL AERONAUTICS AND SPACE ADMINISTRATION

NASA Lewis Research Center
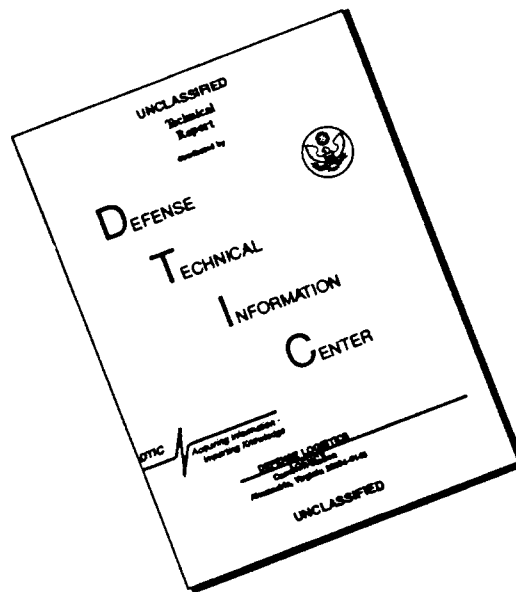Contract NAS3-12047

James R. Faddoul, Project Manager

DISCLAIMER NOTICE

THIS DOCUMENT IS BEST QUALITY AVAILABLE. THE COPY FURNISHED TO DTIC CONTAINED A SIGNIFICANT NUMBER OF PAGES WHICH DO NOT REPRODUCE LEGIBLY.

NOTICE

This report was prepared as an account of Government-sponsored work. Neither the United States, nor the National Aeronautics and Space Administration (NASA), nor any person acting on behalf of NASA:

A.) Make any warranty of representation, expressed or implied, with respect to the accuracy, completeness, or usefulness of the information contained in this report, or that the use of any information, apparatus, method, or process disclosed in this report may not infringe privately-owned rights; or

B.) Assumes any liabilities with respect to the use of, or for damages resulting from the use of any information, apparatus, method or process disclosed in this report.

As used above, "person acting on behalf of NASA" includes any employee or contractor, to the extent that such employee or contractor of NASA or employee of such contractor prepares, disseminates, or provides access to any information pursuant to his employment or contract with NASA, or his employment with such contractor.

FINAL REPORT

LOW THERMAL FLUX GLASS-FIBER TUBING
FOR CRYOGENIC SERVICE

by

C. A. Hall, T. J. Pharo, J. M. Phillips, and J. P. Gille

MARTIN MARIETTA CORPORATION
P. O. Box 179
Denver, Colorado 80201

Prepared for

NATIONAL AERONAUTICS AND SPACE ADMINISTRATION

March 31, 1971

CONTRACT NAS3-12047

NASA Lewis Research Center
Cleveland, Ohio

James R. Faddoul, Project Manager

FOREWORD

The work described herein was conducted by the Martin
Marietta Corporation, Denver Division, under NASA Contract
NAS3-12047. Work was done under the management of the NASA
Project Manager, Mr. James R. Faddoul, Liquid Rocket Technology
Branch, NASA-Lewis Research Center, Cleveland, Ohio.

Contents

ABSTRACT

Thin metallic liners that provide leak-free service in cryogenic propulsion systems are overwrapped with a glass-fiber composite that provides strength and protection from handling damage. The resultant tube is lightweight, strong, and has a very low thermal flux. The resultant reduced boiloff of stored cryogenic propellants yields a substantial weight savings on long-term missions (7 days or greater). Twelve styles of tubing ranging from 1/2 to 5 in. (1.27 to 12.7 cm) in diameter were fabricated and tested at operating temperatures from +70 to $-423^\circ F$ (294 to $20^\circ K$) and operating pressures up to 3000 psi (2068 N/cm^2).

Results for most of the 12 concepts were excellent.

LOW THERMAL FLUX GLASS-FIBER TUBING

FOR CRYOGENIC SERVICE

By Charles A. Hall, Thomas J. Pharo,
John M. Phillips and John P. Gille

Martin Marietta Corporation

SUMMARY

This is the final report of an 18-month program that was con-
ducted under Contract NAS3-12047. The objective of the program
was to develop lightweight, glass-fiber tubing and attendant fit-
tings and seals for use as cryogenic plumbing on space vehicles.
Three different sizes of tubing were selected with four end or
joint configurations on each size. The tubes were then fabricated
(12 specimens of each design) and subjected to thermal, burst, and
cycle testing. The thermal properties were compared with existing
tubing standards to determine the advantages of the glass tubing.

The program consisted of five basic tasks, namely:

Task I   -   Design of Test Specimens and Test
               Apparatus;

Task II   -   Fabrication of Test Specimens and
               Hardware;

Task III   -   Testing;

Task IV   -   Analysis of Test Results;

Task V   -   Reporting.

During Task I, an analysis program assessed thermal, structural,
and fabrication parameters and formed the basis for the tubing de-
sign. Ultimately, thin metallic liners, 0.003 to 0.009 in. thick
(0.0076 to 0.0229 cm), were selected as the primary load-carrying
member. These liners were overwrapped with a glass-fiber composite,
including a cryogenic resin matrix, which strengthened the tube and
protected the tube from handling or flight dynamics damage. This
tubing concept can substantially reduce boil-off and venting require-
ments. Concurrent with this analysis effort, a series of preliminary
tests were performed to aid in selecting materials of construction

(tensile tests), end fitting configurations (leakage tests), and methods of liner fabrication (welding tests). The 12 tubing configurations were selected (and approved by the NASA-LeRC Project Manager) and design drawings were prepared and issued. Test fixture designs, in accordance with the test plan, were also completed during this task.

During Task II, the tubes were fabricated and verified ready for test. A total of 134 specimens were prepared, 12 each of 11 configurations and 2 of the 12th. Tube fabrication included liner welding, joining of the liners to end fittings, instrumentation installation, overwrapping and curing, and a series of in-process leak checks. Much of the metal fabrication was subcontracted to bellows manufacturers. Test fixtures were fabricated concurrent with this effort.

During Task III, the tubes were subjected to a test program that included burst, cycle, torsion, thermal, and leak check testing. All tubes were eventually destroyed by burst or torsion tests.

Task IV consisted of evaluating the results of the test program compared to the analysis program in Task I. Task V consisted of preparing reports including monthly progress reports, a test plan, a design analysis report, and the final report.

Of the 12 original tube configurations, 10 performed very satisfactorily. One design concept affecting 2 tube configurations was abandoned due to an inefficient liner-to-fitting weld. One of these configurations was redesigned to use a new solid-state bonding concept and the other configuration was cancelled. The results of the program clearly verify the advantages in using glass fiber composite lines in cryogenic propellant service. Some of the advantages include low thermal flux, lightweight construction, low heat soak back from engines, rapid chilldown, and strength and handling ease.

Additional work is needed to verify vibration acceptance, extend the diameters to those used in large propulsion systems, improve chilldown time, and eliminate the leakage problems in some designs.

INTRODUCTION

Background

In the continuing development of optimum performance cryogenic propulsion systems, there is considerable interest in the reduction of system heat flux. Thermal optimization on the propellant tanks

and support structures is progressing rapidly, but work on the propellant feed, vent, and pressurization lines has been virtually nonexistent. Considering the high heat leak through conventional tubing systems, it is essential that techniques be developed to produce lines using a low heat leak material or composite materials.

Martin Marietta Corporation proposed to analyze, design, fabricate, and test a series of composite propulsion lines designed to limit the heat transfer through this portion of the propulsion system. The composite lines incorporated a thin metal liner to minimize leakage and provide compatibility with cryogenic propellants such as liquid fluorine. The thin metal lines were overwrapped with a glass-fiber material using a suitable matrix. Because the glass-fiber overwrap is a very good thermal insulator and the thin metal liner has a very small cross-sectional area, the heat conductivity was reduced considerably.

For a plumbing line on a space vehicle that contributes a total heat flux of 1 BTU/hr (.293 Watt), the consumption of LH_2 for this heat flux alone is calculated to be approximately 225 lb (102 kg) for a five-year period. Additional weight penalties are involved because the propellant tank and insulation must be increased by 50 cu ft (1.41 m^3) to accomodate the extra 225 lb (102 kg) of propellant. The boiloff of liquid oxygen will be approximately 500 lb (227 kg) for the same heat flux. If thin metal-lined tubes can be developed that will not substantially reduce mission reliability and will, at the same time, reduce the level of heat conduction, a large payload savings will result.

In a great majority of propulsion systems, the fluid line wall thickness is determined by handling and maintainability, not stresses. Calculations show that an Inconel 718 or stainless steel line with 0.001 in. (0.0025 cm) wall thickness would carry all internal pressure loads for many propulsion feed lines and tank vents. When composite tubing can be fabricated with metal liner wall thickness near 0.001 in. (0.0025 cm) and the handling/maintenance requirements can be supported with a material having a low thermal conductivity, the heat flux will be reduced and the tubing will be lighter. The following problems must be solved before the application of low thermal conductive tubing to a space vehicle:

1) Selection of liner material;

2) Selection of liner thickness;

3) Selection of fabrication techniques;

4) Determination of corrosion factors for FLOX and LF_2;

5) Selection of the overwrap thickness and configuration;

6) Design for proper cycle life and burst pressures; and

3

7) Consideration of mission reliability when confronted with a liner failure.

The objective of the program was to address these problems by developing lightweight, glass-fiber tubing and attendant fittings and seals for use as cryogenic plumbing on upper-stage space vehicles. Three different sizes of tubing were selected with four end or joint configurations on each size. The tubes were then fabricated (12 specimens of each design) and subjected to thermal, burst, and cycle testing. The thermal properties were compared with existing tubing standards to determine the advantages of the glass tubing.

Approach

Specific items that were performed to accomplish the program objectives included:

1) Selecting a set of boundaries for analysis by the computer program;

2) Modifying an existing Martin Marietta analytical model to incorporate the analysis of glass-fiber, metal-lined tubes;

3) Using the analytical model to assist in the design of the metal lined tubes including the selection of an optimum location for the tubes, selection of thermal barriers and effects of various temperatures at each end of the tube;

4) Designing the test articles using several joint designs and three sizes: 1/2-, 2-, and 5-in. (1.27, 5.08, and 12.7 cm) diameter;

5) Preparing the program test plan defining in detail the testing to be conducted;

6) Designing the test fixturing sufficient to perform thermal, burst, torsional, and cyclic testing on the test articles;

7) After design approval, fabricating part of the test articles and the test fixturing;

8) Subjecting 13 initial test articles to burst testing and 1 initial test article to cycle testing and analyzing the data;

9) Incorporating design and fabrication changes resulting from the initial burst and cycle tests and fabricating the remaining articles;

10) Subjecting 55 additional test articles to burst testing;

11) Subjecting a coupon from each size tube to thermal conduction testing;

12) Subjecting 5 articles to thermal heat flux testing;

13) Subjecting 65 articles to temperature/pressure cycle testing followed by burst or torsional testing;

14) Correlating the experimental and analytical data to show the capability of the analytical model to predict the tubing performance; and,

15) Reporting future modifications or changes that would be incorporated into flight-qualified tubing.

The specific assignments in this program were divided into five tasks in accordance with the contract. Task I included the thermal, structural and fabrication analyses and the design of test specimens and test apparatus. In task II, the test articles and the test fixture were fabricated. The test articles were subjected to thermal, burst, torsional, and cycle testing during Task III, followed by the analysis of the results and verification of the model (Task IV). Task V included all reporting.

Task I - Design of Test Specimens and Test Apparatus

The effort in Task I consisted of performing thermal, structural, and fabrication analyses, and reporting the results of these, followed by design of the test items and test fixtures.

Thermal analysis. - A design analysis was performed to define thermal design characteristics for glass-fiber composite plumbing lines of cryogenic propellant tankage. Mission durations of up to five years in space were considered, and propellants for consideration were liquid hydrogen, liquid fluorine, liquid oxygen, liquid methane, and liquid FLOX. The plumbing lines included engine feedlines and tank pressurization lines. Items considered in the analysis included:

1) Optimum placement of glass-fiber tube in the plumbing system (i.e., on warm end, on cold end, or total length of line) based on a nondimensionalized analysis of a simplified propellant plumbing system;

2) Leakage of joints and liner,
   a) Safety and/or mission reliability,
   b) Maximum allowable liquid leak rate (payload penalty);

3) Effect of internal radiation within the line (need for internal radiation barriers and definition of wall emittance);

4) Effects of and thermal limiting values (as compared to stainless steel lines) for wall thickness and liner thickness as a function of thermal conductivity of material, line size, operating pressure, and mission duration;

5) Effect of multilayer insulation or thermal coatings on the outside of the line;

6) Effects of gas or liquid within the line (due to valve leakage into an evacuated line or residual fluid); and,

7) Effect of variable warm end temperatures up to 520°R (238°K), and cold end temperatures corresponding to propellant temperatures.

Thermal comparisons to stainless steel plumbing were made for each of the above items. Design parameters for the glass-fiber composite lines were established based on the goal of significant reduction in heat leak over that of stainless steel lines.

Structural analysis. - Structural analysis was performed to determine the feasibility of specific materials for the structural liner and the composite overwrap. Several parameters were considered appropriate to the identified program for long-term space vehicles and each was used as a criterion.

Specific considerations during this analysis included the liner thickness, the maximum allowable liner stress, the bonding of the glass-fiber overwrap, the effect of gaps between the liner and the overwrap at a variety of cryogenic temperatures including anticipated differential temperatures between the liner and the overwrap, helium permeation, leakage, buckling, torsion, material compatibility and corrosion, and fitting evaluations.

Before making final joint selections, preliminary testing was accomplished to determine leakage characteristics of the joints when subjected to pressure and temperature cycling. Re-torque requirements, both magnitude and frequency, were determined in this test program.

Fabrication analysis. - The welding or joining processes that were evaluated included fusion welding, resistance welding, solid-state bonding,* and seamless tubes. After welding, some heat-treat or hardening process may be necessary, and these processes were briefly evaluated. After fabrication of the thin liner, it was joined to an end fitting in one of three general methods ---

---

* Solid-state bonding, as used in this report, refers to an explosive welding process.

resistance welding, fusion welding or solid-state bonding. Each of these processes were evaluated. In general, for good penetration, the thicker portion of the weld joint should be no more than three times the thickness of the thin member. For example, if the liner wall thickness is 0.002 in. (0.005 cm) the attaching portion of the end fitting should not exceed 0.006 in. (0.015 cm).

The fusion weld concept, with the weld at the end of the assembly, applies to flange-type end fittings. This method of attachment can be cleaned easily and eliminates contaminant trap areas from the assembly.

The resistance welding concept is of particular interest when heat-treatment after welding is undesirable or when dissimilar metals are used for liner and end fitting. The major disadvantage of this concept is that a potential cleaning problem and contaminant trap could exist at the liner end of the fitting.

The solid-state bonding process is particularly useful in joining dissimilar metals such as CRES or Inconel liners to light weight aluminum fittings.

The design analysis of the glass-fiber overwrap for the tubing in this study indicated that it should have sufficient strength and stiffness to carry a share of the internal pressure loads during operation (mainly hoop loads), resist external handling loads, and exhibit the lowest possible thermal conductivity in the axial direction.

Results of this design analysis were presented to the NASA-LeRC Project Manager for approval before initiation of the following design effort.

Design of the test specimens. - Three different glass-fiber composite tubes were designed for a five-year duration mission employing liquid hydrogen, in accordance with criteria developed in the analysis and the design sizes and pressures specified in the contract.

Design of the test fixtures. - Test fixtures were designed for burst, cycle, torsion, thermal, and leak check testing of the tubes and joints. The test apparatus is capable of handling oil or water, liquid nitrogen, and liquid hydrogen for pressurization and cold helium for leak checking.

Designs of the tubes, joints, and test apparatus were submitted to the NASA-LeRC Project Manager for review and approval at completion of the Task I effort.

Task II - Fabrication of Test Specimens and Hardware

During Task II, the tubes were fabricated and verified ready for test. A total of 134 specimens were prepared, 12 each of 11 configurations and 2 of the 12th. Tube fabrication included liner welding, joining of the liners to end fittings, instrumentation installation, overwrapping and curing, and a series of in-process leak checks. Much of the metal fabrication was subcontracted to highly experienced bellows manufacturers. The test fixtures were fabricated concurrent with this effort.

Task III - Testing

Burst, cycle, torsion, and thermal testing was conducted as described below.

Burst test. - Two specimens of each tube and joint combination were pressurized to failure at 70, -320 and -423°F (294, 78, and 20°K).

Cyclic tests. - Two specimens of each tube and joint combination were pressure and temperature cycled. Starting at ambient pressure and temperature, the items were cooled to test temperature, pressurized to design operating pressure, depressurized, and warmed up to ambient temperature. This process was repeated for 200 cycles. The cyclic tests were conducted at 70, -320 and -423°F (294, 78, and 20°K). After each ten cycles, the helium leak rate of each tube and joint combination was determined at test temperature. Following the cyclic test each specimen was held at maximum operating pressure for a 24 hr period and the leak rate measurements repeated. After leak checks were completed, each specimen was pressurized to burst or failed in torsion.

Torsion test. - Representative specimens of each mechanically joined tube were subjected to a torsional test to verify adequate resistance to expected assembly or installation loads.

Thermal tests. - The individual components of heat flux transmitted between the warm end and the cold end for each tube-joint composite style was determined. Temperature profile along the tube length was also measured. In addition, thermal conductivity of the glass-fiber composite/liner combination was individually determined (e.g., sections of the tube were subjected to thermal conductivity testing).

In addition to the primary test program, as noted above, a series of preliminary tests were accomplished. This testing included material tensile testing, fitting evaluation testing, helium permeation testing and gap verification testing.

Task IV - Analysis of Test Results

Data obtained during testing were analyzed to determine the effectiveness of the glass-fiber tubing in cryogenic service. Structural integrity and thermal quality were evaluated and compared to the predicted performance. Recommendations for design improvements based on the above comparison were established. The design criteria established in the initial design phase were updated as indicated by the data analysis. During data analysis all of the identifiable sources of error were accounted for, thereby resulting in acceptably small inaccuracies of the test results.

The following chapters of this report are an account of the program.

TASK I - DESIGN OF TEST SPECIMENS AND TEST FIXTURES

The purpose of this phase of the program was to prepare the design for test specimens and test apparatus for use in evaluating the feasibility of using low thermal flux glass tubing for extended periods. The contractural requirements pertaining to the tube design are listed in the following paragraphs, extracted directly from the contract, Exhibit A, Scope of Work, for the sake of clarity.

"The Contractor shall design three different glass-fiber composite tubes for a five year duration mission employing liquid hydrogen, design sizes and pressures below.

DIAMETER	OPERATING PRESSURE
5" I.D.	200 psi
2" I.D.	200 psi
1/2" I.D.	3000 psi

"In addition, for each of the above tubes, the Contractor shall design two methods of joining the ends of the tube to another fiber-glass section and two methods of joining the ends of the tube to a metal tube section. Semi-permanent methods (joint could be physically ground or cut away allowing a new section to be patched in) may be considered, but at least one completely disconnectable joint (bolted flange, mechanical fastener, or clamp) shall be designed.

"The Contractor shall also design a test apparatus for pressurizing, thermal testing, and leak checking the tubes and joints as specified in Task III below. The test apparatus shall be capable of handling oil or water, liquid nitrogen, and liquid hydrogen for pressurization and cold helium or liquid hydrogen for leak checking. The design shall include the test hardware (e.g., temporary vacuum chamber and plumbing) and test specimen configuration.

"At the conclusion of the design task the designs of the tubes, joints, and test apparatus shall be submitted to the NASA-LeRC Project Manager for review and approval."

The first effort involved in Task I was a design analysis to determine the criteria by which the test specimens would be designed.

After the analysis was completed, test specimen design was accomplished using the information gained, and test fixtures were designed to perform evaluation tests of the specimens.

This report section describes in detail the thermal, structural, and fabrication analyses performed and the resulting designs.

Thermal Analysis

Method of analysis.- To evaluate thermal benefits to be gained by use of glass-fiber overwrapped tubing, a parametric analysis was conducted. The analysis was accomplished by mathematically simulating tube sections of various size, construction, material, and thermal boundary conditions to predict heat transfer rates due to the tubes.

A digital computer program was used to accomplish this analysis. The program uses a conventional finite difference approach to the solution of a thermal network representing the various heat transfer paths. In addition, logic has been incorporated to set up the thermal network for the tube configuration from basic specifications, and to calculate black and grey body view factors for internal radiant heat transfer. Internal tube surfaces were assumed to reflect diffusely.

The thermal network consists of a number of nodes representing the ends and equal length segments of the tube. Adjacent nodes are connected by conductors representing the solid materials; including a metal liner, one or two glass overwrap layers and the contained gas. Each node is connected to every other node by radiative conductors. Any combination of these conductors can be included and the others omitted. Heat fluxes through all conductors depend not only on the temperature gradient, but also on the absolute end point conductor temperatures. Thermal conductivity vs temperature data for all the materials considered were incorporated in the program as polynomial curve fit functions.

Provision is included for the addition of a fixed heat input to each node to simulate heat flux through the insulation. This heat flux is reduced near the hot end of the pipe if the temperature difference across the pipe insulation becomes less than $5^{\circ}R$ ($2.78^{\circ}K$). The insulation heat flux per square foot of tube wall is an input parameter, and can be eliminated if desired. Emissivity of the internal pipe surface is also an input parameter, and internal radiation can be eliminated as an option.

Satisfactory convergence of the thermal network is assumed when no node temperature changes by more than $0.005^{\circ}R$ ($0.00278^{\circ}K$);

and when simultaneously, the net external heat transfer to or from the network is less than 0.1% of the total of heat flux into and out of the network at the hot and cold ends. A survey was made to determine a nodal breakdown of the pipe required to assure satisfactory results. It was found that division of the pipe length into 10, 15, or 20 equal-length segments, depending on the ratio of diameter to length, resulted in a computational inaccuracy of less than 5%.

The following parameters must be specified as input to the program for each tube simulation:

1) Tube inside diameter;

2) Tube length;

3) Liner material and thickness;

4) Overwrap material and thickness;

5) Emissivity of internal tube surface;

6) Sidewall heat flux due to insulation;

7) Contained gas (if any); and

8) End temperatures.

Output from the program includes a description of the tube in accordance with the input data, heat flux to the cold end and other external heat fluxes, temperature of each node, and heat transfer in each conductor.

Results.- To assess the overall thermal performance of the glass-fiber overwrapped tube, and to determine the significance of the various parameters, more than 450 separate tube configurations were evaluated. For each of the tube diameters, 0.5, 2.0, and 5.0 in. (1.27, 5.08, and 12.7 cm) baseline configurations were established. The effects of specific parameters were determined by variation of only the parameter of interest, and frequently tube length, with others remaining at the same values as the baseline case. The following parameters, in addition to tube diameter, define the baseline configurations:

1) Liner material - Stainless steel;

2) Liner wall thickness - 0.002 in. (0.00508 cm);

3) Overwrap material - Circumferentially wrapped S-glass epoxy;

4) Overwrap thickness - 0.030 in. (0.076 cm);

5) Emissivity of liner inside surface - 0.6 (diffuse);

6) Insulation heat flux - 0.1 BTU/hr ft^2 (0.315 W/m^2);

7) Tube contents - Vacuum;

8) End temperatures - 40-400°R (22-222°K); and

9) Tube length - 0.5 to 4 ft (15.24 to 121.92 cm), depending on pipe diameter and variable being investigated.

Comparison of glass and stainless steel tubes. - Figures 1 through 3 give the predicted heat fluxes for glass-fiber overwrapped and all stainless steel tubes. The glass tubes with the lowest heat fluxes are the baseline cases as described above. Except for materials and wall thicknesses, all of the other examples are based on the same assumption. It is noted that the more favorable glass-fiber overwrapped tubes are not as conservative in terms of material thicknesses as would be suggested by structural design analysis results. Therefore, the comparisons given in fig. 1 through 3 tend to show the limit of reduction of heat flux to be gained by use of the glass-fiber overwrap technique.

Liner and overwrap thickness effects. - The effect of increasing the liner thickness was evaluated for the three tube sizes. Results, shown in fig. 4 through 6, show an approximately linear dependence of heat flux on liner wall thickness. A small difference is noted between properties of annealed inconel and inconel in the heat treated and aged condition, with the latter giving approximately the same heat transfer on stainless.

The influence of glass overwrap thickness on overall heat transfer is shown in fig. 7 through 9. As would be expected from the thermal properties of glass-epoxy composites, overall heat transfer is less sensitive to the overwrap thickness. The data presented assures that all the glass fibers are oriented in the hoop direction. The overall thermal conductivity of the glass composite with longitudinal fiber orientation is approximately twice that for the circumferential or hoop orientation.

Radiation effects. - To determine the sensitivity of the overall heat flux through the tube to the surface properties of the liner material, the internal emissivity was varied from 0.1 to 1 assuming diffuse reflectivity. (The emissivity of the pipe ends was assumed to be 1 for all cases.) In addition, the heat fluxes for the various tube configurations were calculated with no radiation. These results are given in fig. 10 through 12. The cases of no radiation are shown as emissivity = 0. By inspection of these results, it can be concluded that the heat transfer is quite insensitive to the emissivity parameter. The fraction of heat transferred by radiation is dependent, as expected, on the ratio of diameter to length. For the case where this ratio is near 1 [5-in. (12.7 cm) diameter, 0.5-ft (15.24 cm) long], approximately 38% of the heat transfer is due to radiation. For the very small ratios of diameter to length, the radiation component of heat transfer is almost negligible.

CONDITIONS FOR ALL CASES

Tube ID = 0.5" (1.27 cm)

Temp. Range = 40-400°R (22-222°K)

Insulation Heat Flux = 0.1 BTU/hr ft² (0.315 W/m²)

Emissivity = 0.6 (Diffuse)

ITEM	LINER WALL THICK.	MAT'L	GLASS DIR.	GLASS WALL THICK.
A	0.002" 0.0051 cm	CRES	Hoop	0.030" 0.0762 cm
B	0.002" 0.0051 cm	CRES	Hoop	0.070" 0.1778 cm
C	0.015" 0.0381 cm	CRES	–	–
D	0.030" 0.0762 cm	CRES	–	–
E	0.050" 0.1270 cm	CRES	–	–
F	0.020" 0.0508 cm	CRES	–	–
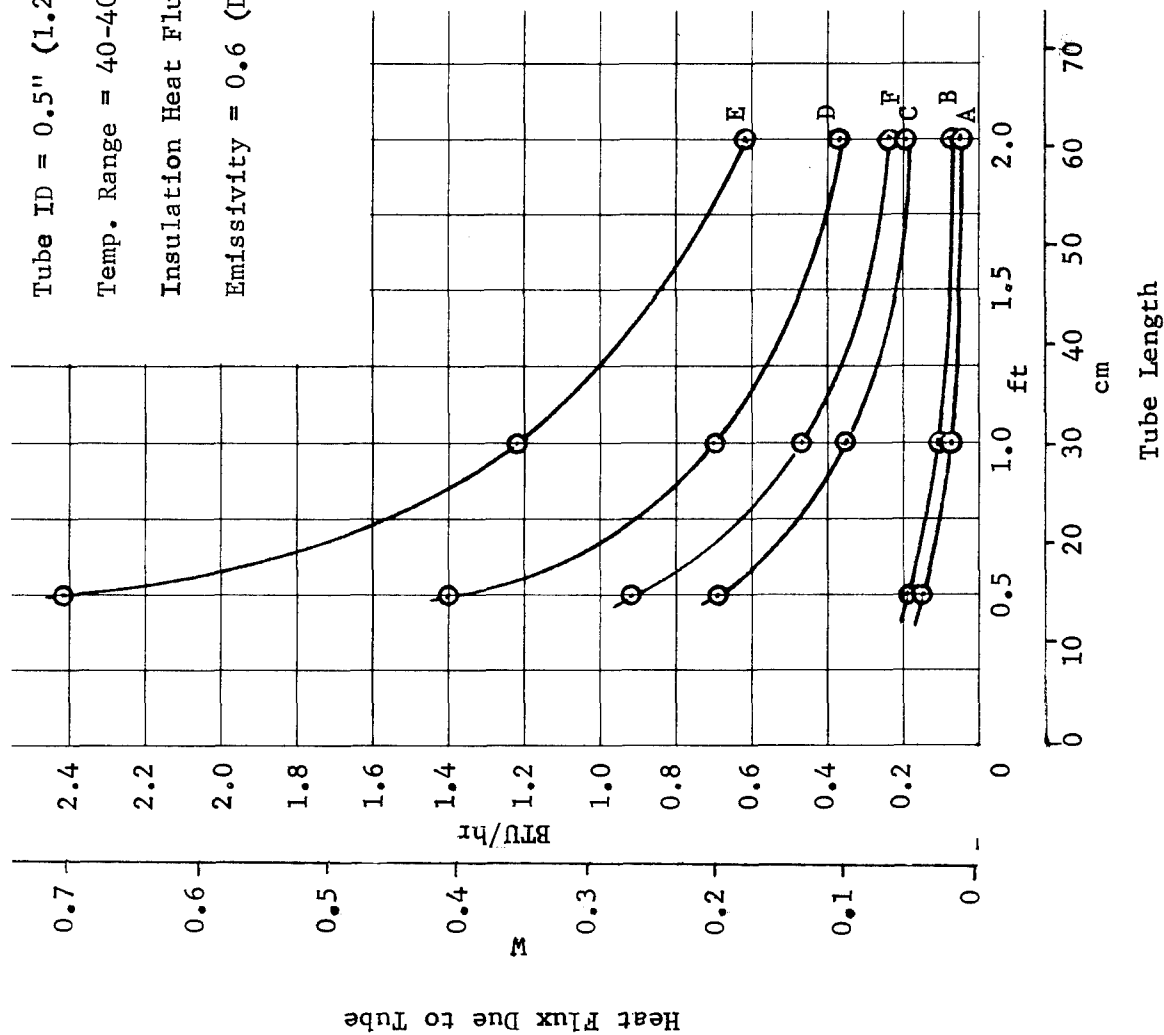
Fig. 1.- Heat Flux vs Tube Length - ½ in. Tube (1.27 cm)

CONDITIONS FOR ALL CASES

Tube ID = 2" (5.08 cm)

Temp. Range = 40-400°R (22-222°K)

Insulation Heat Flux = 0.1 BTU/hr ft^2 (0.315 W/m^2)

Emissivity = 0.6 (Diffuse)

ITEM	LINER WALL THICK.	MAT'L	GLASS DIR.	GLASS WALL THICK.
A	0.002" 0.0051 cm	CRES	Hoop	0.030" 0.0762 cm
B	0.002" 0.0051 cm	CRES	Hoop	0.070" 0.1778 cm
C	0.015" 0.0381 cm	CRES	-	-
D	0.030" 0.0762 cm	CRES	-	-
E	0.020" 0.0508 cm	CRES	-	-

Heat Flux Due to Tube

BTU/hr

W

Tube Length

ft

cm
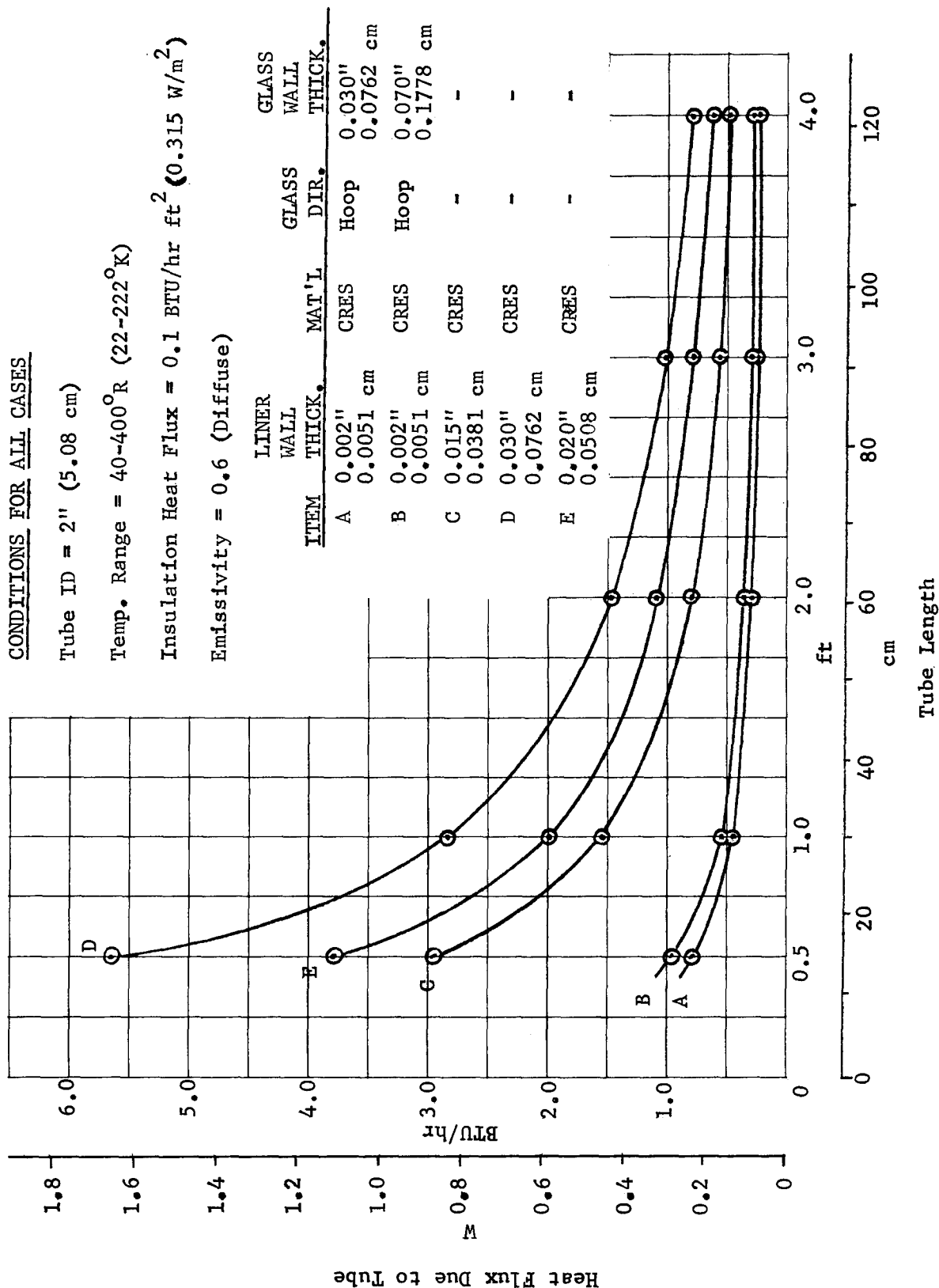
Fig. 2.- Heat Flux vs Tube Length - 2 in. Tube (5.08 cm)

15

CONDITIONS FOR ALL CASES

Tube ID = 5" (12.7 cm)
Temp. Range = 40-400°R (22-222°K)
Insulation Heat Flux = 0.1 BTU/hr ft^2 (0.315 W/m^2)
Emissivity = 0.6 (Diffuse)

ITEM	LINER WALL THICK.	MAT'L	GLASS DIR.	GLASS WALL THICK.
A	0.002" 0.0051 cm	CRES	Long.	0.030" 0.0762 cm
B	0.002" 0.0051 cm	CRES	Hoop	0.070" 0.1778 cm
C	0.002" 0.0051 cm	CRES	Long.	0.070" 0.1778 cm
D	0.030" 0.0762 cm	CRES	-	-
E	0.050 0.127 cm	CRES	-	-
F	0.020" 0.0508 cm	CRES	-	-

Heat Flux Due to Tube

BTU/hr

W

Tube Length

ft

cm
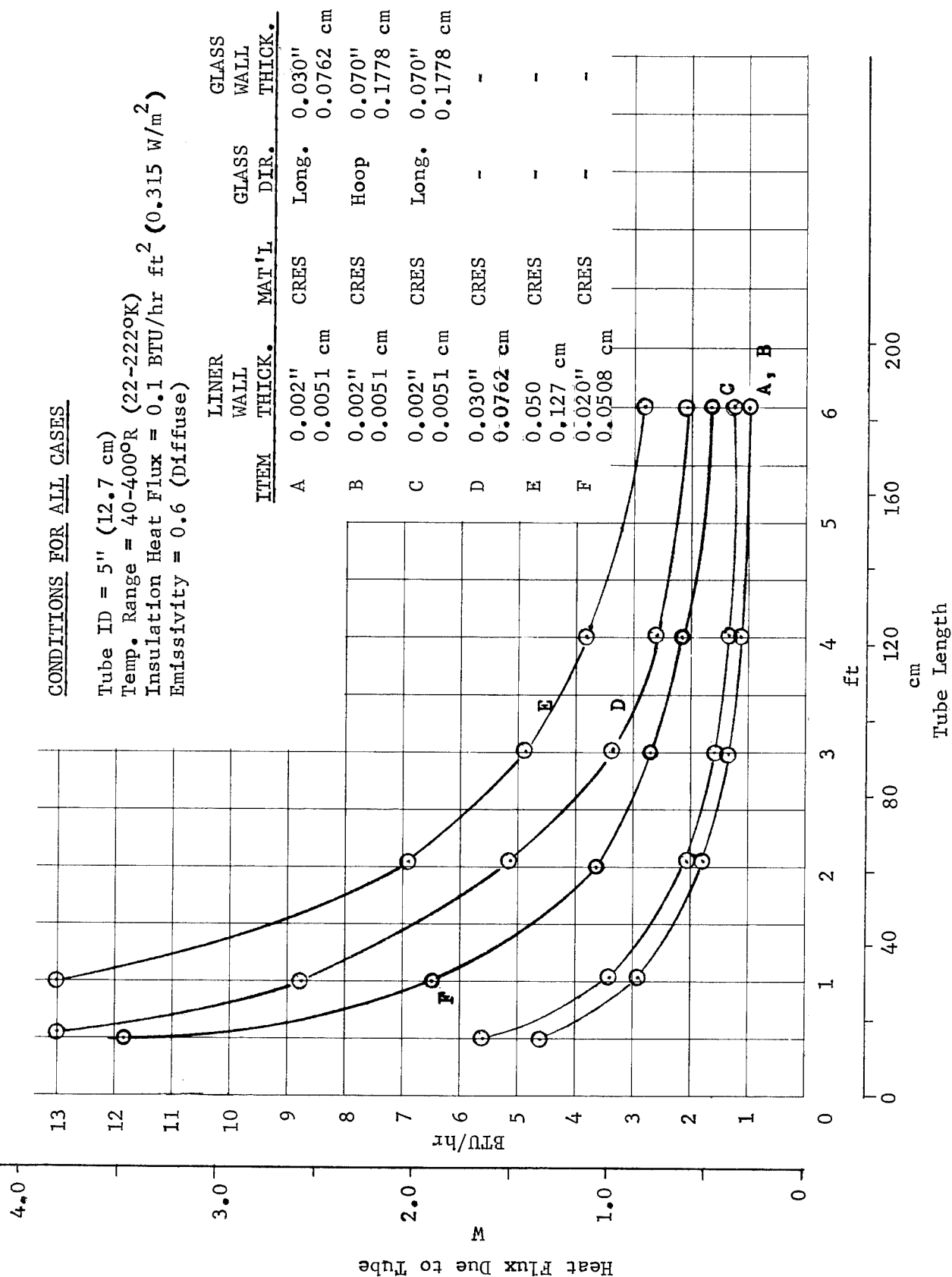
Fig. 3.- Heat Flux vs Tube Length - 5 in. Tube (12.7 cm)

CONDITIONS FOR ALL CASES

Tube ID = 0.5" (1.27 cm)

Liner = Stainless Steel or Inconel 718

Overwrap = 0.030" (0.0762 cm) Hoop Wrapped S. Glass

Temperature Range = 40-400°R (22-222°K)

Insulation Heat Flux = 0.1 BTU/hr ft^2 (0.315 W/m^2)

A – Tube Length = 0.5 ft (15.24 cm)

B – Tube Length = 1 ft (30.48 cm)

C – Tube Length = 2 ft (60.96 cm)

Fig. 4.- Effect of Liner Thickness - ½ in. Tube (1.27 cm)
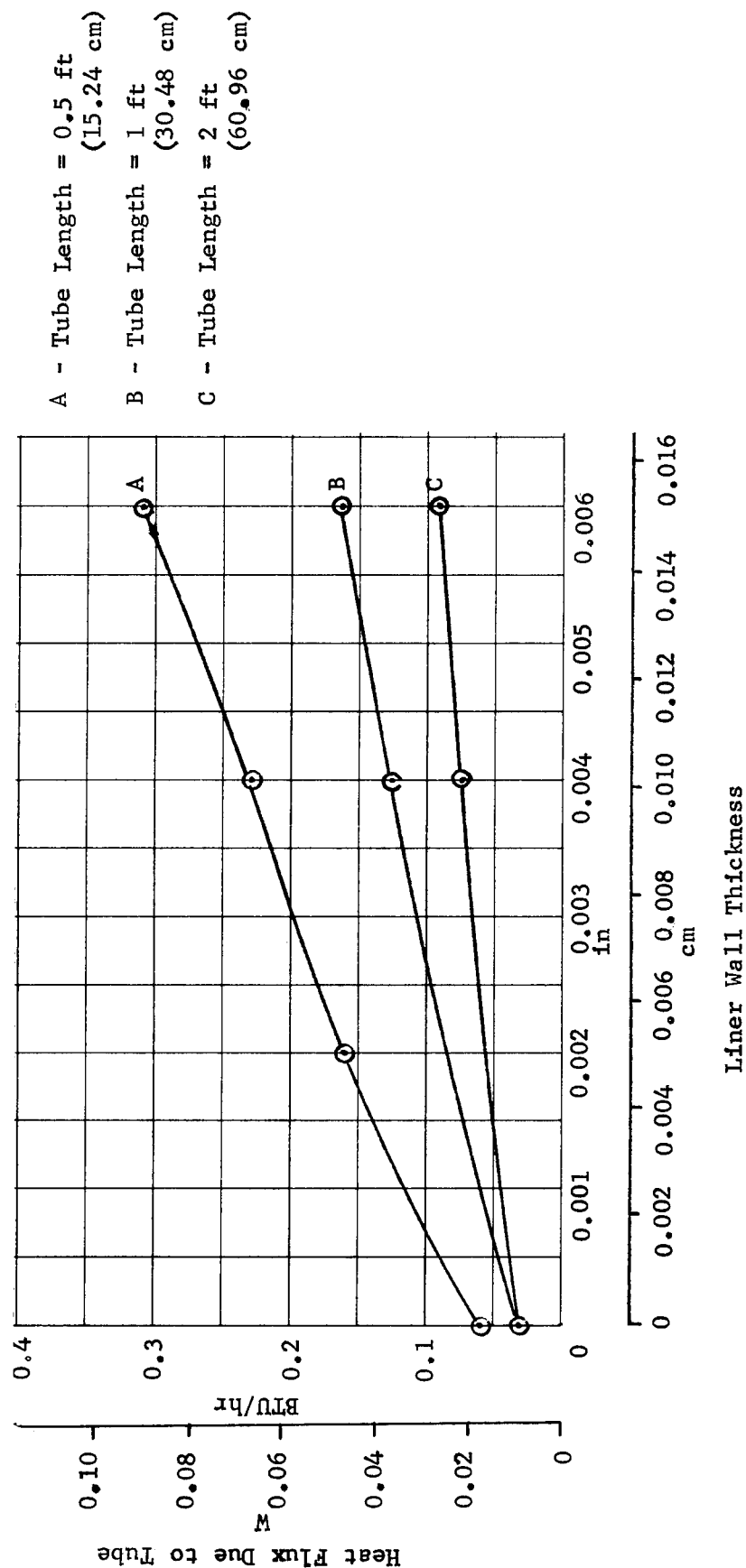
Fig. 5 - Effect of Liner Thickness - 2 in. Tube (5.08 cm)

CONDITIONS FOR ALL CASES

Tube ID = 2" (5.08 cm)
Overwrap = .030" (0.0762 cm) Hoop Wrapped S. Glass
Temp. Range = 40-400°R (22-222°K)
Insulation Heat Flux = 0.1 BTU/hr ft² (0.315 W/m²)

ITEM	LINER MAT'L	LENGTH	
A	CRES	0.5 ft	15.24 cm
B	CRES	1 ft	30.48 cm
C	CRES	2 ft	60.96 cm
D	Inconel 718 Annealed	0.5 ft	15.24 cm
E	Inconel 718 Annealed	1 ft	30.48 cm
F	Inconel 718 Annealed	2 ft	60.96 cm

NOTE: Heat treated Inconel 718 will be the same as curve A, B or C.

Liner Wall Thickness

Heat Flux Due to Tube

CONDITIONS FOR ALL CASES

Tube ID = 5" (12.7 cm)
Overwrap = 0.030" (0.0762 cm) Longitudinal Wrap S. Glass
Temp. Range = 40-400°R (22-222°K)
Insulation Heat Flux = 0.1 BTU/hr ft^2 (0.315 W/m^2)

ITEM	LINER MAT'L	LENGTH
A	CRES	1 ft 30.48 cm
B	CRES	2 ft 60.96 cm
C	CRES	4 ft 121.92 cm
D	Inconel 718 Annealed	1 ft 30.48 cm
E	Inconel 718 Annealed	2 ft 60.96 cm
F	Inconel 718 Annealed	4 ft 121.92 cm

NOTE: Heat treated Inconel 718 will be the same as curve A, B or C.

Liner Wall Thickness

Heat Flux Due to Tube

Fig. 6.- Effect of Liner Thickness - 5 in. Tube (12.7 cm)

19

CONDITIONS FOR ALL CASES

Tube ID = 0.5" (1.27 cm)

Liner = 0.002" (0.0051 cm) Stainless Steel

Overwrap = Hoop Wrapped S. Glass

Temp. Range = 40-400°R (22-222°K)

Insulation Heat Flux = 0.1 BTU/hr ft^2 (0.315 W/m^2)

A - Tube Length = 0.5 ft (15.24 cm)
B - Tube Length = 1 ft (30.48 cm)
C - Tube Length = 2 ft (60.96 cm)
D - Tube Length = 3 ft (91.44 cm)
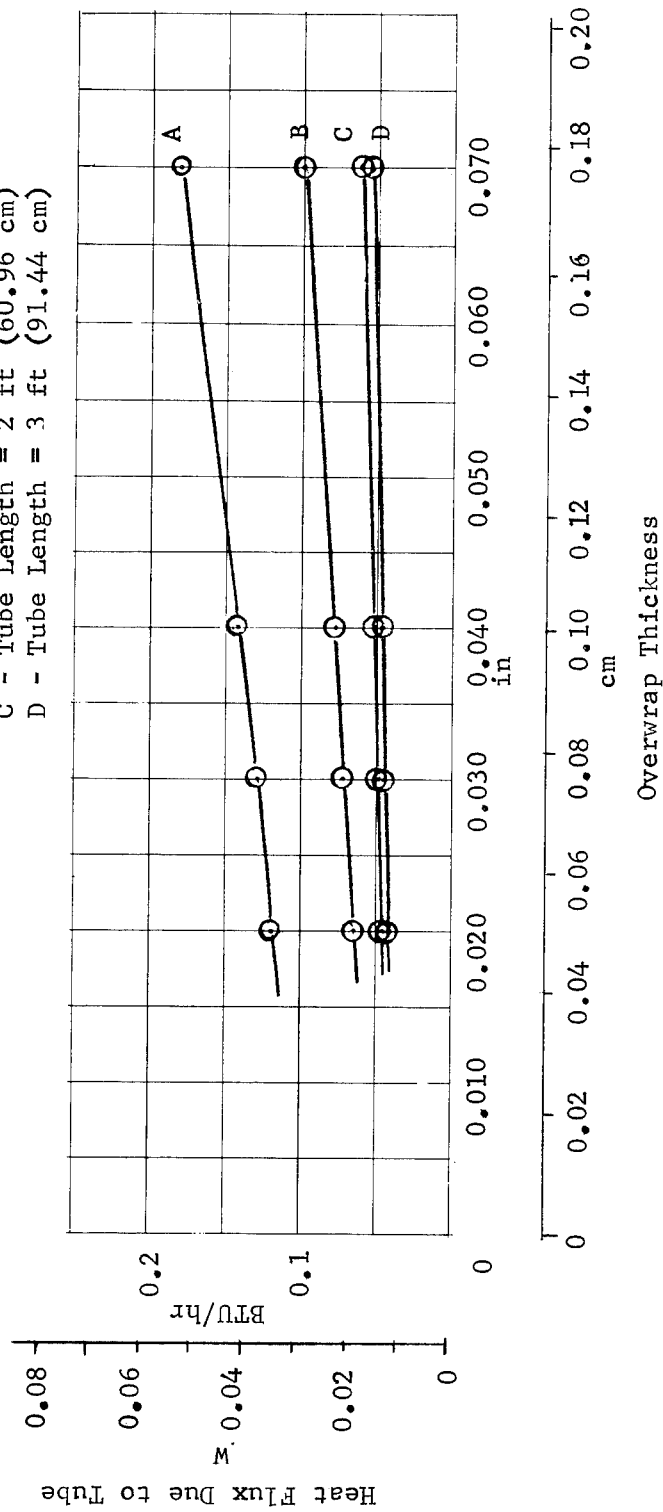
Fig. 7.- Effect of Glass Overwrap Thickness - ½ in. Tube (1.27 cm)

CONDITIONS FOR ALL CASES

Tube ID = 2" (5.08 cm)
Liner = 0.002" (0.0051 cm) Stainless Steel
Overwrap = Hoop Wrapped S. Glass
Temp. Range = 40-400 R (22-222°K)
Insulation Heat Flux = 0.1 BTU/hr ft^2 (0.315 W/m^2)

A - Tube Length = 0.5 ft (15.24 cm)

B - Tube Length = 1 ft (30.48 cm)

C - Tube Length = 2 ft (60.96 cm)
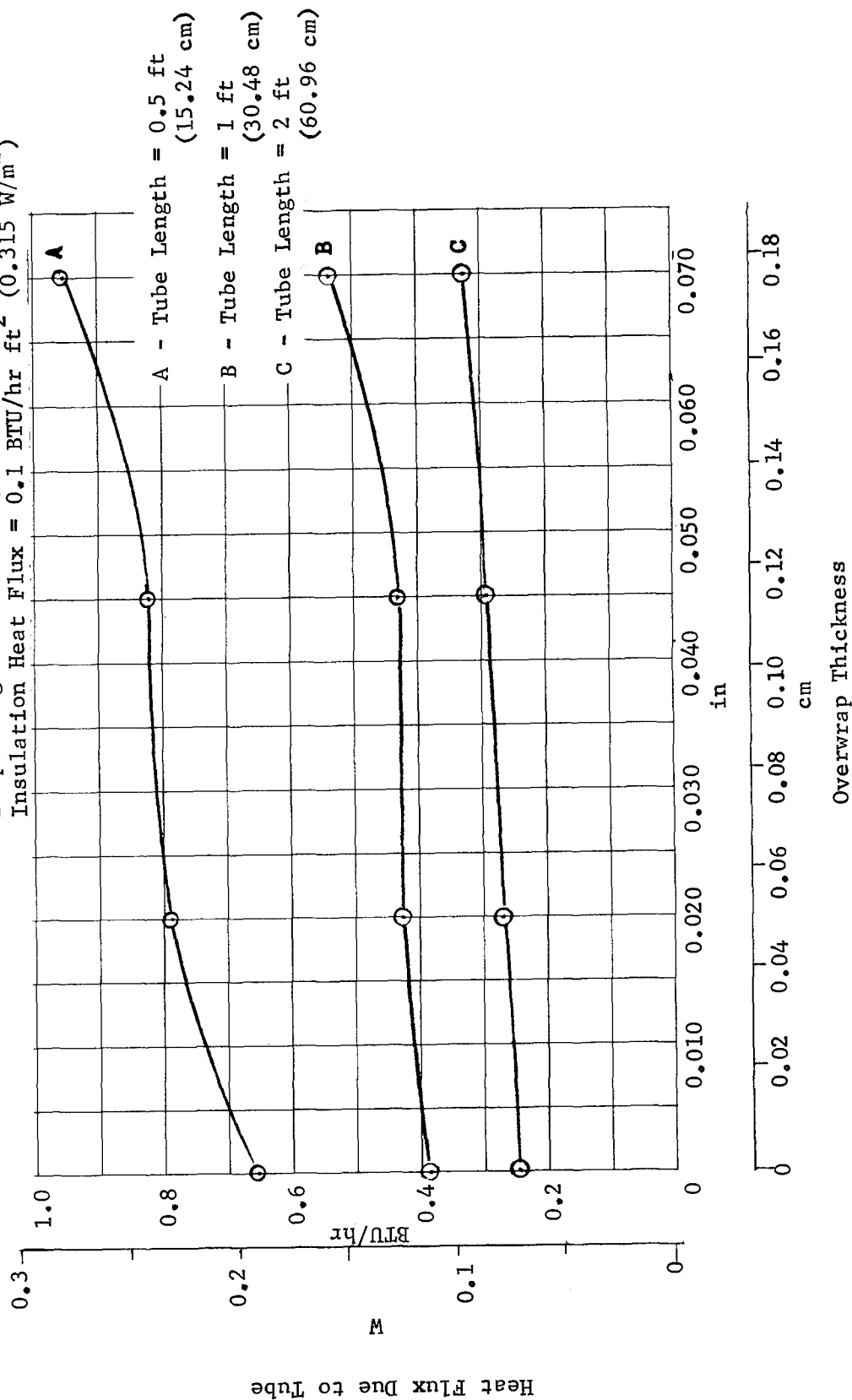
Fig. 8.- Effect of Glass Overwrap Thickness - 2 in. Tube (5.08 cm)

Overwrap Thickness

Heat Flux Due to Tube
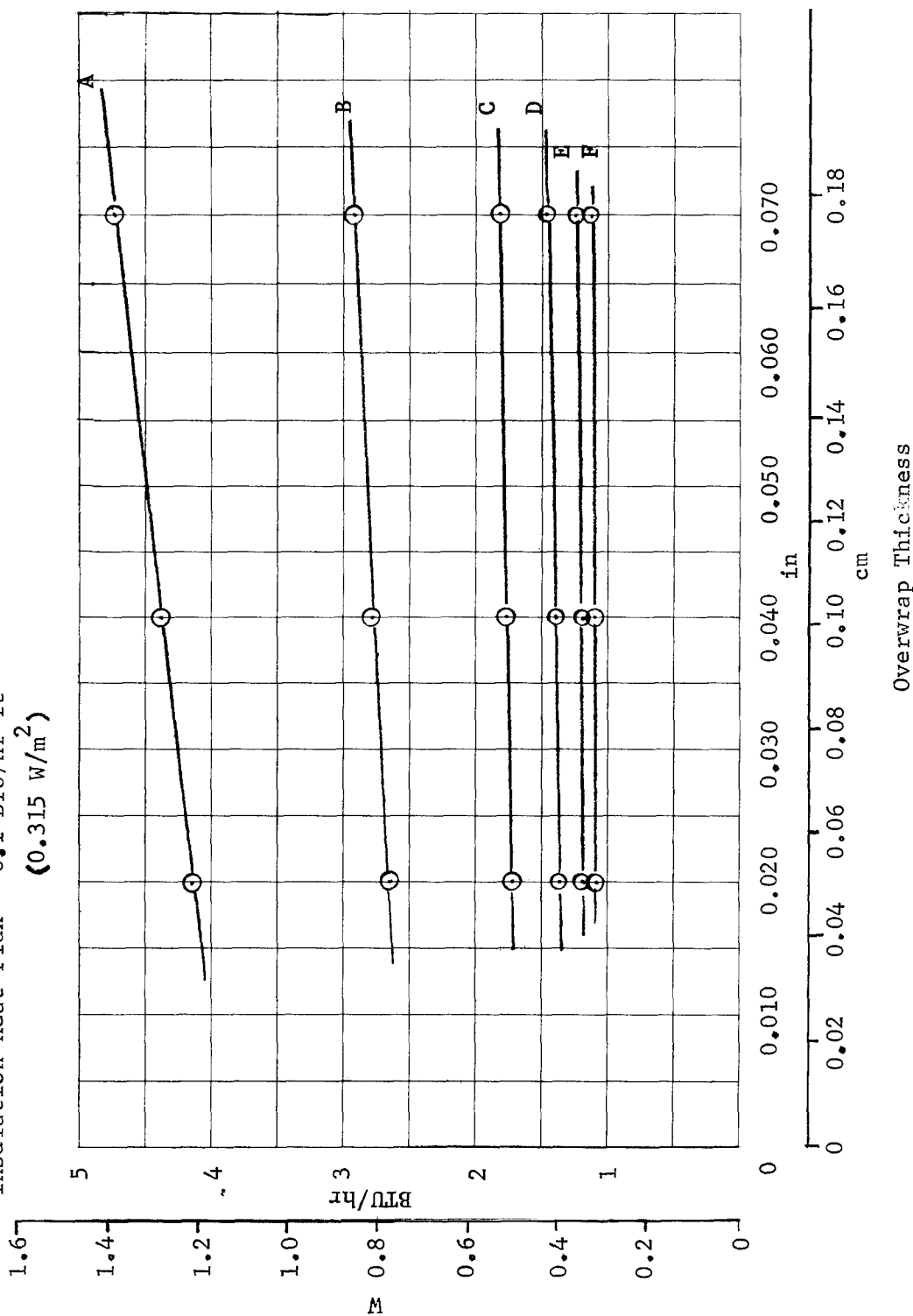
Fig. 9.- Effect of Glass Overwrap Thickness - 5 in. Tube (12.7 cm)

CONDITIONS FOR ALL CASES

Tube ID = 0.5" (1.27 cm)

Liner = 0.002" (0.0051 cm) Stainless Steel

Overwrap = 0.030" (0.0762 cm) Hoop Wrapped S. Glass

Insulation Heat Flux = 0.1 BTU/hr ft^2 (0.315 W/m^2)

A – Tube Length = 0.5 ft (15.24 cm)

B – Tube Length = 1 ft (30.48 cm)

C – Tube Length = 2 ft (60.96 cm)

□ – Level with no radiation

Internal Tube Emissivity

Fig. 10.– Effect of Tube Internal Emissivity – ½ in. Tube (1.27 cm)

CONDITIONS FOR ALL CASES

Tube ID = 2.0 " (5.08 cm)

Temp. Range = 40-400°R (22-222°K)

Liner = 0.002" (0.0051 cm) Stainless Steel

Overwrap = 0.030"(0.0762 cm) Hoop Wrapped S. Glass

Insulation Heat Flux = 0.1 BTU/hr ft^2 (0.315 W/m^2)

A - Tube Length = 0.5 ft (15.24 cm)

B - Tube Length = 1 ft (30.48 cm)

C - Tube Length = 2 ft (60.96 cm)

□ - Level with no radiation

Fig. 11.- Effect of Tube Internal Emissivity - 2 in. Tube (5.08 cm)

CONDITIONS FOR ALL CASES

Tube ID = 5" (12.7 cm)

Liner = 0.002" (0.0051 cm) Stainless Steel

Overwrap = 0.030" (0.0762 cm) Hoop Wrapped S. Glass

Temp. Range = 40-400°R (22-222°K)

Insulation Heat Flux = 0.1 BTU/hr ft^2 (0.315 W/m^2)
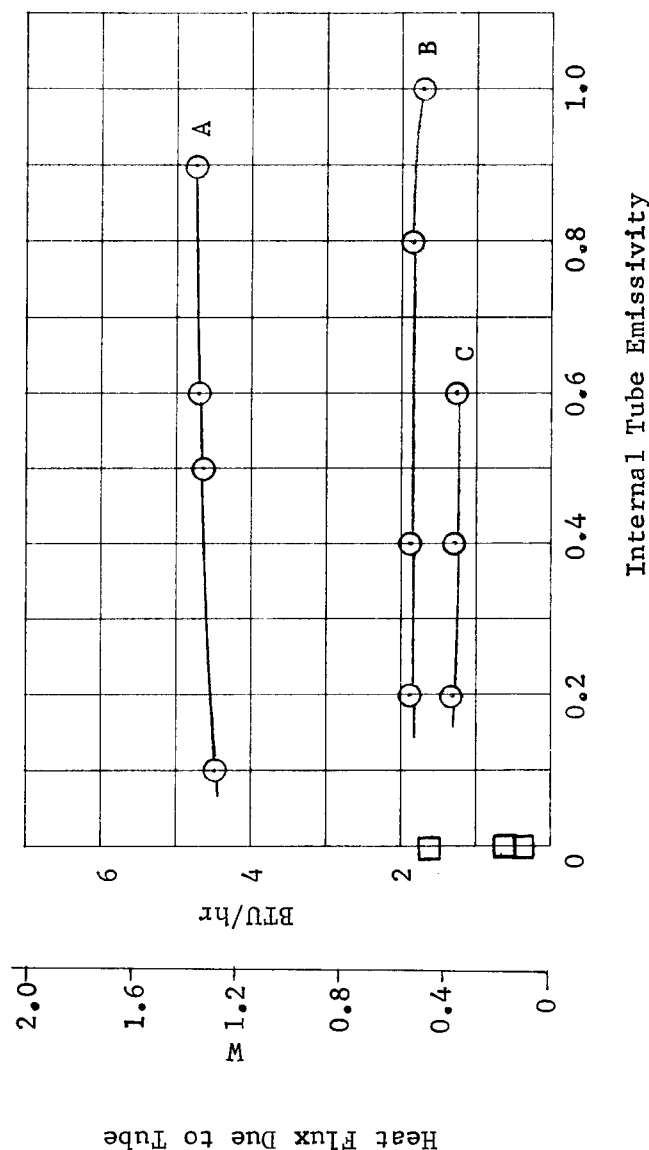
A - Tube Length = 0.5 ft (15.24 cm)

B - Tube Length = 2 ft (60.96 cm)

C - Tube Length = 4 ft (121.92 cm)

□ - Level with no radiation

Fig. 12.- Effect of Tube Internal Emissivity - 5 in. Tube (12.7 cm)

For metal lined tubes, the assumption of diffuse reflectivity of the inside surface introduces some error. However, accurate analysis of radiation heat transfer due to specular infrared reflection is difficult to accomplish because of (1) additional complexity of computation, (2) greater difficulty of measuring specular reflectivity of metal liner, and (3), strong tendency for this property of the metal to change with handling, fabrication processes and environmental exposure. The error resulting from this simplification can be estimated to be as much as 200% of the calculated radient heat transfer for very highly polished surfaces over a limited range of length to diameter ratios. For practical cases, however, and particularly for high ratios of length to diameter (greater than 10), the error is believed to be of minor significance. Further, heat fluxes predicted for the conventional all stainless steel tubes are subject to essentially the same inaccuracy.

Effect of operating temperature. - Because the apparent thermal conductivity of radiation heat paths as well as the conductivity of solid and gas conductors depends on temperature, the hot end temperature is more important than the cold end temperature on heat transmission. This is illustrated in fig. 13 through 15. For this reason, for a long line, an advantage might be gained by coating the uninsulated portion of the line with a material possessing emissivity and absorptivity properties favorable to reducing the line temperature.

Insulation heat flux. - When the heat transfer through a tube is reduced, the effect of its insulation becomes more important. If care is not taken to prevent conduction along the insulation layers (aluminized mylar, for instance), the tube may be thermally short circuited, thereby eliminating any heat reduction that otherwise would be achieved. In the present analysis, a constant heat flux insulation has been assumed, with no conduction in the longitudinal direction of the tube. This would be achieved with multilayer insulation by tapering the insulation thickness to maintain each foil at a constant temperature. Figures 16 through 18 show the effect of the insulation heat flux on total heat flux. The significant conclusion from these results is that for a high sidewall heat flux, the effect of tube length is minimized. This is because the radial heat flux through the insulation acts to increase the heat transfer through the tube toward the cold end and consequently the temperature gradient. Thus the hot end temperature is approached at a shorter distance from the cold end, and the tube appears thermally to be shorter. Because of the insulation heat flux, it is also desirable to place the glass-fiber tube section as near the cold tank as possible.

Effect of contained gas. - All of the results given above assume that the tube interior is evacuated. Because a valve is always required to close a tank-connected line, it is desirable to place this valve near the tank (for very long-term missions), thus permitting the line to be evacuated. However, placing the valve at the warm end of the line permits it to be operated at a more favorable temperature. In a zero-gravity environment, a very little liquid, if any, can remain in the line. Table 1 gives the results of analyses to evaluate the effects of contained gases.

CONDITIONS FOR ALL CASES

Tube ID = 0.5" (1.27 cm)

Tube Length = 1 ft (30.48 cm)

Liner = 0.002" (0.0051 cm) Stainless Steel

Overwrap = 0.030" (0.0762 cm) Hoop Wrapped S. Glass

Insulation Heat Flux = 0.1 BTU/hr ft^2 (0.315 W/m^2)

A - Cold End Temp. = 40°R (22°K)
B - Cold End Temp. = 153°R (85°K)
C - Cold End Temp. = 201°R (112°K)

Hot End Temperature

Heat Flux Due to Tube
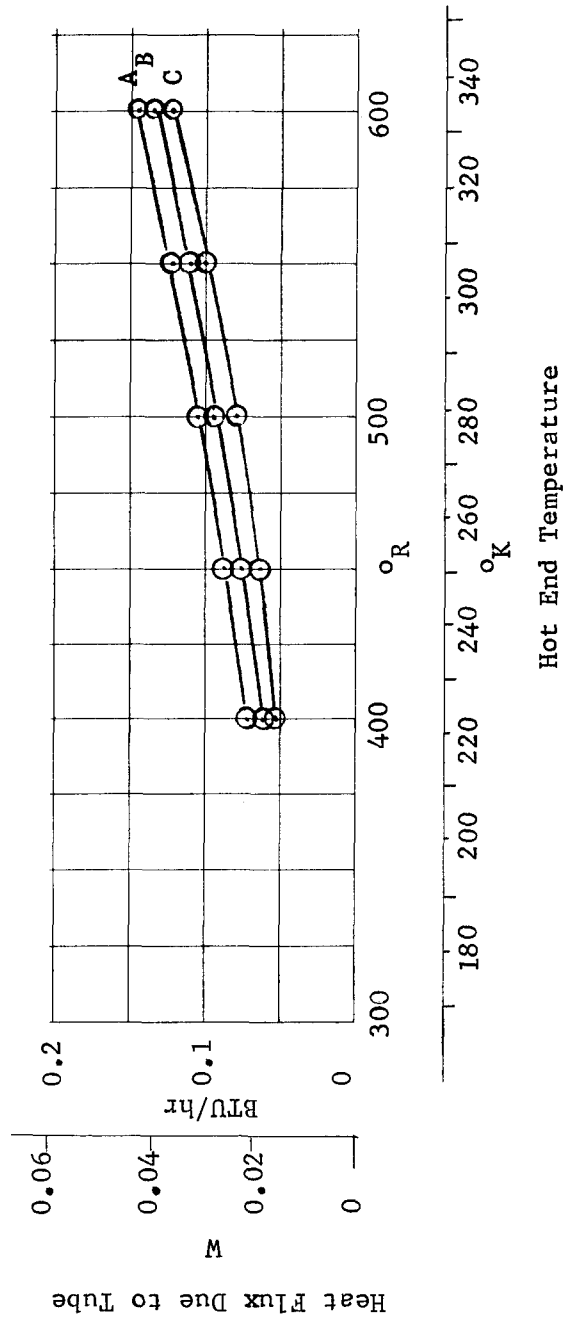
Fig. 13. - Effect of Operating Temperature - ½ in. Tube (1.27 cm)

27

CONDITIONS FOR ALL CASES

Tube ID = 2" (5.08 cm)

Tube Length = 1 ft (30.48 cm)

Liner = 0.002" (0.0051 cm) Stainless Steel

Overwrap = 0.030" (0.0762 cm) Hoop Wrapped S. Glass

Insulation Heat Flux = 0.1 BTU/hr ft^2 (0.315 W/m^2)

A – Cold End Temp. = 40°R (22°K)

B – Cold End Temp. = 153°R (85°K)

C – Cold End Temp. = 201°R (112°K)
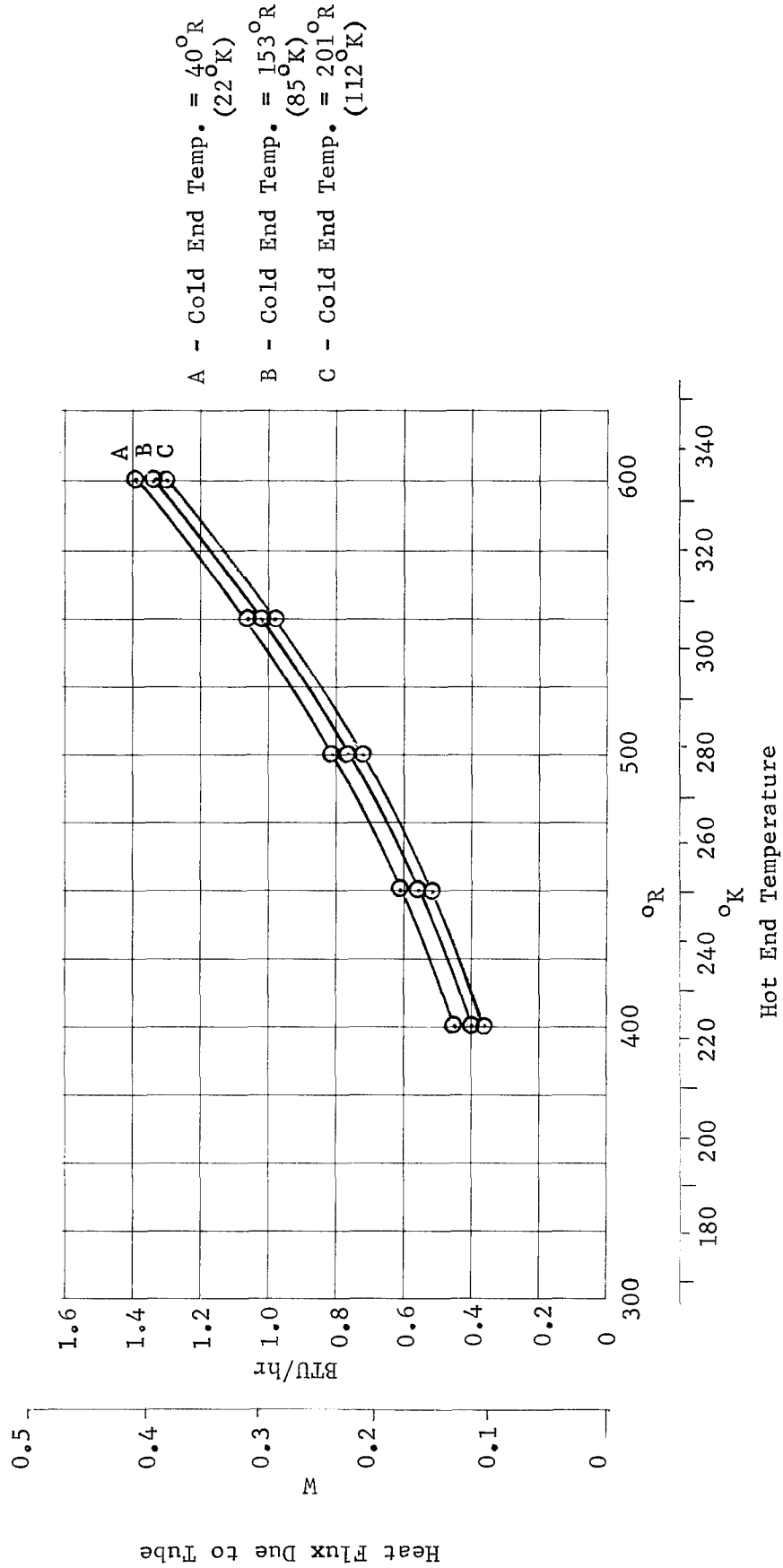
Fig. 14.– Effect of Operating Temperature – 2 in. Tube (5.08 cm)

CONDITIONS FOR ALL CASES

Tube ID = 5" (12.7 cm)

Length = 2 ft (60.96 cm)

Liner = 0.002" (0.0051 cm) Stainless Steel

Overwrap = 0.030" (0.0762 cm) Hoop Wrapped S. Glass

Insulation Heat Flux = 0.1 BTU/hr ft^2 (0.315 W/m^2)

A – Cold End Temp. = 40°R (22°K)

B – Cold End Temp. = 153°R (85°K)

C – Cold End Temp. = 201°R (112°K)
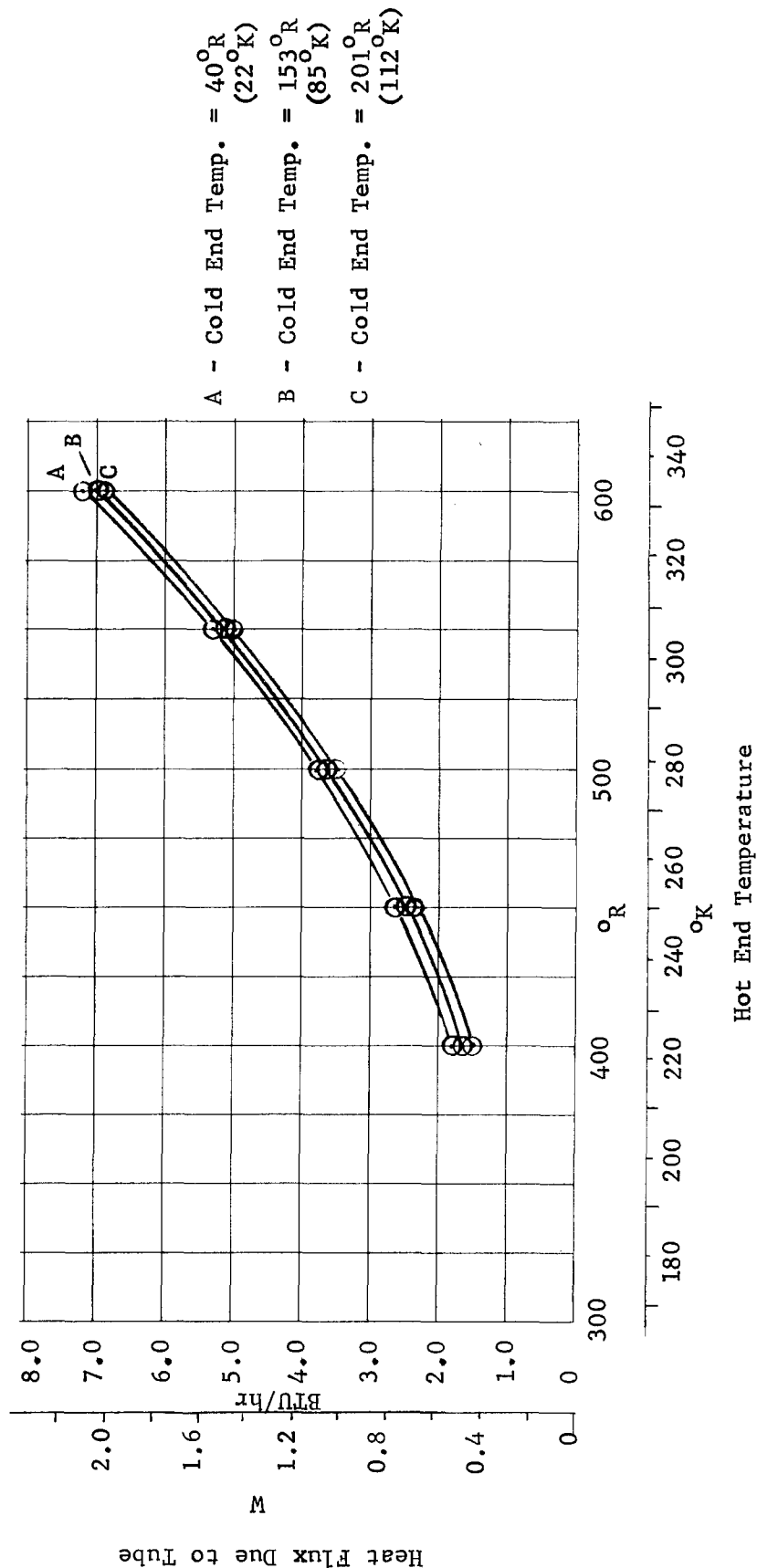
Fig. 15. – Effect of Operating Temperature – 5 in. Tube (12.7 cm)

Hot End Temperature

Heat Flux Due to Tube

CONDITIONS FOR ALL CASES

Tube ID = 0.5" (1.27 cm)

Liner = 0.002" (0.0051 cm) Stainless Steel

Overwrap = 0.030" (0.0762 cm) Hoop Wrapped S. Glass

Temperature Range = 40-400°R (22-222°K)

A - Tube Length = 1 ft (30.48 cm)

B - Tube Length = 2 ft (60.96 cm)

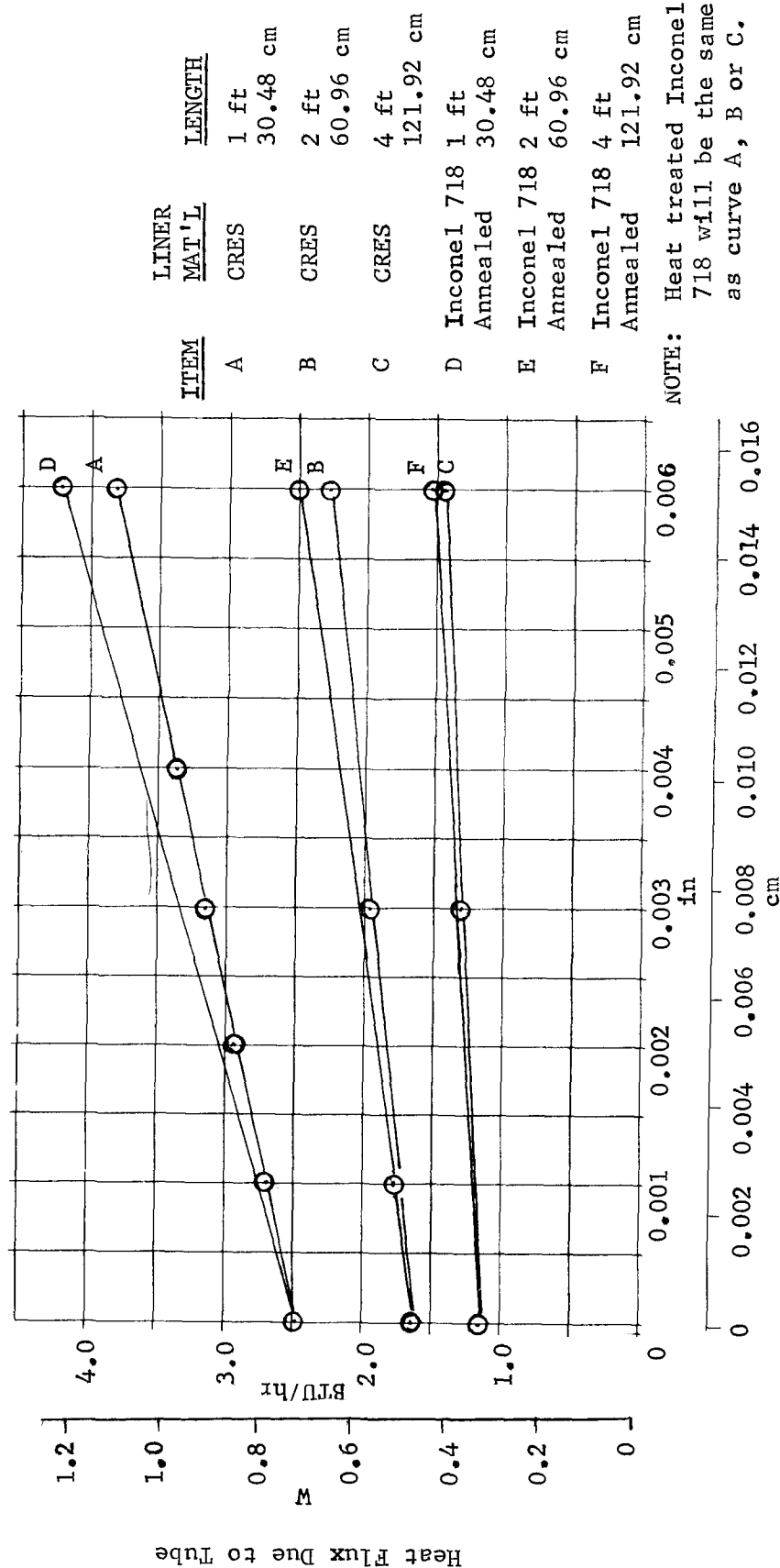C - Tube Length = 3 ft (91.44 cm)
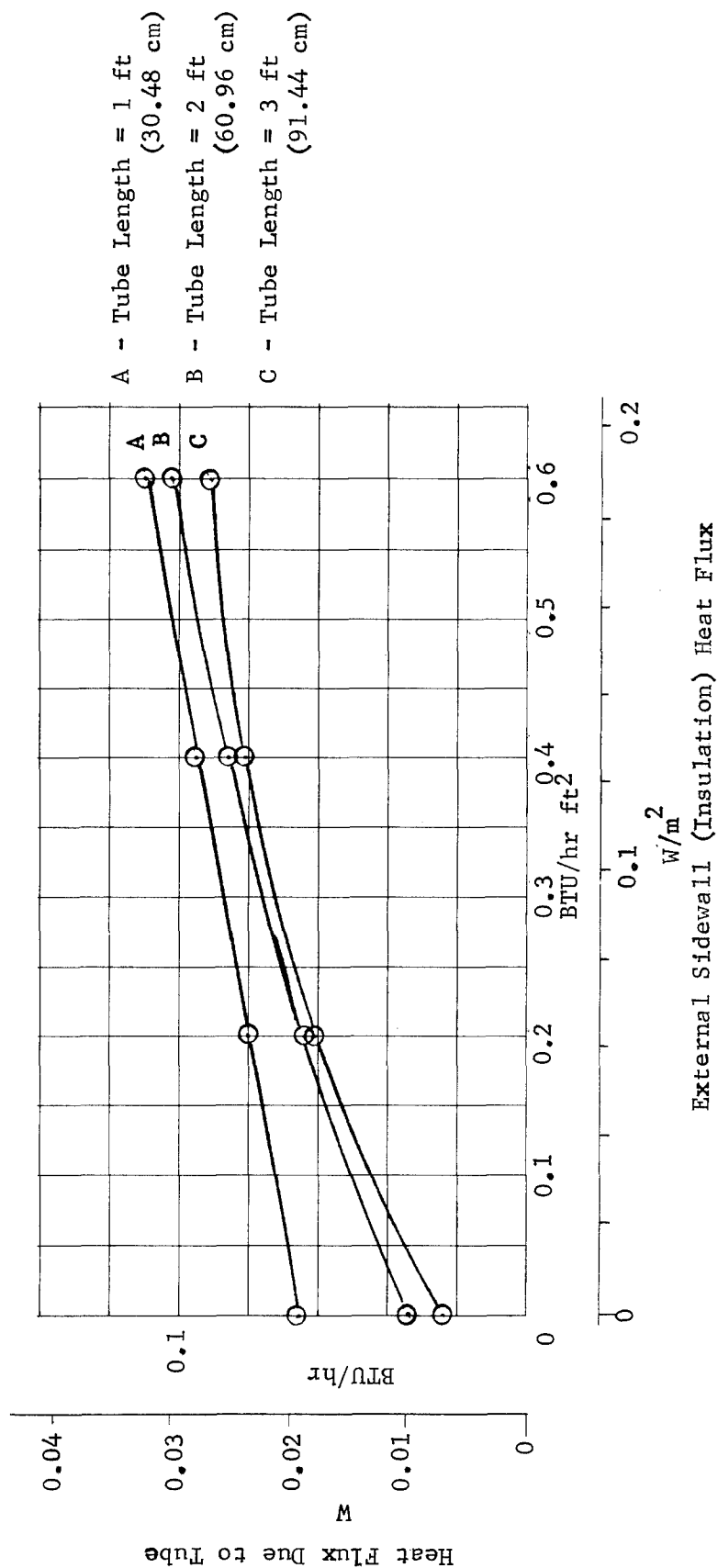
Fig. 16.- Effect of Insulation Heat Flux - ½ in. Tube (1.27 cm)

CONDITIONS FOR ALL CASES

Tube ID = 2" (5.08 cm)

Liner = 0.002" (0.0051 cm) Stainless Steel

Overwrap = 0.030" (0.0762 cm) Hoop Wrapped S. Glass

Temp. Range = 40-400°R (22-222°K)

A — Tube Length = 1 ft (30.48 cm)
B — Tube Length = 2 ft (60.96 cm)
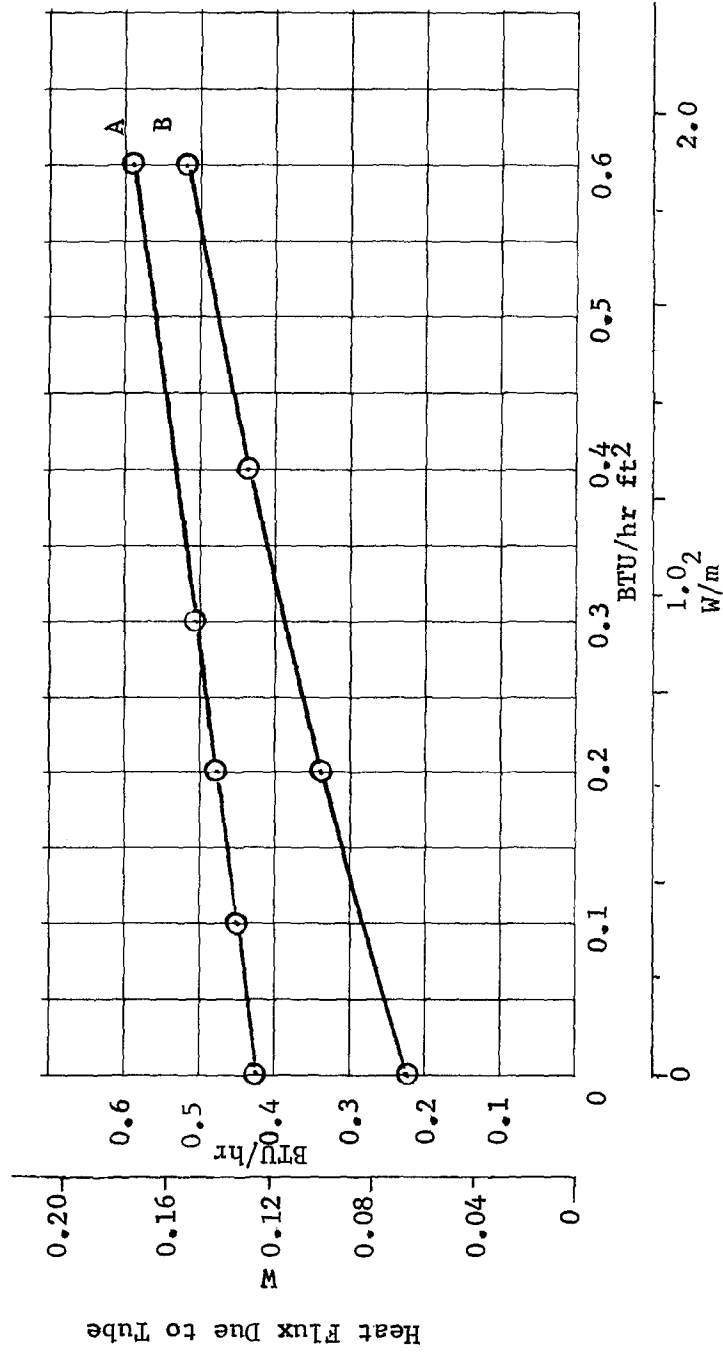
Fig. 17 - Effect of Insulation Heat Flux - 2 in. Tube (5.08 cm)

CONDITIONS FOR ALL CASES

Tube ID = 5" (12.7 cm)

Liner = 0.002" (0.0051 cm) Stainless Steel

Overwrap = 0.030" (0.0762 cm) Hoop Wrapped S. Glass

Temp. Range = 40-400°R (22-222°K)

A – Tube Length = 2 ft (60.96 cm)

B – Tube Length = 3 ft (91.44 cm)

C – Tube Length = 6 ft (182.88 cm)
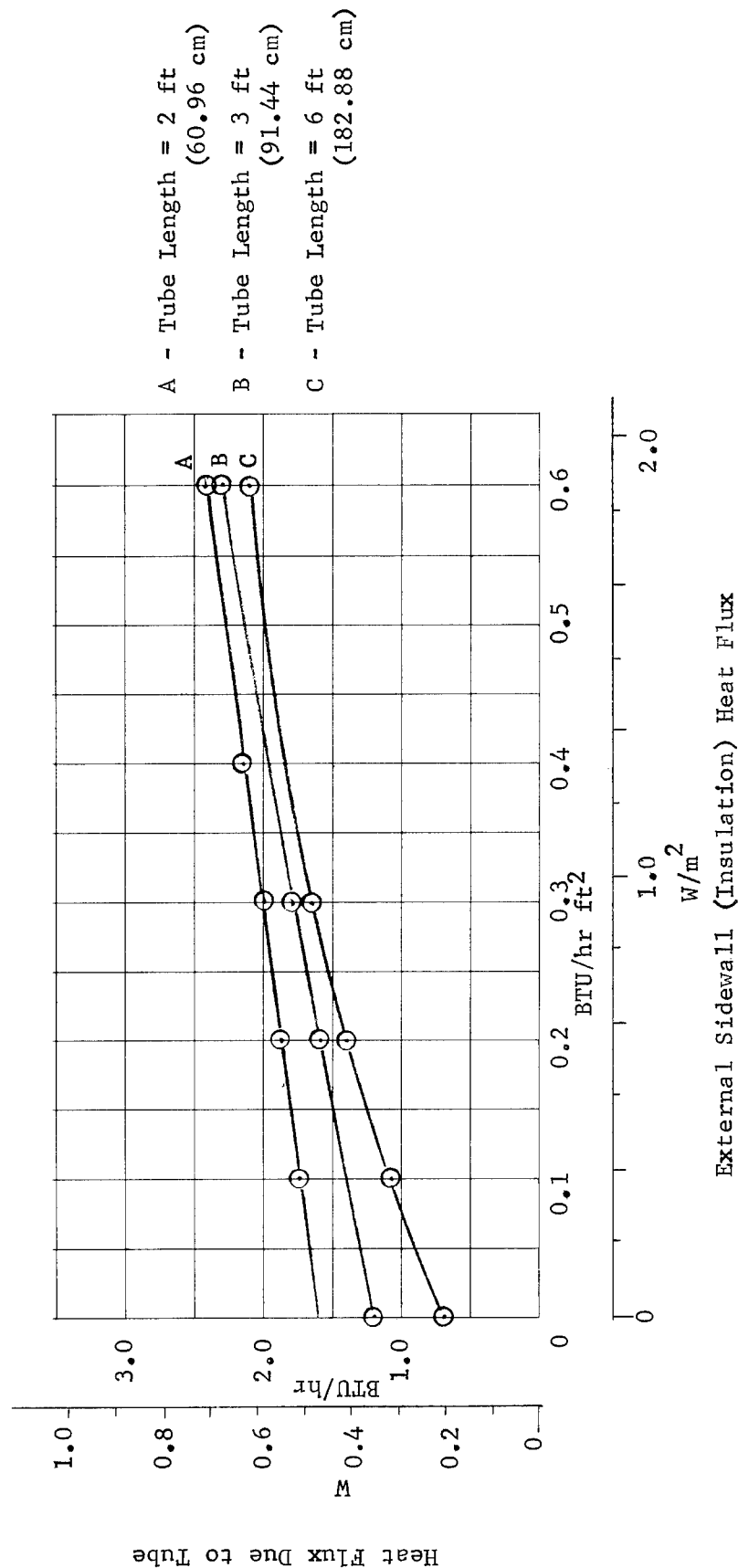
Fig. 18.- Effect of Insulation Heat Flux – 5 in. Tube (12.7 cm)

TABLE 1. – EFFECT OF TUBE CONTENTS ON HEAT TRANSMISSION

Item	Tube ID in.	Tube ID cm	Tube Length ft.	Tube Length cm	Tube Contents	Cold End Temp. °R	Cold End Temp. °K	Heat Flux BTU/hr	Heat Flux W
1	0.5	1.27	1	30.48	Vacuum	40	22	0.104	0.030
2	0.5	1.27	1	30.48	Gaseous Hydrogen	40	22	0.139	0.040
3	0.5	1.27	1	30.48	Gaseous Helium	40	22	0.130	0.038
4	0.5	1.27	1	30.48	Vacuum	153	85	0.093	0.027
5	0.5	1.27	1	30.48	Gaseous Oxygen	153	85	0.097	0.028
6	0.5	1.27	1	30.48	Gaseous Fluorine	153	85	0.089	0.026
7	0.5	1.27	1	30.48	Vacuum	201	112	0.083	0.024
8	0.5	1.27	1	30.48	Methane	201	112	0.089	0.026
9	2	5.08	1	30.48	Vacuum	40	22	0.809	0.237
10	2	5.08	1	30.48	Gaseous Hydrogen	40	22	1.366	0.400
11	2	5.08	1	30.48	Gaseous Helium	40	22	1.299	0.380
12	2	5.08	1	30.48	Vacuum	153	85	0.785	0.230
13	2	5.08	1	30.48	Gaseous Oxygen	153	85	0.829	0.243
14	2	5.08	1	30.48	Gaseous Fluorine	153	85	0.830	0.243
15	2	5.08	1	30.48	Vacuum	201	112	0.718	0.210
16	2	5.08	1	30.48	Methane	201	112	0.793	0.232
17	2	5.08	2	60.96	Vacuum	40	22	0.485	0.142
18	2	5.08	2	60.96	Gaseous Hydrogen	40	22	0.763	0.224
19	2	5.08	2	60.96	Gaseous Helium	40	22	0.730	0.214
20	2	5.08	2	60.96	Vacuum	153	85	0.459	0.134
21	2	5.08	2	60.96	Gaseous Oxygen	153	85	0.495	0.145
22	2	5.08	2	60.96	Gaseous Fluorine	153	85	0.495	0.145
23	2	5.08	2	60.96	Vacuum	201	112	0.438	0.128
24	2	5.08	2	60.96	Methane	201	112	0.476	0.139
25	2	5.08	4	121.92	Vacuum	40	22	0.353	0.103
26	2	5.08	4	121.92	Gaseous Hydrogen	40	22	0.492	0.144
27	2	5.08	4	121.92	Gaseous Helium	40	22	0.476	0.139
28	2	5.08	4	121.92	Vacuum	153	85	0.340	0.099
29	2	5.08	4	121.92	Gaseous Oxygen	153	85	0.357	0.104
30	2	5.08	4	121.92	Gaseous Fluorine	153	85	0.358	0.105
31	2	5.08	4	121.92	Vacuum	201	112	0.328	0.096
32	2	5.08	4	121.92	Methane	201	112	0.347	0.102
33	5	12.7	1	30.48	Vacuum	40	22	5.913	1.73
34	5	12.7	1	30.48	Gaseous Hydrogen	40	22	9.469	2.774
35	5	12.7	1	30.48	Gaseous Helium	40	22	9.058	2.654
36	5	12.7	1	30.48	Vacuum	153	85	5.722	1.676
37	5	12.7	1	30.48	Gaseous Oxygen	153	85	6.199	1.816
38	5	12.7	1	30.48	Gaseous Fluorine	153	85	6.205	1.818
39	5	12.7	1	30.48	Vacuum	201	112	5.537	1.622
40	5	12.7	1	30.48	Methane	201	112	6.041	1.770
41	5	12.7	2	60.96	Vacuum	40	22	3.724	1.091
42	5	12.7	2	60.96	Gaseous Hydrogen	40	22	5.521	1.617
43	5	12.7	2	60.96	Gaseous Helium	40	22	5.317	1.558
44	5	12.7	2	60.96	Vacuum	153	85	3.614	1.059
45	5	12.7	2	60.96	Gaseous Oxygen	153	85	3.855	1.129
46	5	12.7	2	60.96	Gaseous Fluorine	153	85	3.858	1.130
47	5	12.7	2	60.96	Vacuum	201	112	3.506	1.027
48	5	12.7	2	60.96	Methane	201	112	3.760	1.101
49	5	12.7	4	121.92	Vacuum	40	22	2.351	0.689
50	5	12.7	4	121.92	Gaseous Hydrogen	40	22	3.246	0.951
51	5	12.7	4	121.92	Gaseous Helium	40	22	3.146	0.922
52	5	12.7	4	121.92	Vacuum	153	85	2.292	0.672
53	5	12.7	4	121.92	Gaseous Oxygen	153	85	2.911	0.853
54	5	12.7	4	121.92	Gaseous Fluorine	153	85	2.412	0.707
55	5	12.7	4	121.92	Vacuum	201	112	2.232	0.654
56	5	12.7	4	121.92	Methane	201	112	2.357	0.691

*Conditions for All Cases
Liner – 0.002 in. (0.0051 cm) Stainless Steel
Overwrap – 0.030 in. (0.0762 cm) Hoop Wrapped S. Glass
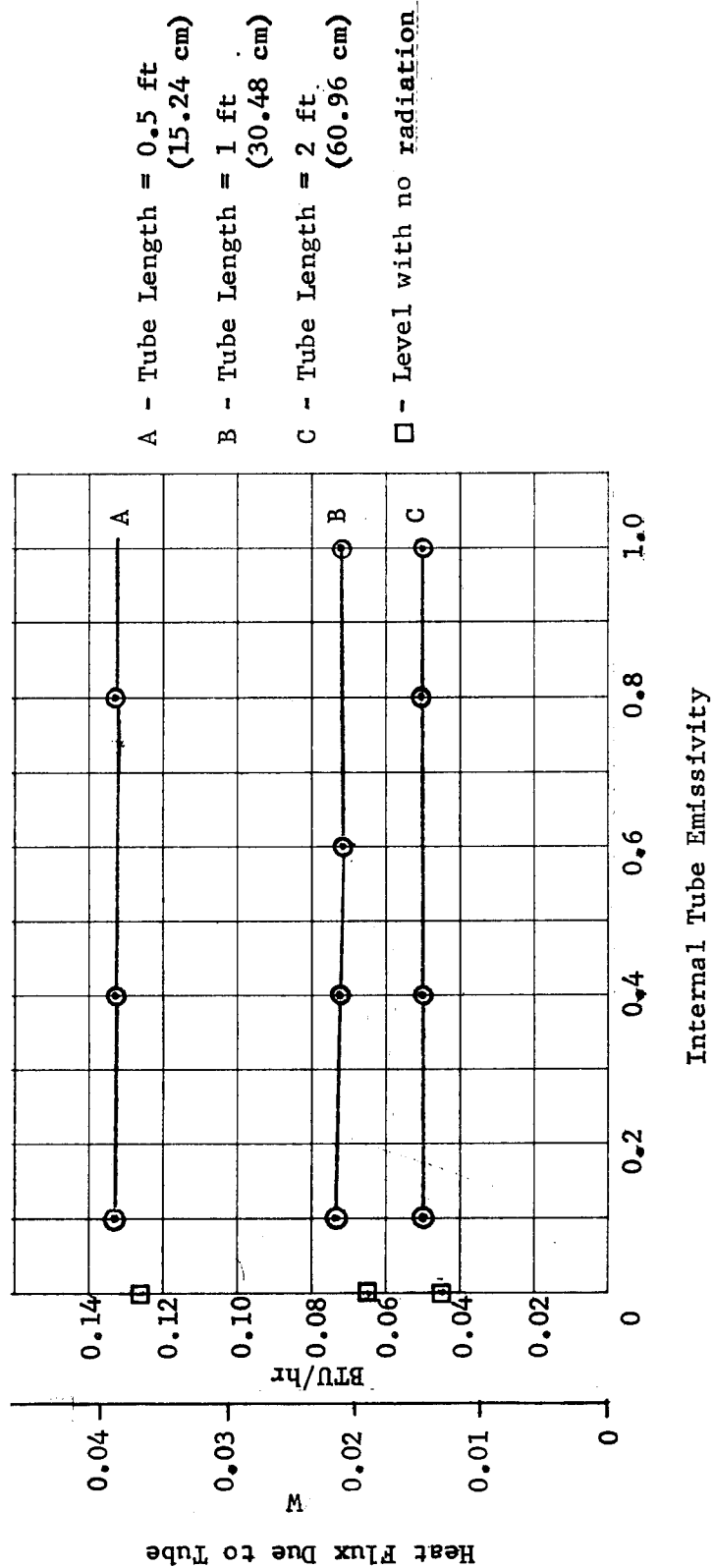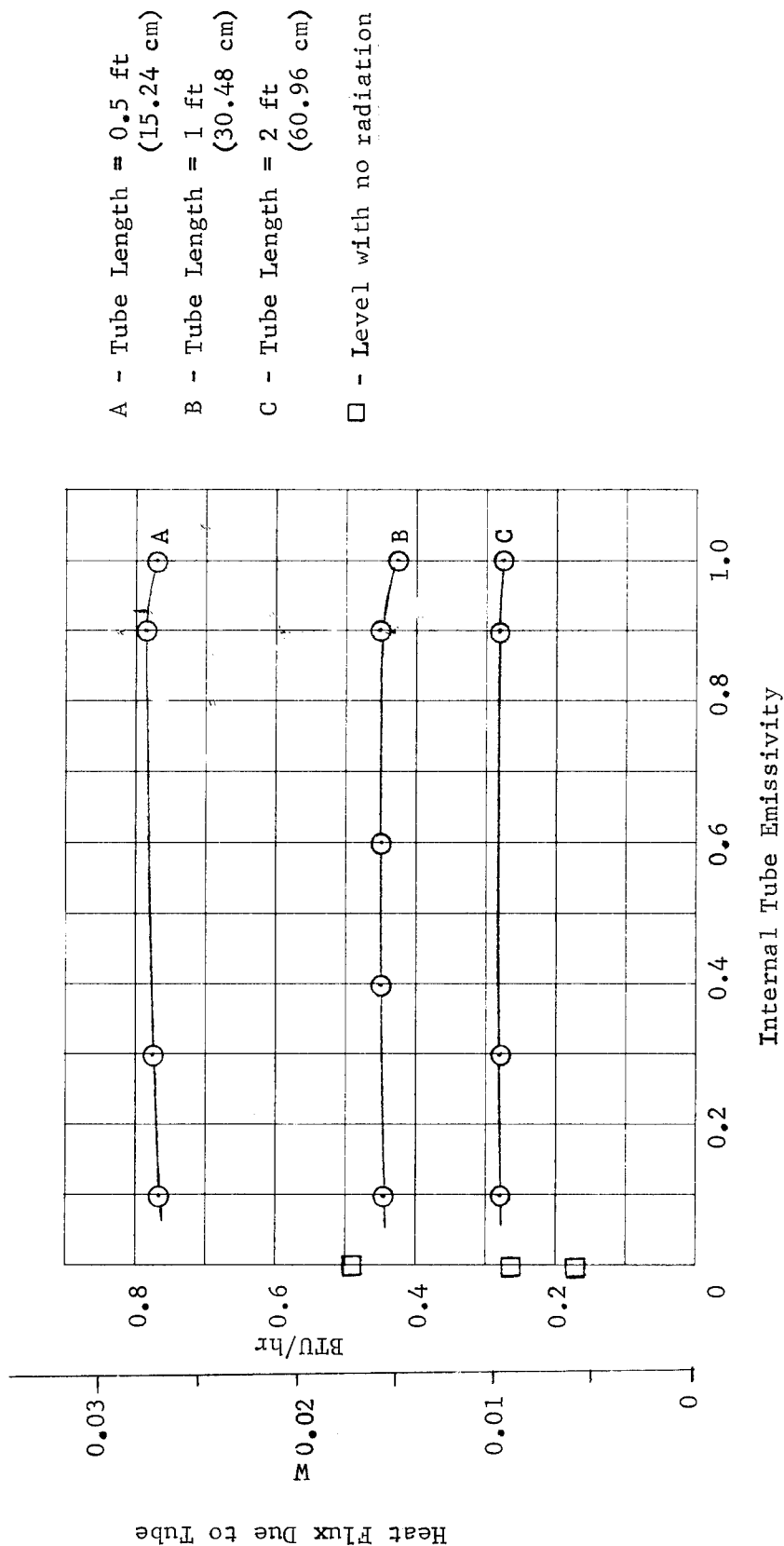Insulation Heat Flux – 0.1 BTU/hr ft^2 (0.315 W/m^2)
Internal Emissivity of Liner – 0.6
Hot End Temperature of 500°R (278°K) for all items

Structural Design Analysis

The structural design analysis was based on an evaluation of the operational requirements of the proposed tubes. These requirements include one or more leak checks at operating pressure and ambient temperature during fabrication and assembly. The tubes would be subjected to bending and torsional loads during handling and installation in a propellant system; and to vibration and dynamic loads during launch and flight of a space vehicle. The tubes would also be subjected to severe thermal stresses and biaxial strain during tank loading, tank pressurization, long-term holds, and propellant outflow when engines were operated.

The operational requirements for long-term space vehicles were considered appropriate to the identified program and were used as criteria during the structural design analysis.

Conditions. - Four distinct conditions regarding the liner temperature and the overwrap temperature were selected for analysis. These conditions were selected as a result of the operational requirements discussed above. After selecting the design configuration resulting from these conditions, a fifth and final analysis verified the results for the critical case and also included a safety factor (by selecting the working pressure (P_w) to be 1.15 times nominal).

The cases which were considered include:

1) Pressurize to working pressure (P_w) while the overwrap is at ambient temperature and the liner is at cryogenic temperature. This condition arises during rapid cooldown;

2) Pressurize to P_w while the liner and the overwrap are both at ambient temperature. This condition arises during leak checks;

3) Pressurize to P_w with the overwrap at the applicable cryogenic temperature. The liner will also be at cryogenic temperature. This condition arises during steady state flow when the line is insulated and the overwrap is nearly adiabatic; and

4) Pressurize to P_w with the overwrap at $\dfrac{T_{amb} + T_{cryo}}{2}$, and the liner at cryogenic temperature. This condition assumes that the outer layer of the overwrap will be at or near ambient temperature and the inner layer of the overwrap will be at the same temperature as the liner. This condition will occur in an uninsulated line during steady state flow.

Liner thickness conditions. - The liner thickness may be sized in a manner that insures all internal pressure loading is carried in the liner, or such that only a portion of the internal pressure loading is carried in the liner with the remaining load carried in the overwrap. The following conditions were used in evaluation of the liner thickness:

1) A minimum thickness so all internally applied loads will be carried in the liner. (In this case the glass-fiber overwrap will provide for easier and safer handling only);

2) Consider the thinnest appropriate liner, such as 0.002 in. (0.0051 cm) for stainless steel and Inconel, and 0.005 in. (0.0127 cm) for aluminum. (In this case the glass-fiber overwrap will be required to support a large portion of the internally applied load); and

3) A nominal thickness so the combined loading in the glass-fiber overwrap and the liner appears to be reasonable. (It may be feasible in this case to carry all longitudinal loading in the liner and some of the hoop load in the overwrap.)

Maximum allowable stress determination - liner. - Several criteria were considered in the selection of the maximum allowable stress in the liner. The major consideration, however, was to restrict stress levels in the liner to the elastic range of the material. Plastic deformation and the resulting compressive loading in the liner after pressure reduction may result in liner buckling, and offers little advantage in reducing weight or heat leak. All acceptable liner thickness are based on the liner remaining in the elastic condition during pressure loading. Other factors that were analyzed included combined stresses, strength reduction due to welding, strength reduction due to weld-heat affected zone, strength changes due to very thin members, and strength changes associated with grain direction. The criteria are detailed in the following:

1) In a thin wall cylinder subjected to internal pressure, the combined stresses are determined by combining the

    hoop stress $\sigma_h = \dfrac{pr}{t}$ and the longitudinal stress, $\sigma_a = \dfrac{pr}{2t}$,

    where p is the tube internal pressure (psia), r is the tube radius (in.), and t is the tube wall thickness (in.). For conditions of biaxial stress, the Hencky - von Mises theory of failure gives results in good agreement with test data for a number of materials. It is the most accurate theory for ductile materials under hydrostatic pressure conditions (Ref 1). This theory suggests that under combined stresses, the yield stress (σ_y) will be

modified as follows:

$$\sigma_h^2 - \sigma_h \sigma_a + \sigma_a^2 = \sigma_y^2$$

where σ_h is a uniaxial stress in the hoop direction and σ_a is a uniaxial stress in the longitudinal direction. Since, from above,

$$\sigma_h = 2 \sigma_a$$

we can substitute in the Hencky-von Mises equation and obtain

$$4 \sigma_a^2 - 2\sigma_a^2 + \sigma_a^2 = \sigma_y^2$$

$$3 \sigma_a^2 = \sigma_y^2$$

and

$$\sigma_a = \frac{\sigma_y}{\sqrt{3}} = 0.57 \sigma_y = \text{allowable longitudinal stress}$$

$$\sigma_h = \frac{2 \sigma_y}{\sqrt{3}} = 1.15 \sigma_y. = \text{allowable hoop stress}$$

This program was not concerned with resolving the additional problems associated with water hammer; assembly misfits and strains associated with them, etc. Specific vehicle working pressures and conditions will require attention to this category;

2) The process of resistance or fusion welding the liner to form a leak tight system causes some reduction in the total tube strength. Estimates of weld efficiency range from 60 to 90% of the base metal strength, but little data existed concerning strength reduction due to welding very thin members. Another area of concern is the heat-affected zone around the weld. In the case of aluminum, heat treating after welding will restore the base metal to its original yield level. In the case of Inconel 718, the short time localized heat is applied may result in little, if any strength reduction, and any strength lost can be recovered by aging. In the case of stainless steel, and in this specific application, cold working of the joint to restore the strength is not very practical and joint strength will be reduced;

3) Strength changes in the liner associated with temperature changes were obtained from the <u>Cryogenic Materials Data Handbook</u> (ref 2), and (ref 3);

4) Strength reduction due to the required pressure and temperature cycling requirements is considered to be negligible. Fatigue strength charts do not apply to less than 1000 cycles;

5) Relatively little data are available for the comparison of strength (σ_y) in very thin members. Surface defects, and surface conditions in general, have a large percentage effect on these thin members;

6) As a somewhat conservative approach, the weaker direction of grain, usually transverse, was used in all calculations.

After considering each of the conditions relating to the maximum allowable stress the following general equation was developed and used for the maximum allowable stress:

$$\sigma_{h_{max}} = \frac{2\sigma_y}{\sqrt{3}} \times (\text{weld efficiency factor}) \times (\text{inverse of safety factor})$$

$$= \frac{2\sigma_y}{\sqrt{3}} (.90) \ (.90)$$

$$\sigma_{h_{max}} = 0.935 \ \sigma_y$$

and by definition
$$\sigma_{a_{max}} = 0.467 \ \sigma_y.$$

A series of tensile tests was performed to determine yield and ultimate stress values and weld efficiency values. Tensile samples consisted of both thin member unwelded coupons and thin member welded coupons. Results of these tests are shown in the Task III Testing section of this report.

<u>Theory on bonding of liner and glass-fiber overwrap.</u> - Results of a recent bonding program (ref 4) indicate the feasibility of physically bonding the liner to the glass-fiber overwrap. This bond, if successful, would permit the transfer of slightly more hoop load and considerably more longitudinal load into the overwrap. However, the stress levels in the liner would result in plastic deformation with a shortening of life. Further, if

the bond failed, the liner would fail immediately because of stress levels or it would fail shortly after the unbonding due to fatigue.

The results of this investigation confirm the desire to prohibit the bonding of the liner and overwrap and, in fact, to apply an antibonding or release agent to the liner before overwrapping.

Design analysis calculations. - The final product of the conditions and criteria is reflected by the actual design calculations for the composite specimen. The general order of these calculations is to first determine the theoretical gap or interference fit created during the overwrap process. Next, the theoretical gap between the liner and the overwrap when the composite is subjected to working temperatures can be calculated. The gap in combination with stress/strain relationships for the metal liner, can be used to determine the portion of the total load in the hoop direction that must be absorbed by the liner before contact with the overwrap. After contact, the loads are transferred to the overwrap as a function of the modulus of elasticity and thickness of the members.

Condition at room temperature. - Before investigating the gap between the metal liner and the glass-fiber overwrap at the cryogenic working temperatures, the gap or condition at room temperature must be evaluated. During the overwrap process the glass-fiber system will be subjected to a tensile load that will subject the liner to a stress that can be identified as

$$P = \frac{T}{r}$$

where P is the liner pressure in lb/in^2 unit stress and T is the tension in pounds per inch of overwrap width and r is the liner radius in inches (ref 5). Empirical data generated by Martin Marietta Corporation using a series of NOL rings were used to calculate the stress strain relationship and to determine the post cure gap or interference due to overwrap tension (see fig. 19). Details of the NOL ring tests are presented in the overwrap tension test discussion on page 120. These empirical data as well as the above equation were used to determine internal pressures and overwrap tension settings used during fabrication.

A requirement of this program was to limit the overwrap imposed stress on the liner to a rather low value with the design goal to achieve the following value at room temperature conditions,

$$0 < \sigma < 10\% \, \sigma_b$$

where σ_b is the allowable compressive, hoop buckling stress for the liner.

Fig. 19.- Effect of Winding Tension Vs. Gap or Interference

□ 3 layers of Hoop Glass (Approximately 0.030" thick) (0.0762 cm)
○ 3 layers of glass (Hoop, Axial, Hoop) (Approximately 0.030" thick) (0.0762 cm)

Liner Diameter = 5.753" (14.61 cm)
Liner Configuration = Solid Stainless Steel Bar
Overwrap = S/HTS with 58-68R Resin System (20%)
    Pre-impregnated, 20 end roving, 16 rovings/inch (6.3 rovings/cm)
Cure = 2 hours at 200°F (366°K), 2 hours from 200°F (366°K) to
    350°F (450°K) and 4 hours at 350°F (450°K).

Gap is defined as the average distance between the liner OD and the
overwrap ID with positive numbers as gap and negative numbers as
interference.

Several methods of controlling this stress level were available and evaluated including the use of low overwrap tension, internal pressure to stabilize the liner during the overwrapping process, independent fabrication of the liner and overwrap to controlled diameters, and a thicker liner so the buckling stress allowable is increased.

The use of a low overwrap tension simplifies fabrication in that no internal pressurization provisions are required. The largest disadvantage of the low tension, say 2 or 3 lb (8.9 or 13.35N) per 20 ends, is in the low quality and poor surface finish of the overwrap. Approximately 6 lb (26.7N) tension per 20 ends is required to provide a high quality surface finish and a well compacted overwrap. A sample 1.25" (3.18 cm) diameter liner was overwrapped without any internal pressure and 2 lb (8.9 N) tension (per 20 ends) and a small cusp was formed in the liner in the area of the longitudinal resistance weld; however, this cusp did not appear to affect the burst pressure of the tube.

To attain a higher quality overwrap configuration and surface finish, internal pressure can be added to the liner during the overwrap process to offset the overwrap tension. This internal pressure will strengthen the liner considerably and can prevent formation of a cusp during the process. The application of pressure can result in an elastic strain in the liner and force the overwrap to a larger null diameter. The release of the pressurization after the overwrap is complete will permit the liner to decrease in diameter to the point of desired compressive stress. Equations for this combination of internal pressure and overwrap tension are not precise and therefore the appropriate levels are best determined empirically. A second sample liner was overwrapped with 25 psig (25.5 N/cm^2) internal pressure and 2 lb (8.9 N) tension (per 20 ends) and a noticeable stiffening of the liner over the unpressurized specimen was observed. No cusp was formed; however, the burst pressure was the same as the other specimen. Of specific interest, the calculated burst pressure of the specimen in the hoop direction was 12 000 psi (8274 N/cm^2) internal pressure and in the longitudinal direction was 1200 psi (827.4 N/cm^2), with actual burst occurring at 1175 psi (810.1 N/cm^2). The failure occurred in the connection of the liner to the end fitting. [Both of the sample tubes were fabricated from a 0.002 in. (0.0051 cm) thick, 1.25 in. (3.18 cm) dia, 304L stainless steel resistance welded liner and 0.030 in. (0.0762 cm) thick hoop wrapped S/HTS glass with the 58-68R resin, 20 ends preimpregnated]. A modification to the internal pressure approach involves the use of a solid mandrel inside the liner during fabrication. The use of this mandrel would be to stiffen the liner and prevent formation of a cusp. One disadvantage in using the solid mandrel is in the inability to elastically strain the liner and control (as noted above) the post cure compressive stress. The solid mandrel is discussed below as a method of preventing buckling during the cure cycle.

Another method of fabrication would involve separate fabrication of the liner and the overwrap to controlled diameters followed by

sliding the overwrap over the liner. Closely controlled diameters would make this method feasible. To slip the overwrap over the liner (with a slight interference fit at ambient temperature) the liner would be cooled to liquid nitrogen temperature to create a gap. After the overwrap and liner are joined the remaining end fitting can be welded to the liner. This process would result in high fabrication costs and probably not be cost effective.

The use of a thicker liner to increase the allowable hoop buckling stress has the disadvantage of increasing the total heat flux. Reviewing the σ_b allowables for the 5 in. (12.7 cm) diameter tube, the stress allowable can be increased almost an order of magnitude by doubling the wall thickness. This method should be used only if the other methods are not acceptable.

In conclusion, the application of a small amount of internal pressure, resulting in a small elastic strain, during the overwrapping and curing process will permit a higher wrap tension and still result in a minimal interference fit (or buckling stress) after the fabrication process is complete. The precise levels of pressure and wrap tension were developed empirically during the early stages of specimen preparation.

Gap at working temperature. As the tube is cooled to cryogenic working temperatures, the liner circumference will be expressed as

$$C_{\ell_{Wt}} = C_{\ell_{rt}} - \Delta C_{\ell_{Wt}}$$

where

$$C_{\ell_{Wt}} = \text{liner circumference at working temperature,}$$

and

$$C_{\ell_{rt}} = \text{liner circumference at room temperature, } 75^\circ F \ (297^\circ K)$$

and

$$\Delta C_{\ell_{Wt}} = C_{\ell_{rt}} (\alpha_{ave}) \left(75^\circ F - T_{Wt} \right)$$

where

$$\alpha_{ave} = \text{average coefficient of linear thermal expansion}$$

and

$$T_{Wt} = \text{working temperature}$$

and the overwrap circumference will be

$$C_{O_{Wt}} = C_{O_{rt}} - \Delta C_{O_{Wt}}$$

where

$$C_{O_{Wt}} = \text{overwrap circumference at working temperature}$$

and

$$C_{O_{rt}} = \text{overwrap circumference at room temperature, } 75^{\circ}F \ (297^{\circ}K)$$

and

$$\Delta C_{O_{Wt}} = C_{O_{rt}} \ (\alpha_{ave}) \ (75^{\circ}F - T_{Wt})$$

This results in a gap between the liner outside diameter and the overwrap inside diameter as follows:

$$GAP_{Wt} = \frac{C_{O_{Wt}} - C_{\ell_{Wt}}}{2\pi}$$

The gaps for various temperature combinations are shown in tables 2 and 3 assuming a zero stress condition in the liner with no gap at ambient temperature.

Stress in liner to close gap to zero. - As internal pressure is applied in the tube, the liner is subjected to the total hoop load until the gap between the liner and the overwrap is reduced to zero as a result of the strain in the liner. The stress in the liner (σ_{ℓ}) at this condition can be defined as

$$\sigma_{\ell} = E_{\ell} \ \epsilon_{\ell}$$

where E is the modulus of elasticity of the liner at the applicable temperature and $\epsilon_{\ell} =$ strain in the liner defined as

TABLE 2. – TEMPERATURE COMBINATION GAPS

Gap between overwrap & liner, hoop wrapped glass (in.)

Temp. Conditions		6061-T6			21-6-9 CRES			304L CRES			INCONEL 718		
		Diameter (in.)			Diameter (in.)			Diameter (in.)			Diameter (in.)		
Overwrap (°F)	Liner (°F)	0.5	2	5	0.5	2	5	0.5	2	5	0.5	2	5
Amb	Amb	0.00	0.00	0.00	0.00	0.00	0.00	0.00	0.00	0.00	0.00	0.00	0.00
Amb	-300	0.00094	0.00378	0.00945	0.00067	0.00027	0.00675	0.00067	0.00270	0.0067	0.00052	0.00208	0.00520
Amb	-423	0.00104	0.00414	0.01035	0.00074	0.00295	0.00737	0.00074	0.00295	0.00737	0.00059	0.00237	0.00592
-423	-423	0.00086	0.00344	0.00860	0.00056	0.00210	0.00562	0.00056	0.00210	0.00562	0.00042	0.00167	0.00418
-174	-423	0.00091	0.00364	0.00910	0.00061	0.00245	0.00612	0.00061	0.00245	0.00612	0.00047	0.00187	0.00467

TABLE 3. – TEMPERATURE COMBINATION GAPS

Gap between overwrap & liner, hoop wrapped glass (cm)

Temp. Conditions		6061-T6			21-6-9 CRES			304L CRES			INCONEL 718		
		Diameter (cm)			Diameter (cm)			Diameter (cm)			Diameter (cm)		
Overwrap (°K)	Liner (°K)	1.27	5.08	12.7	1.27	5.08	12.7	1.27	5.08	12.7	1.27	5.08	12.7
Amb	Amb	0.00	0.00	0.00	0.00	0.00	0.00	0.00	0.00	0.00	0.00	0.00	0.00
Amb	89	0.0024	0.0096	0.0240	0.0017	0.0069	0.0172	0.0017	0.0069	0.0172	0.0013	0.0053	0.0132
Amb	20	0.0026	0.0105	0.0263	0.0019	0.0075	0.0187	0.0019	0.0075	0.0187	0.0015	0.0060	0.0150
20	20	0.0022	0.0087	0.0218	0.0014	0.0053	0.0143	0.0014	0.0053	0.0143	0.0011	0.0042	0.0106
159	20	0.0023	0.0093	0.0231	0.0016	0.0062	0.0155	0.0015	0.0062	0.0155	0.0012	0.0047	0.0119

$$\epsilon_\ell = \frac{C_o - C_\ell}{C_\ell}$$

Rewriting the above equation, we obtain

$$\sigma_{\ell_{Wt}} = E_{\ell_{Wt}} \left(\frac{C_o - C_\ell}{C_\ell} \right)_{Wt}$$

At each combination of loads and temperatures, this stress is desired to be less than the yield stress at the applicable temperature. The poisson's ratio effect was not considered in this analysis.

The results of this analysis are shown in tables 4 and 5, which include the maximum allowable stress $\left(\sigma_{\ell_m}\right)$ and the stress to close the gap to zero $\left(\sigma_{\ell_g}\right)$. In the case where the loads can be carried by a thin liner without closing the gap, the glass fiber overwrap will be a non load member. Tables 6 and 7 list the minimum thicknesses for the liner needed to carry all pressure loads.

Load sharing in liner and overwrap.- When the strain in the liner permits contact between the liner and the overwrap, the remaining loading is absorbed by the liner and the overwrap according to the relationship between the respective modulus of elasticity. Given the stress in the liner at the point of contact with the overwrap σ_{ℓ_g} and given the maximum allowable stress in the liner σ_{ℓ_m}, we can calculate the available stress as

$$\Delta \sigma_\ell = \sigma_{\ell_m} - \sigma_{\ell_g} \quad .$$

The available strain in the liner between contact with the overwrap and the strain associated with the maximum liner stress may be expressed as

$$\Delta \epsilon_\ell = \frac{\Delta \sigma_\ell}{E_\ell}$$

and, by definition, the strain in the overwrap can be expressed as

$$\epsilon_o = \Delta \epsilon_\ell \quad .$$

44

The portion of the internal pressure that will be carried in the liner is expressed by

$$P_{\ell_m} = \frac{\sigma_{\ell_m} t_\ell}{r}$$

where t_ℓ is the liner thickness, r is the nominal tube radius and P_{ℓ_m} is the maximum internal tube pressure associated with the maximum liner stress.

The portion of the internal pressure that will be carried in the overwrap is expressed by

$$P_o = P_w - P_{\ell_m}$$

where P_w is the internal working pressure. Then the stress in the overwrap is

$$\sigma_o = \frac{P_o r}{t_o}$$

or the thickness of overwrap required to carry the internal pressure is

$$t_o = \frac{P_o r}{\sigma_o}$$

Substituting and solving for the overwrap thickness, we have

$$t_o = \frac{\left(P_w - \frac{\sigma_{\ell_m} t_\ell}{r}\right) r}{\sigma_o} = \frac{rP_w - \sigma_{\ell_m} t_\ell}{\sigma_o} = \frac{rP_w - \sigma_{\ell_m} t_\ell}{\Delta \sigma_\ell}\left(\frac{E_\ell}{E_o}\right)$$

The overwrap thickness required for the Inconel 718 liners is shown in tables 8 and 9.

The next step associated with load sharing requires the correction of the von Mises equation to reflect the less than 2:1 relationship between hoop and longitudinal stresses in the liner. If we assume the glass is not bonded or otherwise connected to the liner or end fittings in such a manner as to carry longitudinal load, we must carry all of the axial load in the liner. The solution of the following equation must remain within the allowable liner stress σ_{ℓ_m}

$$\sigma_{\ell_m}^2 = \sigma_h^2 - \sigma_h \sigma_a + \sigma_a^2$$

At this point the liner thickness will require some adjustment, and the calculations will require verification.

TABLE 4.- LINER STRESS ANALYSIS

Temperature conditions		σ_{ℓ_m}	σ_{ℓ_g}	σ_{ℓ_m}	σ_{ℓ_g}	σ_{ℓ_m}	σ_{ℓ_g}	σ_{ℓ_m}	σ_{ℓ_g}
Overwrap (°F)	Liner (°F)	6061-T6	6061-T6	21-6-9	21-6-9	304L	304L	Inco 718	Inco 718
Amb	Amb	39.3	0	63.5	0	56.1	0	142.1	0
Amb	-300	44.4	43.9	164.0	90.3	67.3	85.9	165.5	67.8
Amb	-423	49.5	50.2	215.0	114.8	77.1	88.4	179.5	81.0
-423	-423	49.5	41.9	215.0	93.2	77.1	67.0	179.5	58.0
-174	-423	49.5	45.3	215.0	102.2	77.1	76.1	179.5	67.2

σ_{ℓ_m} = maximum allowable liner stress in psi x 10^{-3}

σ_{ℓ_g} = liner stress to close gap in psi x 10^{-3}

6061-T6 = aluminum σ is independent of liner diameter

21-6-9 = Stainless Steel

304L = Stainless Steel

Inco 718 = Inconel 718

TABLE 5.- LINER STRESS ANALYSIS

Temperature conditions		σ_{ℓ_m}	σ_{ℓ_g}	σ_{ℓ_m}	σ_{ℓ_g}	σ_{ℓ_m}	σ_{ℓ_g}	σ_{ℓ_m}	σ_{ℓ_g}
Overwrap (°K)	Liner (°K)	6061-T6	6061-T6	21-6-9	21-6-9	304L	304L	Inco 718	Inco 718
Amb	Amb	27.1	0	43.8	0	38.7	0	98.0	0
Amb	89	30.6	30.3	113.1	62.3	46.4	59.2	114.1	46.7
Amb	20	34.1	34.6	148.2	79.2	53.2	60.9	123.8	55.8
20	20	34.1	28.9	148.2	64.3	53.2	46.2	123.8	40.0
159	20	34.1	31.2	148.2	70.5	53.2	52.5	123.8	46.3

σ_{ℓ_m} = maximum allowable liner stress in N/cm^2 x 10^{-3}

σ_{ℓ_g} = liner stress to close gap in N/cm^2 x 10^{-3}

6061-T6 = aluminum σ is independent of liner diameter

21-6-9 = Stainless Steel

304L = Stainless Steel

Inco 718 = Inconel 718

TABLE 6.- MINIMUM LINER THICKNESS TO CARRY ALL PRESSURE LOADS

Liner Temp (°F)	Liner thickness to carry all pressure loads, (in.)											
	6061 - T6 Aluminum			304L CRES			Inconel 718			21-6-9 CRES		
	0.5 dia	2 dia	5 dia	0.5 dia	2 dia	5 dia	0.5 dia	2 dia	5 dia	0.5 dia	2 dia	5 dia
+75	0.022	0.0063	0.016	0.016	0.0044	0.011	0.0061	0.002	0.0044	0.0136	0.0039	0.0097
-300	0.020	0.0056	0.014	0.013	0.0037	0.009	0.0052	0.0015	0.0037	0.0056	0.0016	0.0040
-423	0.018	0.005	0.013	0.011	0.0032	0.008	0.0048	0.0014	0.0034	0.0040	0.0012	0.0029

Above dia in inches

Maximum working pressure (P_w) = 1.15 x operating pressure

P_w for 0.5-in. tube = 3467 psia

P_w for 2- and 5-in. tubes = 247 psia

TABLE 7.- MINIMUM LINER THICKNESS TO CARRY ALL PRESSURE LOADS

Liner Temp (°K)	Liner thickness to carry all pressure loads, (cm)											
	6061 - T6 Aluminum			304L Stainless Steel			Inconel 718			21-6-9 Stainless Steel		
	1.27 cm dia	5.08 cm dia	12.7 cm dia	1.27 cm dia	5.08 cm dia	12.7 cm dia	1.27 cm dia	5.08 cm dia	12.7 cm dia	1.27 cm dia	5.08 cm dia	12.7 cm dia
297	0.0559	0.016	0.0406	0.0406	0.0112	0.0279	0.0155	0.0051	0.0112	0.0345	0.0099	0.0246
89	0.0508	0.0142	0.0356	0.033	0.0094	0.0229	0.0132	0.0038	0.0094	0.0142	0.0041	0.0102
20	0.0457	0.0127	0.033	0.0279	0.0081	0.0203	0.0122	0.0036	0.0086	0.0102	0.0031	0.0074

Maximum working pressure (P_w) = 1.15 x operating pressure

P_w for 1.27 cm tube = 2340 N/cm^2

P_w for 5.08 and 12.7 cm tube = 170 N/cm^2

TABLE 8.- REQUIRED OVERWRAP THICKNESSES FOR INCONEL 718 LINERS

Temp	cond	Overwrap thickness (t_o) required for hoop stress control for Inconel 718 liner (unidirectional hoop wrap)		
wrap (°F)	liner (°F)	0.5 dia x 0.004 thick (in.)	2 dia x 0.002 thick (in.)	5 dia x 0.002 thick (in.)
Amb	Amb	0.0068	None required	0.0076
Amb	-423	0.0049	None required	0.0085

Note: These thicknesses are based on a working pressure (P_w) in the 0.5 in. dia tube of 3000 psi and 200 psi for the 2 and 5 in. dia tubes.

TABLE 9.- REQUIRED OVERWRAP THICKNESSES FOR INCONEL 718 LINERS

Temp	cond	Overwrap thickness (t_o) required for hoop stress control for Inconel 718 liner (unidirectional hoop wrap)		
wrap (°K)	liner (°K)	1.27 dia x 0.0102 thick (cm)	5.08 dia x 0.0051 thick (cm)	12.7 dia x 0.0051 thick (cm)
Amb	Amb	0.0173	None required	0.0193
Amb	20	0.0125	None required	0.0216

Note: These thicknesses are based on a working pressure (P_w) in the 1.27 cm dia tube of 2068 N/cm^2 psi and 138 N/cm^2 for the 5.08 cm and 12.7 cm dia tubes.

Liner loads due to glass overwrap thermal characteristics. -
If the glass overwrap is attached firmly to the liner end fittings
or its movement is restricted by the end fittings, consideration
must be given to the liner stresses induced by thermal contraction
or expansion. Derivation of an equation to determine the liner
stresses is presented below:
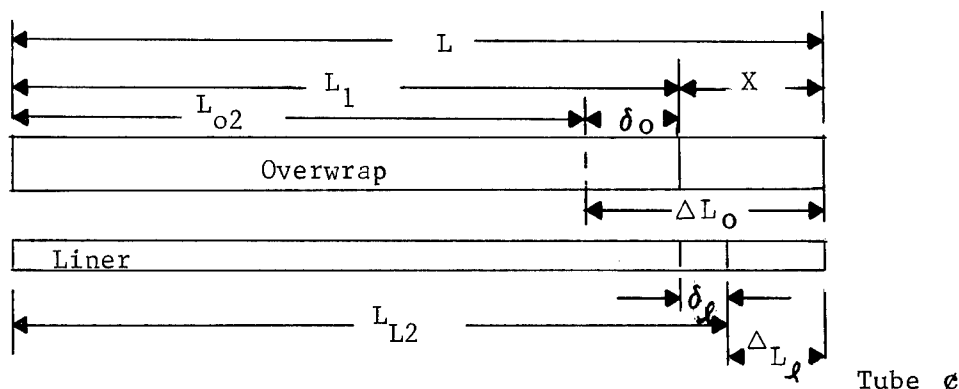
Fig. 20- Determination of Liner Stresses

Consider fig. 20 where the following conditions exist:

1) L is the length at T_1 [cure temperature of $+275^\circ F$ $(408^\circ K)$] of the composite tube. Both overwrap and liner are equal length at cure temperature since the overwrap assumes liner dimensions until curing is completed;

2) L^1 is the length of the composite tube at some temperature T_2;

3) L_{o2} is the length the overwrap would be at some temperature T_2 if it were unrestrained $(L - \Delta L_o)$;

4) L_{L2} is the length of the liner, if unrestrained, at T_2. $(L - \Delta L_\ell)$;

5) δ_o is the deflection in the overwrap resulting from liner loading at T_2;

6) δ_ℓ is the deflection in the liner resulting from overwrap loading at T_2;

7) ϵ_o is the strain in the overwrap at $T_2 = \dfrac{\delta_o}{L_{o2}}$;

8) ϵ_ℓ is the strain in the liner at $T_2 = \dfrac{\delta_\ell}{L_{L2}}$.

9) Free body - the composite is unrestrained.

10) Overwrap and liner both connect to end fitting but no shear bond exists between liner and overwrap elsewhere.

When the liner is cooled to ambient temperature after curing, the stress in the liner and overwrap are increased. Derivation of the liner stress equations is as follows:

$$\Delta L_o = - L \; \alpha_o \Delta T \qquad (1)$$

$$\Delta L_\ell = - L \; \alpha_\ell \Delta T \qquad (2)$$

where α = coefficient of thermal expansion and ΔT is negative (cooling). Because the forces in the overwrap and liner must be equal at equilibrium conditions,

$$\Sigma F \; = \; 0 \quad \text{or} \quad F_o + F_\ell \; = 0 \quad \text{and since}$$

$$F_o = \sigma_o A_o \quad \text{and} \quad F_\ell = \sigma_\ell A_\ell \quad \text{then} \quad \sigma_o A_o + \sigma_\ell A_\ell = 0$$

or $$\sigma_o A_o = - \sigma_\ell A_\ell \quad \text{or} \quad \sigma_o = - \frac{\sigma_\ell A_\ell}{A_o}$$

where F = force, A = cross sectional area and σ = stress.

From fig. 20, the following relations can be obtained:

$$\delta_o \; = \Delta L_o - X$$

$$\delta_\ell \; = \; X - \Delta L_\ell$$

where $\delta_o = \epsilon_o \; L_{o2}$, and $\delta_\ell = - \epsilon_\ell \; L_{L2}$ and, because $\epsilon = \dfrac{\sigma}{E}$

then $\delta_o = \dfrac{\sigma_o}{E_o} L_{o2}$ and $\delta_\ell = - \dfrac{\sigma_\ell}{E_\ell} L_{L2}$. Substituting these values

gives $$\frac{\sigma_o L_{o2}}{E_o} \; = \Delta L_o - X \qquad (3)$$

$$- \frac{\sigma_\ell L_{L2}}{E_\ell} \; = \; X - \Delta L_\ell \qquad (4)$$

adding equations 3 and 4 gives

$$\frac{\sigma_o L_{o2}}{E_o} \; - \; \frac{\sigma_\ell L_{L2}}{E_\ell} = \Delta L_o - \Delta L_\ell \qquad (5)$$

substituting $\sigma_o = -\dfrac{\sigma_\ell\, A_\ell}{A_o}$ into equation 5

$$-\frac{\sigma_\ell\, A_\ell\, L_{o2}}{A_o\, E_o} - \frac{\sigma_\ell\, L_{L2}}{E_\ell} = \Delta L_o - \Delta L_\ell \qquad (6)$$

substituting equations 1 and 2 into (6)

$$-\frac{\sigma_\ell\, A_\ell\, L_{o2}}{A_o\, E_o} - \frac{\sigma_\ell\, L_{L2}}{E_\ell} = -L\,\alpha_o\,\Delta T + L\,\alpha_\ell\,\Delta T$$

since $L_{o2} \cong L_{L2} \cong L$ this may be simplified with neglible error

to

$$-\frac{\sigma_\ell\, A_\ell}{A_o\, E_o} - \frac{\sigma_\ell}{E_\ell} = \Delta T\,(\alpha_\ell - \alpha_o)$$

or

$$\sigma_\ell \left(\frac{A_\ell}{A_o\, E_o} + \frac{1}{E_\ell} \right) = -\Delta T\,(\alpha_\ell - \alpha_o)$$

or

$$\sigma_\ell = \frac{\Delta T\,(\alpha_o - \alpha_\ell)}{\dfrac{A_\ell}{E_o\, A_o} + \dfrac{1}{E_\ell}}$$

and

$$\sigma_c = -\frac{\sigma_\ell\, A_\ell}{A_o}$$

A positive stress indicates tension and a negative stress indicates compression. The ΔT is negative for cooling and positive for warming from cure conditions.

The above equations were used to calculate stresses in both the liner and overwrap due to temperature changes and differences in thermal expansion characteristics of the materials. The results are shown in Table 10. Only those specimens designed to transfer axial loads from the liner to the overwrap required use of these calculations.

TABLE 10. - LINER STRESS DUE TO THERMAL COEFFICIENT GRADIENTS
BETWEEN THE LINER AND OVERWRAP, INCONEL 718 (AXIAL)

Specimen Number *	Tube Diameter		Compressive Stress in Liner	
	in	cm	psi	N/cm^2
CFL 6300605	0.5	1.27	2330	1606
CFL 6300606	0.5	1.27	2330	1606
CFL 6300607	0.5	1.27	2330	1606
CFL 6300609	2.0	5.08	3460	2385
CFL 6300610	2.0	5.08	3460	2385
CFL 6300611	2.0	5.08	3460	2385
CFL 6300612	2.0	5.08	2530	1744
CFL 6300613	5.0	12.70	8300	5722
CFL 6300614	5.0	12.70	8300	5722
CFL 6300615	5.0	12.70	6350	4377
CFL 6300616	5.0	12.70	6350	4377

NOTE: 1. All stress values are calculated with liner and overwrap at -423°F (20°K)

2. Thermal coefficients for liner and composite are based on reference 2 figures D.13.t and H.1.t-1 respectively.

* This column is the identifying drawing number for each tube design.

Buckling stress allowables (axial). - Compression buckling is a failure mode in the thin metal liner. The axial compressive loading may be imposed from the spacecraft structure, from the engine thrust, or from the glass-fiber overwrap. The buckling stresses have been included only for Inconel 718 in tables 11 and 12 because this material was used in almost all applications based on the preceeding calculations.

Buckling stress allowables (hoop). - Compression buckling is a failure mode in the thin metal liner in the hoop as well as the axial direction. The compressive hoop loading may be imposed from the glass-fiber overwrap. The buckling stresses have been included for Inconel 718 and CRES only (see tables 13 and 14) because these materials were used for all applications. A constant modulus of elasticity was used for calculations.

Torque allowables. - Torque may be a failure mode in the thin metal liner. Torque can be applied to the liner during fitting makeup or through the configuration of the propulsion plumbing system. Tables 15 and 16 list the torque allowables for Inconel 718 assuming clamped ends. The values will be somewhat lower if hinged ends are assumed. Results of the torque verification testing are shown in the test section of this report.

Material compatibility and corrosion. - Material compatibility with liquid fluorine must be considered during design of the glass overwrapped tubes. All of the metal liners being evaluated are considered compatible with liquid fluorine. The corrosion rate of 304L CRES in LF_2 varies between 0.25×10^{-4} and 200×10^{-4} in./year $(0.64 \times 10^{-4}$ and 5.1×10^{-4} cm/year), while Inconel corrosion rate in LF_2 is approximately 250×10^{-4} in./year $(640 \times 10^{-4}$ cm/year) depending on the information source (ref 7 and 8). When considering a 5-year mission using LF_2, it becomes obvious that corrosion rates will be a significant factor in propellant line thickness, whether the lines be fiberglass overwrapped or normal type steel lines. The overwrap would be incompatible with liquid or gaseous fluorine and must use liner protection to prevent reactions.

The amount of corrosion allowable in tube thickness is considered to be a specific vehicle design problem. No provisions were made for corrosion allowance during design or fabrication for this contract.

Leakage. - The maximum allowable helium leakage, with the tube pressurize to working pressure was 1×10^{-6} scc/sec. Joint leakage was monitored only for increases during the testing to determine if the glass-fiber tube exerted unusual pressures on the joint in sufficient quantity to cause a leak.

TABLE 11. - BUCKLING STRESS ALLOWABLES, INCONEL 718 (AXIAL)

Liner material	Temp (^{o}F)	Length (in.)	Radius r (in.)	Modulus of Elasticity E (psi)	Thickness t_{ℓ} (in.)	Allowable Stress $\sigma_{c}= 0.3\ E\ \dfrac{t_{\ell}}{r}$ [*] (psi)
Inconel 718	+75	12	0.25	29 x 10^6	0.007	243,600 [†]
	-423		0.25	32 x 10^6	0.007	268,800 [†]
	+75		1.0	29 x 10^6	0.006	52,200
	-423		1.0	32 x 10^6	0.006	57,600
	+75		1.0	29 x 10^6	0.003	26,100
	-423		1.0	32 x 10^6	0.003	28,800
	+75		2.5	29 x 10^6	0.006	20,880
	-423		2.5	32 x 10^6	0.006	23,040
	+75		2.5	29 x 10^6	0.003	8,630
Inconel 718	-423	12	2.5	32 x 10^6	0.003	9,524

[*] Roark, R. J.: _Formulas for Stress and Strain._ 4th edition, McGraw-Hill, 1954, page 273.

[†] σ_{c} exceeds allowable yield stress, therefore failure mode will be other than by buckling.
$\sigma_{c} = 0.3\ E\ \dfrac{t_{\ell}}{r}$ = Buckling stress equation in general agreement with empirical data but about 1/2 of theoretical value.

TABLE 12. - BUCKLING STRESS ALLOWABLES, INCONEL 718 (AXIAL)

Liner material	Temp (^{o}K)	Length ℓ (cm)	Radius r (cm)	Modulus of Elasticity E (N/cm^2)	Thickness t_{ℓ} (cm)	Allowable Stress σ_{c} (N/cm^2)
Inconel 718	297	30.48	0.635	19.99 x 10^6	0.0178	167,900 [*]
	20		0.635	22.06 x 10^6	0.0178	185,300 [*]
	297		2.54	19.99 x 10^6	0.0152	35,990
	20		2.54	22.06 x 10^6	0.0152	39,700
	297		2.54	19.99 x 10^6	0.0076	18,000
	20		2.54	22.06 x 10^6	0.0076	19,860
	297		6.35	19.99 x 10^6	0.0152	14,390
	20		6.35	22.06 x 10^6	0.0152	15,880
	297		6.35	19.99 x 10^6	0.0076	5,950
Inconel 718	20	30.48	6.35	22.06 x 10^6	0.0076	6,570

[*] σ_{c} exceeds allowable yield stress, therefore failure mode will be other than by buckling.

TABLE 13. - BUCKLING STRESS ALLOWABLES (HOOP)

Liner material	Temp (°F)	Liner thickness (in.)	Liner diameter D (in.)	σ_b Allowable (psi)
Inconel 718 or CRES	+75°	0.002	0.5	2.78×10^5 [*]
		0.004	0.5	2.23×10^6 [*]
		0.006	0.5	7.50×10^6 [*]
		0.008	0.5	1.78×10^7 [*]
		0.010	0.5	3.48×10^7 [*]
		0.002	2.0	4.25×10^3
		0.004	2.0	3.48×10^4
		0.006	2.0	1.17×10^5 [*]
		0.008	2.0	2.78×10^5 [*]
		0.010	2.0	5.40×10^5 [*]
		0.002	5.0	2.78×10^2
		0.004	5.0	2.23×10^3
		0.006	5.0	7.50×10^3
		0.008	5.0	1.78×10^4
Inconel 718 or CRES	+75°	0.010	5.0	3.48×10^4

σ_b allowable $= 150,000 \left(\dfrac{t}{D}\right)^3 E;$ (Ref. 6).

$E = 29 \times 10^6$ psi for Inconel 718 and CRES materials (assumed) cryogenic allowables would be approximately 10% higher.

[*] Allowable σ_b exceeds the allowable yield strength therefore, failure mode will be other than by buckling.

TABLE 14.- BUCKLING STRESS ALLOWABLES (HOOP)

Liner material	Temp (^{o}K)	Liner thickness (cm)	Liner diameter D (cm)	σ_b Allowable N/cm^2
Inconel 718 or CRES	297	0.0051	1.27	1.92×10^{5}*
		0.0102	1.27	1.54×10^{6}*
		0.0152	1.27	5.17×10^{6}*
		0.0203	1.27	1.23×10^{7}*
		0.0254	1.27	2.40×10^{7}*
		0.0051	5.08	2.93×10^{3}
		0.0102	5.08	2.40×10^{4}
		0.0152	5.08	8.07×10^{4}*
		0.0203	5.08	1.92×10^{5}*
		0.0254	5.08	3.72×10^{5}*
		0.0051	12.7	1.92×10^{2}
		0.0102	12.7	1.54×10^{3}
		0.0152	12.7	5.17×10^{3}
		0.0203	12.7	1.23×10^{4}
Inconel 718 or CRES	297	0.0254	12.7	2.40×10^{4}

$E = 20 \times 10^{6}$ N/cm^2 for Inconel 718 and CRES materials (assumed) cryogenic allowables would be approximately 10% higher.

* Allowable σ_b exceeds the allowable yield strength, therefore, failure mode will be other than by buckling.

55

TABLE 15. – TORQUE ALLOWABLES, INCONEL 718

Material	Temp (°F)	Mod. elast. E (psi)	Length ℓ (in.)	Radius r (in.)	Thickness t (in.)	$\frac{\ell}{r}$	Allowable shear stress-torsion σ_{st} (psi)	Allowable torque T (in.-lb)
Inconel 718	+75	29 x 10⁶	12	0.25	0.007	48	23,015	63.2
	+75			1.0	0.003	12	2,530	43.0
	+75			1.0	0.006	12	13,941	525.3
	+75			2.5	0.003	4.8	2,049	241.0
	+75	29 x 10⁶		2.5	0.006	4.8	5,250	1236.0
	-423	32 x 10⁶		0.25	0.007	48	25,407	70.0
	-423			1.0	0.003	12	2,795	47.4
	-423			1.0	0.006	12	15,384	580.0
	-423			2.5	0.003	4.8	2,261	266.2
Inconel 718	-423	32 x 10⁶	12	2.5	0.006	4.8	5,793	1364.0

$$\sigma_{st} = E \left(\frac{t}{\ell}\right)^2 \left[3.0 + \sqrt{3.4 + 0.240 \left(\frac{\ell}{tr}\right)^3}\right] \quad \text{for } \frac{\ell}{r} < 7.9 \sqrt[4]{1-\nu^2}\sqrt{\frac{r}{t}}$$

where $\frac{\ell}{r} < 7.9 \sqrt[4]{1-\nu^2}\sqrt{\frac{r}{t}}$ and $\sigma_{st} = KE \left(\frac{t}{r}\right)^{1.35}$ for 5-in. diameter liner and K = 0.62 for

$\frac{\ell}{r} = 4.8$. Values of σ_{st} are for liner only and do not consider any effects of overwrap.

Reference: Roark, R. J.: Formulas for Stress and Strain, 4th edition, McGraw-Hill, 1954 page 353

TABLE 16. - TORQUE ALLOWABLES, INCONEL 718

Material	Temp (°K)	Mod. elast. E (N/cm²)	Length (cm)	Radius r (cm)	Thickness t (cm)	$\frac{\ell}{r}$	Allowable shear stress-torsion σ_{st} (N/cm²)	Allowable torque T (N-m)
Inconel 718	297	20 x 10⁶	30.48	0.635	0.018	48	15,868	7.14
	297			2.54	0.008	12	1,744	4.86
	297			2.54	0.015	12	9,612	59.35
	297	20 x 10⁶		6.35	0.008	4.8	1,413	27.23
	297	22.1 x 10⁶		6.35	0.015	4.8	3,620	139.6
	20			0.635	0.018	48	17,517	7.91
	20			2.54	0.008	12	1,927	5.36
	20			2.54	0.015	12	10,607	65.53
	20			6.35	0.008	4.8	1,559	30.1
Inconel 718	20	22.1 x 10⁶	30.48	6.35	0.015	4.8	3,994	154.1

Fabrication Analysis

This section reports the results of an investigation of
various techniques in fabricating the metal liner used in glass-
fiber tubing. The glass-fiber tubing concept is based on a metal
liner overwrapped with a glass-fiber matrix. This concept calls
for the liner to be as thin as is practical for thermal properties
and still retain the necessary structural integrity. Preliminary
design analysis indicated that metal liner wall thicknesses in the
0.0015 in. (0.0038 cm) to 0.015-in. (0.038 cm) range should be
evaluated.

This information was gathered from engineers and industrial
organizations with extensive experience in the welding of thin
gage materials. The technical information sources included
Martin Marietta's Advanced Materials Technology Laboratory, Battelle
Memorial Institute, and various bellows manufacturers. Liner fab-
rication in four areas was evaluated:

1) Material;

2) Tube fabrication and seam welding;

3) Metal hardening processes; and,

4) End fitting attachment concepts.

Recommendations based on the most favorable characteristics
in each of the categories are included.

Materials. - The metals selected for liner material are all
weldable and compatible with the proposed fluids in the contract.

321 CRES: This stainless steel has excellent welding properties
and is commonly welded by bellows manufacturers in both fusion and
resistance welds in thicknesses of 0.002 in. (0.0051 cm) without
helium leakage. The yield strength and ultimate tensile strength
are superior to most 300 series stainless steels in both ambient
and cryogenic conditions. This material is readily available in
the desired sizes from commercial sources. The cost of this
stainless is the most favorable of the liner materials considered.

The only drawback with 321 CRES, as with all 300 series
stainless steels, is that after fusion welding a relatively large
heat affected zone exists in the weld area, and the structural
properties must be reduced accordingly.

347 CRES: This stainless steel is highly recommended by
bellows manufacturers because of its excellent welding and form-
ing characteristics. The yield strength and tensile strength are
equal to 321 at ambient, but at cryogenic temperatures, it is
about 30% less in yield strength. However, this steel is superior

to all other 300 series stainless steels in strength after welding. This material is also readily available, and its cost is slightly higher than 321.

21-6-9 Armco stainless steel: This stainless steel was specifically developed by the Armco Steel Company to be competitive with the 300 series stainless steels. The composition is similar to that of 347. The steel has excellent welding characteristics, and its strength after welding is superior to 347. This steel was enthusiastically recommended by all engineers contacted. Strength at ambient conditions is 50% more than that of 321, and the yield strength is more than twice that of 321 at cryogenic temperatures; but the ultimate tensile strength of the material is only slightly higher than 321. The material is readily available at a price competitive with 347 CRES.

The main drawbacks with this material is the reduction in strength due to welding and the inability to strengthen the weakened areas with heat treatment.

Inconel 718: This nickel-base alloy is widely used throughout industry in thin-sheet applications. The metal is easily welded in sheets as thin as 0.005 in. (0.013 cm). Fusion welding is not recommended, by some manufacturers, in thicknesses less than 0.005 in. (0.013 cm) because definite leakage characteristics are noted. This metal has superior strength characteristics when compared with any of the stainless steels, generally varying between two and three times the strength of stainless steel.

Because of a high demand for nickel, this metal is not as readily available as the stainless steels. The cost of Inconel 718 is three times greater than stainless steel.

Since little data existed on strength reduction due to welding very thin members, a series of preliminary tensile tests were performed to determine weld strength characteristics. The tensile tests were performed using very thin sheet Inconel 718, 301 CRES and 21-6-9 Armco stainless steel using several welding techniques. The results of these tests are presented in the discussion in the materials tensile tests section of this report.

Tube fabrication and seam welding. - The welding or joining processes that were evaluated included fusion welding, resistance welding and seamless tubes. After welding, some heat-treat or hardening process may be necessary, and these processes were briefly evaluated. After fabrication of the thin liner, it was joined to an end fitting in one of three general methods -- resistance welding, fusion welding, or solid-state bonding. Each of these processes are discussed in this section; but again, not necessarily in order of preference.

Straight seam fusion weld: The most common practice in fabricating thin wall tubes larger than 1-in. (2.54 cm) diameter is to roll a tube to the desired diameter, prepare the butting edges as shown in fig. 21 and fusion weld a seam the length of the tube. Because of highly developed welding techniques, this weld can consistently be made leak free. Also, by plenishing and polishing the weld, the weld area will conform to overall pipe size (no weld buildup inside or outside the tube). This welding process can be used consistently with metal as thin as 0.002 in. (0.0051 cm). The main drawback to this technique is the relatively large heat affected zone in the weld area.

Helically wrapped tubes: This technique for forming tubes requires wrapping a 2 to 3 in. (5.08 to 7.62 cm) strip of metal around a mandrel in the form of a helix and fusion welding the edges. This is shown in fig. 22 where the butting edges are prepared as shown in fig. 21. This method of fabricating tubes has desirable structural properties from hoop stress and forming aspects. This weld can also be plenished and polished. The two undesirable characteristics of this type of fabrication are the very long weld seam that is a potential leak source, and the very large heat affected zone due to the length of weld.

Straight seam resistance welding: This technique for tube fabrication requires the tube to be roll formed to the desired diameter with a slight overlap at the mating surface as shown in fig. 23. An anode is placed in the tube, and a resistance weld is run down the length of the tube. The excess overlap on both the inside and outside of the tube can then be peeled away from the weld. This weld can be made leak free consistently. Also, this type of weld has a minimal heat affected zone and, in most cases, it can probably be ignored from a structural standpoint. This type of weld has two distinct disadvantages-- the inner seam is a possible trap for contaminants, and the overlap area is a potential leak path when attached to an end fitting.

Longitudinal bellows: This concept can be used with either the fusion or resistance welded tube. The tube is made by resistance or seam welding as described earlier. Then, by using existing forming methods, very low amplitude bellows are made along the longitudinal axis as shown in fig. 24. This type of tube would only be of value in cases where the thermal expansion or yield strength of a conventional tube would make its use impractical without the longitudinal bellows.

Seamless drawn tube: Tubes as large as 0.75 in. (1.90 cm) in diameter can be drawn by conventional methods down to wall thicknesses of 0.004 in. (0.010 cm). These tubes have all the obvious advantages of being seamless and, by their nature of manufacture, they are in a hardened condition.

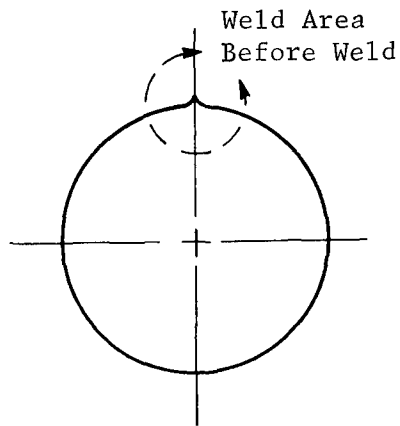Fig. 21.- Preparation of Butting
Edges for Fusion Welding

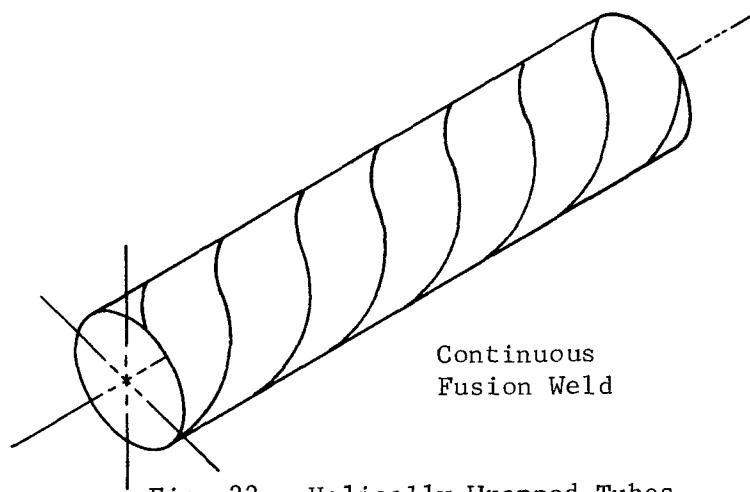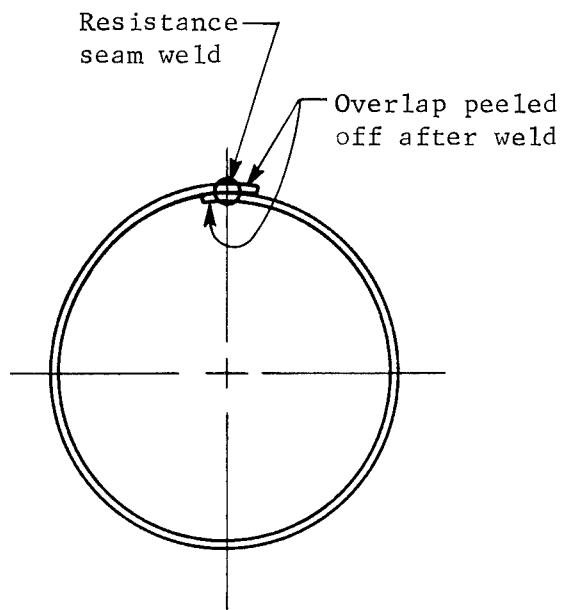
Fig. 22.- Helically Wrapped Tubes

Resistance
seam weld

Overlap peeled
off after weld

Fig. 23.- Resistance Seam Welding
with Overlap

Longitudinal bellows
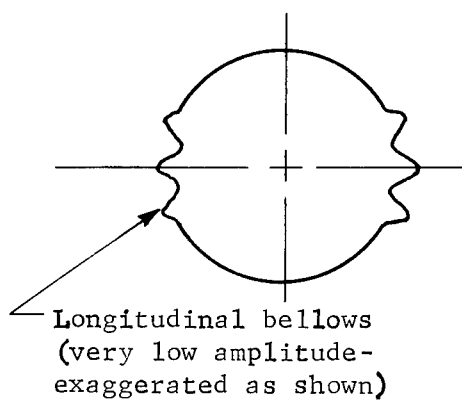(very low amplitude-
exaggerated as shown)

Fig. 24. - Seam Welded, Low
Amplitude Bellows

Heat treating and hardening processes: In all of the afore-
mentioned cases the parent metal would be in some state of hard-
ness due to the rolling mill process used to produce its thick-
ness. After welding, with the exception of resistance welding,
large areas of the tube are annealed (heat affected zone). This
annealed portion of the tube has a very different structural
character than the parent metal; and, therefore, the tube will
not react as a homogenous member under hoop stress, and the combined
hoop stress characteristics are either undesirable or unpredictable.
Under this condition the prime alternative is to anneal the entire
tube. Now the tube acts as a homogenous member but its strength
is greatly reduced. The only method that can be used to harden
stainless steel is to cold work the metal. Thus the tube can be
redrawn over a mandrel as with conventional seamless tubing. This
will reduce the wall thickness and work harden the entire tube.

This redrawing process can also be used for Inconel 718 to
obtain a tube with a wall thickness of less than 0.005 in. (0.013 cm)
without leakage problems. Inconel 718 can be heat treated and
age hardened after welding. An Inconel 718 tube, fabricated from
mill hardened metal and resistance welded, would not normally
require additional heat-treat or aging because the resistance
welding would not greatly reduce its structural capabilities.

End fitting attachment concepts.- The weld method used for
attaching the end fitting to the metal liner can be either a
resistance weld, a fusion weld, or a solid-state bond. In general,
whether the weld be resistance or fusion, it is desirable that
neither portion of the weld joint should be more than three times
the thickness of the thin member. Or, more simply stated, if the
liner wall thickness is 0.002 in. (0.005 cm) the attaching portion
of the end fitting should not exceed 0.006 in. (0.015 cm).

The concept shown in fig. 25, for connecting the liner to
the end fitting, could be applied to flange-type end fittings.
This method of attachment can be cleaned easily and would eliminate
any contaminant trap areas from the assembly.

The concept shown in fig. 26 would be of particular interest
when dissimilar metals are used for liner and end fitting.
This situation would exist when the liner is made from Inconel 718
and the end fitting is a 300 series stainless steel. This concept
would also be very useful where heat-treat and aging after welding
is undesirable, because this method of welding does not create a
significant loss of material strength. The only drawback with this
concept is that a potential cleaning problem and contaminant trap
could exist at the liner end of the fitting. The external band can
carry hoop stresses in the area of weld strength reduction and pre-
vent excessive strain in this weak area.

Machine groove within
3X in. of Flange Edge

Fusion Weld

X in. Thick
Liner
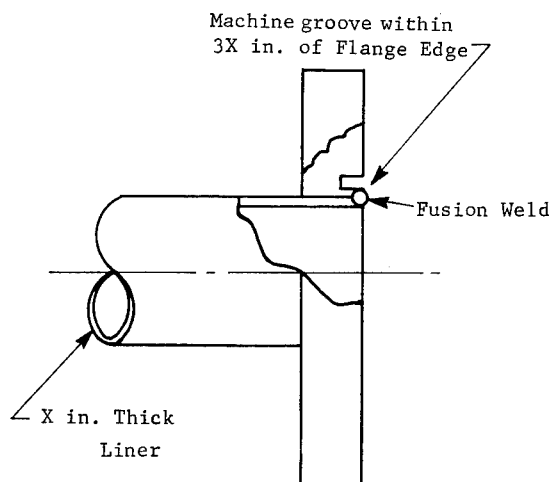
Fig. 25.- Connecting Liner and End
Fitting Using Fusion Weld

2-3X in. Thick Band
Resistance Weld

X in. Thick
Liner

2-3X in. Thick
Flange End

Band Material
(Same as Fitting)
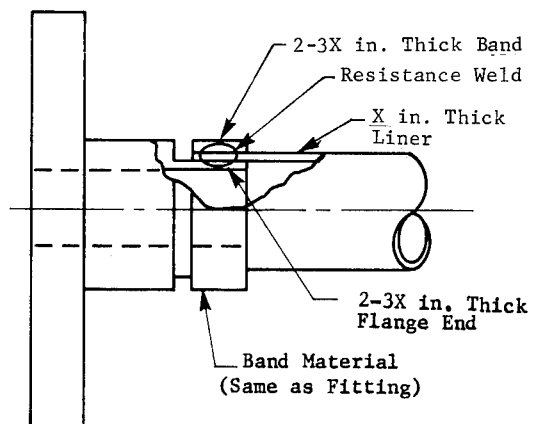
Fig. 26.- Resistance Welding Liner to
End Fitting with Strengthening Band

Fusion Weld
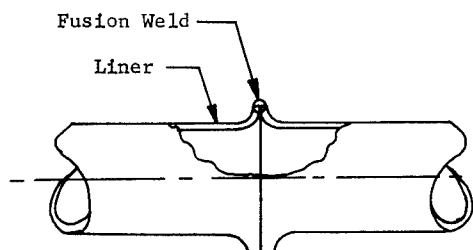
Liner

Fig. 27.- Method of Attaching Two Liners

Resistance Weld

Should Not Exceed
3X in. Liner Thickness
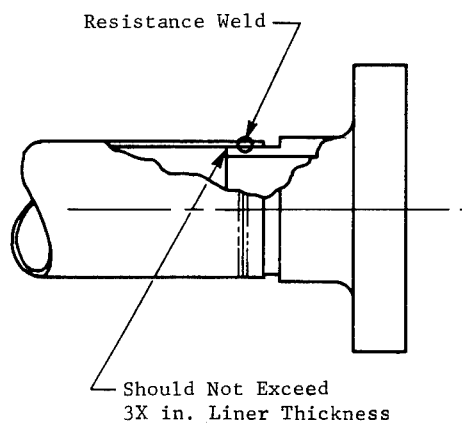
Fig. 28.- Attaching Fitting to Liner Using
Resistance Weld

The concept shown in fig. 27 would be applicable when a liner of this configuration is connected to another liner of similar configuration. This method is used frequently by bellows manufacturers when attaching bellows to end fittings. A disadvantage associated with this method is that it creates potential cleaning problems.

The most straightforward approach to attaching either flange- or threaded-type fittings to the liner is shown in fig. 28. This approach calls for resistance welding the liner to a thin portion of the end fitting. This concept has two shortcomings; first, machining the thin portion of the end fitting will be difficult to keep concentric and, second, to obtain the precise outside diameter required for mating the liner without a gap that would burn through during resistance welding. This method will also present cleaning problems in the flange liner overlap area.

The concept shown in fig. 29 would be applicable when an end fitting, either flange or threaded type, is desired to be connected to the liner. The liner can be inserted into the fitting and bonded using a solid-state technique using a shaped explosive charge. The advantage of this concept is in the strength developed in the joint that exceeds the base metal strength. Two disadvantages associated with this method are that it is new and not completely developed and creates potential cleaning problems.
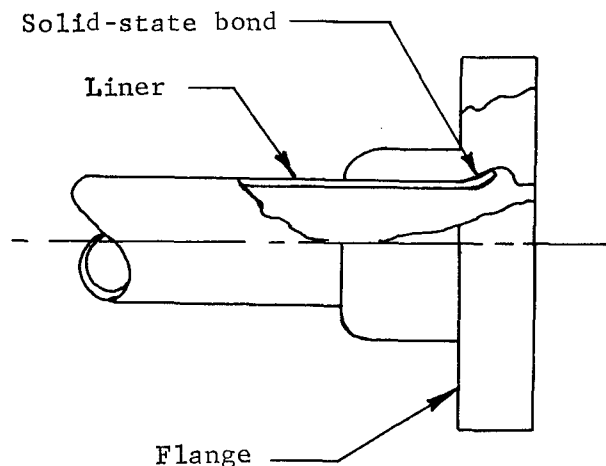
Fig. 29.- Attaching Fitting to Liner Using
Solid-State Bond

Conclusion and recommendations. - The conclusions and recommendations will be covered in three sections. Each section will cover a specific tube size and the fabrication techniques that most favorably lend themselves to these sizes.

0.5-in. (1.27 cm) diameter tube: small diameter tubes (i.e., less than 1 in. or 2.54 cm) are difficult to fabricate using a seam welding technique. However, seamless tubing with diameters as large as 0.75 in. (1.90 cm) and wall thickness as small as 0.004 in. (0.010 cm) are available commercially. This seamless tubing can be drawn using any of the materials discussed in the material section. If a liner thickness less than 0.004 in. (0.010 cm) is required, this tubing could be redrawn (by a specialty company) down to wall thicknesses of 0.0015 in. (0.0038 cm).

The end fitting attaching methods shown in fig. 26 and 28 can be used equally well with flanged, threaded, or weldable end fittings. The method in fig. 26 can be used if the liner is Inconel 718 and the end fitting is stainless steel. The method described in fig. 25 is the most desirable for flanged end fittings.

In conclusion, because the liner is seamless and, therefore, does not present fabrication problems, the final tube design was dictated by strength requirements and end fitting type.

2-in. (5.08 cm) diameter tube: This liner can be fabricated by either straight seam resistance or fusion welding, by solid-state bonding, or by the method described in fig. 22 (helical welding). The helically welded strips have the greatest advantage from a structural standpoint and the poorest from a cost and leakage standpoint. The solid-state bond concept would also be structurally superior. The straight seam fusion weld would have the best leakage characteristics and definitely would have a cost advantage. Both of the fusion welded concepts could be redrawn to attain thinner walls and for cold working purposes.

All of the end fitting attaching concepts apply to this size tubing because threaded and flanged type end fittings are common in this size.

The ultimate tube, from a strength standpoint, is a helically welded Inconel 718 tube redrawn to the desired wall thickness with flanged or butt-welded end fittings, and the whole assembly heat treated and age hardened. This combination is very expensive. At the other end of the cost spectrum, but still retaining structural integrity, is a 21-6-9 tube straight resistance seam welded attached to an end fitting as shown in fig. 25 or fig. 28.

5-in. (12.7 cm) diameter tube: This liner can be fabricated using straight seam resistance welding, fusion welding, or solid-state bonding. All of the materials discussed in the materials section can be used. If stainless steel is fusion welded, the liner should be annealed after welding; and if structural requirements

warrant, the tube could be redrawn. If Inconel 718 is fusion welded, the assembly should be heat treated and age hardened after all welding is complete. If an Inconel 718 liner is used, and the end fitting is stainless, the attachment should be made as shown in fig. 26. All the other attaching concepts shown can be used when the end fitting and liner are similar metals.

End fitting evaluation. - A series of screwed, flanged, and welded end fittings were identified for potential application to cryogenic tubing during this phase of the program. These joints are shown in fig. 30. Before making the final joint selection, preliminary testing was conducted to determine leakage characteristics of the joints when subjected to pressure and temperature cycling. Retorque requirements, both level and frequency, were determined in this test program. Results of the preliminary testing are discussed on page 115. The final joint selections, shown in fig. 31 were based on the following factors:

1) Suitability for cryogenic service;

2) Compatibility with hydrogen, oxygen, methane, FLOX, and fluorine in the gaseous or liquid states;

3) Leakage characteristics at cryogenic temperature;

4) Method of attaching the liner and glass wrap to the joint;

5) The reliability of the joint to provide minimum leakage during pressure and temperature cycling;

6) The total weight of the joint; and

7) The total cost of the joint.

Overwrap fabrication. - The design analysis of the fiberglass overwrap for the tubing in this study indicates that it should have sufficient strength, stiffness and wall thickness to carry a share of the internal pressure loads during operation (mainly hoop loads), resist external handling loads, and at the same time exhibit the lowest possible thermal conductivity in the axial direction. With these criteria in mind, the following recommendations are presented.

Reinforcement: Two commercially available types of glass roving were originally considered; S/HTS glass, and hollow glass. Tests on glass epoxy cylindrical specimens indicated significantly lower axial thermal conductivity in specimens with no axially oriented glass filaments. It was also found that the hollow glass filaments did not offer a significant reduction in thermal conductivity (see results of Thermal Conductivity Test - Hollow Glass Fibers on page 114).
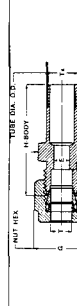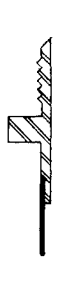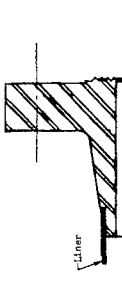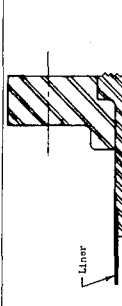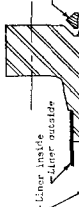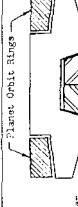
Fig. 30. – Glass-Fiber Tubing for Cryogenic Fluids Joint Evaluation Data Sheet

Manufacturer	Size Available (in.) 0.5	2	5	Type	Gasket Type & Material	Number & Size of Bolts 0.5	2	5	Assembly Torque Req'ts 0.5	2	5	Complete Joint Weight (lb) 0.5	2	5	Complete Joint Cost 0.5	2	5	Liner Attachment	Configuration	Remarks
"B" Nut Conoseal, Aeroquip Corporation, Marman Division, 11224 Exposition Blvd. Los Angeles, Calif. 90064	X			Threaded	Conoseal Steel, Al	N/A	N/A	N/A	400-600 in.-lb			0.15	N/A	N/A	231.00	N/A	N/A	Machine O.D. of Female Butt Weld Flange to Match I.D. of liner. Resistance Weld liner to Flange.		Martin Marietta Corporation has used this joint successfully in high pressure GH2 and He systems, at normal ambient temperature. Operating temperature range specified by mfg. is -450°F to 1500°F. Helium leakage rates of 1 x 10^-8 scc/sec normal with standard gasket & 1 x 10^-10 with special gasket.
Swagelok, Crawford Fitting Co., 29500 Solon Road, Solon, Ohio 44139	X			Threaded	None	N/A	N/A	N/A	Finger Tight + 1¼ Turns			0.20	N/A	N/A	6.10	N/A	N/A	Machine Butt Weld End of Swagelok Male Connector to Match I.D. of Liner. Resistance Weld Liner to Connector.		Martin Marietta Corporation has used this joint in high pressure Helium systems and found it to be "bubble tight" at 7,000 psig and ambient temperature.
MC Flared	X			Threaded	None	N/A	N/A	N/A	475 in.-lb	3500 in.-lb	N/A	0.20	4.5	N/A	6.00	57.00	N/A	Machine One End of Union to Match I.D. of Liner. Resistance Weld Liner to Union.		This joint is used extensively throughout industry for all types of fluid service.
Cajon VCR, Cajon Company, 32550 Old S. Mill Road, Solon, Ohio 44139	X			Threaded	Flat Nickel, Al, OFHC Copper	N/A	N/A	N/A	Finger Tight + ¼ - ½ Turn			0.20	N/A	N/A	21.35	N/A	N/A	Machine Gland on Body End of Coupling to Match I.D. of Liner. Resistance Weld Liner to Gland.		This joint was developed for ultra-high vacuum systems. A sample of this coupling was leak tested by Martin Marietta Corporation with a Helium mass spectrometer with no detectable leakage at 4000 psig.
ASA Raised Face NASA Configuration	X	X	X	Bolted	Flat Copper, Al	8, 1/2 in.	8, 5/8 in.	8, 3/4 in.	580 in.-lb	1100 in.-lb	2100 in.-lb	16	12	38	11.42	32.40	152.56	Machine Weld Neck to Match I.D. of Liner. Resistance Weld Liner to Flange.		Standard Flange with various gaskets is used throughout industry for all types of fluid service. Modified to NASA configuration by machining concentric grooves on sealing surface. A "dead soft" aluminum gasket is used with this configuration.
ASA Lap Joint NASA Configuration	X	X	X	Bolted	Flat Copper, Al	8, 1/2 in.	8, 5/8 in.	8, 3/4 in.	580 in.-lb	1100 in.-lb	2100 in.-lb	16	12	38	9.92	27.06	119.06	Machine Stub Weld End to Match I.D. of Liner. Resistance Weld liner to Stub End.		Same as above
Ring Joint	X	X	X	Bolted	Ring Copper, Al, Steel	8, 1/2 in.	8, 5/8 in.	8, 3/4 in.	580 in.-lb	1100 in.-lb	2100 in.-lb	16	12	38	25.80	54.90	244.00	Machine Weld Neck to Match I.D. of Liner. Resistance Weld liner to Flange.		This joint is used extensively in Martin Marietta Corporation facility high pressure gas and cryogenic liquid systems. The joint has been found to remain "bubble tight" over long periods of service with many cycles from ambient to cryogenic temperatures.

68

Manufacturer	Size Available (in.) 0.5	2	5	Type	Gasket Type & Material	Number & Size of Bolts 0.5	2	5	Assembly[1] Torque Req's 0.5	2	5	Complete Joint[2] Weight (lb) 0.5	2	5	Complete Joint[3] Cost 0.5	2	5	Liner Attachment	Remarks
APCO Flange Accessory Products Co. 12484 East Whittier Blvd Whittier, California 90602	X	X		Bolted	Delta Ring, Steel, Az	4, 5/16 in.	5, 7/16 in.	N/A	275 in.-lb	650 in.-lb	N/A	1.5	5.5	N/A	74.71	94.42	N/A	Machine Weld Neck or ANPT Flange to Match I.D. of Liner. Resistance Weld Liner to Flange, or Extend Liner Through Flange and Fusion Weld Liner to Flange.	Lightweight flange designed to meet the requirements of A.S.M.E. Boiler Code Section VIII. Suitable for cryogenic piping when steel delta ring seal is used.
Granville-Phillips Co. Granville-Phillips Co. 5675 East Arapahoe Ave. Boulder, Colo. 80301	X	X	X	Bolted	Flat OFHC Copper	6, 1/4 in.	8, 5/16 in.	20, 5/16 in.	90 in.-lb	160 in.-lb	140 in.-lb	3	3	6	46.90	130.30	271.40	Machine I.D. of Flange to Match O.D. of Liner. Extend Liner Through Flange and Fusion Weld Liner to Flange.	Joint cost includes bolt set for matched thermal expansion characteristics.
"V" Band Conoseal Aeroquip Corp. – Marman Division 11214 Exposition Blvd. Los Angeles, Calif. 90064	X	X	X	Clamp & Bolt	Conoseal Steel, Az	N/A	1, 1/4 in.	1, 5/16 in.	N/A	70 in.-lb	130 in.-lb	N/A	0.5	2.5	N/A	260.00	575.r0	Machine O.D. of Flange Neck to Match I.D. of Liner. Resistance Weld Liner to Flange.	This joint is used extensively by Martin Marietta Corporation in missile propellant and gas systems.
Graylok Gray Tool Co. P. B. Box 2291 Houston, Texas 77001	X	X	X	Clamp & Bolt	Ring Steel Az Copper	2, 3/8 in.	4, 3/4 in.	4, 1 in.	200 in.-lb	1600 in.-lb	4000 in.-lb	3.5	21	82	58.00	102.00	612.00	Machine O.D. of Butt Weld Hub to Match I.D. of Liner. Resistance Weld Liner to Hub.	Joint cost includes bolt set. This joint is in common use in cryogenic applications and has served very well where rapid cool-down and other conditions are detrimental to sealing efficiency. Helium leakage rates less than 1×10^{-6} scc/sec are considered normal for standard grayloc externals.
ASTRO-GRIP Magnetech – DSD Company Bradley Park East Granby, Conn. 06026	X	X		Clamp & Retainer Ring	Servo-Flex Steel	N/A	N/A	N/A	Planet Orbit Rings Tapped Over the Bracelet Retainer			N/A	4.05	10.6	N/A	135.00	385.00	Machine O.D. of Flange Neck to Match I.D. of Liner. Resistance Weld Liner to Flange.	The seal-groove configuration of this joint is arranged such that if an extreme pressure or temperature surge should occur, so as to cause structural yield of the seal and coupling the deflected seal will adopt a yielded position so as to maintain sealing integrity.
Glass Backed Adapter Martin Marietta Corp. Box 179 Denver, Colorado	X	X		Bolted		TO BE DETERMINED BY MATING FLANGE												Fusion Weld Liner to Adapter Plate	

[1] Torque values are recommended by vendor or taken from Martin Marietta Corporation standards.

[2] Complete joint weight includes mating flange, seal or gasket, and clamp or bolts.

[3] Joint cost includes mating flange, seal or gasket, and clamp. Cost of bolts, nuts, and washers is not included except as noted in Remarks.

Fig. 30. – Glass-Fiber Tubing for Cryogenic Fluids Joint Evaluation Data Sheet (concluded)
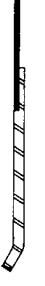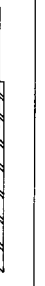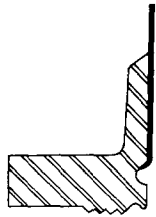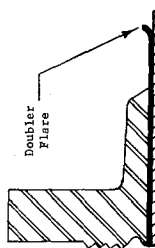
69

Fig. 31.— Test Specimen Identification and Configuration

SPECIMEN IDENTIFICATION NUMBER	SIZE (in.)	LINER						END FITTING			GLASS		
		SERIAL NUMBER	MATERIAL	THICKNESS (in.)	SEAM WELD METHOD	FABRICATION METHOD	HEAT TREAT	TYPE	MATERIAL		THICKNESS (in.)	CONFIGURATION H-HOOP LAYER L-LONGITUDINAL LAYER	END BOND TO LINER
CFL6300605, 1/2", Flared Tube	1/2	1-12	Inconel 718	0.007	Seamless	Drawn	Heat Treat and Age Hardened	AN Flared	Stainless Steel		0.030	H, L, H	Torsion Only
CFL6300606, 1/2", Butt Weld	1/2	13-24	Inconel 718	0.007	Seamless	Drawn	Heat Treat and Age Hardened	Butt Weld	Inconel 718		0.030	H, L, H	Torsion Only
CFL6300607, 1/2", Flat Flanged	1/2	25-36	Inconel 718	0.007	Seamless	Drawn	Heat Treat and Age Hardened As an Assembly	Machined 3/4" APCO Flange	Inconel 718		0.030	H, L, H	Torsion Only
CFL6300608, 1/2", CRES Flared	1/2	37-48	Stainless Steel	0.009	Seamless	Drawn	Hardened	AN Flared	Stainless Steel		0.030	H, L, H	Axial & Torsion
CFL6300609, 2", Butt Weld	2	49-60	Inconel 718	0.003	Helical Fusion Weld	Redrawn from 0.005	Cold Worked	Butt Weld	Inconel 718		0.030	H, L, H	Torsion Only
CFL6300610, 2", Butt Weld	2	61-72	Inconel 718	0.003	Straight Resistance Weld	Not Redrawn	Heat Treat and Age Hardened	Butt Weld	Stainless Steel	Optional	0.030	H, L, H	Torsion Only
CFL6300611, 2", Flat Flanged	2	73-84	Inconel 718	0.003	Helical Fusion Weld	Redrawn from 0.005	Cold Worked	2 1/2" APCO Flange	Inconel 718		0.030	H, L, H	Torsion Only
CFL6300612, 2", NASA Flange (1)	2	85	Inconel 718	0.006	Straight Fusion Weld	Not Redrawn	Annealed	Raised Face NASA Configuration	Stainless Steel		0.030	H, L, H	Axial & Torsion

SPECIMEN IDENTIFICATION NUMBER	SIZE (in.)	LINER						END FITTING				GLASS	
		SERIAL NUMBER	MATERIAL	THICKNESS (in.)	SEAM WELD METHOD	FABRICATION METHOD	HEAT TREAT	TYPE	MATERIAL		THICKNESS (in.)	CONFIGURATION H-HOOP LAYER L-LONGITUDINAL LAYER	END BOND TO LINER
CFL6300612, 2", NASA FLANGE (2)	2	86-96	Inconel 718	0.006	Straight Fusion Weld	Not Re-drawn	Annealed	Raised Face NASA Configuration	Stainless Steel		0.030	H, L, H	Axial & Torsion
CFL6300613, 5", BUTT WELD	5	97-108	Inconel 718	0.003	Straight Resistance Weld	Not Re-drawn	Heat Treat and Age Hardened	Butt Weld	Inconel 718		0.040	H, L, H, H	Torsion Only
CFL6300614, 5", BUTT WELD	5	109-120	Inconel 718	0.003	Straight Fusion Weld	Not Re-drawn	Heat Treat and Age Hardened	Butt Weld	Inconel 718		0.040	H, L, H, H	Torsion Only
CFL6300615, 5", NASA FLANGE	5	121-132	Inconel 718	0.006	Straight Fusion Weld	Not Re-drawn	Annealed	Raised Face NASA Configuration	Stainless Steel		0.040	H, L, H, H	Torsion Only
CFL6300616, 5", STRAP FLANGE (3)	5	133, 134	Inconel 718	0.006	Straight Fusion Weld	Not Re-drawn	Annealed	Conoseal	Stainless Steel		0.040	H, L, H, H	Axial & Torsion

(1) This specimen was redesigned due to an insufficient liner to end fitting weld.

(2) Redesigned specimen to replace the original CFL6300612. This design utilized a solid state (explosive) bonding process to join the liner to the end fitting.

(3) This specimen was cancelled due to an insufficient liner to end fitting weld.

Fig. 31.- Test Specimen Identification and Configuration (concluded)

To produce an overwrap with maximum strength and stiffness, and minimum wall thickness and conductivity, it is recommended that 20 end S/HTS glass roving be used, and that the wrap orientation be mostly circumferential. A small amount of longitudinal glass reinforcement will add to the overall strength and resistance to vibration without adding a severe thermal penalty. Additionally, the longitudinal glass will bring the thermal expansion and contraction of the matrix system to a value near that of the liner, forcing the failure mode of the tube into the liner to fitting joint.

Resin matrix: Several resin systems were considered for the matrix for the glass wrap (NASA LeRC cryo resin no. 2, 58-68R, EPON 828/mPDA, ERLA5617/mPDA, and Adiprene L-100). Generally, the most severe loads are imposed on the resin matrix from handling at room temperature. Therefore, good mechanical properties at room temperature are desired and the resin must also perform reasonably well at cryogenic temperatures. In addition, fabrication with pre-impregnated material (prepreg) rather than wet winding is desirable because closer process control (i.e., resin content, prefabrication quality control) can be attained. The preimpregnation also allows unidirectional layers of axially oriented roving to be easily incorporated into the wrap. Resins from which prepregs are made must have a reasonable shelf life in this catalyzed state (preferably in excess of 2 weeks).

Both the NASA cryo resin no. 2 and Adiprene L-100 are promising for cryogenic service, but their low moduli provide poor protection from rough handling at room temperature. The EPON 828/mPDA system has good room temperature properties and can be cured at $212^{\circ}F$ ($373^{\circ}K$) but has a short shelf life as a prepreg. The ERLA 5617 mPDA system has superior room temperature properties, can be adequately cured at $300^{\circ}F$ ($422^{\circ}K$) and has a reasonable shelf life in prepreg form.

The system considered to best satisfy the resin matrix criteria is 58-68R. This system exhibits good room temperature properties, performs reasonably well at cryogenic temperatures, has a good shelf life in prepreg form, and can be adequately cured at $300^{\circ}F$ ($422^{\circ}K$).

Fabrication parameters: Assuming 20 end S/HTS glass roving is to be used in prepreg form (with 58-68R resin matrix), the following fabrication parameters are recommended:

1) Resin content of the prepreg should be 25 $\pm$ 3%;

2) Internal pressure or a solid mandrel should be used during winding and cure for the liner support, except when using a very low wrap tension;

3) The wrap tension should be 8 pounds $\pm$ 2 lb (35.6 $\pm$ 9 N) per 20 ends for the highest quality of overwrap but may be as low as 2 $\pm$ 1/2 lb (8.9 $\pm$ 2 N) per 20 ends in the event no internal mandrel or pressure is used; and

4) The cure schedule should be 2 hr at 150°F (339°K) followed by 4 hr at 300°F (422°K).

Test Specimen Design

Based on the preceeding analyses, the test specimens were designed. Initially, proposed designs were submitted to the NASA LeRC Project Manager and approved, then slight modifications were found necessary during the actual detailed design effort. Test specimen configurations were finalized and approved prior to start of fabrication. The final design configurations are shown in fig. 31.

Modifications made to the CFL6300612 and cancellation of the CFL6300616 are noted on fig. 31. In addition, the CFL6300615 was modified by the insertion of a doubler between the flange internal diameter and the liner. The doubler was required to strengthen the area because axial strain allowed the flange to separate from the glass, leaving the liner to take all hoop loads in a small area.

Design of the Test Fixtures

Test fixtures for pressurizing, cycle testing, torsion testing, thermal testing, and leak checking the tubes and joints were designed. The test fixtures were capable of handling oil or water, liquid nitrogen, and liquid hydrogen for pressurization and cold helium or liquid hydrogen for leak checking. Schematics and descriptions of each test fixture are included under the Task III section applicable to the specific test being performed.

Designs for the test fixtures were submitted to the NASA LeRC Project Manager to review and approval at completion of the Task I effort.

TASK II. - FABRICATION OF TEST SPECIMENS AND HARDWARE

At the conclusion of the Task I analysis and design effort, the task of fabricating some 140 test items was undertaken. This fabrication effort consisted of the following prime functions:

1) Liner fabrication;

2) Fitting fabrication;

3) Joining the liners and fittings;

4) Mounting the strain gages;

5) Overwrapping and curing the assembly;

6) Welding the end fittings; and

7) Performing the various leak checks.

The materials manufacturing processes, and welding techniques that can be used to produce thin metal liners; along with fitting fabrication and methods of attaching the fittings to the liners, have been previously discussed in the Fabrication Analysis section of Task I. The problems encountered with these processes, during fabrication of the test specimens, are discussed in the following paragraphs. This discussion is followed by a description of the step by step procedure followed in the fabrication of each test specimen configuration. A flow chart, which is necessarily generalized, may help to orient the reader (figure 32). In addition to a discussion of the test item fabrication, the test fixture fabrication is briefly discussed.

Source Evaluation and Selection

A series of vendor evaluations were performed concurrent with Task I with the goal to select several competitive sources and several competitive techniques. Sources were selected in the areas of liner fabrication, fitting fabrication, joining the liners to the fittings, heat treatment, strain gage mounting, overwrapping the tubes, and leak checking the tubes. Vendors or sources were selected on the basis of technical ideas, schedule, cost, management, quality control, and experience.

Fig. 32. – Generalized Fabrication Flow Chart

Fitting Forming → Fitting Machining → Ship Fittings to Tubing Vendor

Resistance Welded

Heat Treat Liner → Resistance Weld Liner

Fusion Welded

Weld Liner → Heat Treat Liner

Fusion Welded and Redrawn

Weld Liner → Redraw Liner

Final Machine Fitting and Weld End Fitting to Liner*

Dye Penetrant Check → Ship to Test Area

Add End Adapters → Low Pressure Helium Leak Check → Mount Strain Gages

Overwrap → Buttweld → Operating Pressure Leak Check → Fabrication Complete

* May be fusion weld, resistance weld, or solid-state bond.

75

The following sources cooperated with NASA and MMC during the performance of this program:

1) Alloy Spotwelders, Los Angeles, California;

2) Metal Bellows Corp., Chatsworth, California;

3) Gardner Bellows Corp., Van Nuys, California;

4) BV Machine Company Inc., Denver, Colorado; and

5) Dr. J. D. Mote, Mr. Jack Snyder, MMC Ordnance Laboratory, Denver, Colorado.

Liner Fabrication

Four different methods of liner fabrication were evaluated during the program. Each of these methods has application and each has advantages and disadvantages. The four methods evaluated were seamless, resistance welded, fusion welded from the final thickness stock, and fusion welded followed by redrawing to the final thickness.

Seamless drawn tube. - Small diameter tubes, less than 1 in. (2.54 cm), are difficult to fabricate by any of the seam welding techniques previously discussed. However, seamless tubing of the desired diameter and wall thickness is commercially available and can be provided using any of the materials discussed in the material selection section. The 1/2 in. (1.27 cm) diameter Inconel 718 and stainless steel liners were fabricated by this method with no process problems.

Resistance welded liner. - This technique for tube fabrication required the tube to be roll formed to the desired diameter with a slight overlap at the mating surface. An anode was placed in the tube and a resistance weld was run down the length of the tube. The excess overlap on both the inside and outside of the tube was then peeled away from the weld on many of the tubes. The overlap was purposely left on several tubes to determine any structural differences, none of which were found. Figure 33 depicts both the peeled and the unpeeled methods. Note that even on the unpeeled liners the overlap is removed in the area of the fitting weld. Because the fabricator can tell much about his weld integrity by peeling away the overlap, and because no structural degradation results, all future work should request peeling the overlap on both the inside and outside surfaces.
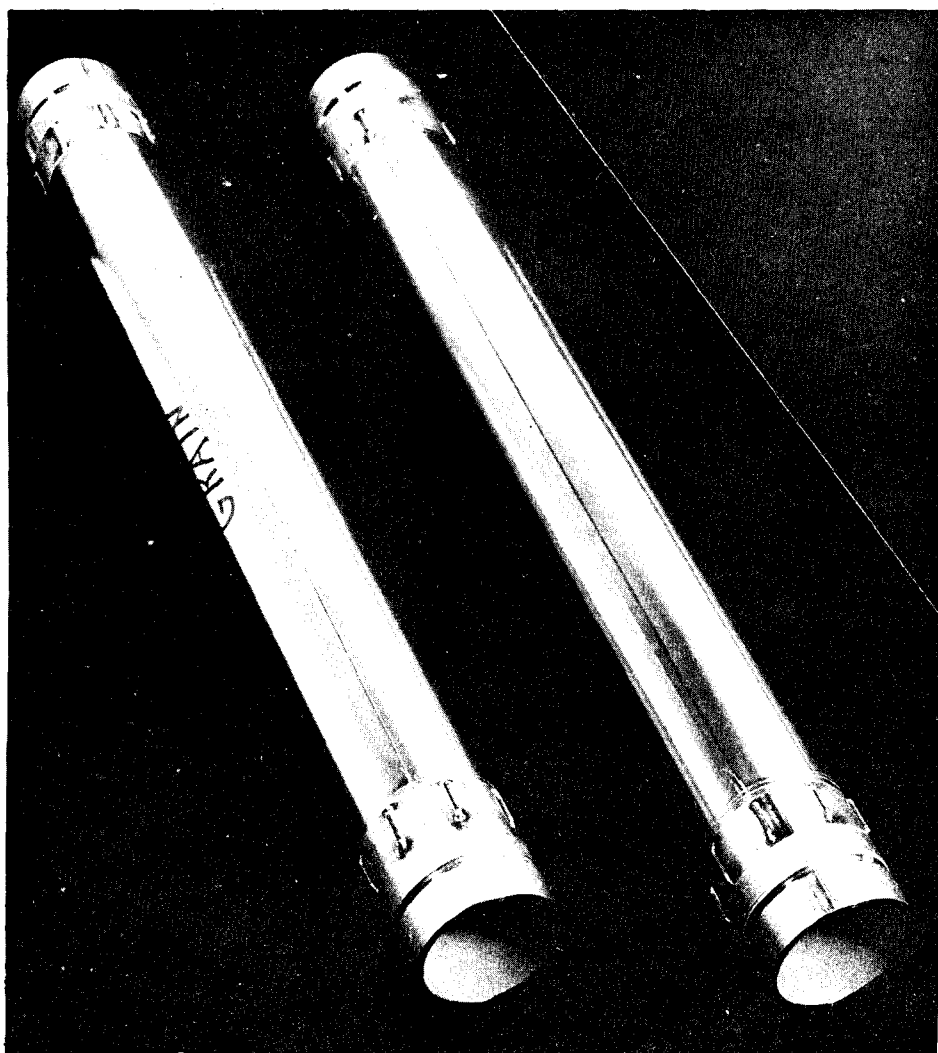
Fig. 33. - Peeled and Unpeeled Resistance Welded Liners

This weld can be made leak free consistently in 1 in. (2.54 cm) and larger diameter tubes. Also, this type of weld has a minimal heat affected zone that can be ignored from a structural standpoint.

Resistance welding is an inexpensive method of fabricating liners and was reported as a new technology disclosure (*) under this contract.

(*) MMC New Technology Disclosure 112 dated 14 January 1970.

Fusion welded - final thickness stock. - The most common practice in fabricating thin wall tubes larger than 1-in. (2.54 cm) diameter is to roll a tube to the desired diameter, prepare the butting edges as shown in fig. 21 and fusion weld a seam the length of the tube. Because of highly developed welding techniques this weld can consistently be made leak free. Also, by plenishing and polishing the weld, the weld area will conform to overall tube size (no weld buildup inside or outside the tube). This welding process can be used consistently with metal thicknesses down to 0.002 in. (0.005 cm).

The main disadvantage of this technique is the relatively large heat affected zone in the weld area. The liner can be heat treated after welding and plenishing, but welding of the liner to end fittings will once again anneal the material. Heat treatment of the final assembly without severe warpage will be difficult.

Fusion welded - redrawn. - As mentioned above, the most common practice in fabricating thin wall tubes larger than 1-in. (2.54 cm) diameter is to roll a tube to the desired diameter, prepare the butting edges and fusion weld a seam the length of the tube. The large areas of the tube that are annealed (heat affected zone) by the welding process have a very different structural character than the parent metal. Therefore, the tube will not react as a homogeneous member under hoop stress, and the combined hoop stress characteristics are either undesirable or unpredictable. Austenitic stainless steel, which is not heat treatable, may be cold worked to restore high strength. To cold work the tube, it can be redrawn over a mandrel as with conventional seamless tubing. This will reduce the wall thickness to that desired, return the tube to a homogeneous status, and strengthen the entire tube. Inconel 718 liners can be cold worked by the same process to restore high strength after seam welding. Plenishing of these liners after weld is unnecessary because redrawing accomplishes the same goals. Fig. 34 depicts a redrawn liner.

CFL 6300609

Fig. 34. - Helically Welded Redrawn Liner

Helically wrapped tubes. - This technique for forming liners requires wrapping a 2 to 3-in. (5.08 to 7.62 cm) strip of metal around a mandrel

in the form of a helix and fusion welding the edges. This is shown in fig. 22 where the butting edges are prepared as shown in fig. 21. This method of fabricating tubes has desirable structural properties from hoop stress and forming aspects. This weld can also be plenished and polished or redrawn.

An advantage to this type of construction will be realized when large diameter tubes are required. Raw stock in widths larger than 12 in. (30.5 cm) is not commercially available. Therefore tubes greater than 3.5 in. (8.9 cm) in diameter would require more than one longitudinal weld.

Heat Treatment

The Inconel 718 used for liner fabrication was heat treated and age hardened on some test specimen configurations. This heat treatment was accomplished in accordance with the following procedure:

1) Wrap the liner in 0.001 in. (0.0025 cm) thick tantalum foil if necessary to eliminate oxidation or discoloration associated with heat treatment in other than a vacuum [0.001 in. (0.0025 cm) thick stainless steel foil may be substituted];

2) Heat to $1750 \pm 25^\circ$F ($1230 \pm 14^\circ$K) for 1 hr then argon quench to 200°F (367°K) max. at a minimum rate of 30°F /min. (16°K/min.);

3) Age at $1400 \pm 15^\circ$F ($1033 \pm 8^\circ$K) for 5 hr then cool to $1175 \pm 25^\circ$F ($909 \pm 14^\circ$K) and hold until total aging time is 8 hr.

Fitting Fabrication

The requirements of the program dictated that a minimum of two types of end fittings be used on the test specimens, one to provide a weldable joint and the other to provide a mechanically disconnectable joint.

The various steps in fitting fabrication are discussed in this section. After forming and machining or flaring, the fittings were joined to the liners. The 2 in. (5.08 cm) and 5 in. (12.7 cm) diameter tubes were pressurized for a leak check prior to overwrap, during overwrap and cure, and again for a leak check after fabrication was

completed. This required that each liner have the capability of being pressurized as a unit. For the liners which used disconnectable joints such as flared fittings or sealing flanges, this was done by simply providing the mating half of the fitting with an adapter appropriate for final testing. For specimens that had buttweld joints the joint was fabricated to include the appropriate adapter. A buttweld type groove was then machined into each end fitting-adapter combination at a location which corresponded to where another tube would be welded during a system assembly.

To demonstrate the weldability of this type of joint, this groove was filled using normal welding techniques after other fabrication was completed. Heat input into the composite was controlled by the use of heat sinks and controlled welding rates. In most cases a single butt-weld pass was adequate because the machined groove was not excessively deep. This groove is clearly visible in fig. 33. A chill ring used during the welding is shown in fig. 35 and weld speed was controlled so as to limit the glass-fiber temperature to a maximum of 250°F (394°K).
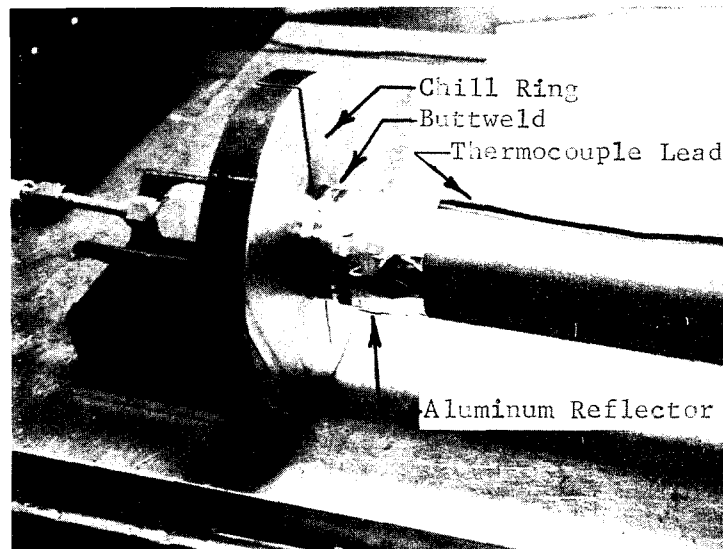
Fig. 35.- Chill Ring

For the 1/2 in. (1.27 cm) tubes with the butt weld end fitting configuration the adapter was welded in place after overwrapping, using the above techniques.

In production work these same or similar adapters would be added to facilitate fabrication. In the case of the buttweld joints the adapters would be removed after fabrication by machining an identical style of buttweld end configuration at the end of the tube. For this program two different size adapters were used. A 1/4 in. (0.635 cm) diameter flared tube was used on the burst test specimens and a 3/4 in. (1.90 cm)

80

diameter flared union was used on the cycle test specimens (to provide increased flow rates to the specimen during cycling).

Load Transfer to the Overwrap

A method of transferring torsional loads into the overwrap was desired. The application of a release agent during overwrap required the addition of a separate device to affect this transfer. The addition of small pins oriented longitudinally underneath the overwrap facilitated this transfer. The pins which were welded to or inserted into the end fittings are shown in fig. 33.

Both torsional and longitudinal load transfer was desired on some tubes. For these applications the pins were replaced by a knurl on each end fitting. Release agent was not applied in the knurled area so the resin system would fill the voids and provide load transfer through shear. These load transfer methods are apparent in several figures throughout this report.

Joining Liners and End Fittings

The leak free joining of the liners to the end fittings was one of the most difficult aspects of the program. Three basic methods of joining were employed including fusion welding, resistance welding, and solid-state bonding.

Fusion welding.- The concept shown in fig. 25, for connecting the liner to the end fitting, was applied to flange-type end fittings. This method of attachment, shown in fig. 36, can be cleaned easily and eliminated any contaminant trap areas from the assembly. The concept does not use any filler material, and it depends on an even heating of all joint components to obtain a reliable weld. Fusion welding resulted in leak-free, high strength, reliable welds and is recommended for use in any further work. Significantly, dissimilar materials such as Inconel 718 and stainless steel can be joined reliably.

Another fusion welding concept (fig. 37) would be applicable when an end fitting, either flange or threaded type, is fusion welded to the liner. This method is used frequently by bellows manufacturers when attaching bellows to end fittings. This concept could be easily applied when welding a glass-fiber tube to another line without using end fittings. One disadvantage associated with this method is that it creates potential cleaning problems. Another disadvantage is the lack of strength of the weld. For the weld to be structurally sound, both members must be of similar heat capacity. In addition, the materials should be of equal strength as the joint strength will be the same as the weaker material. The joint design can be used when both members are of the same material, and the same thickness.
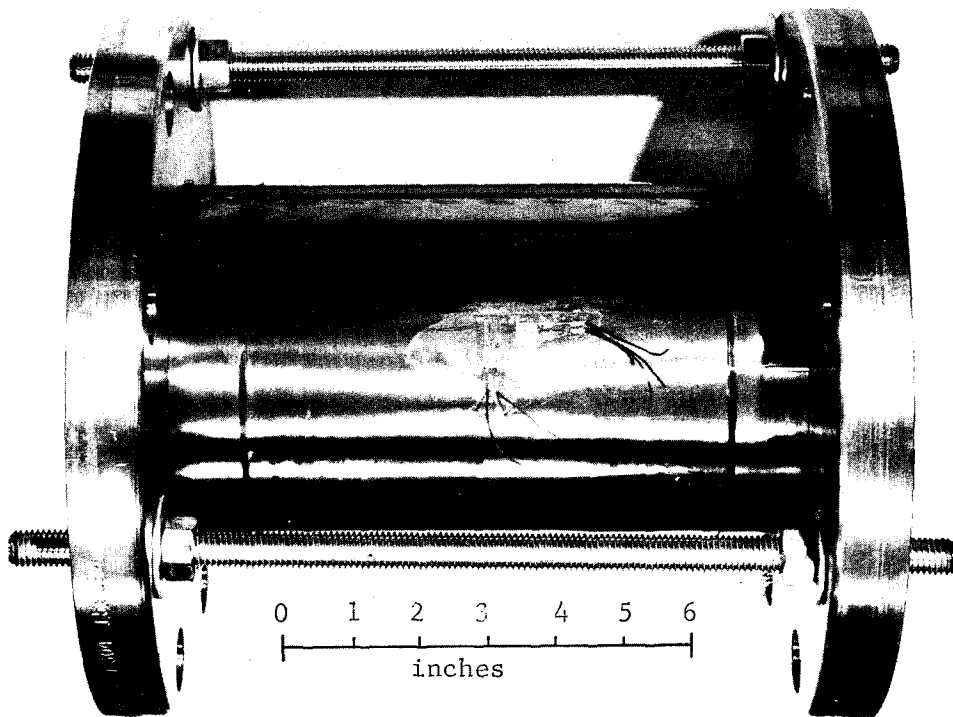
Fig. 36.- Fusion Welded Tube Assembly
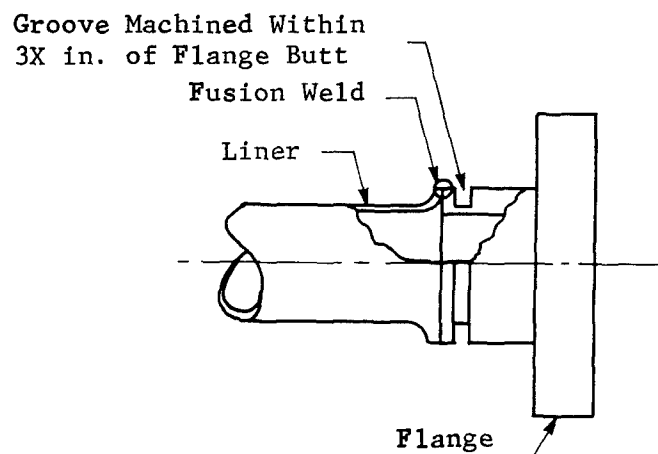
Fig. 37.- Fusion Welding Liner to End Fitting

Resistance welding.- The most straightforward approach to attach-
ing either flange or threaded type fittings to the liner is shown in
fig. 38. This approach calls for resistance welding the liner to a
thin portion of the end fitting.

Resistance Weld

May Exceed 3 Times Liner Thickness
When Stitch Welded.
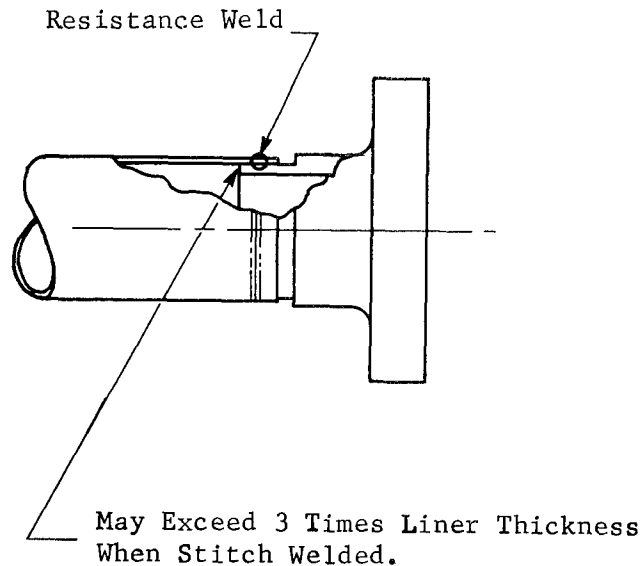
Fig. 38.- Resistance Welding Fitting to Liner Using Stitch Welder

Two different methods of resistance welding were used during this
program. The first method used an anode inside the tube and rotating
cathode on the outside of the tube. This cathode was in constant
contact with the tube and current was applied at predetermined intervals.
A tube fabricated by this method is shown in Fig. 39. The second method,
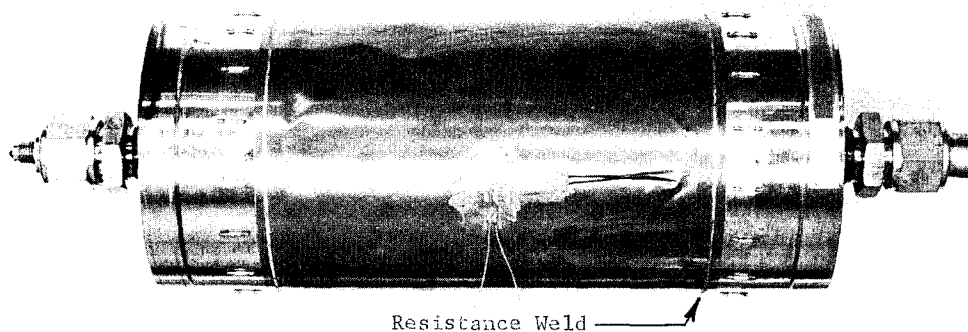
Resistance Weld

Fig. 39.- Fitting Resistance Welded to Liner,
5 in. (12.7 cm) Diameter Tube

commonly referred to as stitch welding, differed only in that the cathode was brought into contact with the tube momentarily for each spot weld. Using the stitch welder, successful welds were made when the inner material was many times thicker than the liner. Dissimilar metals such as Inconel 718 and stainless steel are reliably joined with these methods.

The major advantages of resistance welding include reliability, relative lack of cost, and the elimination of an annealed heat affected zone. A disadvantage of resistance welding is the cleaning problem in the flange to liner overlap area. The cleaning problem may preclude the use of this style in fluorine or FLOX but not liquid oxygen, liquid hydrogen, or methane.

The stitch welding method was not particularly successful on many of the 1/2 in. (1.27 cm) diameter tubes because it was plagued by development problems and leaks -- these problems were largely overcome on later tubes by improved procedures and better quality control. Investigations revealed that control of the stinger current and its tip size will help alleviate these problems.

Solid state bonding.- A highly desirable method of joining the liner to the end fittings uses an explosive or solid-state bonding technique. This method of joining the two parts provides a joint that is in excess of 100% of the base metal strength and as such forces the failure to another location. The few disadvantages such as leakage can probably be overcome with more development. The joint is low cost, strong, easily inspectable, and cleanable. Figure 29 depicts the solid state bond.

Shipping Unfinished Tubes

An area that required special attention was the shipping of the unwrapped tubes from Los Angeles to Denver. Special packaging by the vendors helped control the problem, but several boxes were grossly mishandled in transit, and the liners were buckled. Figure 36 shows representative packaging techniques. This tube and rod assembly was installed in a heavy cardboard box that was slotted to accept the flanges and restrain the tube snugly. Boxes that received proper handling, were in all cases, adequate and prevented damage.

Of importance to this concept, the damage, such as shown in fig. 40 did not alter the burst pressure or cycle life of the tubes. In most cases, the internal pressure associated with the overwrapping operation minimized the dings. A substantial finding, therefore, is the liners do not have to be completely free of scratches, dents, and dings to properly function.

With the exception of the 5 in. (12.7 cm) diameter design with heavy NASA flanges, all tubes could be safely handled without internal
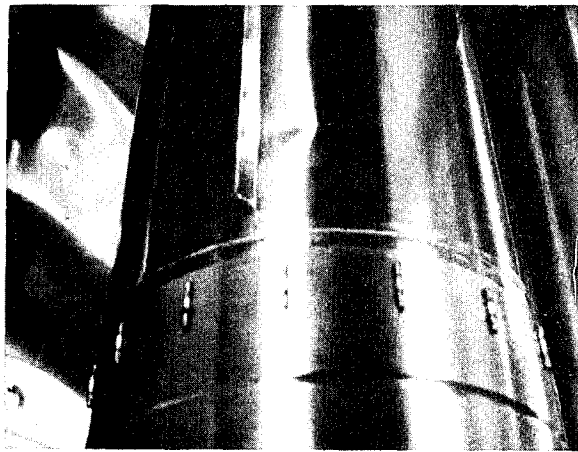
Fig. 40.- Oil Can Ding, Serial Number 99

pressure or other protective devices. As an added precaution 8 to 10 psig (13.8 to 15.2 N/cm^2) internal pressure was applied during most handling operations.

Strain Gage Installation

The primary instrumentation for the tubing consisted of biaxial strain measurements. It was planned to be able to determine the strain at or near the points of failure -- this was not accomplished. After the test program began, a review of the strain gage data indicated the desirability to locate all gages on a specific tube design at the same location; that is, if the axial gage is always 6.0 in. (15.24 cm) from the end, the data should be able to be correlated. The different designs have different friction factors between the overwrap and the liner and, therefore, several gages would have been required on any one tube to plot the movement of the liner (strain) with respect to distance from the end.

To arrive at the location criteria, Martin Marietta reviewed what was desired from strain instrumentation. The following is a list of desirable knowledge:

1) Determine the gap between the liner and overwrap at cryogenic temperature;

2) If possible, locate the strain gage at the failure point and not affect the failure;

3) Determine whether the gap closed before plastic deformation of the liner occured;

4) Determine that the liner did not exceed the yield stress below working pressure;

5) Determine the modulus of elasticity of the composite tube (liner and overwrap);

6) Determine the load that is transferred to the glass in the axial direction; and

7) Verify the consistency of a design.

Strain gages located 180° from the longitudinal weld and nearly centered between the end fittings satisfied a maximum number of these goals.

Except for a few prototype tubes, one hoop and one axial strain gage, or a rosette containing both, were applied to the outside of the liner. The strain gage wires were attached to a terminal board and small lead wires were mated to the terminal board, as shown in fig. 41, and fed through the over wrap at a later time.

2 in. (5.08 cm) Dia — Liner
Strain Gage ———
Terminal Board
Lead Wires
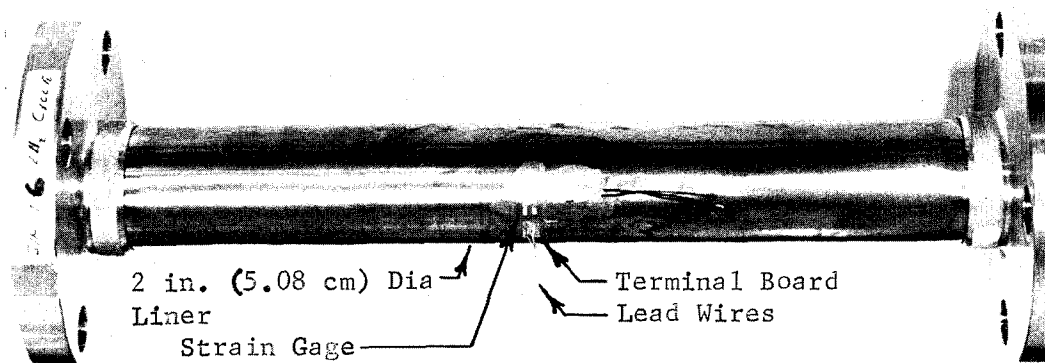
Fig. 41.- Strain Gage Installation

On some prototype tubes, strain gages were mounted inside the liner to obtain compressive loads in the liner created by the overwrapping process. These strain gages were for room temperature use only and the Eastman 910 adhesive was cured without any elevated temperature. The gages became inoperative during the overwrap and cure cycle, but had served the purpose intended.

On some prototype tubes strain gages were also mounted outside the glass-fiber system. These gages were used to verify the gap between the liner and overwrap at cryogenic temperatures. They were also to be used to determine the load-sharing between the liner and the overwrap. As anticipated many of these became inoperative during cooldown or pressurization of the tube. Strain gages mounted on the overwrap were not planned to be used as prime data because of inaccuracies or failures associated with the resin system crazing.

Different strain gages were used for the ambient and the cryogenic tubes for the prime reason that rosettes were easily procured for ambient temperature application while only single strain gages were readily available for cryogenic service. Strain gage installation criteria is shown in table 17.

Sometime before installing the gages on a tube, the tube was cleaned with acid, a water rinse, and flushed with freon. Immediately before bonding the gages to the liner, the metal was thoroughly rinsed with methyl ethyl ketone (MEK). The tube was pressurized to 10 psig (15.2 N/cm) during the strain gage installation and curing to prevent localized buckling. The strain gages were covered with a thin sheet of Teflon, followed by a rubber pad laid on top of the strain gage area, and then tightly wrapped with adhesive backed aluminum tape. After the gage was cured the excess adhesive was removed by scraping or sanding, and the entire area was smoothed out to minimize the stress riser. A strain gage continuity check was performed at this stage of the fabrication process and again after the overwrap operation was completed with a third and final continuity verification just before test.

After the overwrap cycle was complete, the burst specimens were equipped with longer wires and connectors. The cycle test items were assembled into the test fixture without connectors.

TABLE 17. - STRAIN GAGE INSTALLATION CRITERIA

Ambient Service Inside Liner	Gage Adhesive Cure Temp. Range/Adhesive	Automation Industries C9-125-R2T Rosette Eastman 910 Instantaneous with Pressure -100°F to $+150^{\circ}$F (200°K to 339°K) $+180^{\circ}$F is max. (355°K)
Ambient Service Outside Liner	Gage Adhesive Cure Temp. Range/Adhesive	Automation Industries C9-125-R2T Rosette Automation Industries GA-5 165°F (347°K) for 4 hours (slow rise rate) -425°F to $+275^{\circ}$F (19°K to 408°K)
Ambient Service Outside Glass	Gage Adhesive Cure Temp. Range/Adhesive	BLH Type C-8 Eastman 910 Instantaneous with Pressure -100°F to $+150^{\circ}$F (200°K to 339°K)
Cryogenic Service Inside Liner	Gage Adhesive Cure Temp. Range/Adhesive	Automation Industries S741-R2T-300 Rosette Eastman 910 Instantaneous with Pressure -100°F to $+150^{\circ}$F (200K to 339°K) $+180^{\circ}$F is max. (355°K)
Cryogenic Service Outside Liner	Gage Adhesive Cure Temp. Range/Adhesive	Automation Industries S-741 2 at Right Angle Automation Industries GA-5 165°F (347°K) for 4 hours (slow rise rate) -425°F to $+200^{\circ}$F (19°K to 367°K) 300°F permissible (422°K)
Cryogenic Service Outside Glass	Gage Adhesive Cure Temp. Range/Adhesive	BLH DLB-MK35-4A-S13 Automation Industries GA-5 165°F for 4 hours (slow rise rate) -425°F to $+275^{\circ}$F (19°K to 408°K)

Overwrapping and Curing

After the strain gages were mounted and cured, the tubes were overwrapped with a system consisting of glass-fibers and a cryogenic resin system. This system was then subjected to elevated temperatures to cure the overwrap.

Glass-fiber and resin system. - The glass fiber systems selected for use on this program consisted of S-HTS glass for the hoop and early longitudinal wrappings and E-HTS glass for the longitudinal wrappings when the 10 to 1 prefabricated mat was used. The S-HTS glass was 20 end roving and was preimpregnated with a cryogenic resin matrix, 58-68R. The resin content was controlled to between 20 and 25%. Prepreg batches were large enough to overwrap three or four large diameter tubes. A maximum allowable shelf life, in a refrigerated condition, of one week assured a good system. The preimpregnation coating tower is shown.
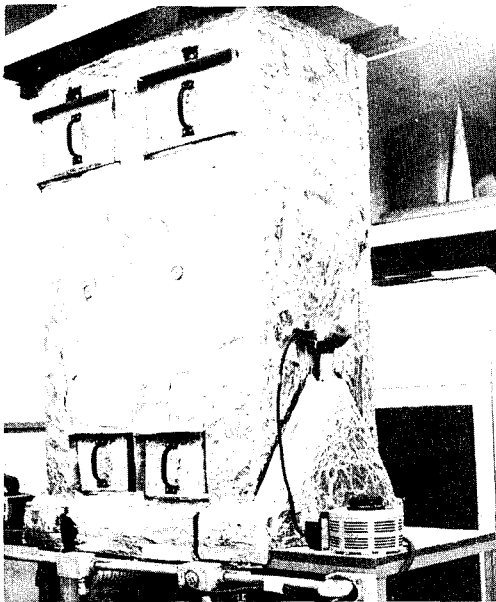
The resin content of each tower run was calculated, and recorded in the inspection log for each tube.

During the fabrication process the weight of overwrap material applied to each style of tube was determined. These data can be used to verify the relative light weight of the tubing. The test data are summarized in tables 18 and 19.

Overwrap method. - In all cases, the tube was overwrapped using a preimpregnated glass-fiber and resin system. For hoop wraps the tube was installed in a filament-winding machine (fig. 42 and 43) which had a linear movement of 0.06 in. (0.15 cm) per revolution. Machine speed was variable and was adjusted to 40 rpm for the 1/2 in. diameter (1.27 cm) tubes and 15 rpm for the 2 and 5 in. diameter (5.08 and 12.70 cm) tubes.

Before beginning the overwrap process, the larger diameter tubes were pressurized to 20 to 25 psig (22 to 25.5 N/cm^2) and this pressure was maintained until completion of the cure cycle. Early experiments involving the venting of pressure before cure met with failure in that the liner seam weld collapsed (see fig. 44). The 1/2 in. (1.27 cm) diameter tubes were not pressurized but were overwrapped while a solid mandrel was inserted inside
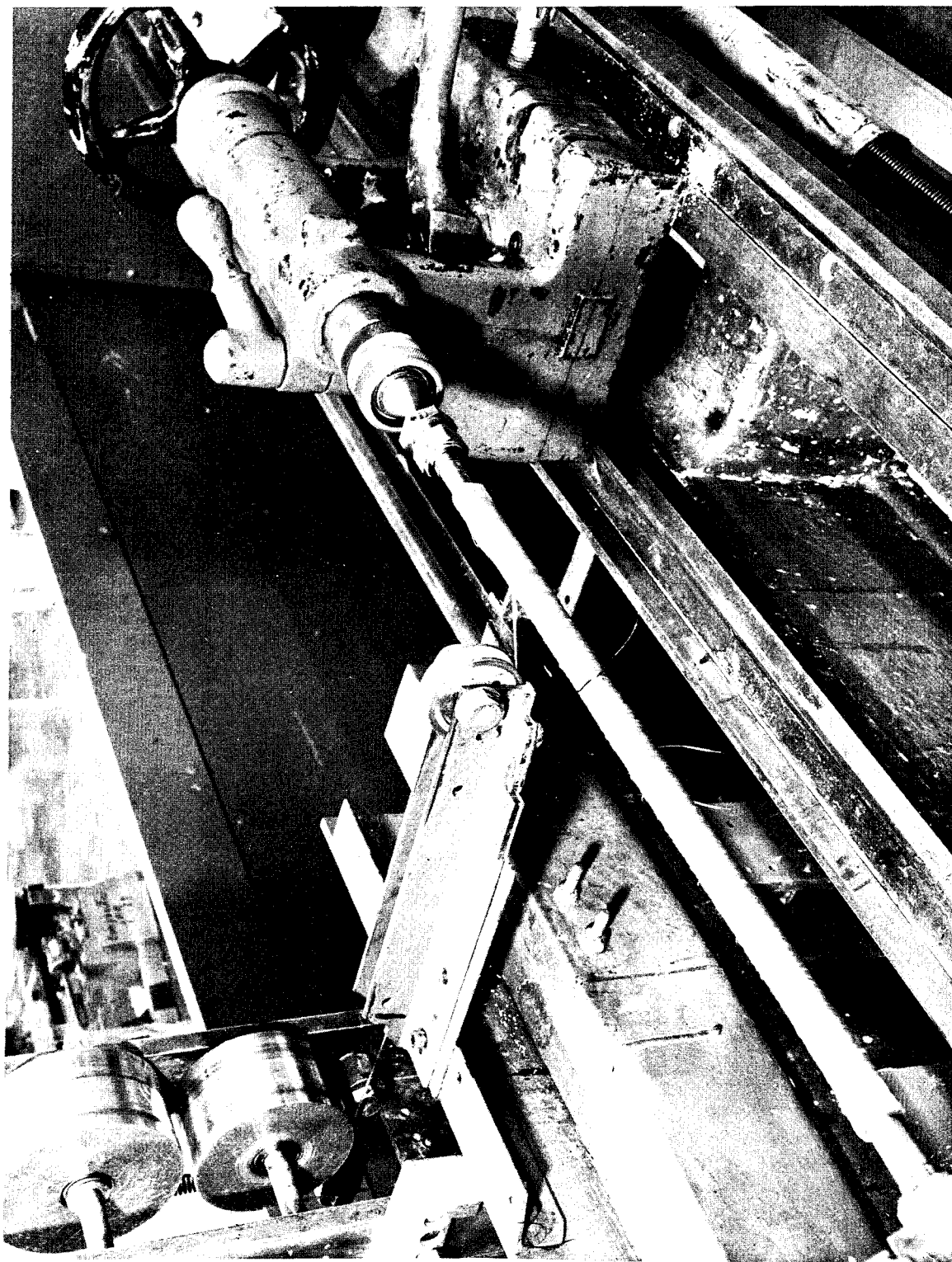
Fig. 42. - Filament-Winding Machine 1/2 in. (1.27 cm) Diameter Tubes
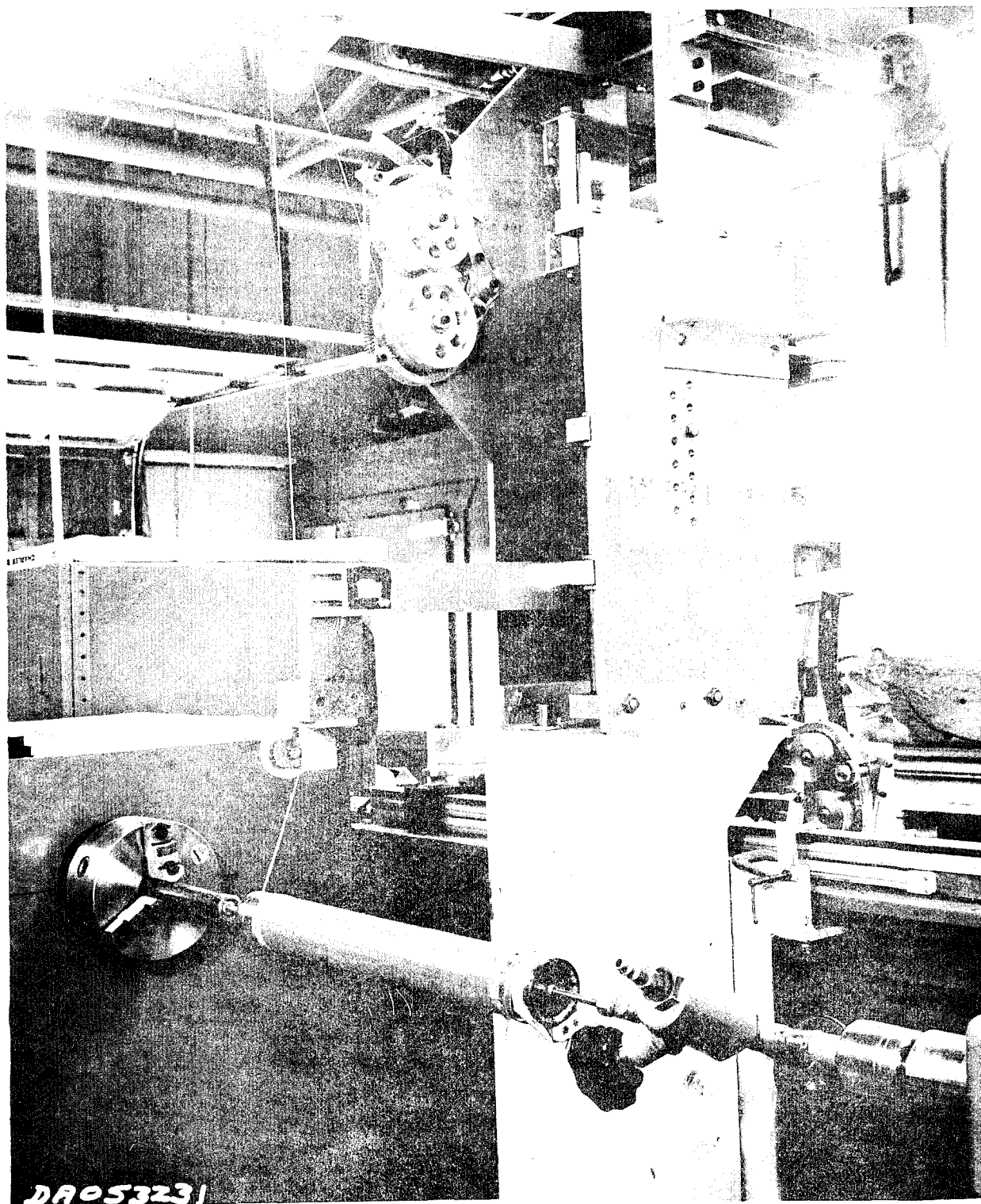
Fig. 43. – Filament-Winding Machine, 2 in. (5.08 cm) and 5 in. (12.7 cm) Diameter Tubes

TABLE 18. - WEIGHT ANALYSIS AND COMPARISON WITH CONVENTIONAL TUBES

Diameter (in.)	Liner Thickness (in.)	Overwrap Thickness (in.)	Calculated (1b/ linear in.)	Actual weight (1b/linear in.)		
				Liner	Composite	Total
1/2	0.007	0.030	0.00684	0.0033	0.0037	0.0070
1/2	0.009	0.030	0.00764	0.0042	0.0037	0.0079
1/2*	0.020	N/A	0.00911			
2	0.003	0.040	0.02348	0.0056	0.0213	0.0269
2	0.006	0.030	0.02463	0.0113	0.0159	0.0272
2	0.003	0.030	0.01903	0.0056	0.0160	0.0216
2*	0.030	N/A	0.05460			
5	0.003	0.040	0.05990	0.0141	0.0464	0.0605
5	0.006	0.050	0.08560	0.0282	0.0580	0.0862
5	0.006	0.040	0.07410	0.0282	0.0468	0.0750
5*	0.050	N/A	0.22750			

Note:

The weight of end fittings is not considered because any configuration will require end connections.

* Conventional stainless steel tube. Not a composite.

TABLE 19. - WEIGHT ANALYSIS AND COMPARISON WITH CONVENTIONAL TUBES

Diameter (cm)	Liner thickness (cm)	Overwrap thickness (cm)	Calculated weight (N/linear cm)	Actual Weight (N/linear cm)		
				Liner	Composite	Total
1.27	0.0178	0.0762	0.0120	0.0058	0.0065	0.0123
1.27	0.0229	0.0762	0.0134	0.0074	0.0065	0.0139
1.27*	0.0508	N/A	0.0160			
5.08	0.0076	0.1016	0.0411	0.0098	0.0373	0.0471
5.08	0.0152	0.0762	0.0431	0.0198	0.0278	0.0476
5.08	0.0076	0.0762	0.0333	0.0098	0.0280	0.0378
5.08*	0.0760	N/A	0.0956			
12.70	0.0076	0.1016	0.1049	0.0247	0.812	0.1059
12.70	0.0152	0.1270	0.1499	0.0494	0.1015	0.1509
12.70	0.0152	0.1016	0.1298	0.0494	0.0819	0.1313
12.70*	0.1270	N/A	0.3981			

Note:

The weight of end fittings is not considered because any configuration will require end connections.

* Conventional stainless steel tube. Not a composite.

the liner. This mandrel was of a slightly smaller diameter than
the liner and, therefore, was easily removed after the cure cycle.
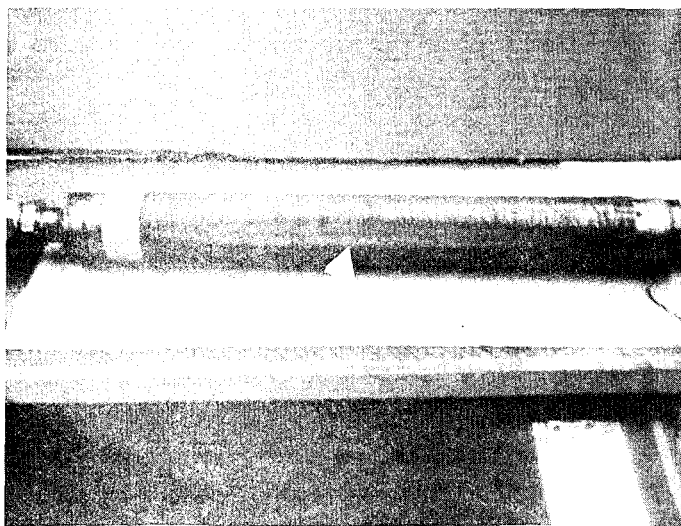
Fig. 44. - Post Overwrap Showing
Buckle, Serial No. 63

Machine tension settings (overwrap tension) were determined
empirically during the overwrapping of the prototype tubes. The
2 lb (8.89 N) per 20 end roving tension was abondoned because of
undesirable roughness on the finished product. Wrap tensions
were adjusted until the aesthetic appearance and the internal
pressure required to offset the pressure on the liner were optimized.
Final wrap tensions are shown in the accompanying table.

Tube diameter		Liner thickness		Machine tension	
(in.)	(cm)	(in.)	(cm)	(lb)	(N)
0.5	1.27	0.007	0.0178	3	13
0.5	1.27	0.009	0.0229	3	13
2	5.08	0.003	0.0076	3	13
2	5.08	0.006	0.0152	3	13
5	12.70	0.003	0.0076	4 or 6*	18 or 26*
5	12.70	0.006	0.0152	4	18

* Either 4# or 6# (18 or 26N) machine tension was used according
  to the specific design.

The initial step in the overwrap process was the application of a silicone release agent to the liner. This release agent was applied to all tubes in all areas of overwrap contact except for the knurls which were designed to adhere to the resin system.

The hoop layers were all 20 end rovings, applied at 16 turns to the inch (6.3 turns to the cm) with machine tensions as discussed. In the early stages of the fabrication effort, the longitudinal glass-fiber was hoop wrapped on a drum, cut from the drum, and then fit to the tube at a 90° direction to the hoop windings. This method was soon abandoned in favor of 10 to 1 prefabricated glass-fiber, which was fitted to the tube with the 10 fiber direction being longitudinal. The latter method saved considerable time and also enhanced the appearance of the finished tube. In all cases, at least one and as many as two layers of hoop overwrap were applied over the longitudinal layer.

The instrumentation, which consisted of strain gages and a thermocouple required special handling during the overwrapping process. The strain gages that were bonded to the liner included small wires that were guided through the various layers of the overwrap. The machine was stopped in the area of the wiring and the overwrap was guided into place as the lathe was turned slowly by hand. This hand fitting operation resulted in only a minor discontinuity in the overwrap and only one tube failed in this area. Several of the fragile wires were severed at the tube interface during this operation, most of them were repaired and operated satisfactorily. The thermocouple was added underneath the last hoop layer, near one end of the tube. The thermocouples were Thermoelectic Corporation, type G/G with fiber-glass insulation. The AWG #30 unshielded wires with a twisted and soldered exposed loop are made of copper and constantan.

When the overwrap process was completed the tubes were removed from the lathe, and without removing the solid mandrel or venting the pressure, the tubes were installed in the cure oven.

Cure cycle.- The 58-68R resin matrix requires a cure cycle at elevated temperatures. Several combinations of time and temperature are acceptable. For this program the cure temperature profile shown in the accompanying sketch was used. Several tubes were cured simultaneously in a 5 x 6 x 8 ft (152 x 183 x 244 cm) oven. The cure oven is of the forced-air type and has a maximum temperature of 650°F (615°K). Temperature repeatability is ensured by programmer control of the oven temperature vs time. Actual data from the cure cycle, including any anomolies, were entered in test specimen logs.
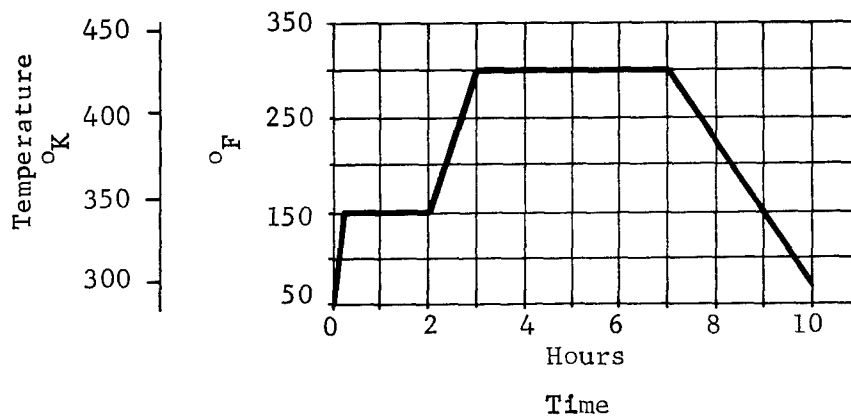
This method of curing the tubes resulted in two somewhat undesirable side-effects. First, a layer of thin Teflon sheet was wrapped around the tube where the overwrap was terminated as an aid in holding this loose end in place until the resin matrix was cured. This left an area where the resin matrix was unusually dry appearing. The second undesirable aspect resulted from not rotating the tubes while curing. The resin matrix tended to slump and leave a dry appearance on the top of the tube and an overly shiny appearance on the bottom (fig. 45). The slump often dripped to the floor of the oven and left a protrusion on the tube. Neither of these side-effects altered the strength of the tube but both would be undesirable where aesthetics is important.
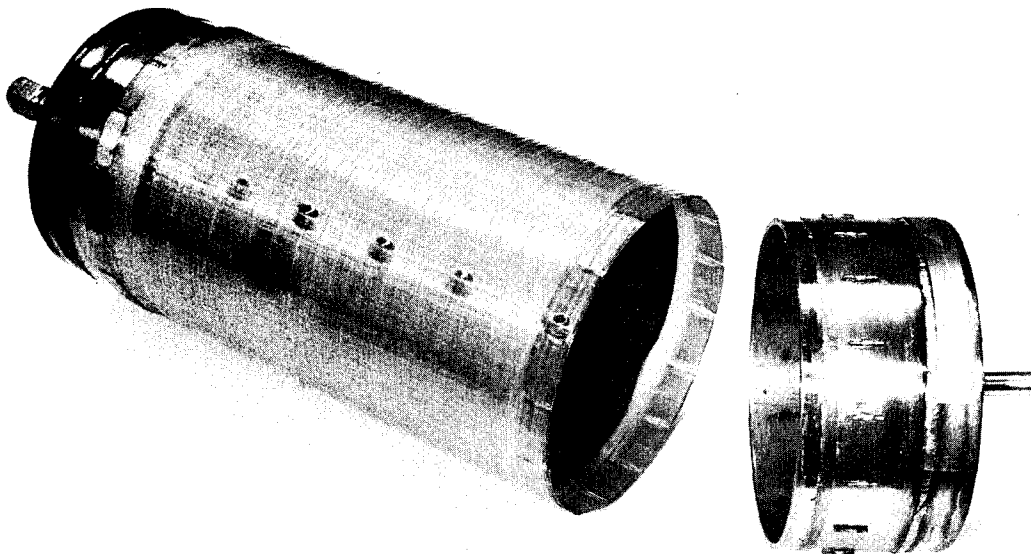
Fig. 45 . - Post Cure Showing Resin Slump.

Leak Checks

To determine the leak-free integrity of the tubes, they were subjected to a series of leak checks during the fabrication process. These checks were performed on the liner before the end fittings were installed and on the tube assembly both before and after the overwrapping process.

Liner leak checks. - After the 2 and 5 in. (5.08 and 12.70 cm) tube liners were fabricated, they were subjected to a dye penetrant leak check. This step was completed by the vendors as a part of the fabrication quality assurance program. Original plans to leak check the liners with helium were abandoned because of the lack of tooling to perform a positive pressure helium leak check and because any vacuum applied to the inside of the liner (for a helium wash leak check) would result in collapsing the liner. The dye penetrant method proved to be suitable.

Pre-overwrap leak checks. - After attaching the fittings to the liner, a second dye penetrant check (the first leak check for the small seamless tubes) was performed at and adjacent to these welds. This test was also accomplished by the tube vendors. Results of these tests are included in the test item inspection logs.

After receipt of the tubes at the MMC Cold Flow Laboratory, an internal pressure helium leak check was performed on each tube in accordance with the sketch. The pressure level for this leak check was usually 25 psig (25.5 N/cm^2) with some 1/2 in. diameter (1.27 cm) tubes checked at 200 psi (138 N/cm^2). Safety restrictions precluded leak checks at operating pressure until the overwrap system was installed and cured. A helium mass spectrometer with a sensitivity of approximately 1×10^{-10} scc/sec of helium was used for these tests. The mass spectrometer probe with a rubber gathering cup was used to search for leaks at all joints. Results of these tests are included in the test item inspection logs and are summarized at the end of this section.

Helium Supply

Safety shield for use while pressurizing

Rubber Cup Tipped Probe
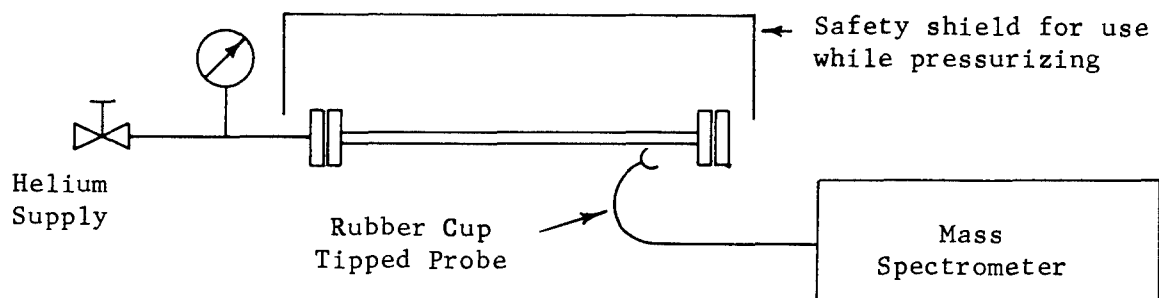
Mass Spectrometer

Post-overwrap leak checks. - After the tubes were overwrapped
and cured, a 200 psi (138 N/cm^2) for the 2 and 5 in. dia. (5.08
and 12.70 cm) tubes and a 3000 psi (2068 N/cm^2) for the 1/2 in.
dia (1.27 cm) tubes, leak check was performed using a helium mass
spectrometer. For this test, the test items were enclosed in a
bag and the mass spectrometer probe was inserted into the bag.
This method of leak checking, referred to as accumulation test-
ing, is excellant if there are no leaks in the tube. The method
is not considered to be quantitative in nature because the leak-
ing helium will accumulate in the bag and replace the nitrogen
gas or air that was originally in the bag but was withdrawn by
the mass spectrometer. In cases of marginal leakage, the system
(bag, tube, and mass spectrometer) was compared to a known
standard leak and this calibration was used to calculate the
quantitative leak (ref. 9).
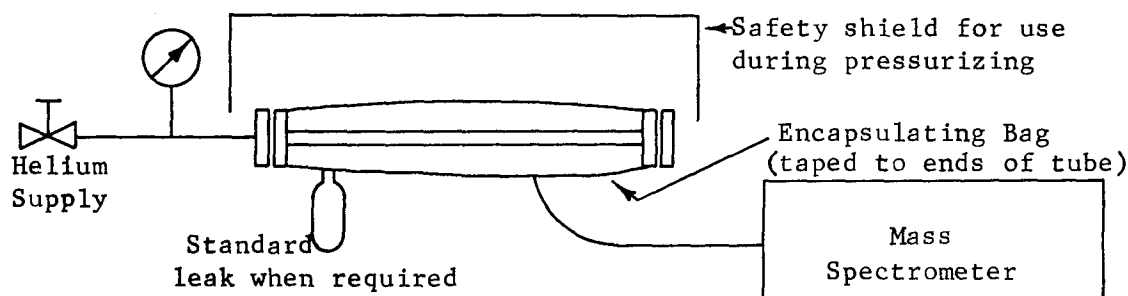
Again, the results of these leak checks were entered in the
test item inspection log and are summarized at the end of this
section.

Results. - The results of these leak checks are tabulated
in table 20. As noted, several of the tubes had leakage rates
in excess of the 1 x 10^{-6} scc/sec allowable. These tubes were
subjected to a material review board and appropriate corrective
action was initiated. Because of the methods used during
cryogenic cycle testing, tubes that indicated any appreciable
leakage were subjected only to burst testing.

In general the tubes can be reliably manufactured without
measurable leakage. A requirement of any production program
resulting from this study should be a mass spectrometer leak
check, with no measurable leakage, before overwrapping the tube.

TABLE 20. - LEAKAGE RATES

Specimen[f] Number	Pre Overwrap 25 psig (25.5 N/cm^2) He Pressure			Post Overwrap Operating Pressure He		
	No. of Leak Free Tubes	Acceptable Leak Rate ($<1 \times 10^{-6}$ scc/sec)	Unacceptable Leak Rate	No. of Leak Free Tubes	Acceptable Leak Rate	Unacceptable Leak Rate
CFL6300605	11	1	0	7	5	0
CFL6300606	12	0	0	9	3	0
CFL6300607	8	4	0	8	3	1[a]
CFL6300608	11	1	0	6	5	1[b]
CFL6300609	10	2	0	8	3	1
CFL6300610	12	0	0	10	2	0
CFL6300611	11	1	0	9	3	0
CFL6300612	0	0	1			
CFL6300612 (redesign)	6	2	3[c]	5	3	3[c]
CFL6300613	10	2	0	6	4	2[d]
CFL6300614	8	4	0	6	4	2[e]
CFL6300615	5	4	3	5	4	3[d]

a. Used as an ambient temperature burst test specimen without repair.

b. Was changed to LH$_2$ burst test item without repair.

c. The out of spec leaks received MRB action and the leaks were repaired with a cryogenic epoxy. Additional changes in the bonding procedure assisted in fabrication of leak free bonds.

d. These tubes were used as burst items where effects of leakage are minimal.

e. Retest on serial no. 116 revealed the tube leak rate was acceptable for ambient cycle. The other leaking tube was changed to a LN$_2$ burst article where effects of leakage are minimal.

f. This column is an identifying drawing number for each tube design.

It is significant that once a tube is leak free it usually remains leak free throughout the extensive overwrap and cycle test programs.

Specific leakage problems were experienced on several designs. The 1/2 in. dia (1.27 cm) high-pressure tubes frequently indicated leakage at the resistance welded joint to the end fitting but this leakage was usually within the specification limits. The probable cause of this leakage problem is the tip diameter of the stitch welder. The 1/2 in. (1.27 cm) tube has a small contact area and, therefore, cannot receive proper welding current. Other areas of close control required in this size tube are cleanliness, fit-up, and thickness of the two welded materials. The tubes fabricated during the latter part of the program have considerably better characteristics than the early development models.

One design style was eliminated from the program as a result of poor weld quality that resulted in excessive leakage. The lack of fusion was clearly evident and reasons for this failure are included in the discussion of the specific tube.

A third type of assembly that exhibited leakage was the solid-state bonded concept. This concept was initiated late in the program, and the development problems are not yet completely solved. Close control of the groove depth and shape, cleanliness, and fit-up tolerances will eliminate the leakage problems with this joint style.

Test Specimen Fabrication

The following paragraphs discuss the step by step procedure that was followed during the fabrication of the test specimens. The purpose of this discussion is to denote the materials, processes, and welding techniques that were used; and the problems that were encountered in the fabrication of each test specimen configuration. The test specimens will be discussed in three groups according to diameter. Except where noted herein all processes and welding techniques used were identical to those discussed in the preceeding section.

1/2 in. (1.27 cm) diameter.- All liners in this group were fabricated from commercially available seamless drawn tubing of desired wall thickness. The glass overwrap configuration was also common to all test specimens in this group. The overwrap was 0.030 in. (0.076 cm) thick and consisted of two layers of hoop wound glass separated by one longitudinal layer of 10 to 1 woven glass mat.

CFL6300605: The liners for this test specimen configuration were 0.007 in. (0.018 cm) wall, Inconel 718 tubing. The liners were cut to the proper length, then heat treated and age hardened prior to attaching the end fittings.

The AN flared end fittings for this design were made from 1/2 in. (1.27 cm) diameter stainless steel tubing. The fittings were machined to fit the inside diameter of the liner. Four longitudinal pins were then welded to the fittings to provide a torsional bond for the glass overwrap. The fittings were then attached to the liners by resistance welding using a stitch welder. A representative test specimen at this stage of fabrication is shown in fig. 46.
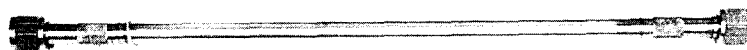
CFL 6300608

CFL 6300606

CFL 6300605

Fig. 46.- Resistance Welded 1/2 in. (1.27 cm) Diameter Tubes

The next steps in the fabrication process were the installation of strain gages and a low pressure helium leak check. The glass over-wrap was then applied and cured, and the test specimens were leak checked at operating pressure. This step completed the test specimen fabrication process. A completed test specimen of this configuration is shown in fig. 49 at the end of this section.

CFL6300606: The liners for this configuration were identical to the liners for the CFL6300605 configuration and were heat treated and age hardened by the same procedure.

The test joint for this configuration was a buttweld and was made from 1/2 in. (1.27 cm) Inconel 718 tubing. The end of the fitting was originally to be flared to provide a mechanical connection for test purposes, but difficulties with the Inconel 718 work hardening during flaring brought about a change to weld on threaded connectors. The end fittings were attached to the liner by a resistance weld using a stitch welder and the fabrication process was completed in the same manner as the previous configuration. After the overwrap and cure processes were completed a weld bead was added to the buttweld groove.

A representative test specimen, before overwrapping is shown in fig. 46 and a completed test specimen is shown in fig. 49.

CFL6300607: The liners for this configuration were the same as the previous configuration but were heat treated and aged after the end fittings were attached.

The end fittings for this configuration were 3/4 in. (1.90 cm) APCO flanges machined from a billet of Inconel 718. The fittings were attached to the liner by the fusion welding technique shown in fig. 25. The specimens were then heat treated and age hardened as an assembly. After completing the heat treatment, the strain gages were installed and a low pressure helium leak check was performed. The glass overwrap was then applied and cured. After the first layer of overwrap was applied, four pins were inserted into holes in each end fitting and the remaining two layers of glass were wrapped over these pins. The completed test specimen is shown in fig. 49.

CFL6300608: The liners for this test specimen configuration were 0.009 in. (0.023 cm) wall, stainless steel tubing.

The AN flared end fittings for this design were made from 1/2 in. (1.27 cm) diameter stainless steel tubing. A knurl was applied to the end fittings to provide both axial and torsional bonding of the glass overwrap and the fittings were machined to fit the inside diameter of the liners.

Fabrication of this test specimen configuration was then completed in the same manner as the CFL6300605 design.

2 in. (5.08 cm) diameter.- All liners in this group were fabricated from Inconel 718 sheet. The glass overwrap configuration for all specimens in this group was 0.030 in. (0.076 cm) thick and consisted of two layers of hoop wound glass separated by a longitudinal layer of 10 to 1 woven glass mat.

CFL6300609: The liners for this test specimen were fabricated from 0.005 in. (0.013 cm) thick Inconel 718 sheet. The sheet was cut in strips and formed into tubes by the helically wrapped-fusion weld technique. The tubes were then redrawn to a final thickness of 0.003 in. (0.0076 cm).

The test joint for this configuration was a buttweld and was machined from Inconel 718. Eight longitudinal pins were welded to the fittings to provide a torsional bond for the glass overwrap. The fittings were then machined to fit the inside diameter of the liner and attached to the liner by resistance welding.

The next steps in the fabrication process were the installation of strain gages and a low pressure helium leak check. The glass overwrap was then applied and cured. After the overwrap was cured the buttweld was completed and the specimens were leak checked at operating pressure. This step completed the fabrication process. A completed test specimen is shown in fig. 49.

CFL6300610: The liners for this test specimen configuration were fabricated from 0.003 in. (0.0076 cm) thick Inconel 718 which was heat treated and age hardened as flat foil. The liners were roll formed to the desired diameter with a slight overlap at the mating surfaces. The seam was then welded by resistance welding and the excess overlap was peeled from both the inside and outside of the tube on selected specimens.

The test joint for this configuration was a buttweld and was made from stainless steel tubing.

The remaining steps in the fabrication process for this test specimen design were identical to the CFL6300609 configuration. A completed test specimen is shown in fig. 49.

CFL6300611: The liners for this test specimen configuration were fabricated from 0.003 in. (0.0076 cm) Inconel sheet by the same method used on the CFL6300609 configuration.

The end fittings for this configuration were $2\frac{1}{2}$ in. (6.35 cm) APCO flanges machined from a billet of Inconel 718. The fittings were attached to the liners by fusion welding as shown in fig. 25. After the end fittings were attached to the liners the strain gages were installed and a low pressure helium leak check was performed. The glass overwrap was then applied and cured. After the first layer of overwrap was applied, pins were inserted into holes in each end fitting and the remaining two layers of glass were applied over the pins. The test specimens were then subjected to a helium leak check at operating pressure to complete the fabrication process. A completed test specimen is shown in fig. 49 at the end of this section.

CFL6300612: The liners for this test specimen configuration were fabricated from 0.006 in. (0.015 cm) thick Inconel 718 sheet and welded by straight seam fusion welding.

The end fittings for this configuration were stainless steel raised face flanges machined to the NASA serration configuration.

The flange shoulders were knurled to provide both an axial and torsional bond for the glass overwrap. On the original design the end fittings were attached to the liners by fusion welding as shown in fig. 37. This technique, when applied to members with vastly different heat capacities, produces a weld which is not structurally sound. Figure 47 shows this configuration with the failed weld and fig. 48 is a magnified photograph of the weld area showing a definite lack of fusion. Note that the roughness in the liner area is release agent that was applied before attempting to overwrap the tube. Although this design was recommended by several vendors, its strength is dependent on equal heat flow to both sides of the weld and this would reduce its strength to that of the stainless steel end fitting, about 40% of the strength of the Inconel liner. If the end fittings were made of high strength Inconel, this joint could be fabricated with equal heat areas and would probably be reliable. After fabricating one test specimen this method of attaching the end fittings to the liners was abandoned. The end fittings for the remaining test specimens of this design were attached to the liners by the solid-state bonding technique shown in fig. 29.

The remaining steps in the fabrication procedure for this configuration were the same as the CFL6300609 configuration except that no buttweld was required. A completed test specimen is shown in fig. 49.

5 in. (12.7 cm) diameter.- All liners in this group were fabricated from Inconel 718 sheet. The glass overwrap configuration was common to all test specimens in this group except for two specimens of the CFL6300615 configuration which had four layers of hoop wound glass. The overwrap was 0.040 in. (0.102 cm) thick and consisted of a layer of hoop wound glass, then a longitudinal layer of 10 to 1 woven glass mat, followed by two additional layers of hoop wound glass. The overwrap was applied and cured by the procedure previously discussed.

CFL6300613: The liners for this test specimen configuration were fabricated from 0.003 in. (0.0076 cm) thick Inconel 718 sheet. The material was heat treated and age hardened as flat foil. The liners were roll formed to the desired diameter and the seam was welded by resistance welding as shown in fig. 23.

The test joint for this configuration was a buttweld. The end fittings were roll formed from flat Inconel 718 sheet and seam welded. Sixteen longitudinal pins were welded to each end fitting to provide a torsional bond for the glass overwrap. The fittings were then machined to fit inside the liners and were attached to the liners by resistance welding. After the fittings were attached to the liners, end plug adaptors were welded to the fittings to provide a mechanical joint for test purposes.

The next steps in the fabrication process were the installation of strain gages and a low pressure helium leak check. The glass overwrap
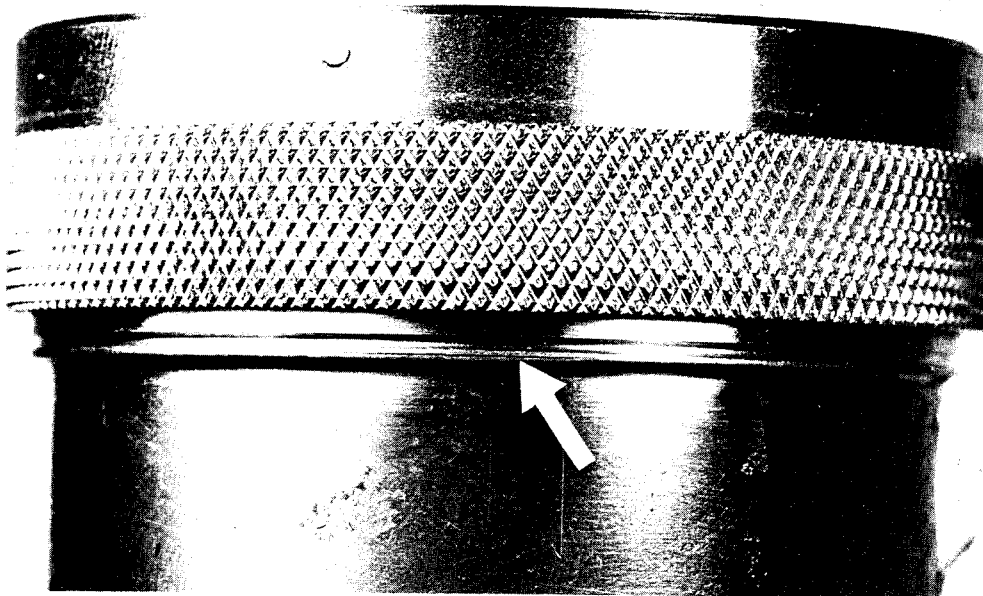
Fig. 47. - Cracked Weld Area,
Serial Number 85
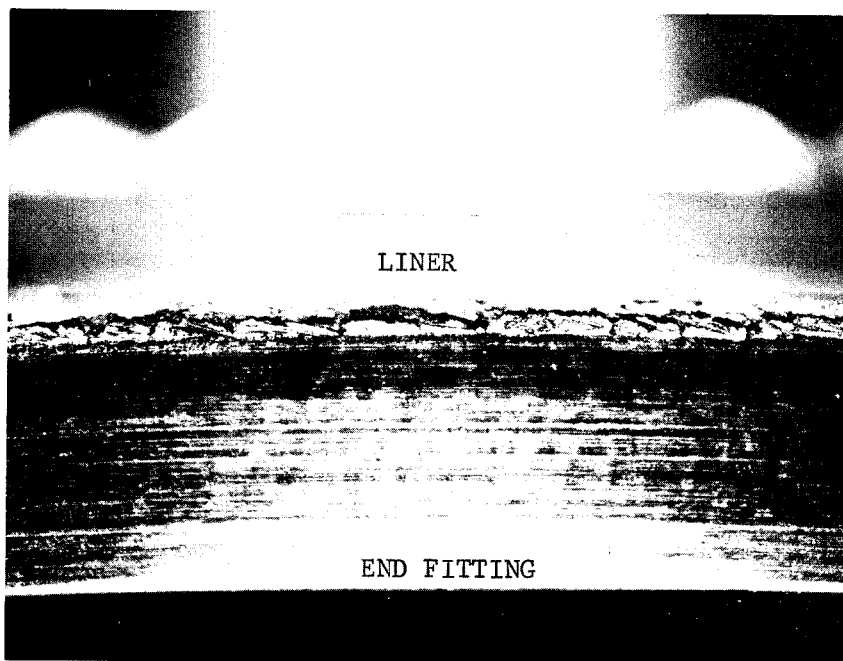
Fig. 48. - Photograph Showing Lack of
Fusion, Serial Number 85

was then applied and cured. The buttweld was then completed and the test specimen were leak checked at operating pressure. A completed test specimen is shown in fig. 49.

CFL6300614: The liners for this test specimen configuration were fabricated from 0.003 in. (0.0076 cm) thick Inconel 718 sheet. The liners were roll formed to the desired diameter and seam welded by fusion welding. After completing the seam weld, the liners were heat treated and age hardened before the end fittings were installed.

End fitting configuration and the remaining steps in the fabrication process for this test specimen design were identical to the CFL6300613 configuration. A completed test specimen is shown in fig. 49.

CFL6300615: The liners for this test specimen configuration were fabricated from 0.006 in. (0.015 cm) thick Inconel 718 sheet. The liners were roll formed to the desired diameter and seam welded by fusion welding. The liners were plenished after welding but were not heat treated.

The end fittings for this configuration were stainless steel raised face flanges machined to the NASA serration configuration. The end fittings were attached to the liners by fusion welding as shown in fig. 25. After the end fittings were attached to the liners, the strain gages were installed and a low pressure helium leak check was performed. The glass overwrap was then applied and cured. After the first layer of overwrap was applied, sixteen pins were inserted into holes in each end fitting and the remaining layers of glass were applied over the pins. The test specimens were then subjected to a helium leak check at operating pressure to complete the fabrication process.

The burst test pressure of the first two specimens of this design was below the acceptable level. The results of a failure analysis showed that as the liner elongated the end flange separated from the glass overwrap. This left the liner unsupported in this area and hence a premature hoop failure occurred. A photograph of this failure is shown in the test section of this report. The failure analysis also showed circumferential cracks in the glass overwrap indicating axial load transfer from the liner to the glass even though a release agent had been applied to the liner. The inability of the overwrap (all hoop wound glass on these two specimens) to absorb these loads contributed to the premature failure. This problem was corrected on the remaining test specimens by adding a doubler that extended past the end of the flange on each end of the liner and by including a layer of longitudinal glass in the overwrap configuration. As a result of these preliminary tests the planned all hoop glass overwrap on the CFL6300611 design was changed to include a layer of longitudinal glass.

CFL6300616: The liners for this test specimen configuration were fabricated of the same material and by the same method as the CFL6300615 configuration.

The end fittings for this configuration were stainless steel Conoseal flanges. The flanges were attached to the liners by the fusion weld technique as shown in fig. 37. The end fittings were knurled to provide both an axial and torsional bond for the glass overwrap. After the end fittings were attached to the liners, the strain gages were installed and a low pressure helium leak check was performed. The glass overwrap was then applied and cured and the specimens were leak checked at operating pressure. This step completed the fabrication process.

The burst test pressure of the first two specimens of this configuration was below the acceptable level. The premature failure was due to lack of strength in the weld.

Fabrication of Test Fixtures

The test fixtures were fabricated and installed in accordance with the system design after approval by the NASA-LeRC Project Manager. Fabrication was accomplished by the Engineering Model Shop and by the Cold Flow Laboratory. After fabrication, proof pressure or hydrostatic tests were accomplished to verify fixture structural integrity. All components and subsystems were then cleaned to Martin Marietta cleaning specifications for the appropriate fluid service. After installation, all fixtures were functionally tested to verify proper operation and leak checks were performed to verify fixture integrity and suitability for intended service.

Except for a modification required for the tube joint heat flux test, an existing calorimeter was used for all thermal testing. Fabrication of special tube containers that limited the axial temperature differential between the tube and the environment were added to the program to obtain more adequate thermal data.

Fabrication Costs

Future selection of composite tubes for cryogenic applications will be influenced by fabrication costs. Using the costs accrued during this program, including tooling, and other non-recurring costs, the financial obligations can be estimated. For clarity, these costs do not include quality control or cleaning and packaging although each will be required in production operations. Included in the costs are leak checks before and after overwrapping, a proof test, and all fabrication costs. A quantity of 12 tubes was chosen. The accompanying table summarizes these costs.

106

Tube dia		Tube length		Liner thickness final		Liner fab				Heat treat	Fitting style	Liner to fitting weld	Overwrap config	Cost per tube *
(in)	(cm)	(in)	(cm)	(in)	(cm)	Resistance	Seamless	Fusion	Fusion/redrawn					
0.5	1.27	48	121.9	.007	.018		X			X	Buttweld	Resistance	HLH	$120
0.5	1.27	48	121.9	.009	.023		X				Flat flange	Fusion	HLH	163
2.0	5.08	48	121.9	.003	.008	X				X	Buttweld	Resistance	HLH	247
2.0	5.08	48	121.9	.006	.015			X			Buttweld	Resistance	HLH	240
2.0	5.08	48	121.9	.003	.008				X		Flat flange	Fusion	HLH	291
5.0	12.7	48	121.9	.003	.008	X				X	Buttweld	Resistance	HLHH	462
5.0	12.7	48	121.9	.003	.008			X		X	Buttweld	Resistance	HLHH	456

*Including all materials, tooling, end fittings, fabrication and assembly costs.

Conclusions

Figure 49 includes photographs of all types of the finished assemblies. No major problems arose during fabrication except those already noted. All eleven remaining designs, and the concepts that they employ are usable and can be fabricated with a high reliability.

Recommendations

There exist several items that require further investigation but, in these sizes, these items can be resolved in a preproduction investigation. The items, regarding fabrication, which merit additional attention include:

1) Ability to provide leak free resistance welding of 1/2 in. diameter (1.27 cm) liners to end fittings;

2) Ability to provide leak free solid-state bonding;

3) Aesthetic improvement of the overwrap surface finish;

4) Extension of fabrication materials into those less susceptible to hydrogen embrittlement than Inconel 718; and,

5) Use of a more machinable alloy than Inconel 718 for fittings.

CFL 6300610

CFL 6300608
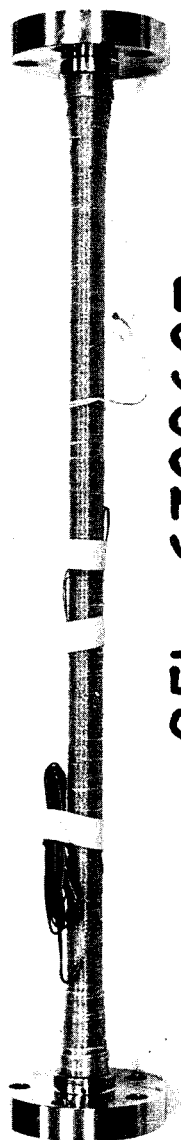
CFL 6300607

CFL 6300606

Fig. 49. - Photographs of Finished Test Specimen
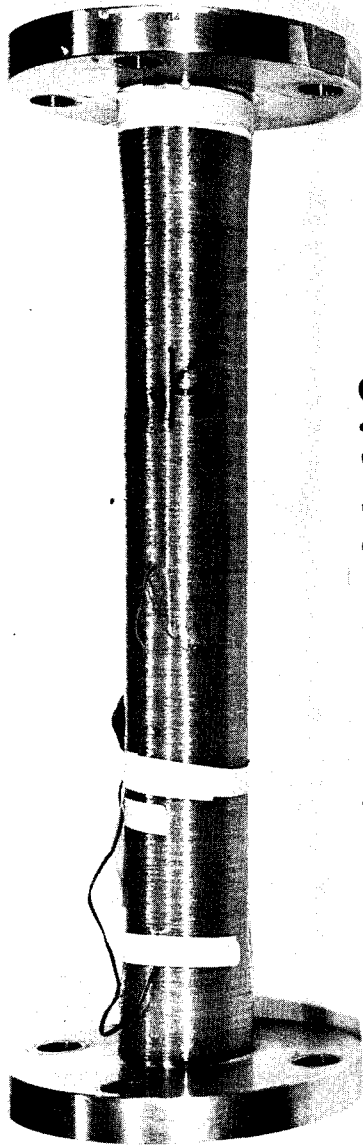
CFL 6300612

CFL 6300613

Fig. 49. - Photographs of Finished Test Specimen (Continued)

109
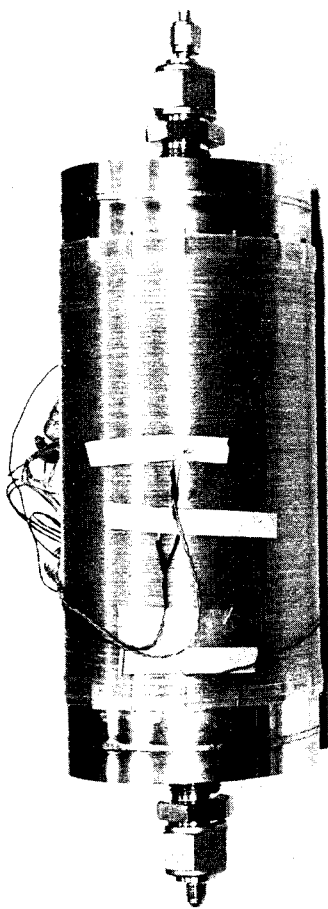
CFL 6300614

CFL 6300611
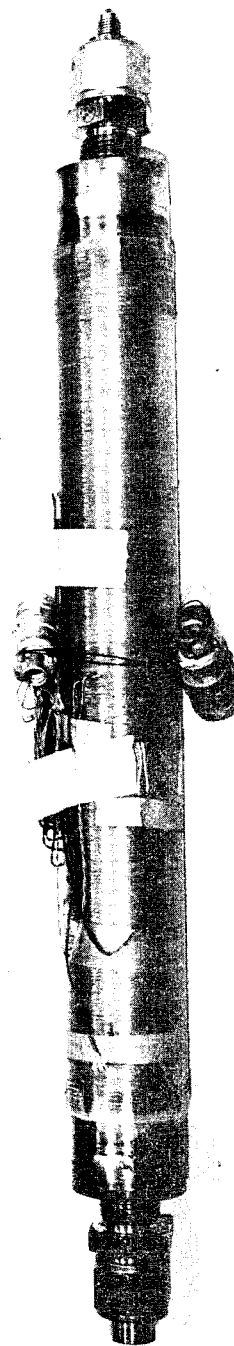
CFL 6300609

Fig. 49. - Photographs of Finished Test Specimen (Continued)
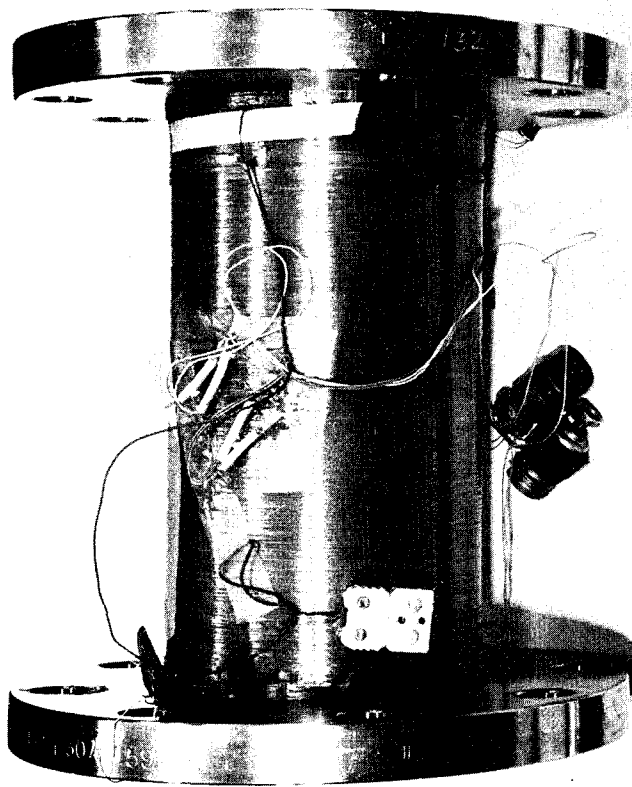
CFL 6300615
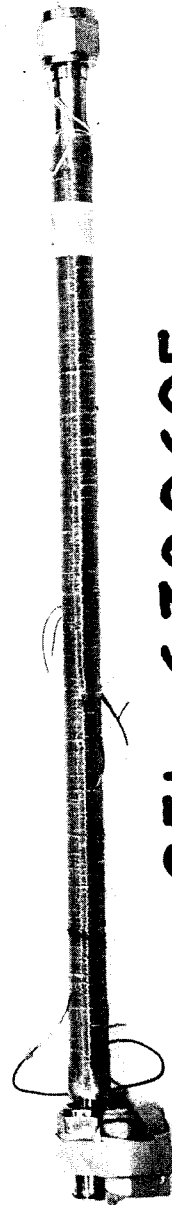
CFL 6300605

Fig. 49. - Photographs of Finished Test Specimen (Concluded)

111

TASK III-TESTING

The objectives of Task III were to (1) verify the structural integrity of the composite test specimens, (2) establish the thermal conductivity of the specimens in the axial direction as a function of temperature, and (3) establish a representative heat flux through the test specimen.

Test Plan

To satisfy the first objective of Task III, the following test program was to be conducted:

1) Burst tests - Specimens of each design were to be subjected to burst tests at ambient, liquid nitrogen, and liquid hydrogen temperatures. Two identical specimens were to be tested at each temperature;

2) Cycle tests - Specimens of each design were to be subjected to 200 pressure and temperature cycles from ambient to operating temperature and from zero psig to operating pressure. Two identical specimens were to be tested at operating temperatures of ambient, -320°F (78°K), and -423°F (20°K). The 2 and 5 in. (5.08 and 12.7 cm) specimens were to be cycled to an operating pressure of 200 psi (138 N/cm^2) and the 1/2 in. (1.27 cm) specimens were to be cycled to an operating pressure of 3000 psi (2068 N/cm^2);

3) Extended load tests - After completing pressure and temperature cycle testing, the test specimens were to be pressurized to operating pressure at operating temperature and held at these conditions for a period of 24 hr;

4) Torsion tests - After completing the extended load test, representative specimens were to be torsion-tested by applying torque along the centerline of the specimen until a failure of the liner or glass wrapping was evident; and,

5) Postcycle burst tests - The cycle test specimens that were not torsion tested were to be burst tested at their respective operating temperatures.

The second objective of Task III was to determine the thermal conductivity of the composite test specimens. This was to be accomplished by subjecting a small sample of each size test specimen to a bath of LN_2 or LH_2 at one end, a controlled heat source at the other end, and measuring the heat input or cryogen boiloff to establish the heat flux. Using this flux and a measured temperature difference across the specimen, an apparent thermal conductivity was to be calculated.

The third objective of Task III was to determine the heat flux through the tube/joint of representative test specimens. This objective was to be met by a test method very similar to the thermal conductivity test except that a complete test specimen would be used.

The Task III testing was completed with no significant deviation from the planned test program.

Facility and Instrumentation

All testing performed during this program was conducted at the Martin Marietta Denver Division facilities. Burst and cycle testing was conducted at the Cold Flow Laboratory and thermal testing was conducted at the Propulsion Research Laboratory.

Each test specimen was instrumented to provide biaxial strain measurement of the liner during burst and cycle testing. The strain gages were bonded to the outside of the liner at the midpoint prior to applying the glass overwrap. On particular test specimens, additional strain gages were mounted to measure the strain on the inside of the liner and/or the outside of the glass overwrap.

A thermocouple was also mounted on each test specimen for temperature measurement. The thermocouple was installed during glass overwrapping prior to applying the last layer of glass. Additional thermocouples were added to the test specimens that were subjected to thermal testing. These thermocouples were bonded to the outside of the glass overwrap.

During burst testing, the failure pressure of each test specimen was determined by continuously recording the output of a pressure transducer mounted on one end of the test specimen. Burst test temperatures were determined by recording the output of thermocouples located in the test environment plus the output of the thermocouple mounted on one of the four test specimens. The pressure in the test specimens during cycle testing was determined by continuously recording the output of

pressure transducers mounted on the inlet and outlet manifolds. During cycle testing the temperatures in the system were determined by recording the output of the thermocouples mounted on each test specimen plus the output of a thermocouple located at the inlet of each pair of test specimens or on the tubing spool connecting the two specimens.

For all burst tests the outputs of the pressure transducers, strain gages, and thermocouples were recorded on 6 channel Sanborn direct-writing recorders. During cycle testing, pressure and strain gage outputs were recorded on Sanborn recorders and thermocouple outputs were recorded by a Honeywell 24-channel multipoint recorder. A detailed description of the transducers and data acquisition system components is included as Appendix A.

Preliminary Testing

Concurrent with the Task I analysis effort, preliminary testing was performed to verify and supplement the analysis. These tests included thermal conductivity determination, helium permeation, fitting evaluations, overwrap gap determination, material tensile tests, and prototype liner burst tests.

Thermal conductivity tests for hollow glass fibers. - A limited test was conducted to obtain thermal conductivity data for a composite structural material of hollow glass fibers in an epoxy matrix. The objective of the test was to determine if the thermal conductivity of the hollow glass composite was significantly less than that of S-glass composites. The specimen configuration tested was a cylindrical tube section with glass fibers wrapped circumferentially. Two samples were tested at temperatures varying from 36 to 500°R (20 to 278°K).

Analysis of the test data shows that there is no appreciable difference in thermal conductivity between hollow glass fiber composites and solid S-glass composites.

Test method: After installation of the test equipment in the thermal test fixture discussed on page 184, the chamber was pumped down to approximately 10^{-4} torr (0.013 N/cm^2). The heat sink tank was then filled with liquid hydrogen and the system allowed to cool for approximately 24 hr. This permitted the system to reach a cold equilibrium condition and, at this point, power was applied to the lower heater. A power setting estimated to produce a differential temperature across the sample of approximately 30°R (16°K) was selected. Data were recorded every half hour until the temperatures of the system again stabilized. The power setting was then decreased to a value calculated to produce a differential temperature half that produced by the first power

114

setting. Again, the temperatures of the system were allowed to stabilize, with data taken every half hour.

Data reduction: The thermal conductivity of the specimen can be directly calculated from the steady-state test data (i.e., steady power input and constant end temperature). The transient data obtained during the warmup period were reduced with the aid of a computer program that includes corrections and compensations for energy losses through lead wires, effects of thermal masses, etc.

Results: The thermal conductivity calculated from the steady-state data indicates there is no measurable difference between hollow glass-fiber composites and solid S-glass-fiber composites. For comparison, the calculated thermal conductivity for hollow glass-fiber composite is $0.038 \frac{BTU}{ft\ hr\ ^{O}R} \left(0.00046 \frac{W}{m\ ^{O}K} \right)$ at $59\ ^{O}R$ $(33\ ^{O}K)$. This compares with a thermal conductivity of S-glass-fiber composite of $0.039 \frac{BTU}{ft\ hr\ ^{O}R} \left(0.00047 \frac{W}{m\ ^{O}K} \right)$ at $59\ ^{O}R$ $(33\ ^{O}K)$ discussed in reference 10. Since in all probability the thermal conductivities of the two composites will be similar at all temperatures, neither composite offers a thermal advantage.

Helium permeation test. - A 0.002-in. (0.005 cm) thick stainless steel liner which had been resistance-welded to form a 1.25 in. (3.2 cm) diameter tube, and then resistance-welded to modified conoseal end fittings, was subjected to a helium permeation test. The purpose of the test was to determine if, under prolonged exposure to pressurized helium, the helium would permeate the thin metal tube. At the end of a two week test period, no permeation was sensed by a helium mass spectrometer with a sensitivity of 3×10^{-10} scc/sec of helium.

Fitting evaluation tests. - A preliminary test program was conducted to evaluate the leakage characteristics of the selected end fittings and seals at cryogenic temperatures. The objectives of the test were to (1) determine the capability of the joints to provide essentially zero leakage when pressurized with helium to operating pressure at ambient and cryogenic temperatures, and (2) establish the retorque requirements for the joints.

Test equipment: The end fittings and seal combinations that were subjected to the preliminary evaluation test are described in Table 21.

TABLE 21. - EVALUATION TEST JOINTS

Joint description	Size		Seal type	Seal material
	in.	cm		
V-Band conoseal	6	15.2	Conoseal	Aluminum, stainless steel
NASA flange-150 lb	5	12.7	Flat gasket	1100 Dead soft aluminum
ASA flange-150 lb	5	12.7	Flexatallic gasket	Stainless steel and Teflon
APCO flange	2½	6.35	Delta ring	Aluminum, stainless steel
NASA flange-150 lb	2	5.08	Flat gasket	1100 Dead soft aluminum
ASA flange-150 lb	2	5.08	Flexatallic gasket	Stainless steel and Teflon
APCO flange	3/4	1.9	Delta ring	Aluminum, stainless steel
AN fitting	1/2	1.27	Del seal	Aluminum, copper

The joints to be tested were assembled in the test fixture as shown in fig. 50. The 2 and 5 in. (5.08 and 12.7 cm) joints were tested simultaneously at an operating pressure of 200 psi (138 N/cm^2). The 3/4 and 1/2 in. (1.9 and 1.27 cm) joints were tested at an operating pressure of 3000 psi (2068 N/cm^2).

Test procedure: Before assembly, the sealing surfaces of each fitting and seal were inspected for visible signs of poor workmanship or handling damage. The joints were then assembled in accordance with the manufacturers recommendations or standard practices. The system was then pressurized with gaseous helium to operating pressure and leak-checked with a helium mass spectrometer using the probe test method. After completing the ambient leak-checks, the joints were cooled down and stabilized at cryogenic temperature by flowing liquid nitrogen through the system. Each joint was then helium-leak-checked at cold temperature. The system was then warmed up to ambient temperature by purging with gaseous nitrogen and the helium leak check was repeated. The torque on the flange bolts and/or AN fittings was then checked to determine if the bolts had loosened. The bolts and/ or fittings were then retorqued and the test sequence was repeated.
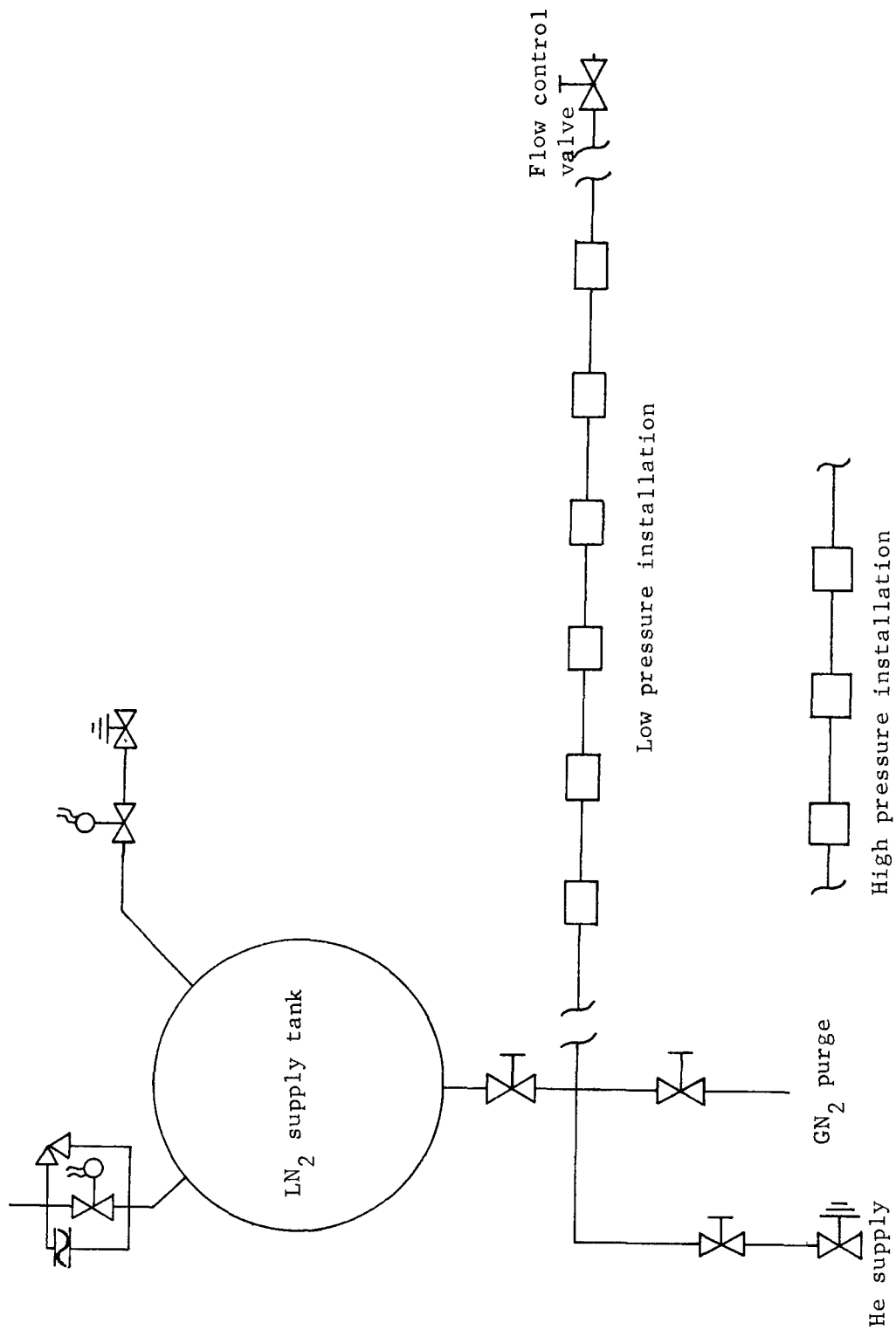
Fig. 50. - Test Fixture Schematic, Preliminary Fitting Evaluation Test

Results: The results of the evaluation test of the selected joints are presented in the following paragraphs:

3/4 in. (1.90 cm) APCO flange. - This joint was assembled with the flange bolts torqued evenly to 275 in.-lb (31 N-m). The joint was then subjected to three ambient and one cold pressure cycle. The joint showed a slight leak when pressurized cold. The joint was retorqued and leak-checked at ambient and cold temperature with zero leakage. The joint was then subjected to five pressure and temperature cycles, followed by ambient and cold leak checks with zero leakage. Bolt torque was checked and found to be relaxed to 225 in.-lb (25 N-m). The joint was then subjected to an additional 20 pressure and temperature cycles. Leak checks at ambient and cold temperature after the tenth and twentieth cycles showed zero leakage. The performance of this joint was considered satisfactory and testing was discontinued.

1/2 in. (1.27 cm) AN flared fitting. - This fitting, assembled without a Del seal, and torqued to the maximum recommended torque of 750 in.-lb (85 N-m) plus one flat on the B-nut, would not seal when pressurized to 3000 psi (2068 N/cm^2) with helium at ambient temperature. Testing of this joint was therefore discontinued.

The 1/2 in. (1.27 cm) AN fitting assembled with an aluminum Del seal showed leakage at ambient temperature when torqued to the maximum recommended torque of 750 in.-lb (85 N-m) plus one flat of the B-nut. The fitting was disassembled and the sealing surfaces of the union and flare were polished. The fitting was then reassembled with new Del seals and showed zero leakage at ambient and cold temperature when torqued at 750 in.-lb (85 N-m) plus one flat. The fitting was then subjected to 10 pressure and temperature cycles and showed leakage at ambient temperature. The torque on the fitting was checked and found to be relaxed to 650 in.-lb (73 N-m). The fitting was retorqued but the leakage was not stopped. Additional testing of a new assembly showed that the retorquing operation after pressure and temperature cycling would eliminate leakage at ambient temperature but not at cold temperature. The testing of this joint was discontinued.

The 1/2 in. (1.27 cm) AN fitting assembled with a copper Del seal showed zero leakage when torqued at 750 in.-lb (85 N-m). This fitting showed a slight leak at cold temperature after completing five pressure and temperature cycles. The torque on the fitting was checked and found to be relaxed to 600 in.lb (68 N-m). The fitting was retorqued to 750 in.-lb (85 N-m) and completed 10 pressure and temperature cycles with zero leakage and no further decrease in torque. The performance of the joint was considered satisfactory and testing was discontinued.

2½ in. (6.35 cm) APCO flange. - This joint was assembled
with a stainless steel delta ring seal, with 275 in.-lb (31 N-m)
bolt torque, and the joint was then subjected to pressure and
temperature cycling. After completing 10 pressure and temperature
cycles, the joint showed a slight leak when leak-checked at cold
temperature. Bolt torque was checked and found to be relaxed to
240 in.-lb (27 N-m). The joint was retorqued and subjected to
an additional 10 pressure and temperature cycles. Leak checks at
ambient and cold temperatures showed zero leakage. The performance
of this joint was considered satisfactory and testing was discon-
tinued.

6 in. (15.2 cm) Conoseal. - This joint was assembled with a
stainless steel conoseal gasket and the clamp T-bolt was torqued
to 170 in.-lb (19 N-m). The joint was then subjected to pressure
and temperature cycling. After completing five pressure and temp-
erature cycles, the torque on the T-bolt was checked and found to
be relaxed to 150 in.-lb (17 N-m). The joint showed zero leakage
when leak-checked at ambient and cold temperature. The unchanged
joint was then subjected to 10 additional pressure and temperature
cycles. Leak checks at ambient and cold temperatures after these
cycles showed zero leakage. The performance of this joint was con-
sidered satisfactory and testing was discontinued.

2 and 5 in. (5.08 and 12.7 cm) ASA flanges. - These joints
were assembled with Flexatallic gaskets and the flange bolts were
torqued in accordance with vendor recommendations to provide the
proper gasket load. The joint would not seal when pressurized
with helium at 200 psi (138 N/cm^2) and ambient temperature. Bolt
torque was then increased to the maximum recommended values but
the joint still did not seal. Testing of this joint was there-
fore discontinued.

2 and 5 in. (5.08 and 12.7 cm) NASA flanges. - The configura-
tion of these flanges during initial testing was full face serration
[11 serrations on the 2 in. (5.08 cm) flange and 14 serrations on
the 5 in. (12.7 cm) flange.] The flanges were assembled with a
1/8 in. (0.3 cm) soft aluminum (1100-0) gasket and the flange bolts
were torqued evenly to 360 in.-lb (41 N-m) for the 2 in. (5.08 cm)
and 540 in.-lb (61 N-m) for the 5 in. (12.7 cm) joint. After five
pressure and temperature cycles, the joints leaked. The bolt torque
was then increased and the pressure and temperature cycles were re-
peated with the same results. This process was repeated, increasing
the bolt torque in increments to a maximum of 1,800 in.-lb (203 N-m).
The joint showed leakage after cycling at each torque level. The
test was repeated with new gaskets with similar results.

The gaskets were then modified by reducing the outside dia-
meter so the gasket would contact only four of the flange serrations.
The joints were assembled with the modified gaskets and the flange
bolts were torqued to 1,800 in.-lb (203 N-m). The joints were then
subjected to one pressure and temperature cycle and retorqued. This
process was repeated until the torque value did not relax more than
60 in.-lb (7 N-m), a total of five retorquing operations. The joints
were then subjected to 16 pressure and temperature cycles with zero
leakage at ambient and cold temperature. The performance of the
joints was then considered satisfactory and testing was discontinued.

The results clearly indicate that not all joint configurations
are acceptable. From previous discussions, however, it is noted
that configurations selected (see Fig. 31) for this program utilize
sound joints.

Overwrap tension tests. - A series of NOL rings were fabri-
cated and tested. The primary purpose of the test was to verify
the gap or interference between the glass and an inflexible mandrel.
The rings were wrapped on a 5.753 in. (14.613 cm) diameter thick
walled stainless steel cylinder. One set of rings was all hoop
wrap, 3 layers at 16 threads/inch (6.3 threads/cm), and wrap tension
varying from 2 lb (8.9 N) per 20 ends up to 14 lb (62 N) per 20
ends. The other set of rings was a combination of hoop and axial
wrap with a single axial wrap in between hoop layers (3 total layers).
The threads per inch and tension were the same as the other set of
rings.

After winding, the cylinders were oven-cured 2 hr at 200°F
(367°K), 2 hr from 200 to 350°F (367 to 450°K), and 4 hr at 350°F
(450°K). After cure, the mandrel was cooled in LN$_2$ to remove the
cylinders. Rings, 1/4 in. (0.64 cm) wide, were machined from the
cylinders. A photograph of these rings is shown below.
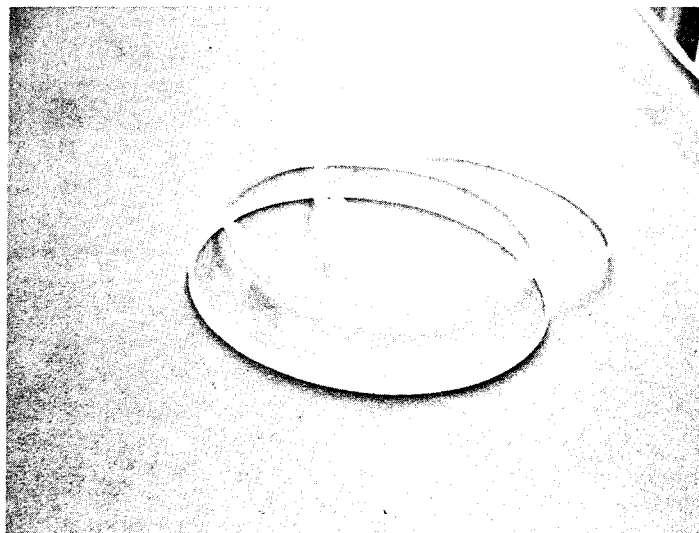
The inside diameter data can be used to determine the interference fit between the overwrap and a metal liner. Internal pressure in the thin liner may be used to offset this interference, or any part of it, after fabrication. For example, if all hoop, 6 lb (27 N)/ 20 end tension was used, the interference would be 0.003 in (0.008 cm) on the diameter. If internal pressure could be applied so that the liner is strained 0.0015 in. (0.004 cm) after overwrapping (prior to cure), then relief of the pressure after cure would result in no gap or interference. The springback data in the following table is a measurement of the distance between the ends of the ring after the ring is cut as shown. The minus sign indicates overlap.
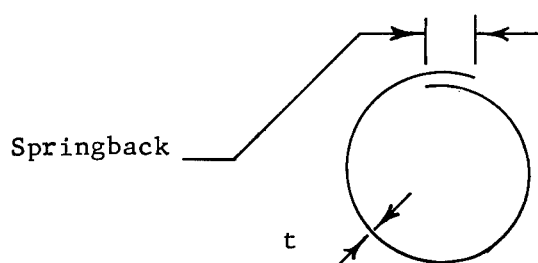
These data can be used to determine the bending stress in the overwrap according to

$$\sigma_{Bending} = E\,\epsilon$$

where   E is approximately 9.0×10^6 psi (6.2×10^6 N/cm^2) for all the hoop rings and 7.0×10^6 psi (4.8×10^6 N/cm^2) for the mixed rings

and

$$\epsilon = Strain = \frac{t\left(D_1 - D_2\right)}{D_1 D_2}$$

where D_1 is the original diameter at the midsurface of the ring and D_2 is the diameter after the ring is cut. Since D_2 is difficult to measure, we can compute it as

$$D_2 = D_1 - \frac{(Springback + Cut\ Width)}{\pi}$$

where the cut width is the width of the saw blade which was 0.03 in. (0.08 cm).

The following tables show the pertinent data on these rings.

Wrap	Wrap Tension (lb.)	Inside diameter (in.) of uncut ring.	Springback (inches)	Bending stress (psi)
All hoop	2	5.754	-0.55	1620
All hoop	6	5.750	-0.55	1530
All hoop	10	5.746	-0.76	2130
All hoop	14	5.743	-0.98	2760
Hoop/axial/hoop	2	5.753	-0.84	1830
Hoop/axial/hoop	6	5.750	-1.10	2420
Hoop/axial/hoop	10	5.747	-1.37	3040
Hoop/axial/hoop	14	5.744	-1.46	3260

Wrap	Wrap Tension (N)	Inside diameter (cm) of uncut ring	Springback (cm)	Bending Stress (N/cm^2)
All hoop	9	14.615	-1.40	1120
All hoop	27	14.605	-1.40	1050
All hoop	44	14.595	-1.93	1470
All hoop	62	14.587	-2.49	1900
Hoop/axial/hoop	9	14.613	-2.13	1260
Hoop/axial/hoop	27	14.605	-2.79	1670
Hoop/axial/hoop	44	14.597	-3.48	2100
Hoop/axial/hoop	62	14.590	-3.71	2250

Material tensile tests. - A literature search for the tensile properties of ultrathin metal foils was not successful. In recognition of the theory that surface conditions in thin foil may have a large effect on the tensile stress allowables, a series of tests were performed to determine the design allowables. Associated with the base metal strengtns, some information regarding weld strengths and mixed metal weld strengths (weld 301 CRES to Inconel 718) was desired. The combinations of welding, heat treating, and mixed metal welds were selected as typical of the combinations that were to be used for liner and fitting fabrication in this contract.

Test specimens: A number of tensile test specimens were fabricated using both resistance-welding and fusion-welding techniques. The resistance-welded specimens are listed in table 22 and the configuration of these specimens is shown in fig. 51. The fusion-welded specimens are listed in table 23 and the configuration of these specimens is shown in fig. 52. Specimens of the parent metals were also tested to provide a basis for comparison.

Test results: The test program for Inconel 718 included annealed and heat-treated specimens in fusion-welded, resistance-welded, and base metal configurations. The indicated yield stress (the area of interest in this program), under properly controlled heat-treat and aging, indicates the fusion-weld (butt weld, no filler) will develop more than 90% of the base metal yield strength. The resistance-weld (continuous spot welds) method results in 100% of the base metal strength even if welded after the heat treatment. A yield allowable of 160,000 psi (110,000 N/cm^2) and an ultimate tensile allowable of 176,000 psi (121,000 N/cm^2) will be used for ambient temperature allowables.

The test program for 301 CRES indicates a considerable reduction in tensile strength due to resistance-welding (75% of base metal) and an even larger reduction in tensile strength after fusion welding (66% of base metal). After fusion welding 301 CRES to Inconel 718, the 301 CRES failed at 54% of base metal strength.

The data for 21-6-9 CRES contains considerable scatter, which was attributable to test methods. A tensile allowable of 112,000 psi (77 000 N/cm^2) seems appropriate even when joined by fusion welding [the fusion weld samples were tested as the typical "dog bone" configuration while the other data were obtained from straight 1/2 in. (1.27 cm) wide samples].

The results of the testing are tabulated in table 24 and 25.

TABLE 23. -
FUSION-WELDED TENSILE TEST COMBINATIONS

Item	Material Size (in.)	Material Size (cm)	Material
1	0.0025 / 0.0025	0.0063 / 0.0063	718 Inconel / 718 Inconel
2	0.004 / 0.004	0.010 / 0.010	718 Inconel / 718 Inconel
3	0.004 / 0.004	0.010 / 0.010	718 Inconel / 301 CRES
4	0.002 / 0.002	0.005 / 0.005	21-6-9 / 21-6-9
5	0.002 / 0.0025	0.005 / 0.0063	21-6-9 / 301 CRES
6	0.004 / 0.004	0.010 / 0.010	301 CRES / 301 CRES

TABLE 22. -
RESISTANCE-WELDED TENSILE TEST COMBINATIONS

Item	Material Size (in.)	Material Size (cm)	Material
1[a]	0.0025 / 0.0025	0.0063 / 0.0063	718 Inconel / 718 Inconel
2	0.0025 / 0.0025	0.0063 / 0.0063	718 Inconel / 718 Inconel
3	0.004 / 0.004	0.010 / 0.010	718 Inconel / 718 Inconel
4	0.004 / 0.004	0.010 / 0.010	718 Inconel / 301 CRES
5	0.002 / 0.002	0.005 / 0.005	21-6-9 CRES / 21-6-9 CRES
6	0.002 / 0.0027	0.005 / 0.007	21-6-9 CRES / 301 CRES
7	0.004 / 0.004	0.010 / 0.010	301 CRES / 301 CRES
8[b]	0.004 / 0.0025 / 0.004	0.010 / 0.0063 / 0.010	301 CRES / 718 Inconel / 301 CRES

a   Items 1 and 2 to be welded at two different weld heats in the optimum range.

b   See fig. 51 detail A

Plan View

4" ± 1/16   4" ± 1/16

Cut Line For Coupons (3 Per Weld Sample)

1"   5"

See Note [a]

Notes:

a. Weld sample butting edges may be prepared in this fashion prior to welding. After welding weld area to be nearly flush with parent sheet surfaces.

b. Weld samples identified in Table 23.

Fig. 52.- Fusion - Welded Tensile Test Coupon Configuration[b]

Plan View

4¼" ± 1/16   ¢ of Weld   4¼" ± 1/16

1"   5"

Cut Line For Test Coupons (3 Per weld sample)

718 Inconel

H[b]   3/8   Detail A[c]

Notes:

a. Materials and size to be welded are listed in Table 22.

b. (H) for single weld not to exceed 1/4 in.

c. Detail A applys to item no. 8, Table 22.

Fig. 51.- Resistance - Welded Tensile Test Coupon Configuration[a]

TABLE 24. — TENSILE TEST RESULTS

MATERIAL	THKNS.	METHOD OF JOINING	CONDITION	σ_u (KSI)	NO. OF SAMPLES	SCATTER KSI	σ_y (KSI)	NO. OF SAMPLES	SCATTER KSI	FAILURE ZONE[c]	NOTES
Inconel 718	.0025	None	Heat Treated & Aged[a]	180.9	6	+1.8 / -2.4	164.1	6	+4.4 / -3.2		
Inconel 718	.0025	None	Heat Treated & Aged[b]	175.2	3	+10.8 / -8.8	154.7	3	+6.2 / -5.1		
Inconel 718	.0025	Fusion Welded	Heat Treated & Aged[a]	182.6	2	+0.9 / -3.3	168.2	2	±2.7	1-HAZ, 1-Base Metal	
Inconel 718	.0040	None	Heat Treated & Aged[a]	180.2	3	+3.3 / -4.2					
Inconel 718	.0040	None	Heat Treated & Aged[b]	170.0	2	±5.1	151.3	2	±3.3		
Inconel 718	.0040	Fusion Welded	Heat Treated & Aged[a]	178.0	1		156.0	1		HAZ	Welded After H.T. & Aging
Inconel 718	.0040	Resistance Welded	Heat Treated & Aged[b]	176.7	3	+3.0 / -2.3	164.4	3	+2.3 / -1.6	HAZ	
Inconel 718	.0025	None	Annealed	71.3	3	+1.8 / -1.3	52.8	3	+1.8 / -2.0		
Inconel 718	.0025	Resistance Welded	Annealed	77.0	5	+3.5 / -3.6	49.9	5	+0.7 / -1.7	1-HAZ, 4-Base Metal	
Inconel 718	.0025	Fusion Welded	Annealed	88.6	4	+6.0 / -7.1	49.1	4	+1.7 / -1.1	Base Metal	
Inconel 718 and 301 CRES (.004")	.0025	Resistance Welded	Annealed	78.7	3	+5.1 / -3.7	51.0	3	±0.6	Base Metal	Inconel 718 Failed
Inconel 718	.0040	None	Annealed	94.8	2	±1.8	59.8	3	+0.4 / -0.2	Base Metal	
Inconel 718	.0040	Fusion Welded	Annealed	114.1	3	+3.7 / -2.7	54.9	3		Base Metal	
Inconel 718	.0040	Resistance Welded	Annealed	86.7	1		58.7	1		Base Metal	
Inconel 718 and 301 CRES (.004)	.0040	Resistance Welded	Annealed	89.5	2	±6.1	61.0	2	±1.8	Base Metal	
21-6-9	.0020	None		100.5	2	+3.5 / -1.9	82.2	1			Not Dog Bones
21-6-9	.0020	Resistance Welded		96.9	6	+1.2 / -1.9	75.4	4	+1.6 / -1.1	1-HAZ, 5-Base Metal	Not Dog Bones
21-6-9	.0020	Fusion Welded		112.1	3	+2.5 / -4.3	73.0	3	+0.3 / -0.2	2-HAZ, 1-Base Metal	
21-6-9 and 301 CRES (.0025)	.0020	Fusion Welded		117.1	3	+4.8 / -2.7	78.0	3	+1.0 / -1.6	HAZ	21-6-9 Failed
21-6-9 and 301 CRES (.0025)	.0020	Resistance Welded		108.8	1		84.6	1		HAZ	21-6-9 Failed
301 CRES	.0040	None	Full Hard	206.9	2	±1.6					
301 CRES	.0040	Fusion Welded	Full Hard	135.6	3	+5.2 / -5.8	108.0	3	+4.7 / -2.5	HAZ	
301 CRES	.0040	Resistance Welded	Full Hard	153.2	5	+13.5 / -8.2				HAZ	
301 CRES and Inconel 718 (.0040)	.0040	Fusion Welded	Full Hard	105.6	3	+4.4 / -2.7				HAZ	301 CRES Failed

a Heat treat was performed by Vac-Hyd Processing Corp. The heat treatment was performed in a vacuum furnace at 5 x 10^{-4} Torr as follows:
   (1) 1950° ± 15°F for 10 minutes; (2) Rapid cooled to room temperature; (3) Aged at 1400° ± 15°F for 10 hours;
   (4) Furnace cooled to 1200° ± 15°F and held at this temperature until total aging time is 20 hours.
   The samples were wrapped in a .001 inch tantalum foil to retain the bright finish on the Inconel.

b Heat treat was performed by the Martin Marietta Corporation. The heat treatment was performed in a furnace without vacuum capabilities.
   (1) 1325° ± 15°F for 8 hours; (2) Furnace cooled to 1250° ± 15°F; (3) Held at 1150° ± 15°F for 18 hours.
   The samples were wrapped in a .001 inch stainless foil to prevent surface oxidation. However, oxidation of surface did occur.

c HAZ = Heat Affected Zone.

MATERIAL	TKNS.	METHOD OF JOINING	CONDITION	$\sigma_u \times 10^{-3}$ N/cm²	NO. OF SAMPLES	SCATTER N/cm² $\times 10^{-3}$	$\sigma_y \times 10^{-3}$ N/cm²	NO. OF SAMPLES	SCATTER N/cm² $\times 10^{-3}$	FAILURE ZONE[c]	NOTES
Inconel 718	0.006	None	Heat Treated & Aged[a]	124.7	6	+1.2/-1.7	113.1	6	+3.0/-2.2		
Inconel 718	0.006	None	Heat Treated & Aged[b]	120.8	3	+7.4/-6.0	106.7	3	+4.3/-3.5		
Inconel 718	0.006	Fusion Welded	Heat Treated & Aged[a]	125.9	2	+0.6/+2.3/-2.9	116.0	2	+1.9	1-HAZ, 1-Base Metal	
Inconel 718	0.010	None	Heat Treated & Aged[a]	124.2	3						
Inconel 718	0.010	None	Heat Treated & Aged[b]	117.2	2	+3.5	104.3	2	+2.3		
Inconel 718	0.010	Fusion Welded	Heat Treated & Aged[a]	122.7	1		108.0	1		HAZ	Welded After H.T. & Aging
Inconel 718	0.010	Resistance Welded	Heat Treated & Aged[b]	121.8	3	+2.0/-1.6	113.3	3	+1.6/-1.1	HAZ	
Inconel 718	0.006	None	Annealed	49.2	3	+1.2/-0.9	36.4	3	+1.2/-1.4		
Inconel 718	0.006	Resistance Welded	Annealed	53.1	5	+2.4/-2.5	34.4	5	+0.5/-1.2	1-HAZ, 4-Base Metal	
Inconel 718	0.005	Fusion Welded	Annealed	61.1	4	+4.1/-4.9	33.8	4	+1.1/-0.8	Base Metal	
Inconel 718 and 301 CRES (.004")	0.006	Resistance Welded	Annealed	54.3	3	+3.5/-2.6	35.2	3	+0.4	Base Metal	Inconel 718 Failed
Inconel 718	0.010	None	Annealed	65.4	2	+1.2/-1.9	41.2	3	+0.1/-0.1	Base Metal	
Inconel 718	0.010	Fusion Welded	Annealed	78.7	3	+2.6/-1.9	37.9	3	+0.3/-0.1	Base Metal	
Inconel 718	0.010	Resistance Welded	Annealed	59.8	1		40.5	1		Base Metal	
Inconel 718 and 301 CRES (.004)	0.010	Resistance Welded	Annealed	61.7	2	+4.2	42.1	2	+1.2	Base Metal	
21-6-9	0.005	None		69.3	2	+2.4	56.7	1			Not Dog Bones
21-6-9	0.005	Resistance Welded		66.8	6	+0.8/-1.3	52.0	4	+1.1/-0.8	1-HAZ, 5-Base Metal	Not Dog Bones
21-6-9	0.005	Fusion Welded		77.3	3	+1.7/-3.0	50.3	3	+0.2/-0.1	2-HAZ, 1-Base Metal	
21-6-9 and 301 CRES (.0025)	0.005	Fusion Welded		80.7	3	+3.3/-1.9	53.8	3	+0.7/-1.1	HAZ	21-6-9 Failed
21-6-9 and 301 CRES (.0025)	0.005	Resistance Welded		75.0	1		58.3	1		HAZ	21-6-9 Failed
301 CRES	0.010	None	Full Hard	142.7	2	+1.1					
301 CRES	0.010	Fusion Welded	Full Hard	73.5	3	+3.6/-4.0	74.5	3	+3.2/-1.7	HAZ	
301 CRES	0.010	Resistance Welded	Full Hard	105.6	5	+9.3/-5.7				HAZ	
301 CRES and Inconel 718 (.0040)	0.010	Fusion Welded	Full Hard	72.8	3	+3.0/-1.9				HAZ	301 CRES Failed

a   Heat treat was performed by Vac-Hyd Processing Corp. The heat treatment was performed in a vacuum furnace at 0.07 $\times 10^{-4}$ N/cm² as follows:
(1) 1350° ± 8°K for 10 minutes; (2) Rapid cooled to room temperature; (3) Aged at 1042° ± 8°K for 10 hours;
(4) Furnace cooled to 930° ± 8°K and held at this temperature until total aging time is 20 hours.
The samples were wrapped in a 0.0025 cm tantalum foil to retain the bright finish on the Inconel.

b   Heat treat was performed by the Martin Marietta Corporation. The heat treatment was performed in a furnace without vacuum capabilities.
(1) 1000° ± 8°K for 8 hours; (2) Furnace cooled to 960° ± 8°K; (3) Held at 902° ± 8°K for 18 hours.
The samples were wrapped in a 0.0025 cm stainless foil to prevent surface oxidation. However, oxidation of surface did occur.

c   HAZ = Heat Affected Zone.

Prototype liner burst test. - Two existing 1.25 in. (3.2 cm)
diameter tubes were overwrapped with three layers of hoop-wound
S/HTS glass with a 58-68R resin system and subjected to a burst
test. The purposes were to (1) determine if 2 lb (8.9 N) of tension
for 20 ends resulted in a satisfactory overwrap configuration, (2)
determine if 2 lb (8.9 N) of tension would crush an unsupported
0.002 in. (0.005 cm) thick liner, (3) determine if 2 lb (8.9 N) of
tension would crush a supported (by internal GN_2 pressure) 0.002
in. (0.005 cm) thick liner, (4) resolve any fabrication problems,
(5) determine the burst pressure and failure mode, and (6) determine
if cure temperatures would create a buckling failure in the liner.

The fabrication and test program was considered very successful.
The tube that was overwrapped without internal pressure was bowed
considerably during and after overwrap in the area of the longitudi-
nal resistance weld. The addition of internal pressure during
winding and cure eliminated this bowing. The cure temperature did
not cause any buckling of the thin liner. The burst pressures of
the test items were 1150 and 1175 psi (793 and 810 N/cm^2). This
was a hydrostatic, ambient temperature, test at a pressure rise rate
of about 400 psi (276 N/cm^2) per minute. The calculated burst pres-
sure was 950 psi (655 N/cm^2) without considering any longitudinal
glass strength. The additional strength is attributed to the glass
bond and its contribution to the allowable burst pressure. The
failure mode was at the hoop resistance weld heat-affected zone (see
fig. 53 and 54). The disappointing feature of the 2 lb (8.9 N)
tension/20 ends overwrap is a generally poor appearance. The tube
handling characteristics are good and a technician will not damage
the liner with normal handling abuse. A side benefit of the test was
that the one tube liner, badly wrinkled during liner fabrication,
did not fail as a result of these wrinkles.

Fig. 54. - Tube After Overwrap and Burst

DA051400

Fig. 53. - Tubing Liner Showing Resistance Welds

Burst Testing

The specific objectives of the burst test program were to (1) validate the assumptions made during the structural analysis, (2) determine and/or compare the efficiencies of the fabrication methods including resistance welds, fusion welds, and solid-state bonding, (3) determine the burst pressure of the test specimens as a function of temperature, and (4) verify the structural integrity of the end joints.

Test fixtures. - A schematic diagram of the test fixture used for ambient burst testing of the low pressure test specimens is shown in fig. 55. The test specimen and the ullage tank were installed in a vertical attitude with the top of the ullage tank slightly higher than the top of the test specimen. Vent valves were installed on the tops of the ullage tank and test specimen to bleed air out of the system during water fill. Gaseous nitrogen from the 5000 psi (3447 N/cm^2) facility storage was used as the pressurization medium.

The test fixture used for ambient burst testing of the high-pressure test specimens is shown schematically in fig. 56. The test specimen was installed in a vertical attitude so the top of the specimen was lower than the water level in the water supply tank. The fitting at the inlet to the instrumented gage was loosened to bleed the air out of the test specimen during water fill. The original design of the test fixture used a hydrostatic pump to increase the pressure in the test specimen. During the initial testing, it was found that the pressure rise rate produced by this pump could not be adequately controlled when the test item was leak free. The hydrostat pump was therefore replaced with a gas booster pump on which the output pressure could be controlled by regulating the supply pressure. Gaseous nitrogen was used as the pressurization medium.

A schematic of the test fixture used for all cryogenic burst testing is shown in fig. 57. The test fixture was designed to permit the simultaneous testing of four test specimens. The test specimens were separated by barriers so the bursting of one specimen would not damage the adjacent specimens. The test specimens were suspended from the cryostat lid in a vertical attitude with the pressurization and pressure transducer lines passing through the lid. Isolation valves were installed in the pressurization lines so one test specimen could be pressurized to burst without pressurizing the other specimens. An orifice and bypass valve were also installed in the pressurization line to allow a high gas flow into the test specimens during cool-down and fill and to restrict the flow during pressurization. Thermocouples were located in the cryostat to monitor liquid level during fill and test. Gaseous nitrogen was used as the pressurization medium during tests at liquid nitrogen temperature and gaseous hydrogen was used as the pressurization medium during tests at liquid hydrogen temperature.

Gage

GN₂ Shutoff
Valve

Vent

Ullage
Tank

Press
Transducer

Vent

Test
Item

Temp

Strain
Gages

GN₂
Supply

Gage

Water
Supply

Orifice
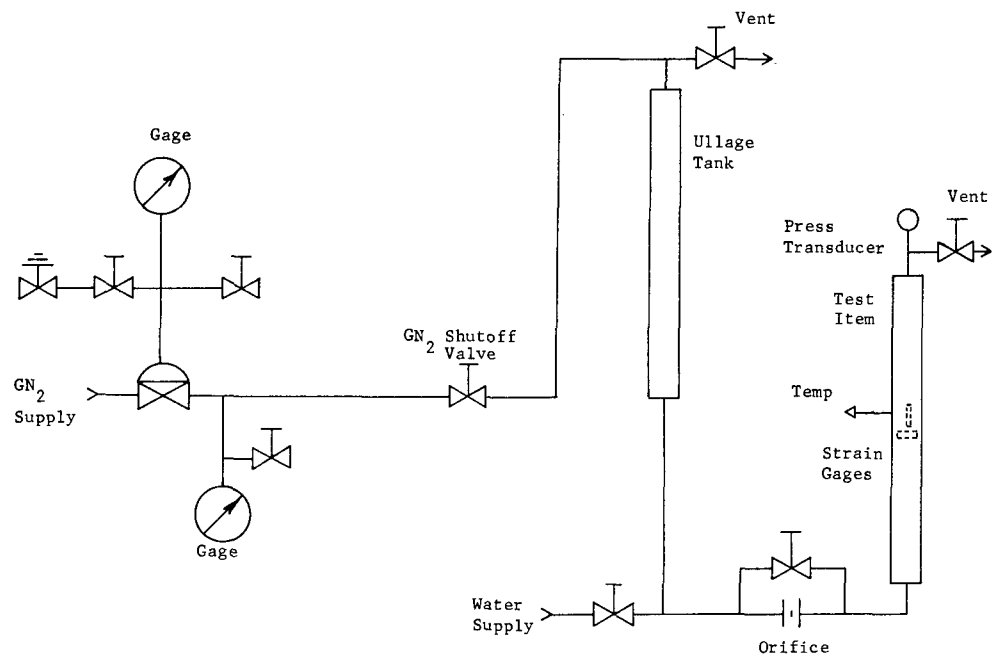
Fig. 55. - Test Fixture Schematic, Low-Pressure Ambient Burst Test

Gage

Water Supply
Tank

Instrumented
Gage

Test
Item

Temp

Strain
Gage

GN₂
Supply

Gage

Booster
Pump
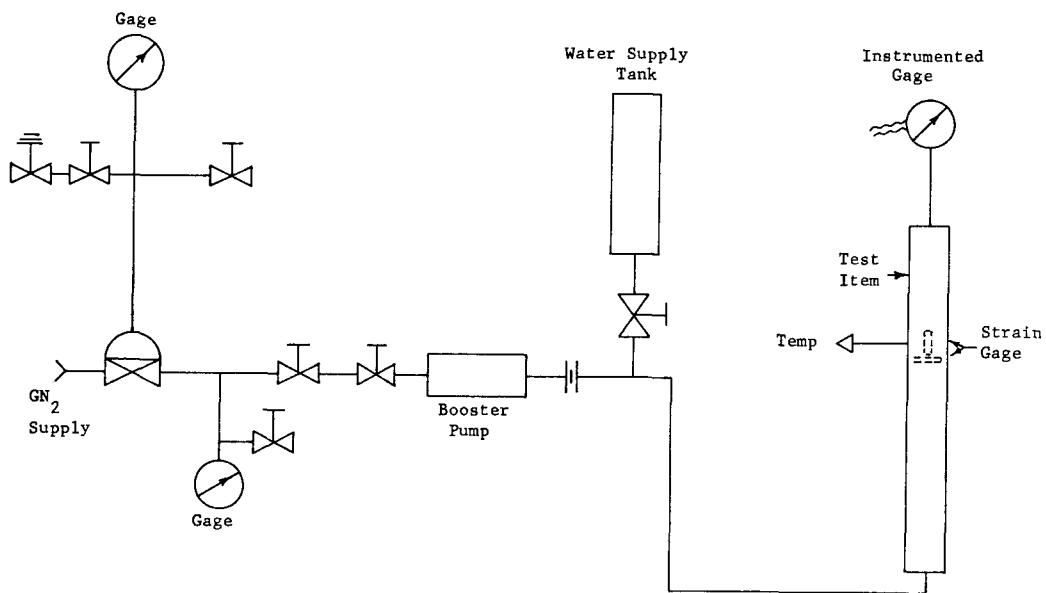
Fig. 56. - Test Fixture Schematic, High-Pressure Ambient Burst Test

131
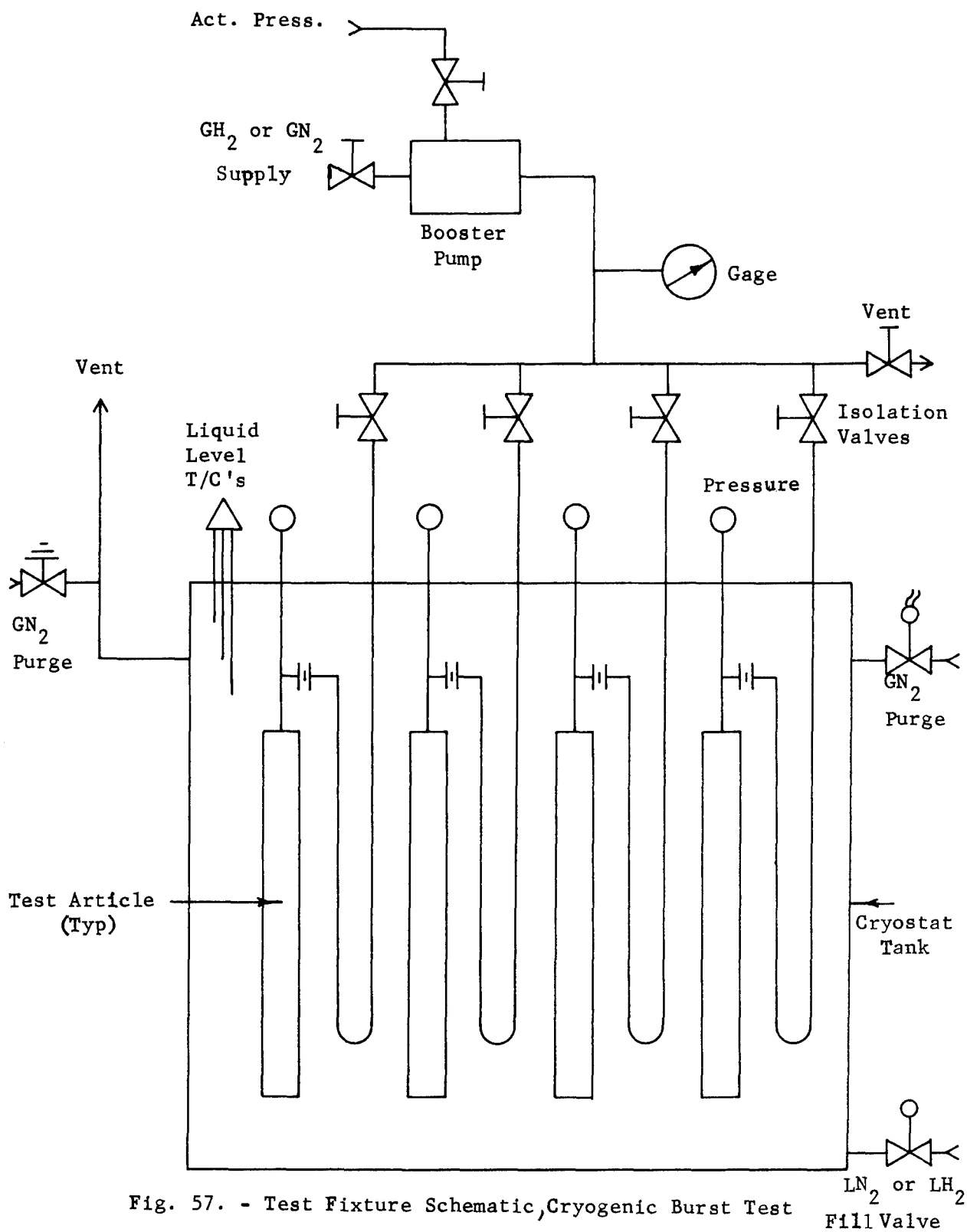
Fig. 57. – Test Fixture Schematic, Cryogenic Burst Test

Test method. - The ambient burst tests of the low-pressure test specimens were performed with the test specimens installed in the test fixture as shown in fig. 55. Before filling the test specimen with water, the system was pressurized to operating pressure with gaseous nitrogen and all connections were bubble leak checked. All leaks except test specimen leaks were repaired before proceeding. With the orifice bypass valve and the vent valves at the top of the test specimen and ullage tank open, the system was filled with clean demineralized water through the water fill valve. The system was filled to a gas-free condition as evidenced by water flow from the top of the test specimen and the top of the ullage tank. All valves were then closed and the pressure transducer and strain gages were balanced to zero output. The instrumentation recorders were then calibrated; annotated with date, test title, and test specimen serial number; and started at a chart speed of 2.5 mm/sec. The gaseous nitrogen pressure in the system was then increased at a controlled rise rate to maintain a strain rate not exceeding 1% per minute, until test specimen failure was indicated by visible leakage or rupture. The pressure in the system was then reduced to zero and the test specimen was inspected to determine the failure mode.

The ambient burst tests of the high-pressure specimens were performed with the test specimens installed in the test fixture as shown in fig. 56. The burst tests of the high-pressure test specimens were conducted using the same method as for the low-pressure specimens except that a gas booster pump was used to increase the pressure to the point of failure.

The cryogenic burst tests of both the low-pressure and high-pressure test specimens were performed with the test specimens installed in the test fixture as shown in fig. 57. The test method discussed in the following paragraphs is for testing at liquid nitrogen temperature only. The same procedure was followed for the testing at liquid hydrogen temperature except that gaseous hydrogen was used as the pressurant gas and the cryostat tank was filled with liquid hydrogen.

After installing the test specimens in the test fixture the system was pressurized with gaseous nitrogen to operating pressure and all connections were bubble leak checked. All leaks except test specimen leaks were repaired before proceeding. The cryostat lid with the test specimens attached was then mounted on the cryostat tank and the test specimens were pressurized to approximately 25% of operating pressure with gaseous nitrogen. This pressure was maintained in the test specimens while the cryostat tank was filled with liquid nitrogen. As the cryostat filled, the pressurant gas in the test specimens liquefied so that when the cryostat tank was full the test specimen was submerged in and filled with liquid nitrogen. When the system temperatures were stabilized, the pressure

in the test specimens was reduced to zero so the pressure transducer and strain gage outputs could be balanced to zero. The orifice bleed valve, manifold vent valve, and the test specimen isolation valves were closed and the instrumentation recorders were calibrated and annotated. The isolation valve to one test specimen was then opened and the system pressure was increased at a controlled rate until the test specimen failed. This sequence was repeated until the four specimens had been tested. The system pressure was then decreased to zero and the cryostat tank was drained. The test specimens were then inspected to determine the failure mode.

To reduce the chances of system leaks, the test fixture was modified when testing the high pressure test specimens. After completing the cool-down and fill of the test specimens and cryostat tank by the above procedure, the pressurization line was plumbed direct from the gas booster outlet to the test specimen. The gas booster pump was then used to increase the pressure in the system until test specimen failure occurred. This procedure was repeated for each of the other three test specimens.

Test results and discussion. - To present the results of the burst test program, the test specimens will be divided into three groups with respect to the diameter of the test specimens. The first group of test specimens to be discussed will consist of the 1/2 in. (1.27 cm) diameter high-pressure test specimens. The second group of test specimens to be discussed will consist of the 2 in. (5.08 cm) diameter low-pressure test specimens. The third group of test specimens to be discussed will consist of the 5 in. (1.27 cm) diameter low-pressure test specimens.

The change in slope of the strain readings for the 2 in. (5.08 cm) and 5 in. (12.7 cm) diameter tubes can be attributed to closing the gap between the liner and the overwrap. This slope change is present in the cryogenic testing only, confirming the absence of a gap at ambient temperatures. The empirical gap was the same magnitude as the calculated gap. Any gap in the 1/2 in. (1.27 cm) diameter tubes was not evident in the data.

Out of the first group of 48 high-pressure test specimens, 43 specimens were subjected to burst tests and 5 specimens were subjected to torsion tests. The results of the torsion tests are discussed in a later section. Twenty-four of the test specimens were subjected to burst tests with no other structural testing performed and the remaining specimens were burst tested after being subjected to pressure and temperature cycling and extended load tests. The results of the burst tests on each design are tabulated in table 26 through 29 and the average pressure vs strain at the three test temperatures for each design are plotted on fig. 58 through 61. The pressure vs strain curves reflect the average values at failure of all specimens tested at each temperature.

This page intentionally left blank.

TABLE 26.- BURST TEST DATA, PART NO. CFL6300605

Serial no.	Test temperature °F	Test temperature °K	Pressure at failure lbs/in²	Pressure at failure N/cm²	% Strain at failure Axial	% Strain at failure Hoop	Pressure rise rate lbs/in²-sec	Pressure rise rate N/cm²-sec
1	Amb	Amb	10,530^f	7,260^f	0.28	0.74	220	150
2	Amb	Amb	11,400^f	7,870^f	0.23	0.63	11,400	7,860
3	-320	78	9,950^e	6,870^e	0.24	0.93	70	50
4	-320	78	10,000^f	6,900^f	0.27	0.48	310	210
5	-423	20	7,680^e	5,300^e	0.18	c	270	190
6	-423	20	7,990^e	5,540^e	0.11	0.56	200	140
7^a	Amb	Amb	8,380^f	5,770^f	0.26	0.47	170	120
8^b								
9^a	-423	20	9,470^e	6,530^e	0.21	0.55	260	180
10^a	-423	20	7,350^e	5,070^e	0.10	0.39	190	130
11^a	-320	78	7,000^e	4,830^e	0.15	c	620	430
12^b								

Design operating pressure: 3000 psi (2068N/cm²) Minimum acceptable burst pressure: 6000 psi (4136N/cm²)

Calculated Burst Pressure:
$\quad$ 70°F (294°K) $\quad$ 9,800 psig (6,760 N/cm²)
$\quad$ -320°F (78°K) $\quad$ 12,375 psig (8,530 N/cm²)
$\quad$ -423°F (20°K) $\quad$ 12,880 psig (8,880 N/cm²)

Standard Notes:
a$\quad$ Post Cycle Burst Test Specimen
b$\quad$ Torsion Test Specimen
c$\quad$ Strain Gage Non-Operating
d$\quad$ Strain Gage Failed before Test Item Failure, Curve Extrapolated
e$\quad$ Leakage Failure
f$\quad$ Weld Failure (Liner to End Fitting Adaptor)
g$\quad$ Maximum pressure capability of fixture - did not fail tube.

Test Specimen Description
Dimensions: $\quad$ 0.5 in. (1.27 cm) diameter x 18 in. (45.72 cm) long.
Liner: $\quad$ 0.007 in. (0.018 cm) Inconel 718, Seamless Drawn Tube, Heat Treated & Age Hardened
End Fitting: $\quad$ AN Flared, Resistance Weld or Liner
Glass: $\quad$ 0.030 in. (0.076 cm), Hoop-Longitudinal-Hoop

Fig. 59. - Pressure vs Strain, CFL6300606, 1/2 in. (1.27 cm) Diameter, Butt Weld

NOTES:

1. Curves represent average of all specimens burst tested at each temperature including leakage failures.

2. a - Axial strain

   h - Hoop strain

TABLE 27.- BURST TEST DATA, PART NO. CFL6300606

Serial no.	Test temperature		Pressure at failure		% Strain at failure		Pressure rise rate	
	°F	°K	lbs/in²	N/cm²	Axial	Hoop	lbs/in²-sec	N/cm²-sec
13	Amb	Amb	13,900[f]	9,580[f]	0.40	0.82	730	500
14	Amb	Amb	12,030[f]	8,290[f]	0.45	0.74	860	590
15	-320	78	16,000[g]	11,030[g]	1.03	1.18	300	210
16	-320	78	17,000[g]	11,720[g]	0.66	1.07	610	920
17	-423	20	10,780[e]	7,430[e]	0.20	0.37	280	190
18	-423	20	10,900[e]	7,520[e]	0.27	0.84	310	210
19[a]	Amb	Amb	10,430[e]	7,190[e]	0.53	c	290	200
20[a]	Amb	Amb	10,300[e]	7,100[e]	0.43	0.82	220	150
21[a]	-423	20	9,080[e]	6,260[e]	c	0.33	180	120
22[a]	-423	20	14,860[f]	10,250[f]	0.38	c	250	170
23[a]	-320	78	15,250[f]	10,510[f]	0.39	0.67	220	150
24	-320	78	16,500[f]	11,380[f]	0.78	1.26	300	210

Design operating pressure: 3000 psi (2068N/cm²) Minimum acceptable burst pressure: 6000 psi (4136N/cm²)

Calculated Burst Pressure: 70°F (294°K)   9,800 psig (6,760 N/cm²)
                              -320°F (78°K)   12,375 psig (8,530 N/cm²)
                              -423°F (20°K)   12,880 psig (8,880 N/cm²)

Standard Notes:

a Post Cycle Burst Test Specimen
b Torsion Test Specimen
c Strain Gage Non-Operating
d Strain Gage Failed before Test Item Failure, Curve Extrapolated
e Leakage Failure
f Weld Failure (Liner to End Fitting Adaptor)
g Maximum Pressure Capability of Fixture - Did not Fail Tube

Test Specimen Description
Dimensions: 0.5 in. (1.27 cm) diameter x 18 in. (45.72 cm) long
Liner: 0.007 in. (0.018 cm) Inconel 718, Seamless Drawn Tube, Heat Treated and Age Hardened
End Fitting: Butt Weld, Resistance Weld to Liner
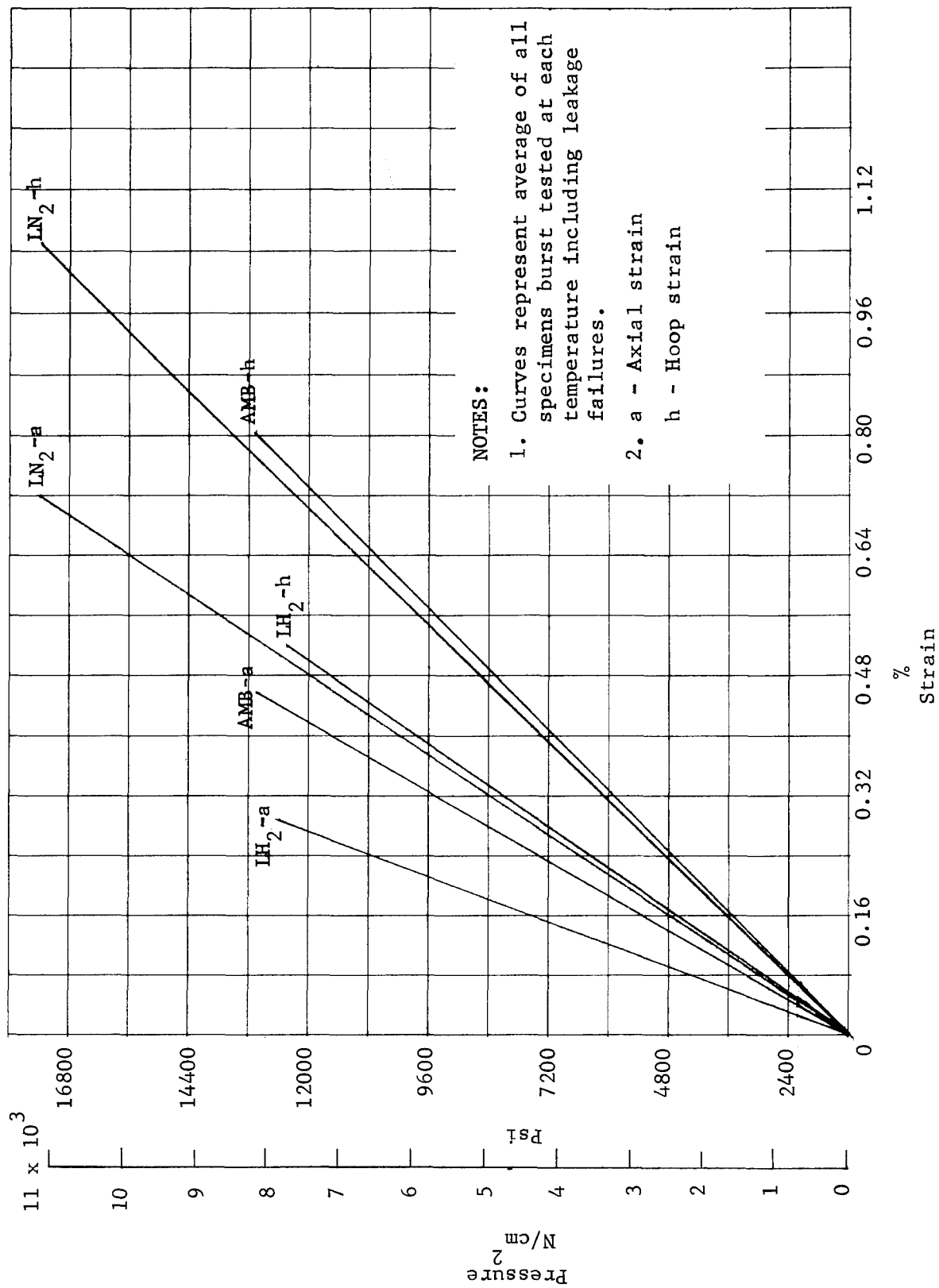Glass: 0.030 in. (0.076 cm) Hoop-Longitudinal-Hoop

139

Fig. 60. – Pressure vs Strain, CFL6300607, 1/2 in. (1.27 cm) Diameter, Flat Flange

TABLE 28.- BURST TEST DATA, PART NO. CFL6300607

Serial no.	Test temperature		Pressure at failure		% Strain at failure		Pressure rise rate	
	°F	°K	lbs/in²	N/cm²	Axial	Hoop	lbs/in²-sec	N/cm²-sec
25	Amb	Amb	10,680[f]	7,360[f]	0.69	1.11	120	80
26	Amb	Amb	13,050[f]	9,000[f]	0.52	1.05	480	330
27	-320	78	16,000[f]	11,030[f]	0.94	1.07	230	160
28	-320	78	17,000[g]	11,720[g]	1.09	1.93	290	200
29	-423	20	10,190[e]	7,030[e]	0.20	0.54	230	160
30	-423	20	9,150[e]	6,310[e]	0.19	0.43	510	350
31[a]	Amb	Amb	11,190[e]	7,720[e]	0.51	0.87	290	200
32[b]								
33[a]	-423	20	15,150[e]	10,450[e]	0.59	0.96	190	130
34[a]	-423	20	15,300[f]	10,550[f]	0.67	1.11	210	140
35[a]	-320	78	15,400[f]	10,620[f]	c	0.72	180	120
36[b]								

Design operating pressure: 3000 psi (2068N/cm²) Minimum acceptable burst pressure: 6000 psi (4136N/cm²)

Calculated Burst Pressure: 70°F (294°K)   9,800 psig (6,760 N/cm²)
                            -320°F (78°K) 12,375 psig (8,530 N/cm²)
                            -423°F (20°K) 12,880 psig (8,880 N/cm²)

Standard Notes:

a Post Cycle Burst Test Specimen
b Torsion Test Specimen
c Strain Gage Non-Operating
d Strain Gage Failed before Test Item Failure, Curve Extrapolated
e Leakage Failure
f Weld Failure (Liner to End Fitting Adaptor)
g Maximum Pressure Capability of Fixture - Did not Fail Tube

Test Specimen Description
Dimensions: 0.5 in. (1.27 cm) diameter x 18 in. (45.72 cm) long
Liner: 0.007 in. (0.018 cm) Inconel 718, Seamless Drawn Tube, Heat Treated and Age Hardened
End Fitting: Machined 0.75 in. (1.90 cm) APCO Flange, Fusion Weld To Liner As An Assembly
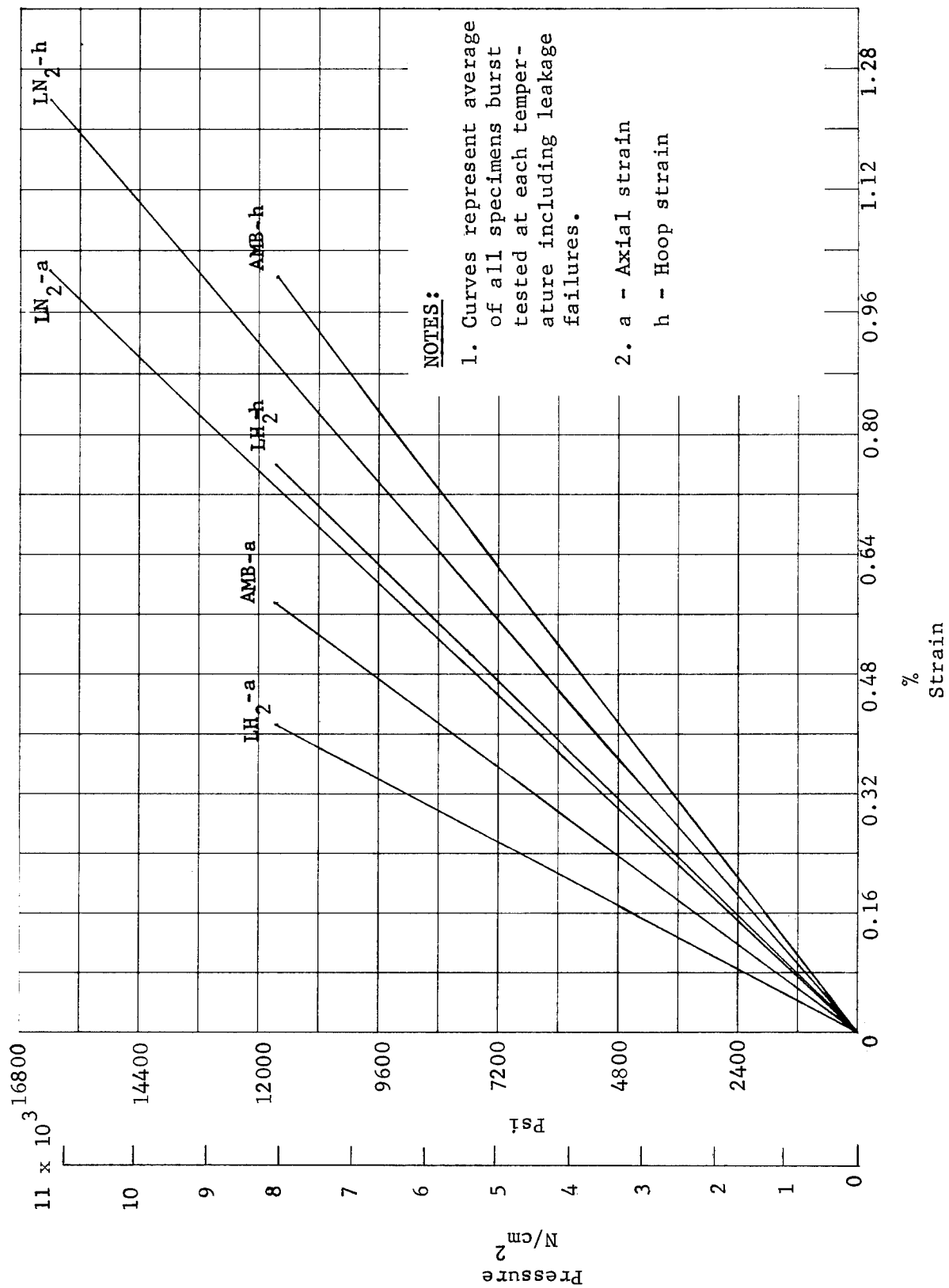Glass: 0.030 in. (0.076 cm), Hoop Longitudinal-Hoop
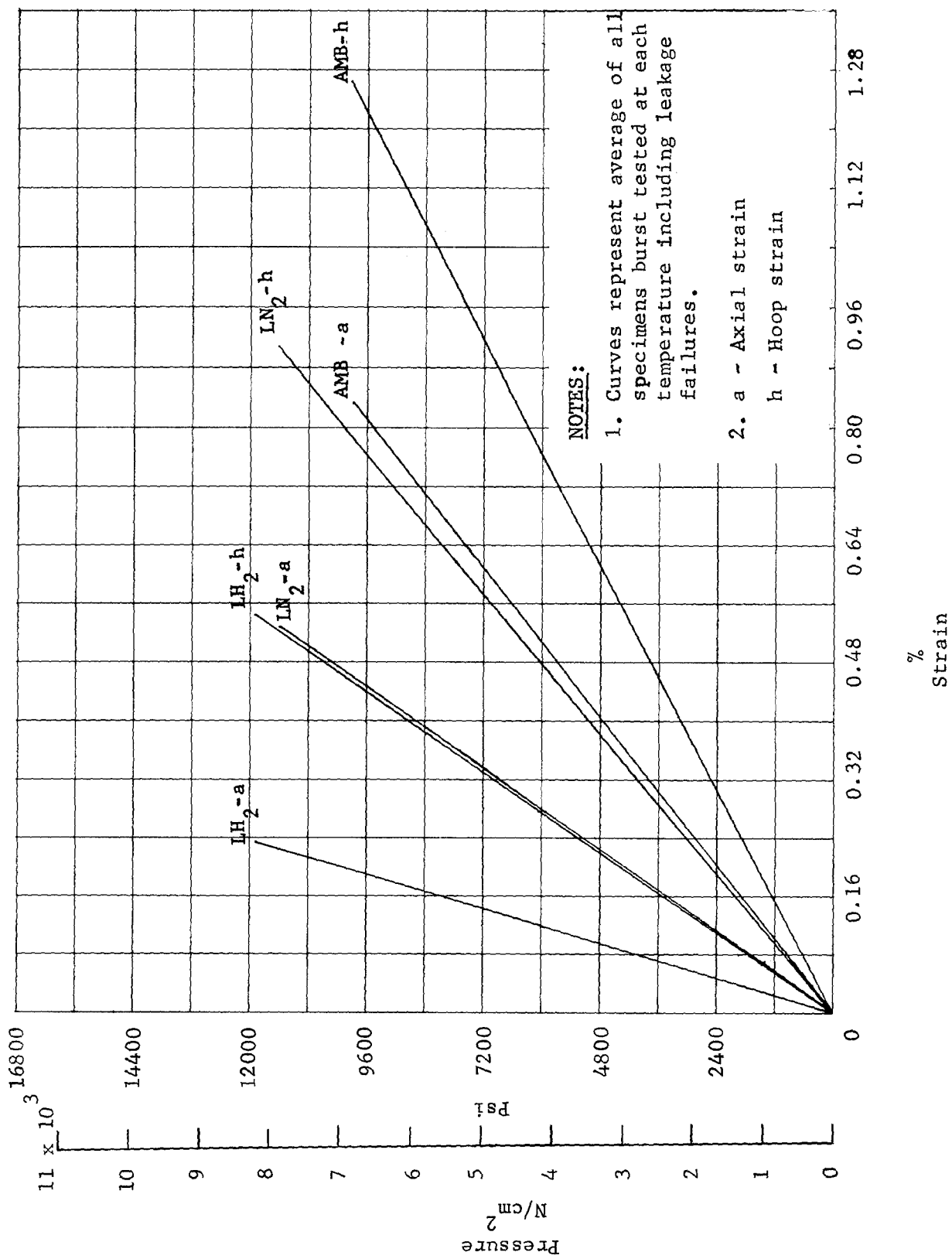
Fig. 61. — Pressure vs. Strain, CFL6300608, 1/2 in. (1.27 cm) Diameter, AN Flared

TABLE 29.- BURST TEST DATA, PART NO. CFL6300608

Serial no.	Test temperature		Pressure at failure		% Strain at failure		Pressure rise rate	
	°F	°K	lbs/in²	N/cm²	Axial	Hoop	lbs/in²-sec	N/cm²-sec
37	Amb	Amb	11,880	8,190	0.99	1.69	70	50
38	Amb	Amb	9,980^f	6,880^f	0.83	1.23	360	250
39	-320	78	11,180^e	7,710^e	0.99	1.11	100	70
40	-320	78	8,300^e	5,720^e	0.38	0.75	440	300
41	-423	20	13,520^e	9,320^e	0.21	0.62	190	130
42	-423	20	10,000^e	6,900^e	c	0.71	320	220
43^a	Amb	Amb	7,950	5,480	0.69	0.87	160	110
44^b								
45^a	-423	20	13,350^e	9,210^e	0.16	0.41	260	180
46^a	-423	20	11,650^e	8,030^e	0.21	0.44	400	280
47^a	-320	78	15,830^f	10,910^f	c	1.37	430	300
48^a	-320	78	10,420^e	7,180^e	0.21	0.43	420	290

Design operating pressure: 3000 psi (2068N/cm²) Minimum acceptable burst pressure: 6000 psi (4136N/cm²)

Calculated Burst Pressure: 70°F (294°K)   7,776 psig (5,360 N/cm²)
                           -320°F (78°K)   9,331 psig (6,430 N/cm²)
                           -423°F (20°K) 10,653 psig (7,340 N/cm²)

Standard Notes:

a Post Cycle Burst Test Specimen
b Torsion Test Specimen
c Strain Gage Non-Operating
d Strain Gage Failed before Test Item Failure, Curve Extrapolated
e Leakage Failure
f Weld Failure (Liner to End Fitting Adaptor)
g Maximum Pressure Capability of Fixture - Did not Fail Tube

Test Specimen Description
    Dimensions: 0.5 in. (1.27 cm) diameter x 18 in. (45.72 cm) long
    Liner: 0.009 in (0.0230 cm) Stainless Steel, Seamless Drawn Tube, Hardened
    End Fitting: AN Flared, Resistance Weld To Liner
    Glass: 0.030 in. (0.076 cm) Hoop-Longitudinal-Hoop

The primary failure mode for the first group of test specimens was determined to be leakage failure. A leakage failure occured when the gas booster pump, because of its very low volumetric output and pumping speed, was unable to increase the system pressure faster than it leaked off. The specific location of the leaks was not determined because in no case did failure occur at less than two times the design operating pressure. The failure modes for each design in the first group of test specimens are presented in the following paragraphs:

CFL6300605, 1/2 in. (1.27 cm), flared tube: Two test specimens were torsion tested and six failed due to leakage. Of the four remaining specimens, the resistance weld joining the liner to the end fitting adapter failed due to insufficient weld penetration on two of the tubes. Typical failure is shown in fig. 62.
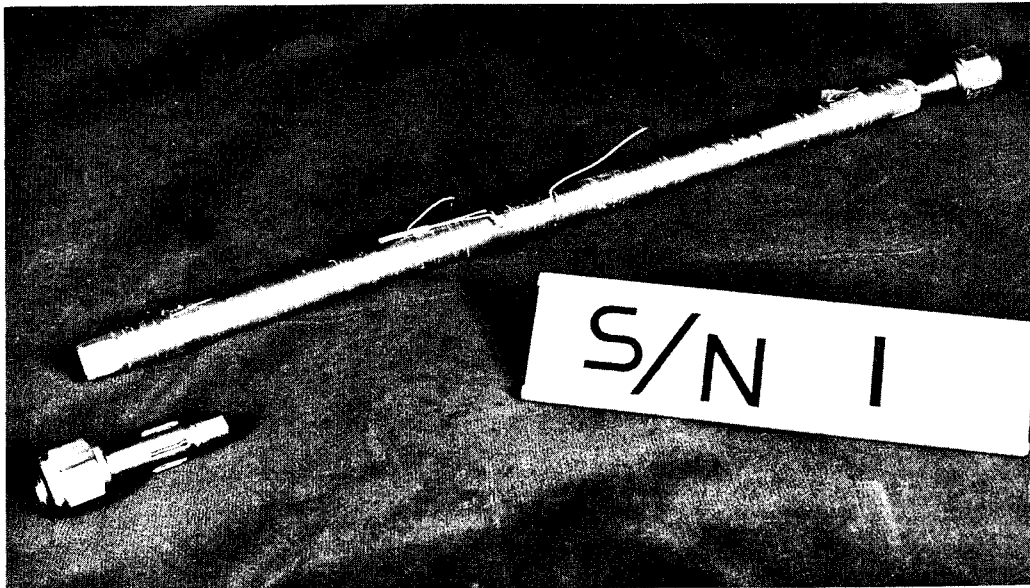
Fig. 62. - Failure Mode, CFL6300605

CFL6300606, 1/2 in. (1.27 cm), butt weld: Five specimens failed due to leakage. Five specimens failed due to liner failure in the heat-affected zone adjacent to the resistance weld joining the liner to the end fitting adapter. This failure is shown in fig. 63. Two specimens showed no evidence of failure when pressurized to the maximum capability of the test fixture.

CFL6300607, 1/2 in. (1.27 cm), flat flanged: Two test specimens were torsion tested and four failed due to leakage. Five specimens failed due to liner failure at the inside edge of the flange (see fig. 64). The remaining test specimen showed no evidence of failure when pressurized to the maximum capability of the test fixture.

Fig. 63. - Failure Mode, CFL6300606
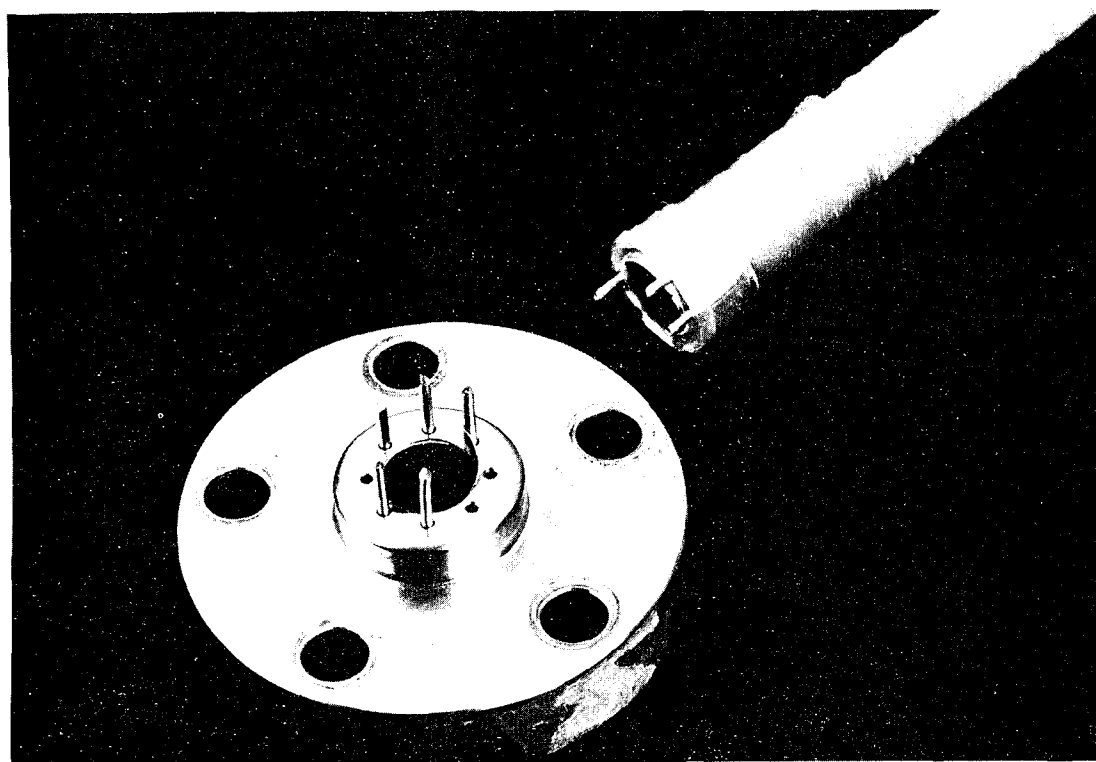
Fig. 64. - Failure Mode, CFL6300607

CFL6300608, 1/2 in. (1.27 cm), CRES flared: One test speci-
men was torsion tested and seven failed due to leakage. On two
test specimens the resistance-weld joining the liner to the end
fitting adapter failed due to insufficient weld penetration (similar
to fig. 63). The two remaining test specimens (S/N's 37 and 43)
failed at the center of the tube at the point where a strain gage was
bonded to the liner. This failure is shown in fig. 65. The data
scatter at ambient temperature is attributed to load transfer from
the liner to the overwrap as a result of friction. This load transfer
is indicated by the actual burst pressures being higher than the
calculated burst pressure.
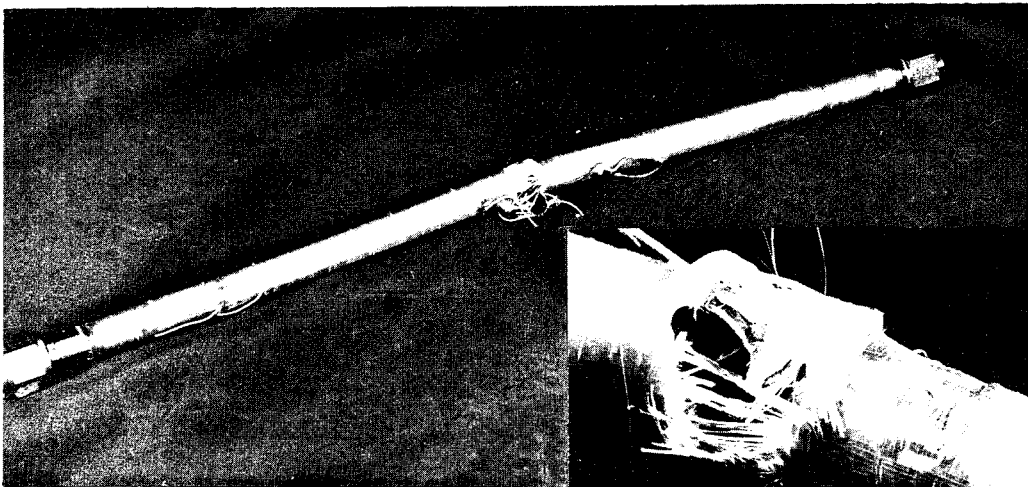
Fig. 65. - Failure Mode on Two CFL6300608 Tubes

Out of the second group of 48 low-pressure test specimens,
44 specimens were subjected to burst tests and 3 were subjected
to torsion tests. The remaining specimen, CFL6300612-S/N 93 was
destroyed after completing pressure and temperature cycling
testing. Twenty four of the test specimens were subjected to
burst testing with no other structural tests being performed and
the remaining specimens were subjected to burst tests after com-
pleting pressure and temperature cycling and extended load tests.
The resuts of the burst tests on each design are given in tables
30 through 33 and the average pressure vs strain at the three
test temperatures for each design are plotted in fig. 66 through
69. The pressure vs strain curves reflect the average values at
failure of all specimens tested at each temperature.

When testing the low pressure test specimens, the pressure
capabilities of the test fixtures made it possible to pressurize
the specimens to burst failure even though leakage may have occured
before burst. The failure modes for each design in the second
group of test specimens are presented in the following paragraphs:

This page intentionally left blank.

Fig. 66. — Pressure vs Strain, CFL6300609, 2 in. (5.08 cm) Diameter, Butt Weld

Notes:

1. Curves represent average of all specimens burst tested at each temperature

2. All specimens were pressurized to a burst failure

3. a - Axial strain

   b - Hoop strain

148

TABLE 30.- BURST TEST DATA, PART NO. CFL6300609

Serial no.	Test temperature		Pressure at failure		% Strain at failure		Pressure rise rate	
	°F	°K	lbs/in²	N/cm²	Axial	Hoop	lbs/in²-sec	N/cm²-sec
49	Amb	Amb	1,470[f]	1,010[f]	0.23	0.38	50	30
50	Amb	Amb	1,530[f]	1,050[f]	0.29	0.40	40	25
51	-320	78	800[f]	550[f]	0.22	0.74	100	70
52	-320	78	1,060[f]	730[f]	0.43	0.82	90	60
53	-423	20	1,750[f]	1,210[f]	0.40	0.53	20	10
54	-423	20	1,540[f]	1,060[f]	0.34	0.46	30	20
55[a]	Amb	Amb	1,290[f]	890[f]	0.20	0.42	40	25
56[a]	Amb	Amb	1,090[f]	750[f]	0.21	0.30	50	30
57[a]	-423	20	1,680[f]	1,160[f]	0.25	0.44	190	130
58[a]	-423	20	1,600[f]	1,110[f]	0.28	0.49	110	80
59[a]	-320	78	1,520[f]	1,050[f]	0.21	0.34	50	30
60[a]	-320	78	1,620[f]	1,120[f]	0.31	0.76	60	40

Design operating pressure: 200 psi (138N/cm²) Minimum acceptable burst pressure: 400 psi (276N/cm²)

Calculated Burst Pressure: 70°F (294°K)   840 psig (580 N/cm²)
                             -320°F (78°K)   1,060 psig (730 N/cm2)
                             -423°F (20°K)   1,100 psig (760 N/cm²)

Standard Notes:
a Post Cycle Burst Test Specimen
b Torsion Test Specimen
c Strain Gage Non-Operating
d Strain Gage Failed before Test Item Failure, Curve Extrapolated
e Leakage Failure
f Weld Failure (Liner to End Fitting Adaptor)

Test Specimen Description

Dimensions: 2.0 in. (5.08 cm) diameter x 18 in. (45.72 cm) long
Liner: 0.005 in. (0.013 cm) Inconel 718, Helical Fusion Weld Redrawn To 0.003 in.(0.008 cm),
                                                                                 Cold Worked
End Fitting: Butt Weld, Resistance Weld to Liner
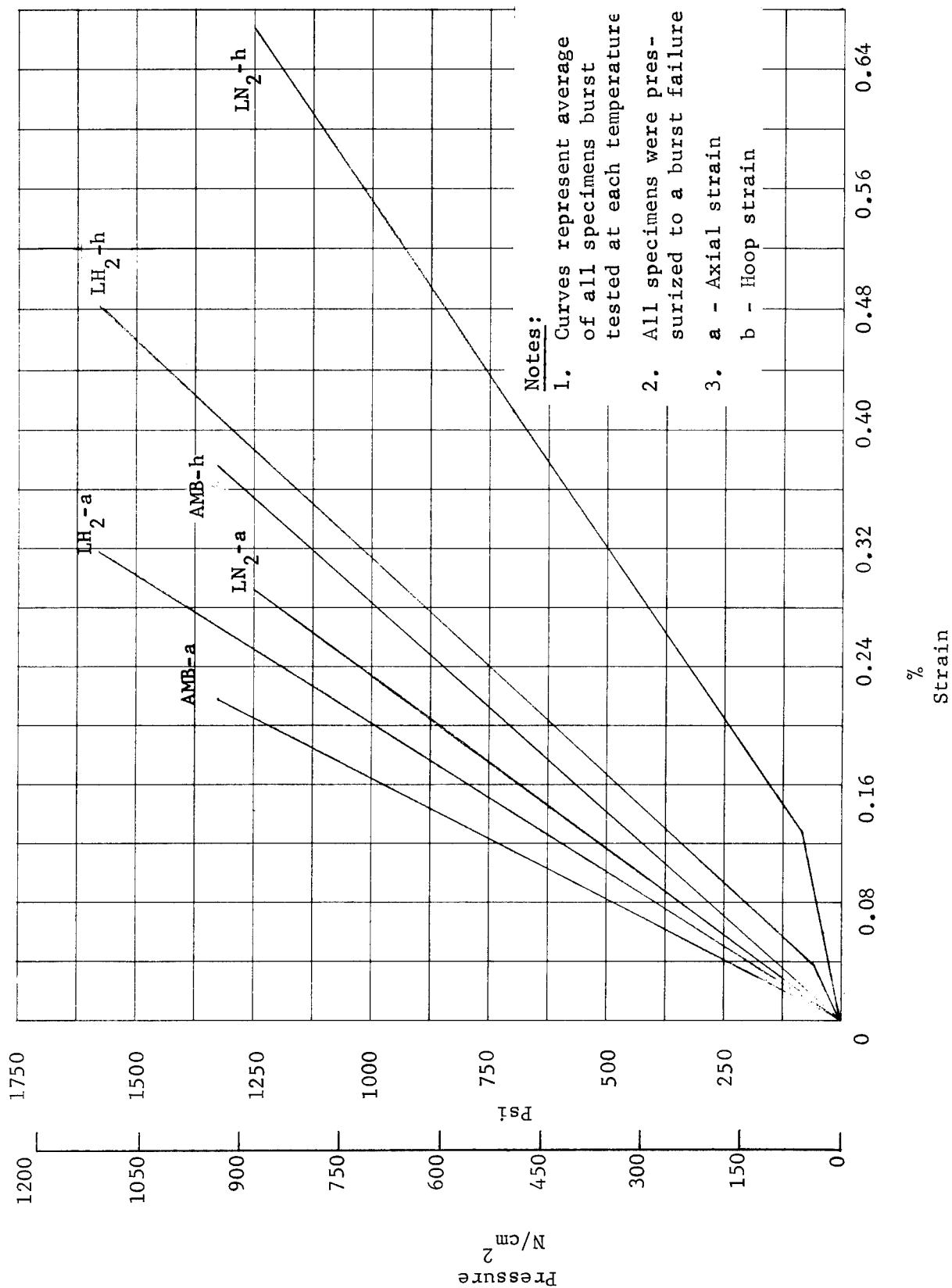Glass: 0.030 in. (0.076 cm) Hoop-Longitudinal-Hoop

149
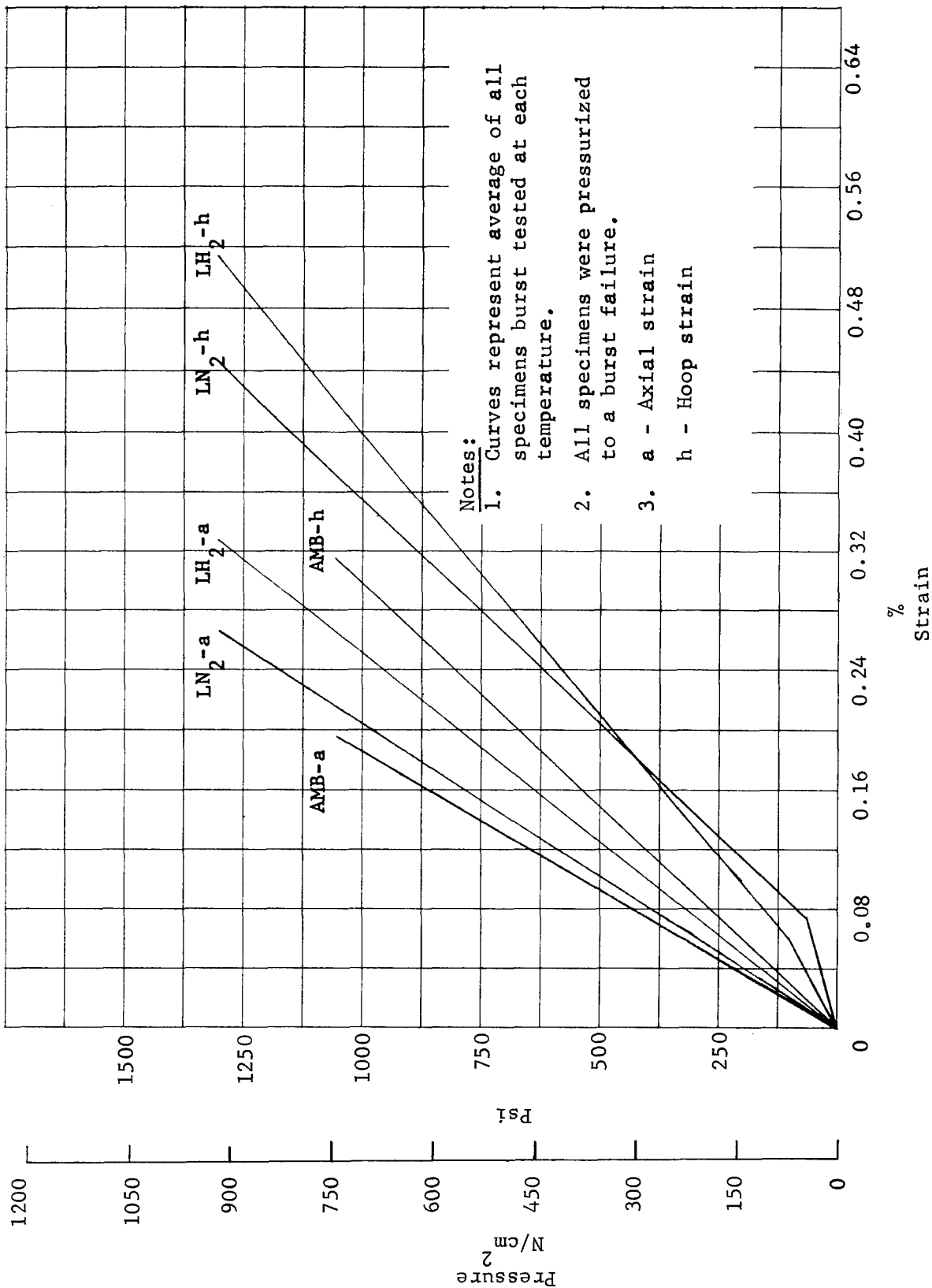
Fig. 67. – Pressure vs Strain, CFL6300610, 2 in. (5.08 cm) Diameter Butt Weld

150

TABLE 31.- BURST TEST DATA, PART NO. CFL6300610

Serial no.	Test temperature		Pressure at failure		% Strain at failure		Pressure rise rate	
	°F	°K	lbs/in²	N/cm²	Axial	Hoop	lbs/in²-sec	N/cm²-sec
61	Amb	Amb	1,180[f]	820[f]	0.19	0.42	10	10
62	Amb	Amb	1,020[f]	700[f]	0.19	0.35	40	30
63	-320	78	1,470[f]	1,010[f]	0.32	0.57	10	10
64	-320	78	1,280[f]	880[f]	0.28	0.38	10	10
65	-423	20	1,330[f]	920[f]	0.38	0.69	10	10
66	-423	20	1,320[f]	910[f]	0.35	0.45	20	15
67[a]	Amb	Amb	1,150[f]	790[f]	0.17	0.22	50	30
68[a]	Amb	Amb	1,090[f]	750[f]	0.22	0.28	60	40
69[a]	-423	20	1,340[f]	920[f]	0.28	0.40	110	80
70[a]	-423	20	1,400[f]	970[f]	0.29	0.51	80	60
71[a]	-320	78	1,370[f]	950[f]	0.23	0.47	20	15
72[a]	-320	78	1,280[f]	880[f]	0.24	0.36	70	50

Design operating pressure: 200 psi (138N/cm²) Minimum acceptable burst pressure: 400 psi (276N/cm²)

Calculated Burst Pressure: 70°F (294°K)   1,050 psig (720 N/cm²)
                              -320°F (78°K)   1,330 psig (910 N/cm²)
                              -423°F (20°K)   1,380 psig (950 N/cm²)

Standard Notes:
a Post Cycle Burst Test Specimen
b Torsion Test Specimen
c Strain Gage Non-Operating
d Strain Gage Failed before Test Item Failure, Curve Extrapolated
e Leakage Failure
f Weld Failure (Liner to End Fitting Adaptor)

Test Specimen Description

Dimensions: 2.0 in. (5.08 cm) diameter x 18 in. (45.72 cm) long
Liner: 0.003 in. (0.008 cm) Inconel 718, Straight Resistance Weld Tube Not Redrawn, Heat
End Fitting: Butt Weld, Resistance Weld To Liner   Treated and Age Hardened
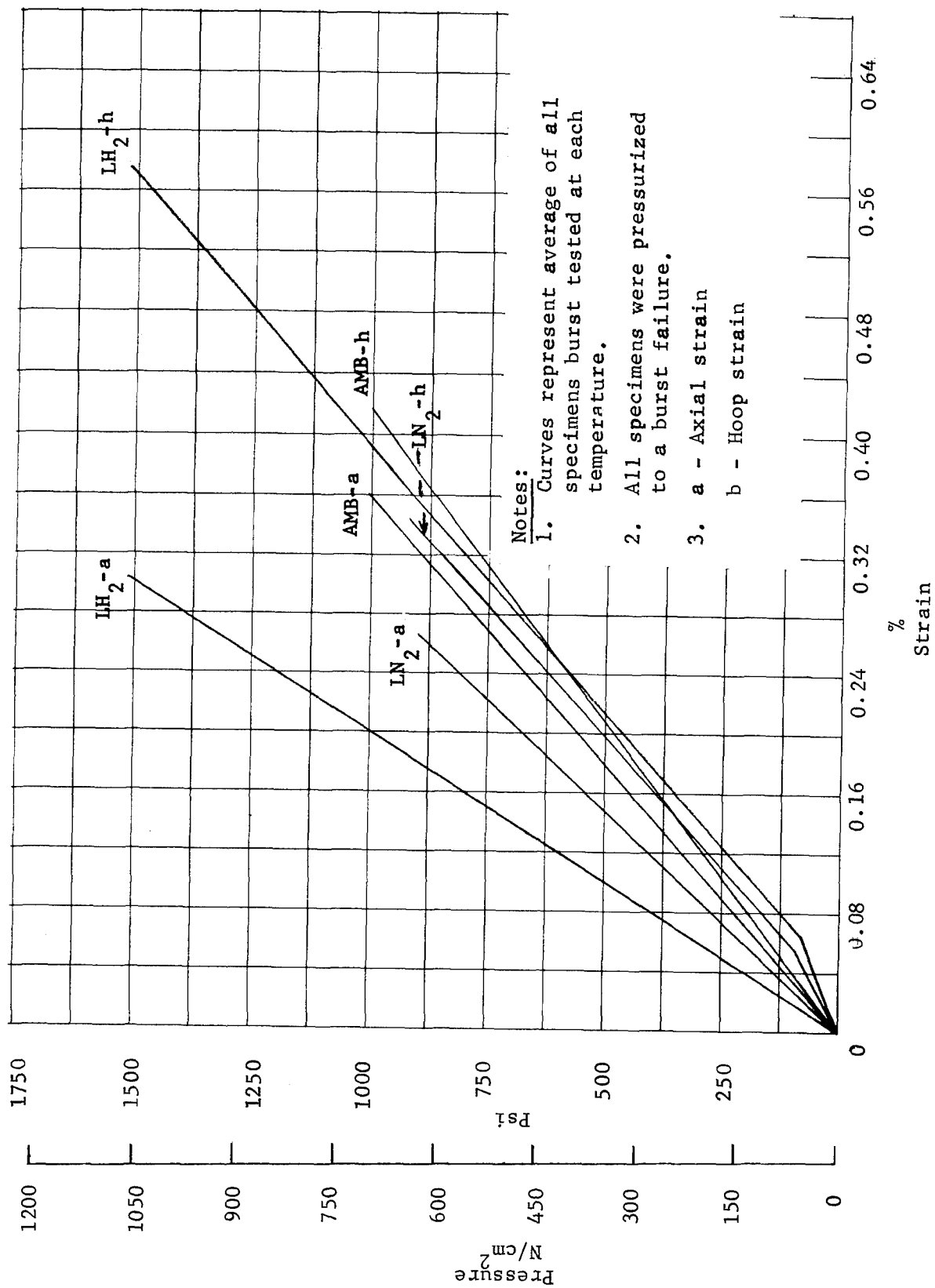Glass: 0.030 in. (0.076 cm) Hoop-Longitudinal-Hoop

151

Fig. 68. - Pressure vs Strain, CFL6300611, 2 in. (5.08 cm) Diameter, Flat Flange

TABLE 32.– BURST TEST DATA, PART NO. CFL6300611

Serial no.	Test temperature		Pressure at failure		% Strain at failure		Pressure rise rate	
	°F	°K	lbs/in²	N/cm²	Axial	Hoop	lbs/in²-sec	N/cm²-sec
73	Amb	Amb	1,060^f	730^f	0.19	0.33	30	20
74	Amb	Amb	1,050^f	720^f	0.25	0.34	30	20
75	-320	78	810^f	560^f	0.40	0.46	80	60
76	-320	78	1,200^f	830^f	0.27	0.30	20	15
77	-423	20	1,570^f	1,080^f	c	0.49	10	10
78	-423	20	1,770^f	1,220^f	0.41	1.03	10	10
79^a	Amb	Amb	900^f	620^f	0.80	c	70	50
80^b								
81^a	-423	20	1,000^f	690^f	0.19	0.29	40	30
82^a	-423	20	1,700^f	1,170^f	0.32	0.49	30	20
83^{ag}	-320	78	600^f	410^f	0.13	0.25	30	20
84^b								

Design operating pressure: 200 psi (138N/cm²) Minimum acceptable burst pressure: 400 psi (276N/cm²)

Calculated Burst Pressure:
    70°F (294°K)   680 psig (470 N/cm²)
    -320°F (78°K)   910 psig (630 N/cm²)
    -423°F (20°K)   1,060 psig (730 N/cm²)

Standard Notes:
a Post Cycle Burst Test Specimen
b Torsion Test Specimen
c Strain Gage Non-Operating
d Strain Gage Failed before Test Item Failure, Curve Extrapolated
e Leakage Failure
f Weld Failure (Liner to End Fitting Adaptor)
Other Notes:
g Premature failure attributable to bulged liner
Test Specimen Description
    Dimensions: 2.0 in. (5.08 cm) diameter x 18 in. (45.72 cm) long
    Liner: 0.005 in. (0.013 cm) Inconel 718, Helical Fusion Weld Tube Redrawn To 0.003 in.(0.008 cm)
    End Fitting: Machined 2.5 in. (6.35 cm) APCO Flange, Fusion Weld To Liner   Cold Worked
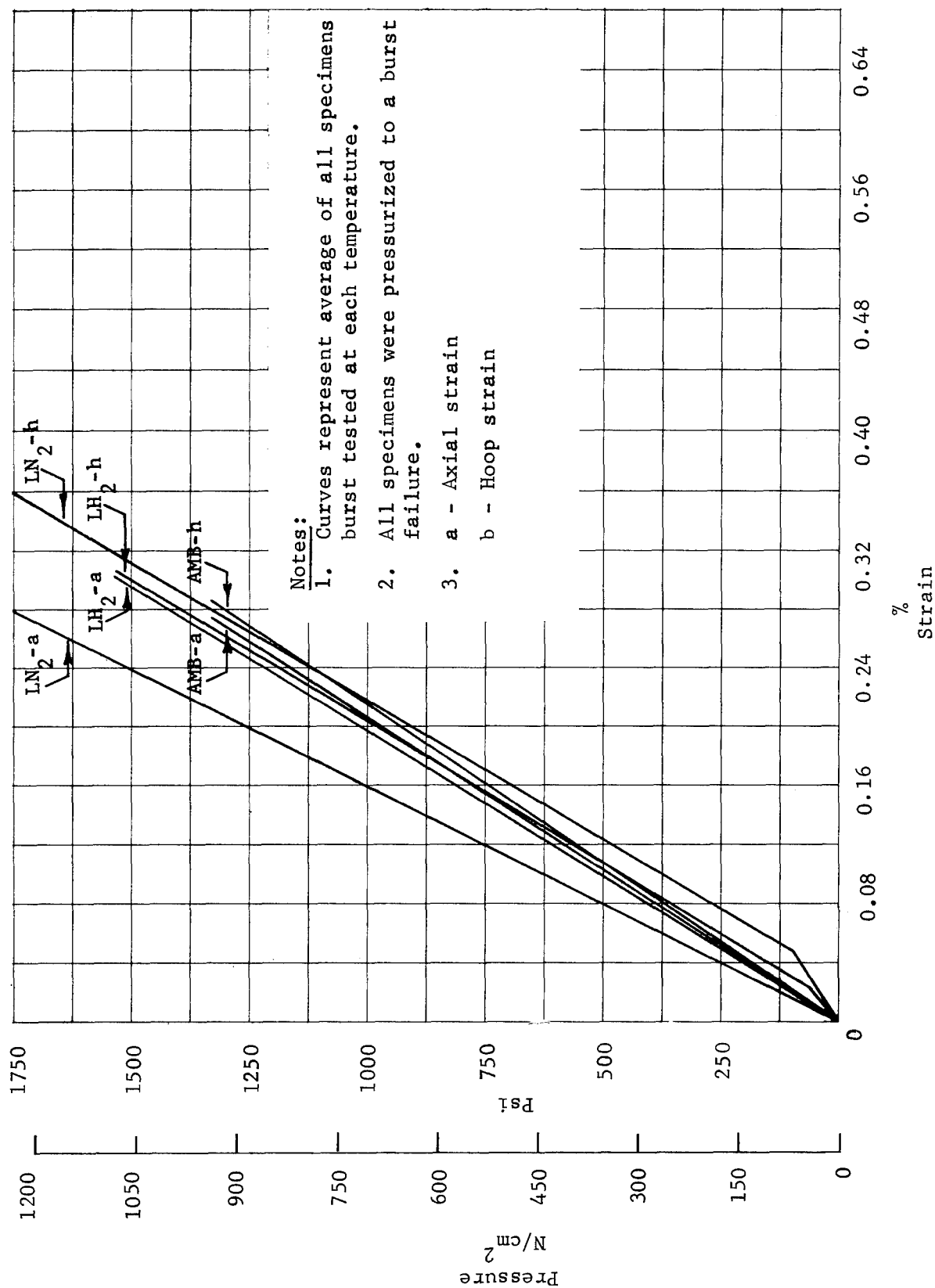   Glass: 0.030 in. (0.076 cm), Hoop-Longitudinal-Hoop

Fig. 69. - Pressure vs Strain, CFL6300612, 2 in. (5.08 cm) Diameter, NASA Flange

TABLE 33.- BURST TEST DATA, PART NO. CFL6300612

Serial no.	Test temperature		Pressure at failure		% Strain at failure		Pressure rise rate	
	°F	°K	lbs/in²	N/cm²	Axial	Hoop	lbs/in²-sec	N/cm²-sec
85g								
86	Amb	Amb	950[f]	660[f]	0.19	0.19	20	15
87	-320	78	1,620[f]	1,120[f]	0.18	0.22	40	30
88	-320	78	1,700[f]	1,170[f]	0.30[d]	0.52	20	15
89	-423	20	1,590[f]	1,100[f]	0.30	0.24	10	10
90	-423	20	1,240[f]	860[f]	c	0.18	20	15
91[a]	Amb	Amb	1,700[f]	1,170[f]	0.36	0.37	60	40
92[b]								
93[h]								
94[a]	-423	20	1,800[f]	1,240[f]	0.30[d]	0.49	20	15
95[a]	-320	78	2,050[f]	1,410[f]	c	0.34	20	15
96[a]	-320	78	1,670[f]	1,150[f]	0.37	c	20	15

Design operating pressure: 200 psi (138N/cm²) Minimum acceptable burst pressure: 400 psi (276N/cm²)

Calculated Burst Pressure:
70°F (294°K)   1,370 psig (940 N/cm²)
-320°F (78°K)   1,820 psig (1,260 N/cm²)
-423°F (20°K)   2,110 psig (1,460 N/cm²)

Standard Notes:
a Post Cycle Burst Test Specimen
b Torsion Test Specimen
c Strain Gage Non-Operating
d Strain Gage Failed before Test Item Failure, Curve Extrapolated
e Leakage Failure
f Weld Failure (Liner to End Fitting Adapter)
Other Notes:
g Cancelled prior to Burst Test
h Destroyed
Test Specimen Description:
Dimensions: 2.0 in. (5.08 cm) diameter x 18 in. (45.72 cm) long
Liner: 0.006 in. (0.015 cm) Inconel 718, Straight Fusion Weld Tube Not Redrawn, Annealed
End Fitting: Raised Face NASA Configuration Flange, Solid-State Bonded to Liner Except S/N 85
Glass: 0.030 in. (0.076 cm) Hoop-Longitudinal-Hoop

CFL6300609, 2 in. (5.08 cm) butt weld: All 12 specimens of this design were pressurized to a burst failure. The failure for all specimens was due to liner failure in the heat-affected zone adjacent to the resistance weld joining the liner to the end fitting adapter. This was the expected mode of failure and is shown in fig. 70.
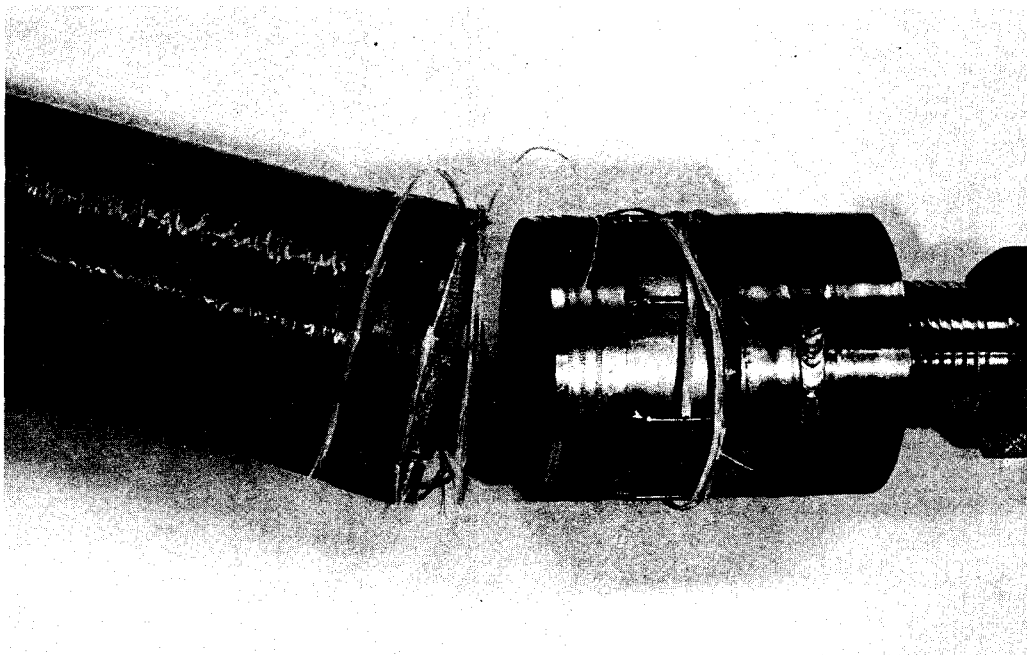
Fig. 70. - Failure Mode, CFL6300609

CFL6300610, 2 in. (5.08 cm) butt weld: All 12 specimens of the design were pressurized to a burst failure. The failure for all specimens was due to liner failure in the heat-affected zone adjacent to the resistance weld joining the liner to the end fitting adapter. This failure is shown in fig. 71.

CFL6300611, 2 in. (5.08 cm) flat flanged: Two specimens of this design were torsion tested. The remaining 10 specimens were pressurized to a burst failure. The failure of all specimens was due to liner failure in the heat-affected zone adjacent to the fusion weld joining the liner to the end fitting. This failure is shown in fig. 72. The data scatter for this design can be attributed to inadequate control of the liner weld to the end fitting which resulted in varying weld penetration.

CFL6300612, 2 in. (5.08 cm) NASA flange: After fabricating and testing one specimen of this design, it was determined that the fusion-weld joining the liner to the end fitting was of insufficient strength. This specimen was therefore redesigned to incorporate a solid-state bonding technique to join the liner to
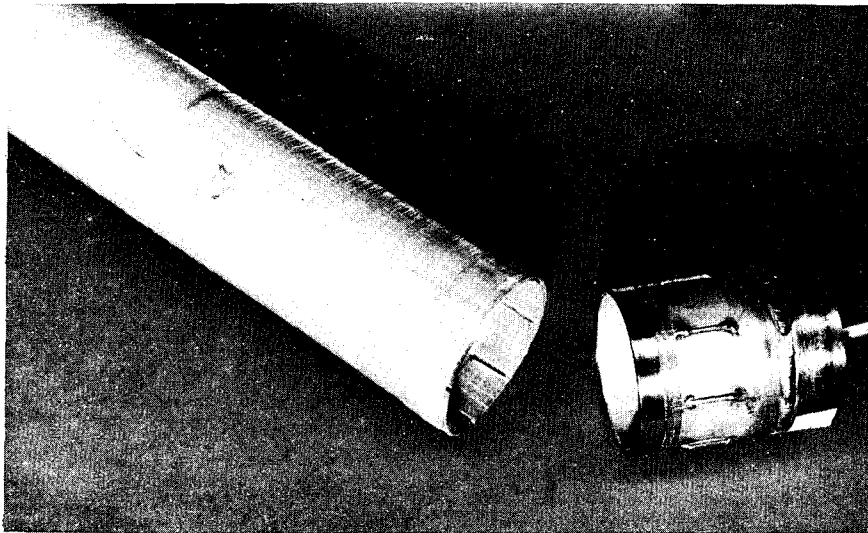
Fig. 71. - Failure Mode, CFL6300610
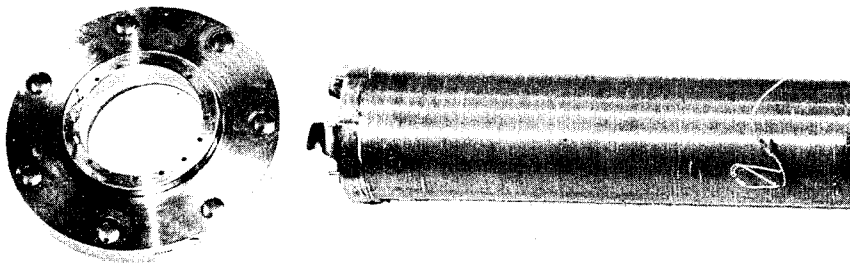
Fig. 72. - Failure Mode, CFL6300611

the end fittings. Eleven specimens of the new design were fabricated and tested. One specimen was subjected to torsion test, and one specimen was destroyed in handling after completing pressure and temperature cycling. The nine remaining specimens were pressurized to a burst failure. The failure mode for these specimens was liner failure at the inside edge of the end flange as expected and is shown in fig. 73.
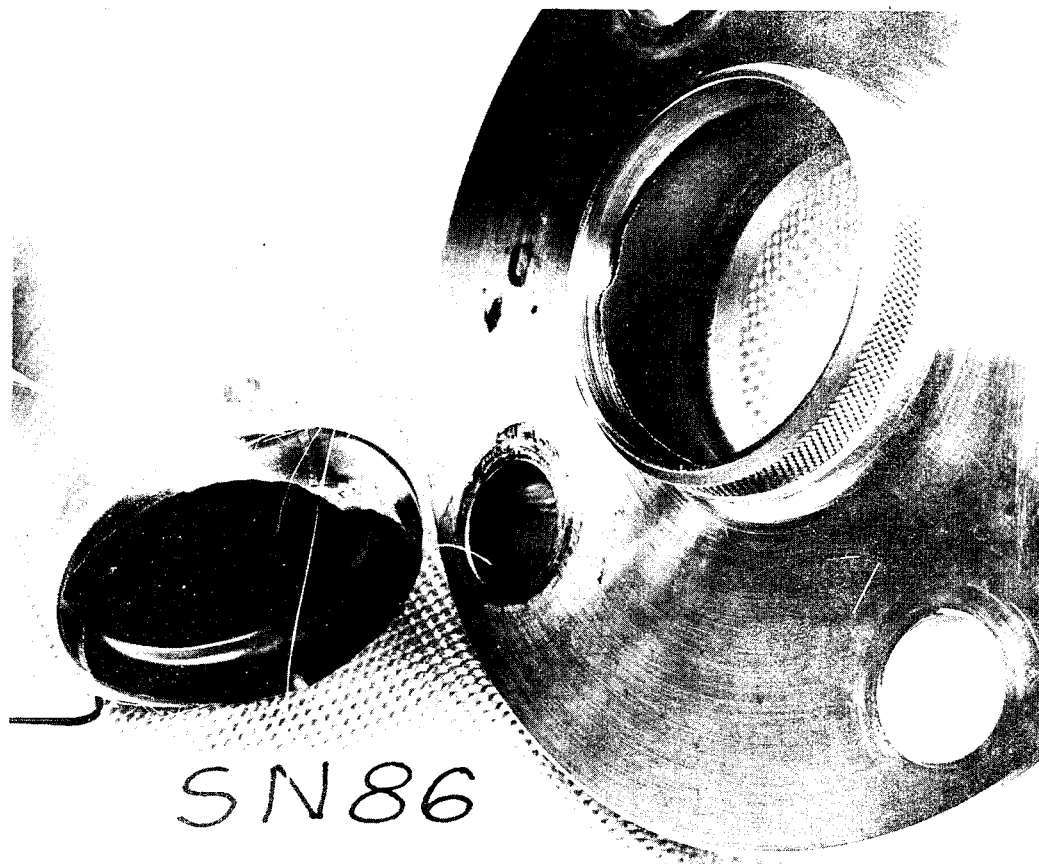
Fig. 73. - Failure Mode, CFL6300612

The third group of test specimens consisted of three designs
with 12 specimens of each design and one design with two specimens.
Out of this group of 38 low-pressure test specimens, 33 were sub-
jected to burst test and two were torsion tested. One of the
torsion test specimens was burst tested after completing torsion
testing. Three specimens were damaged in the cycle test fixture
before test and one specimen had the flanges removed to provide
a thermal conductivity test specimen. Twenty of the test speci-
mens were subjected to burst testing with no other structural
tests being performed, and the remaining specimens were subjected
to burst tests after completing pressure and temperature cycling
and extended load tests. The results of the burst tests on each
design are given in tables 34 through 37 and the average pressure
vs strain at the three test temperatures for each design are plotted
in fig. 74 through 77. The pressure vs strain curves reflect the
average values at failure of all specimens tested at each tempera-
ture.

This page intentionally left blank.

Fig. 74. - Pressure vs Strain, CFL6300613, 5 in. (12.7 cm) Diameter, Butt Weld

Notes:
1. Curves represent average of all specimens burst tested at each temperature.
2. All specimens were pressurized to a burst failure.
   a - burst failure.
3. a - Axial strain
   h - Hoop strain

TABLE 34.- BURST TEST DATA, PART NO. CFL6300613

Serial no.	Test temperature °F	Test temperature °K	Pressure at failure lbs/in²	Pressure at failure N/cm²	% Strain at failure Axial	% Strain at failure Hoop	Pressure rise rate lbs/in²-sec	Pressure rise rate N/cm²-sec
97	Amb	Amb	430[f]	290[f]	0.13	0.26	50	35
98	Amb	Amb	410[fg]	280[fg]	0.18	0.28	40	30
99	-320	78	510[f]	350[f]	0.20	0.28	30	20
100	-320	78	390[fh]	270[fh]	0.22[d]	0.32[d]	10	10
101	-423	20	490[f]	340[f]	0.25	0.25[d]	10	10
102	-423	20	450[f]	310[f]	0.23	0.38	10	10
103[a]	Amb	Amb	440[f]	300[f]	0.25	c	20	15
104[a]	Amb	Amb	420[f]	290[f]	0.18	0.22	20	15
105[a]	-423	20	530[f]	360[f]	0.35	0.46	10	10
106[i]								
107[a]	-320	78	560[f]	390[f]	0.17	c	40	30
108[a]	-320	78	400[fh]	270[f]	0.21	0.32	40	30

Design operating pressure: 200 psi (138N/cm²) Minimum acceptable burst pressure: 400 psi (276N/cm²)

Calculated Burst Pressure: 70°F (294°K)   420 psig (290 N/cm²)
                             -320°F (78°K)   530 psig (370 N/cm²)
                             -423°F (20°K)   550 psig (380 N/cm²)

Standard Notes
a Post Cycle Burst Test Specimen
b Torsion Test Specimen
c Strain Gage Non-Operating
d Strain Gage Failed before Test Item Failure, Curve Extrapolated
e Leakage Failure
f Weld Failure (Liner to End Fitting Adapter)
Other Notes:
g All Hoop Overwrap
h Liner was Buckled During Overwrap
i Destroyed
Test Specimen Description
Dimensions: 5.0 in. (12.7 cm) diameter x 12 in. (30.48 cm) long
Liner: 0.003 in. (0.008 cm) Inconel 718, Straight Resistance Weld Tube Not Redrawn, Heat
End Fitting: Butt Weld, Resistance Weld To Liner   treated and Age Hardened
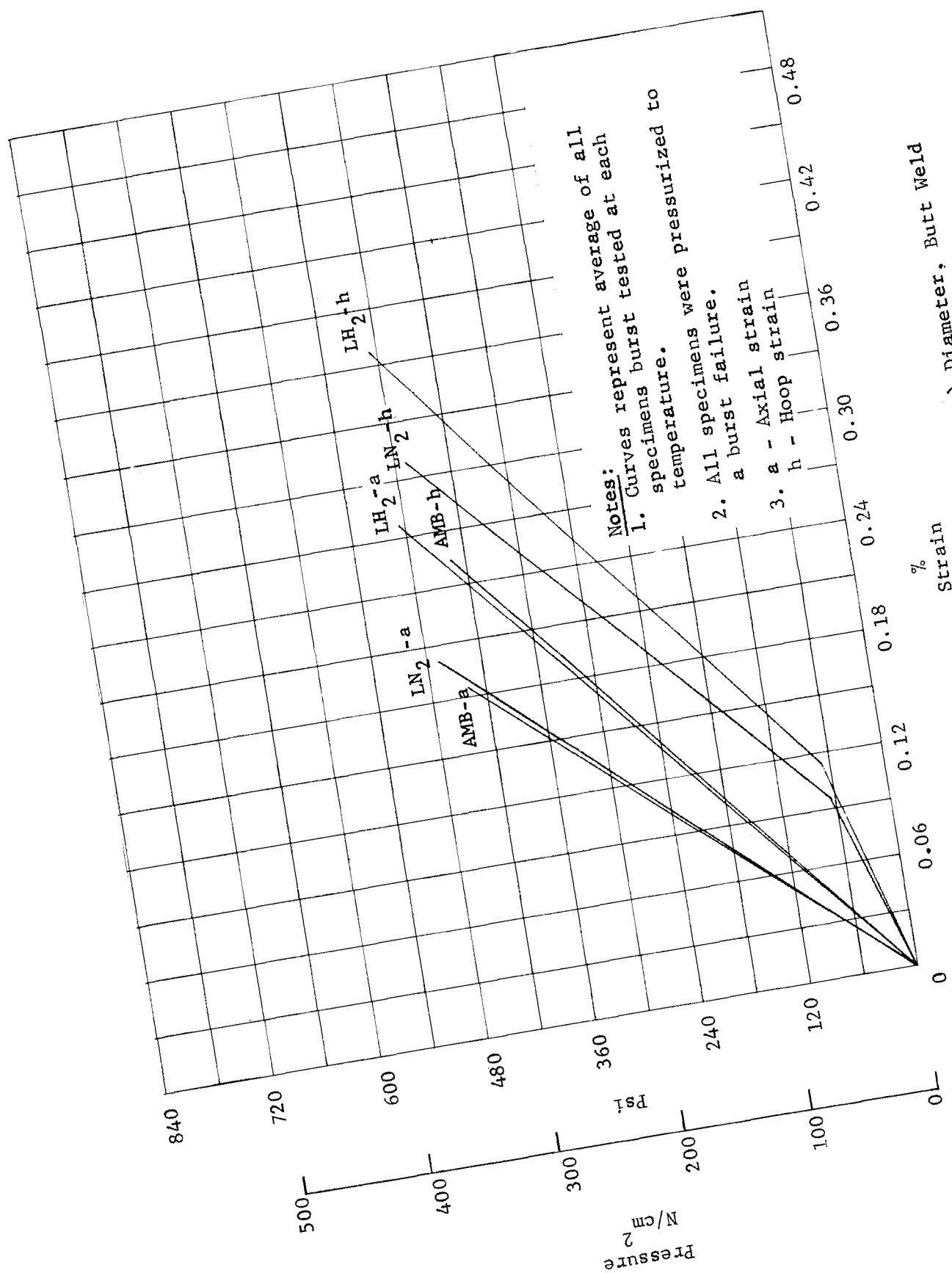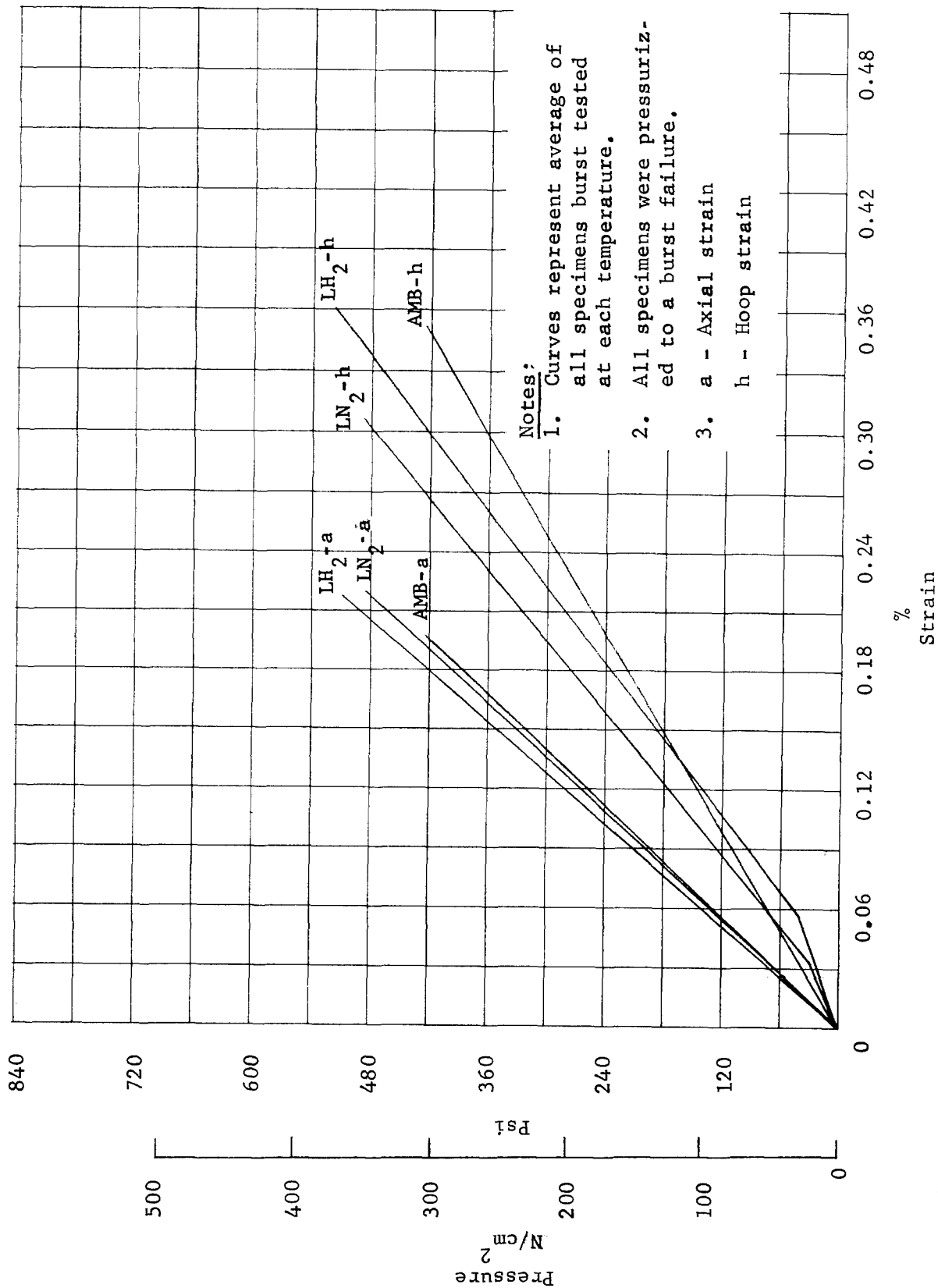Glass: 0.040 in. (0.10 cm) Hoop-Longitudinal-Hoop-Hoop

161

Fig. 75. – Pressure vs Strain, CFL6300614, 5 in. (12.7 cm) Diameter, Butt Weld

TABLE 35.— BURST TEST DATA, PART NO. CFL6300614

Serial no.	Test temperature		Pressure at failure		% Strain at failure		Pressure rise rate	
	°F	°K	lbs/in²	N/cm²	Axial	Hoop	lbs/in²-sec	N/cm²-sec
109	Amb	Amb	390[f]	270[f]	0.17	0.42	10	10
110	Amb	Amb	440[f]	310[f]	0.24	0.55	10	10
111[g]								
112	-320	78	510[f]	350[f]	0.23	0.31	10	10
113	-423	20	530[f]	370[f]	0.25[d]	0.29	10	10
114	-423	20	530[f]	370[f]	0.29	0.31	10	10
115[a]	Amb	Amb	400[f]	280[f]	0.16	0.23	40	30
116[a]	Amb	Amb	440[f]	310[f]	0.22	0.20	20	15
117[a]	-423	20	520[f]	360[f]	c	0.33	20	15
118[a]	-423	20	520[f]	360[f]	0.18	0.48	10	10
119[a]	-320	78	440[f]	310[f]	0.20	c	10	10
120[a]	-320	78	510[f]	350[f]	0.23	c	30	20

Design operating pressure: 200 psi (138N/cm²) Minimum acceptable burst pressure: 400 psi (276 N/cm²)

Calculated Burst Pressure:
70°F (294°K)   420 psig (290 N/cm²)
-320°F (78°K)   530 psig (370 N/cm²)
-423°F (20°K)   550 psig (380 N/cm²)

Standard Notes:
a Post Cycle Burst Test Specimen
b Torsion Test Specimen
c Strain Gage Non-Operating
d Strain Gage Failed Prior to Test Item Failure, Curve Extrapolated
e Leakage Failure
f Weld Failure (Liner to End Fitting Adapter)
Other Notes: g No Data Obtained During Burst

Test Specimen Description
Dimensions: 5.0 in. (12.7 cm) diameter x 12 in. (30.48 cm) long
Liner: 0.003 in. (0.008 cm) Inconel 718, Straight Fusion Weld Tube Not Redrawn, Heat Treated and Age Hardened
End Fitting: Butt Weld, Resistance Weld to Liner
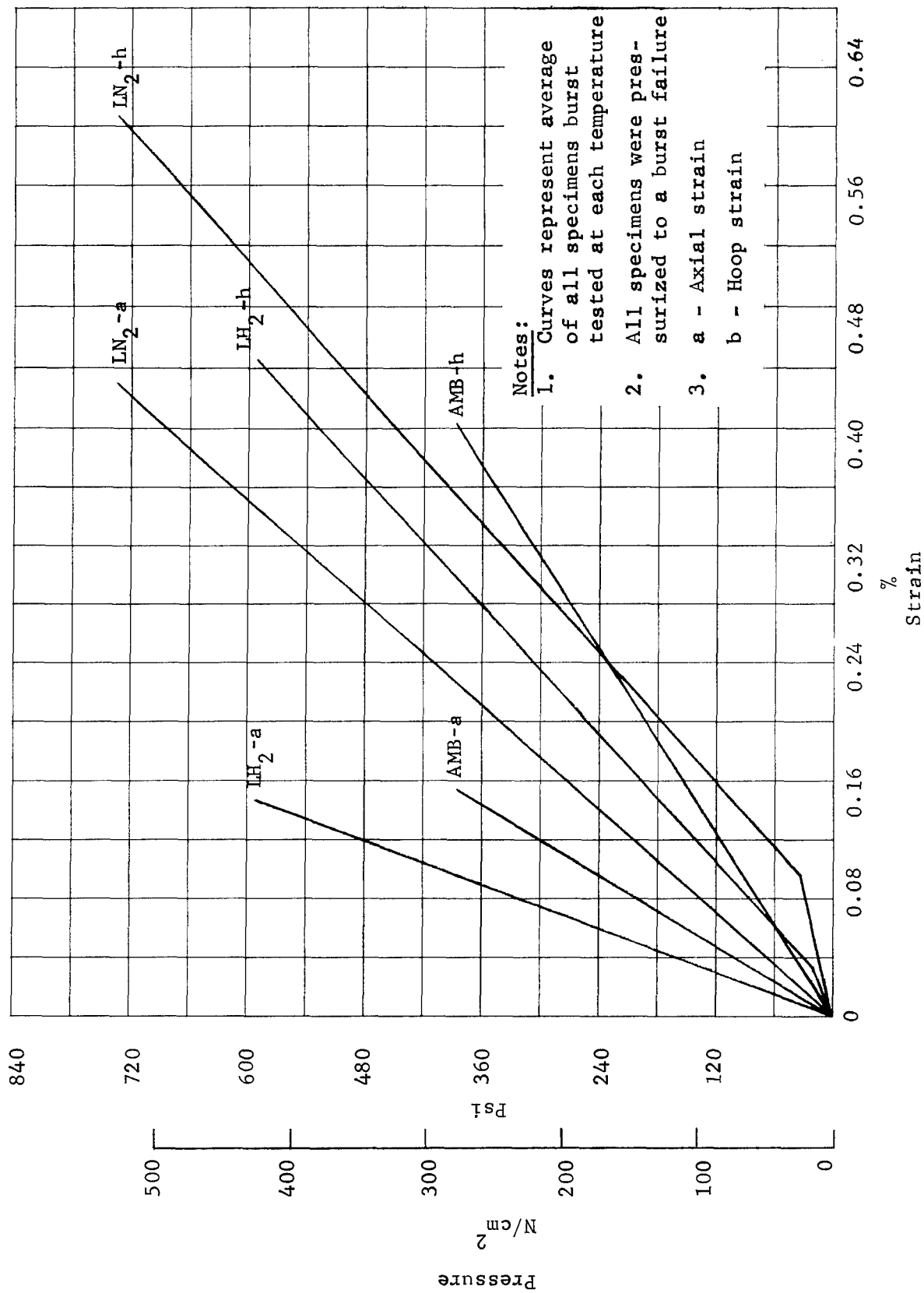Glass: 0.040 in. (0.10 cm) Hoop-Longitudinal-Hoop-Hoop

Fig. 76. - Pressure vs Strain, CFL6300615, 5 in. (12.7 cm) Diameter, NASA Flange

164

TABLE 36.- BURST TEST DATA, PART NO. CFL6300615

Serial no.	Test temperature		Pressure at failure		% Strain at failure		Pressure rise rate	
	°F	°K	lbs/in²	N/cm²	Axial	Hoop	lbs/in²-sec	N/cm²-sec
121	Amb	Amb	370[fgj]	250[fgj]	0.15	0.18	10	10
122	Amb	Amb	310[fg]	210[fg]	0.12	0.13	10	10
123	-320	78	490[fj]	330[fj]	0.20	0.35	10	10
124	-320	78	800[f]	550[f]	0.47	0.68	10	10
125	-423	20	650[f]	450[f]	0.14	0.44	10	10
126	-423	20	520[f]	360[f]	c	c	10	10
127[ai]								
128[b]								
129[ah]								
130[ah]								
131[ab]	-320	78	790[f]	540[f]	0.65	0.78	10	10
132[ab]	-320	78	850[f]	590[f]	0.38	c	10	10

Design operating pressure: 200 psi (138N/cm²) Minimum acceptable burst pressure: 400 psi (276 N/cm²)

Calculated Burst Pressure:
    70°F (294°K)   550 psig (380 N/cm²)
    -320°F (78°K)   730 psig (500 N/cm²)
    -423°F (20°K)   850 psig (580 N/cm²)

Standard Notes:
a Post Cycle Burst Test Specimen
b Torsion Test Specimen
c Strain Gage Non-Operating
d Strain Gage Failed before Test Item Failure, Curve Extrapolated
e Leakage Failure
f Weld Failure (Liner to End Fitting Adapter)

Other Notes:
g After These Premature Failures, This Article was Redesigned
h Destroyed as a result of system lockup with cryogenics in system
i Thermal Flux Test
j No Axial Glass-Fiber Layer - Hoop - Hoop - Hoop - Hoop
Test Specimen Description

Dimensions: 5.0 in. (12.7 cm) diameter x 12 in. (30.48 cm) long
Liner: 0.006 in. (0.015 cm) Inconel 718, Straight Fusion Weld Tube Not Redrawn, Annealed
End Fitting: Raised Face NASA Configuration Flange, Fusion Weld to Liner
Glass: 0.040 in. (0.102 cm) Hoop-Longitudinal-Hoop-Hoop
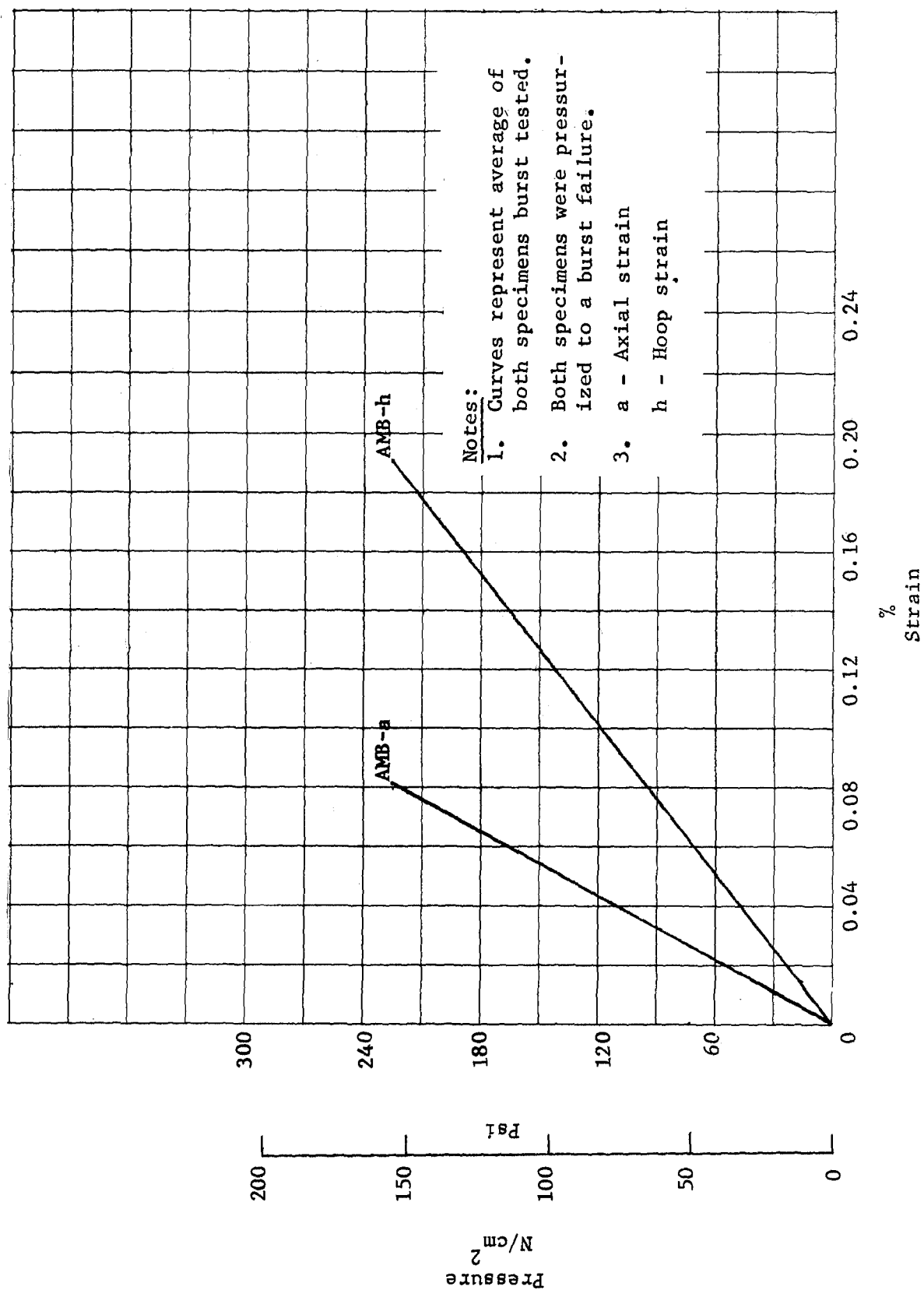
Fig. 77. - Pressure vs Strain, CFL6300616, 5 in. (12.7 cm) Diameter, Conoseal

166

TABLE 37.- BURST TEST DATA, PART NO. CFL6300616 [a]

Serial no.	Test temperature		Pressure at failure		% Strain at failure		Pressure rise rate	
	°F	°K	lbs/in^2	N/cm^2	Axial	Hoop	lbs/in^2-sec	N/cm^2-sec
133	Amb	Amb	200	141	b	b	10	10
134	Amb	Amb	230	161	0.08	0.19	10	10

Design operating pressure: 200 psi (138 N/cm^2) Minimum acceptable burst pressure: 400 psi (276 N/cm^2)

Calculated Burst Pressure: 70°F (294°K)   550 psig (380 N/cm^2)

Other Notes:

a This design cancelled due to inadequacy of weld strength
b Strain Gage Non-Operating

Test Specimen Description

Dimensions: 5.0 in. (12.7 cm) diameter x 12 in. (30.48 cm) long
Liner: 0.006 in. (0.015 cm) Inconel 718, Straight Fusion Weld Tube Not Redrawn, Annealed
End Fitting: Conoseal Strap Flange, Fusion Weld to Liner
Glass: 0.040 in. (0.10 cm) Hoop-Longitudinal-Hoop-Hoop

The failure modes for each design in the third group of test specimens are presented in the following paragraphs.

CFL6300613, 5 in. (12.7 cm) butt weld: One specimen of this design, S/N 106, was accidently overpressurized at the beginning of pressure and temperature cycle testing. The remaining test specimens were pressurized to a burst failure. The failure mode for this design was due to liner failure in the heat-affected zone adjacent to the resistance weld joining the liner to the end fitting adapter. This failure is shown in fig. 78.
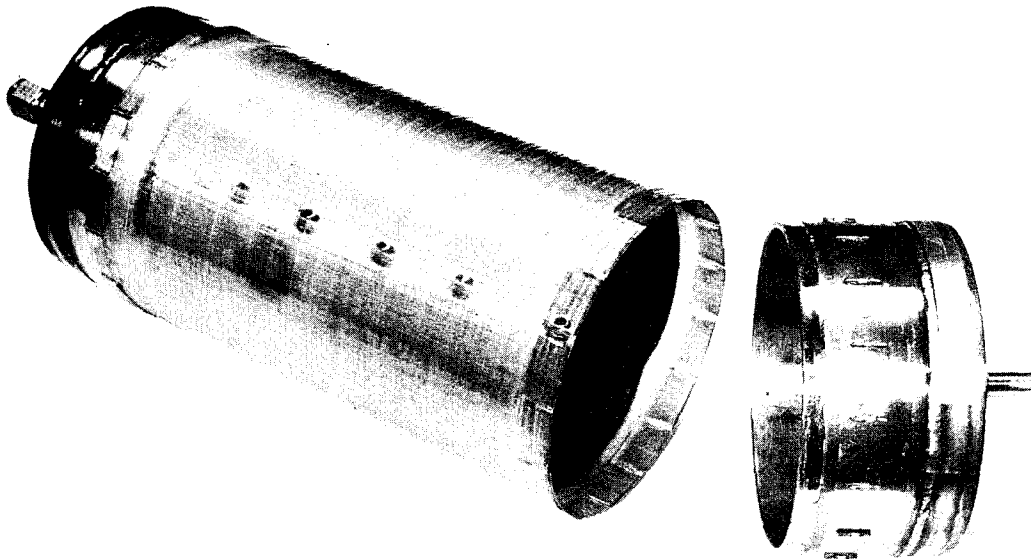
Fig. 78. - Failure Mode, CFL6300613 and CFL6300614

CFL6300614, 5 in. (12.7 cm) butt weld: All 12 specimens of this design were pressurized to a burst failure. The failure mode for all specimens was liner failure in the heat-affected zone adjacent to the resistance weld joining the liner to the end fitting adapter. This failure is shown in fig. 78.

CFL6300615, 5 in. (12.7 cm) NASA flange: One specimen of this design, S/N 127, had the flanges removed after cycle testing to provide a specimen for thermal testing and was not subjected to burst or torsion test. The flanges were removed so the test item would fit the thermal test fixture. Two specimens were subjected to torsion tests, S/N 128 and S/N 132, with S/N 132 then being burst tested. Two specimens, S/N 129 and S/N 130, were accidently overpressurized at the beginning of pressure and temperature cycle testing. The remaining test specimen were pressurized to a burst failure. The results of the burst tests on the first two specimens showed the

168

burst pressure on this design was less than twice the design operating pressure. The failure was due to liner failure at the inside edge of the flange. As the liner strained in the axial direction, the glass pulled away from the flange leaving the liner unsupported in this area. This failure is shown in fig. 79. This design was changed to include a doubler that extended out past the edge of the flange. The doubler was flared slightly to prevent damage to the liner during assembly. Failure of the redesigned specimens was due to longitudinal liner failure. This failure is shown in fig. 80.

Fig. 79. - Failure Mode, CFL6300615
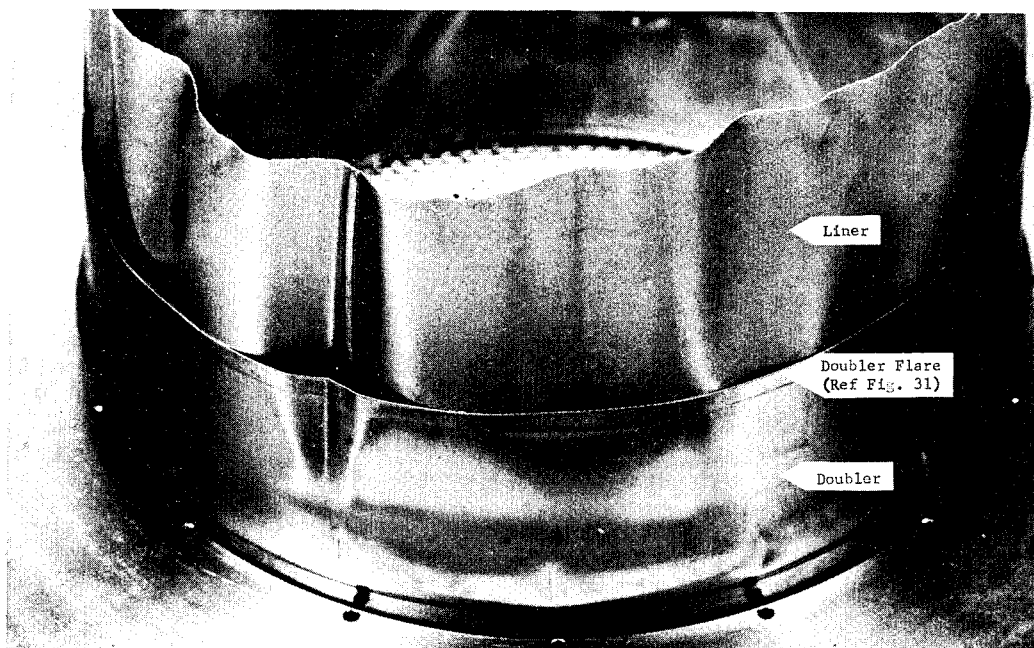
Fig. 80. - Failure Mode, CFL6300615, Redesign

CFL6300616, 5 in. (12.7 cm) strap flange: Two specimens of
this design were fabricated and tested. These specimens failed
at a pressure just over operating pressure due to insufficient
strength in the fusion weld joining the liner to the end fitting
(see fig. 81). This design was therefore cancelled from the test
program.
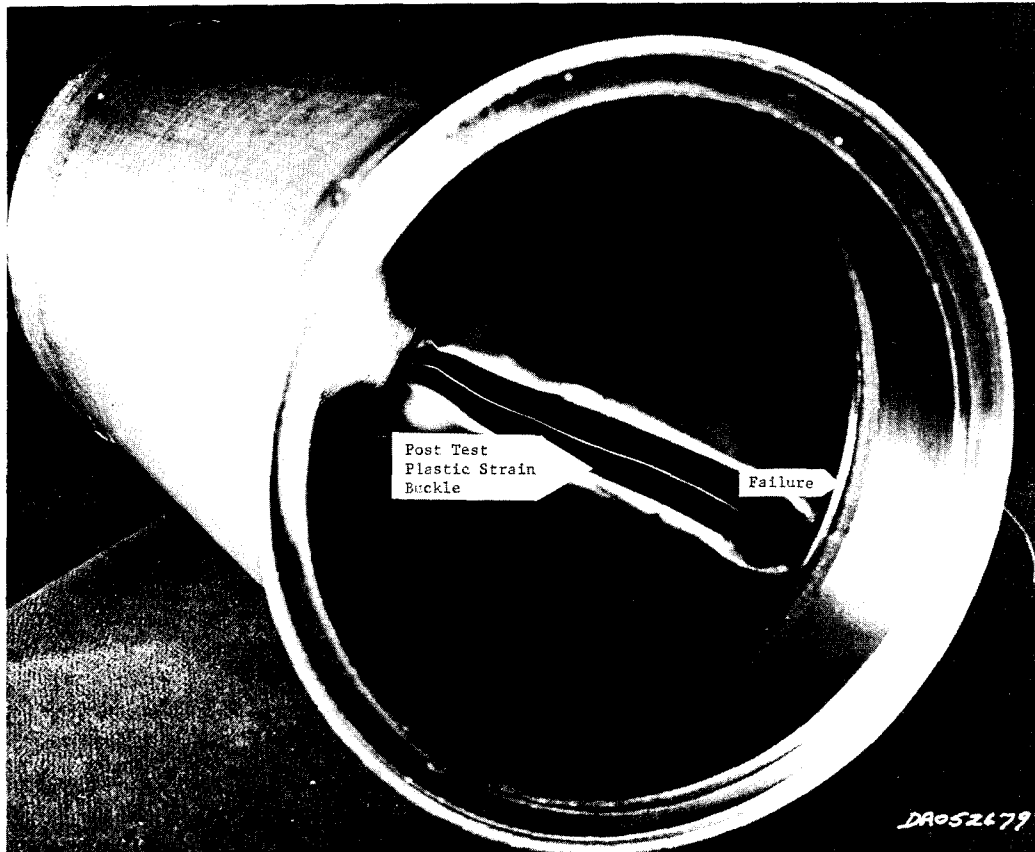
Fig. 81. - Failure Mode, CFL6300616

Pressure-Temperature Cycle and Extended Load Test

The objective of this test program was to investigate the
feasibility of using glass-fiber tubing in a cryogenic system as
tank pressurization and propellant outflow plumbing. During the
design phase of the test program a fatigue life goal of at least
200 pressure-temperature cycles was established. The purpose of
the cycle testing was to verify that this design goal had been
achieved.

Test fixtures. - A schematic of the test fixture used for the
ambient cycle test is shown in fig. 82. One end of the test speci-
mens was capped and the opposite ends were manifolded together so

170
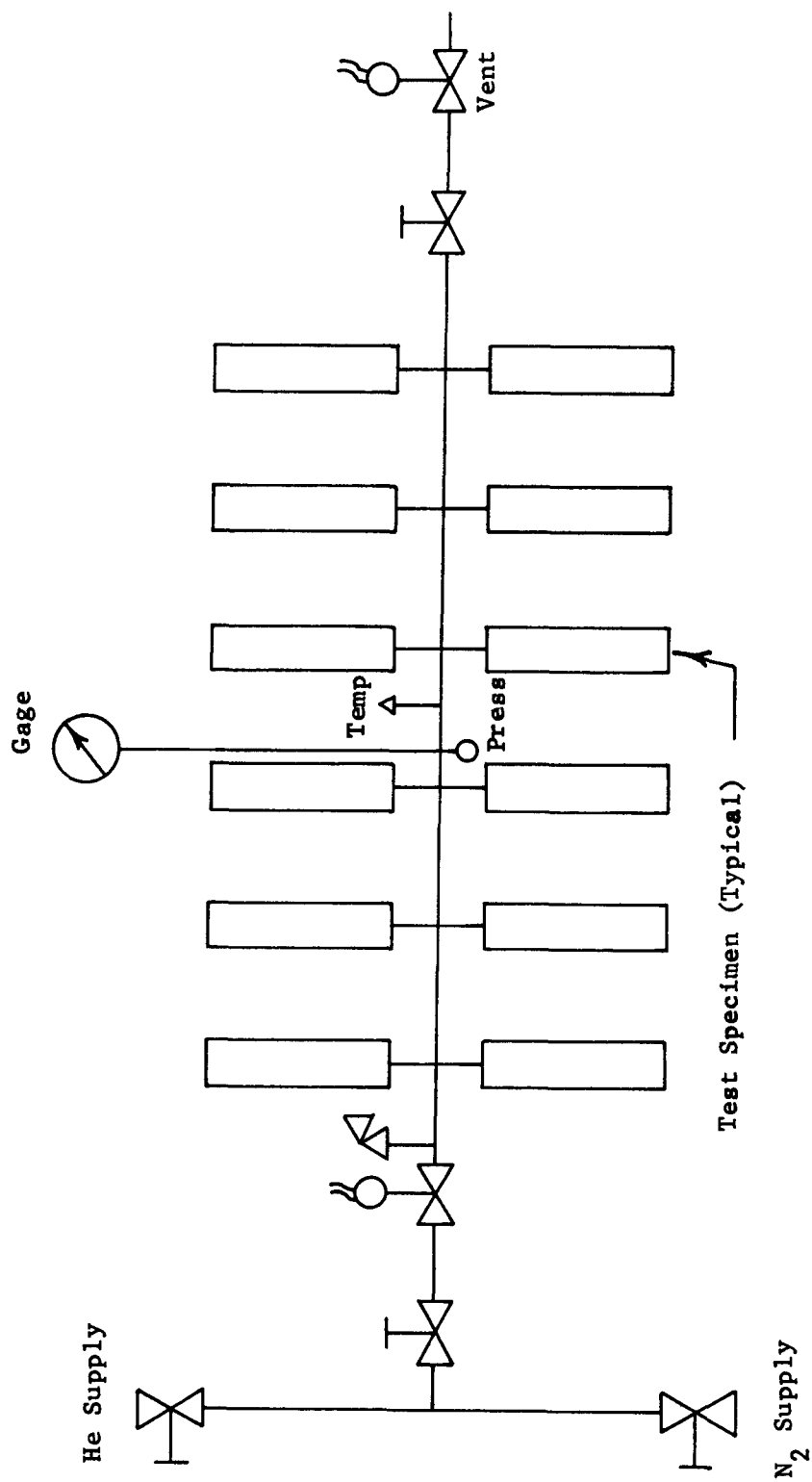
Fig. 82. - Test Fixture Schematic, Ambient Cycle Test

171

that all specimens were pressurized simultaneously. The pressurization and vent rates were controlled by throttling valves located at the inlet and outlet of the manifold. The pressurization medium was gaseous nitrogen at ambient temperature.

A schematic of the test fixture used for cryogenic cycle tests is shown in fig. 83. Two identical specimens of each design were mounted in series in a flow loop suspended from the vacuum chamber lid. The inlet and outlet lines passed through the lid to the inlet and outlet manifolds, respectively. An isolation valve was installed in the inlet lines to control flow through each loop. The nitrogen gas used as the pressurization medium was precooled by flowing through a liquid nitrogen heat exchanger before entering the test specimens. The liquid nitrogen used to cool down the test specimens to liquid nitrogen temperature was supplied from the facility storage system. Liquid hydrogen was supplied to the test fixture from 1500-gal (5.7 m^3) trailers. The pressurization rate was controlled by an orifice in the pressurization line and the isolation valves in each flow loop. The vent rate was controlled by a throttle valve in the vent line.

<u>Test method-ambient cycle</u>. - After installing the test specimens in the ambient cycle test fixture, the system was pressurized to operating pressure with gaseous nitrogen, and all test fixture connections were leak checked with soap solution. All leaks except test specimen leaks were corrected before proceeding with the test. Each test specimen was then enclosed in a polyethylene bag. The system was then pressurized to operating pressure with helium and each specimen was leak checked with a helium mass spectrometer using the probe test method. Leakage was recorded at 30 second intervals for a 5-minute period to establish the pretest leakage rate of each test specimen. The pressure cycles were performed by opening the pressurization valve and allowing the system pressure to increase to operating pressure. The inlet throttling valve was adjusted so that strain rate of the test specimens did not exceed 1%/min. The pressurization valve was then closed and the vent valve was opened. The vent rate was controlled by adjusting the outlet throttling valve as required. This sequence was repeated until nine pressure cycles had been completed. On the tenth cycle gaseous helium was used to pressurize the system and each specimen was again leak checked for a 5-minute period. This procedure was repeated with a leak check on every tenth pressure cycle until a total of 200 pressure cycles were completed. After completing the final leak check, the test specimens were subjected to an extended load test by pressurizing the system to operating pressure and maintaining the pressure for a 24 hr period. At the end of the 24 hr period, the test specimens were again leak checked.
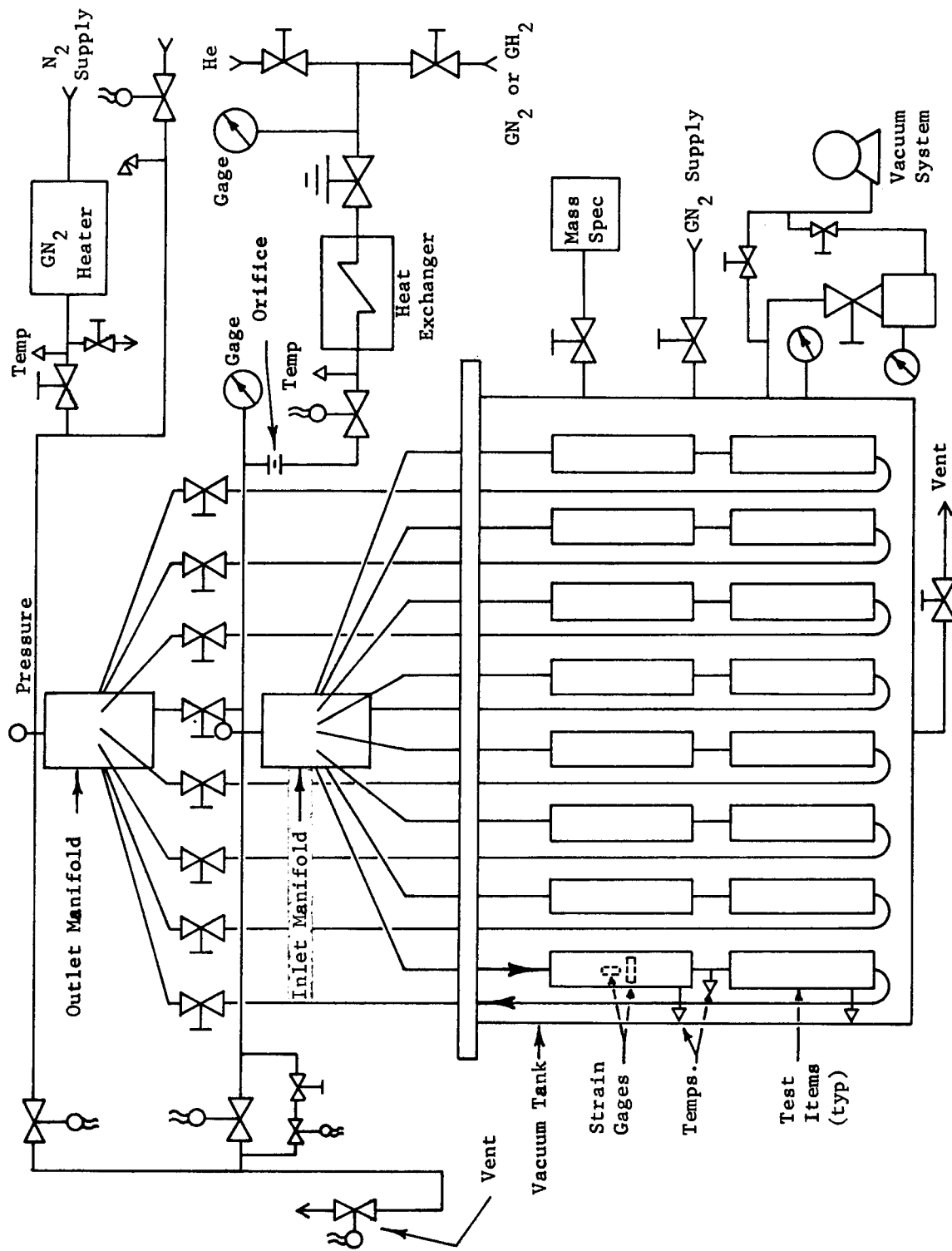
Fig. 83. - Test Fixture Schematic Cryogenic Cycle Test

Test method-cryogenic cycle. - The test specimens that had NASA flanges as end fittings were subjected to a retorque operation before installation in the test fixture. This operation consisted of assembling the joints and torquing the bolts to the specified torque value then cooling the joints by flowing liquid nitrogen through the test specimen. The joint was then returned to ambient temperature and the bolts were retorqued. This operation was repeated for five cycles.

When the test specimens were installed in the cryogenic cycle test fixture (fig. 84 and 85), all connections inside of the vacuum chamber, except those test specimen connections intended to be a part of the test, were seal welded to eliminate all leakage into the chamber, except test specimen leakage. The pressure-temperature cycles were performed by cooling the test specimens to operating temperature, pressurizing to operating pressure, venting the pressure and warming the specimen to ambient temperature. The vacuum chamber was evacuated before starting the cooldown and the vacuum was maintained throughout the test. The test specimens were cooled down by flowing liquid nitrogen or liquid hydrogen from the supply through the inlet manifold and the test specimens into the outlet manifold and an outlet vent. This flow was continued until all test specimens were stabilized at operating temperature. The isolation valves in the test item inlet lines were adjusted so that all specimens were cooled at nearly the same rate. When the test specimens were stabilized at operating temperature, the cryogen flow was stopped and the test specimens were pressurized to operating pressure with cold gas. The pressurization valve was then closed and the pressure in the test specimens was vented through the vent valve. The pressurization and vent rates were controlled so as not to exceed a test specimen strain rate of 1%/min. The test specimens were then warmed up to ambient temperature by flowing hot gaseous nitrogen from the nitrogen heater through the inlet manifold and the test specimens into the outlet manifold and out the vent. This sequence was repeated until nine cycles had been completed. On the tenth cycle the specimens were pressurized with cold helium and a leak check was performed using a helium mass spectrometer connected to the vacuum chamber. The helium leakage into the chamber was monitored for a time period sufficient to establish the increase rate and/or achieve a steady state rate. The pressure-temperature cycles were repeated with a leak check on every tenth cycle until a total of 200 cycles were completed. Assuming a constant system sensitivity, the leakage rate in scc/sec for an increment of time was monitored and compared to the leakage rate observed on preceeding leak checks for the same increment of time. That is, if after 5 minutes, the leakage rate for cycle 1 was 1×10^{-7} scc/sec and after 5 minutes on cycle 10 the leakage rate was 1×10^{-7} scc/sec, then it was assumed there was no tube degradation. At the conclusion of the 200 cycles each tube was individually leak checked and the results were compared to the results of the individual tube pretest leak check to verify the above assumptions.
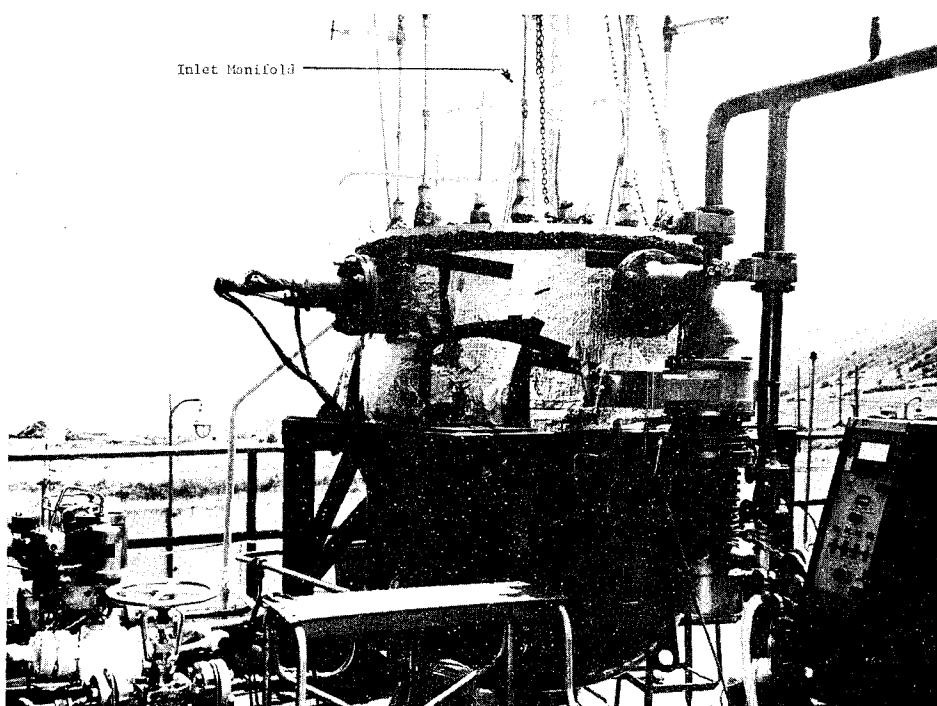
Inlet Manifold

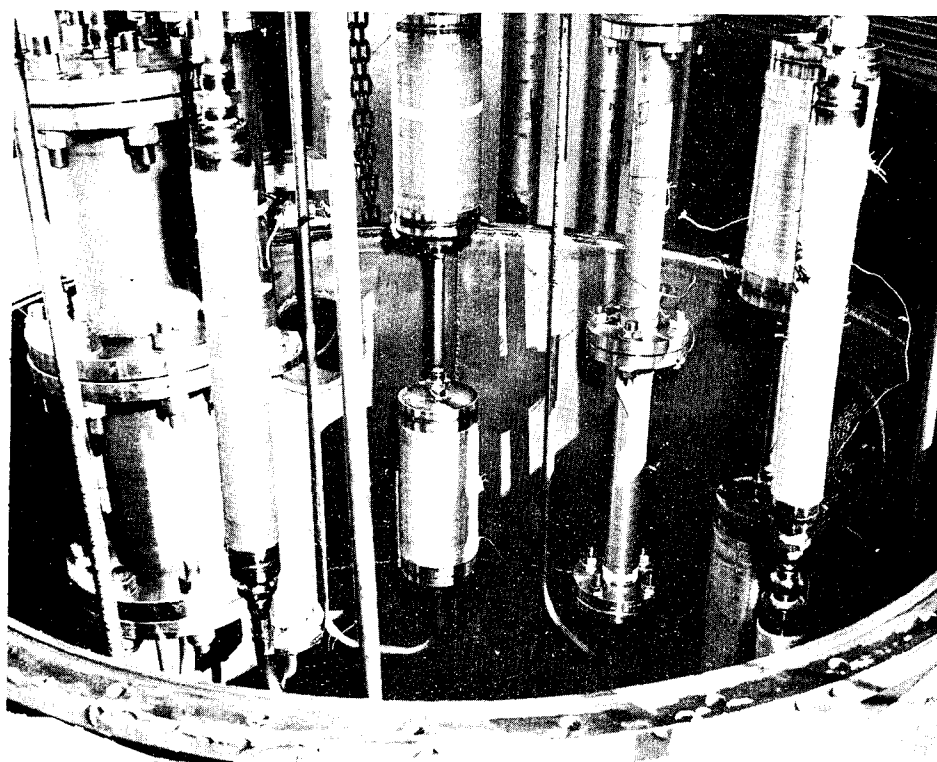Fig. 84. - Cryogenic Cycle Test Fixture

Fig. 85. - Test Specimen Installation - Cryogenic Cycle Test

Test results and discussion. - The results of the leak checks performed at 10 cycle intervals during all pressure-temperature cycle testing showed no increase in the leakage characteristics of any test specimen as a result of the 200 pressure-temperature cycles. The leak checks after cycling verified no significant change in leakage rates. Plots of pressure, temperature and strain vs time for a typical cycle on representative test specimens are included as fig. 86 through 89. All tubes successfully passed the 24-hr extended load test. Results of the burst test after extended load are included in the burst test section.

Torsion Tests

The purpose of the torsion testing was to determine the strength of the test specimens when subjected to torsional loading that may be encountered during assembly and installation of pressurization and propellant outflow lines.

Test method and equipment. - To perform the torsion tests one end of the test specimen was clamped in a fixed position with the test specimen in a vertical attitude. A torque wrench of the proper range was then attached to the free end of the specimen so that torque could be applied along the centerline of the test specimen. During the application of torque, care was taken to assure that no bending loads were imposed on the test specimen.

Test results and discussion. - The results of the torque test are tabulated in table 38 and discussed in the following paragraphs:

CFL6300605, 1/2 in. (1.27 cm), flared tube: Two specimens of this design were subjected to the torsion test. The failure mode on both specimens was a circumferential crack in the glass overwrap and a subsequent buckling of the liner. The end bond of the glass overwrap to the liner remained intact. This failure is shown in fig. 90.

CFL6300607, 1/2 in. (1.27 cm), flat flanged: Two specimens of this design were subjected to the torsion test. The failure mode of these specimens was identical to that described above.

CFL6300608, 1/2 in. (1.27 cm), CRES flared: One specimen of this design were subjected to the torsion test. The failure mode on this specimen was identical to that described above.

CFL6300611, 2 in. (5.08 cm), flat flanged: Two specimens of this design was subjected to the torsion test. The failure mode on both specimens was buckling of the liner after failure of the end bond between the glass overwrap and the liner. This failure is shown in fig. 91.
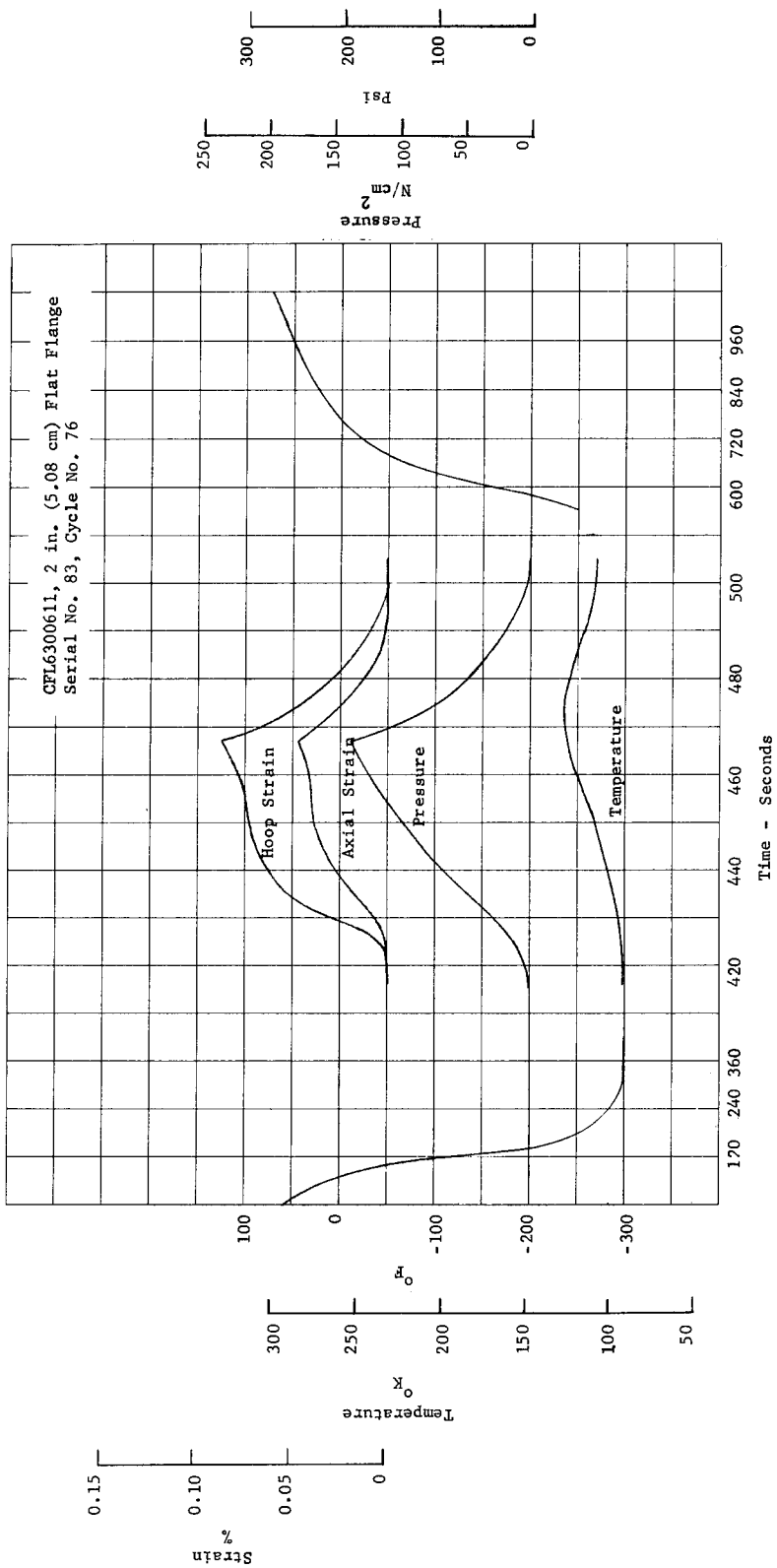
Fig. 86. - Strain, Pressure, and Temperature vs Time, Low Pressure Liquid Nitrogen Cycle

177
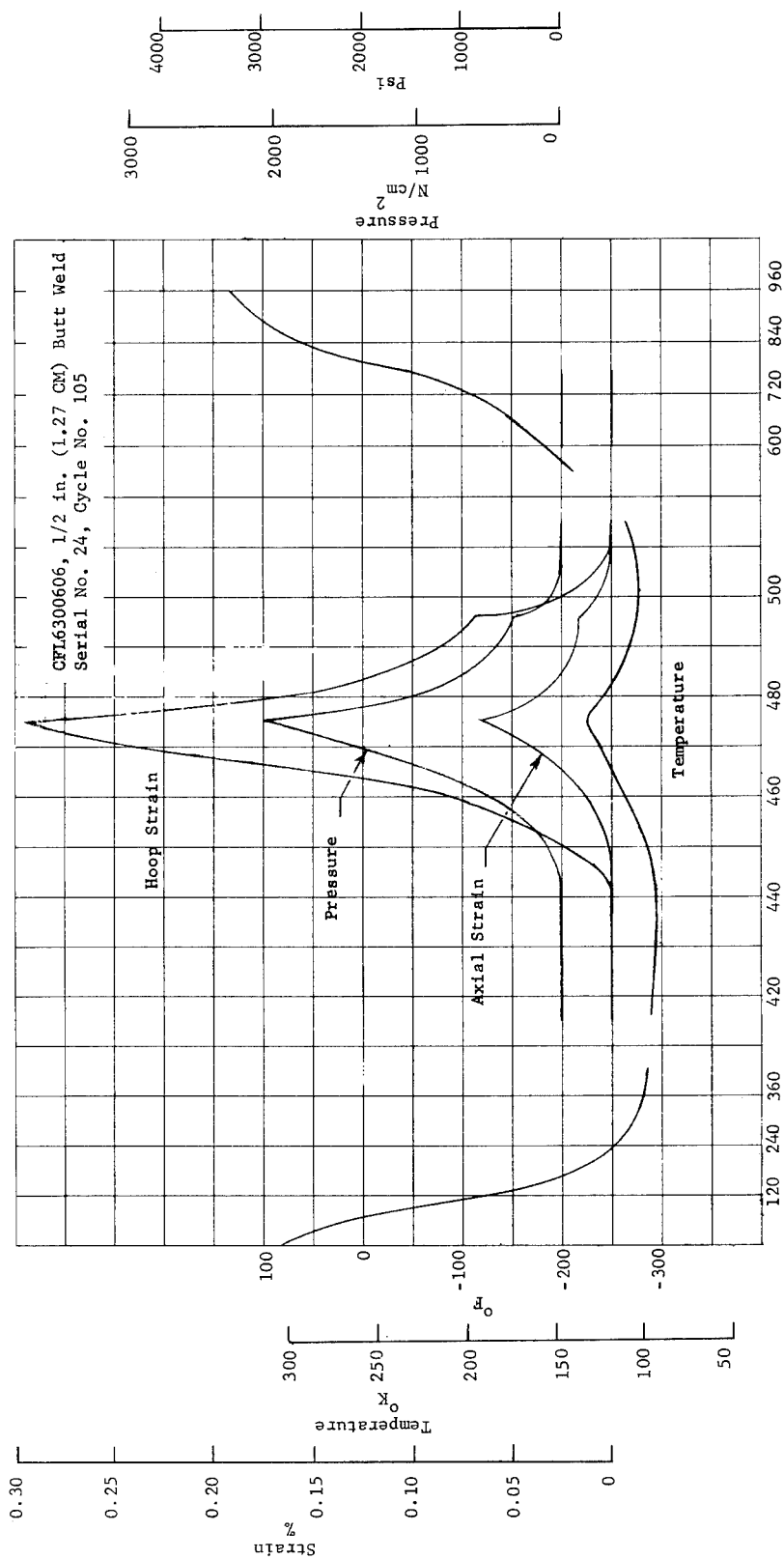
Fig. 87. - Strain, Pressure, and Temperature vs Time, High Pressure Liquid Nitrogen Cycle

178
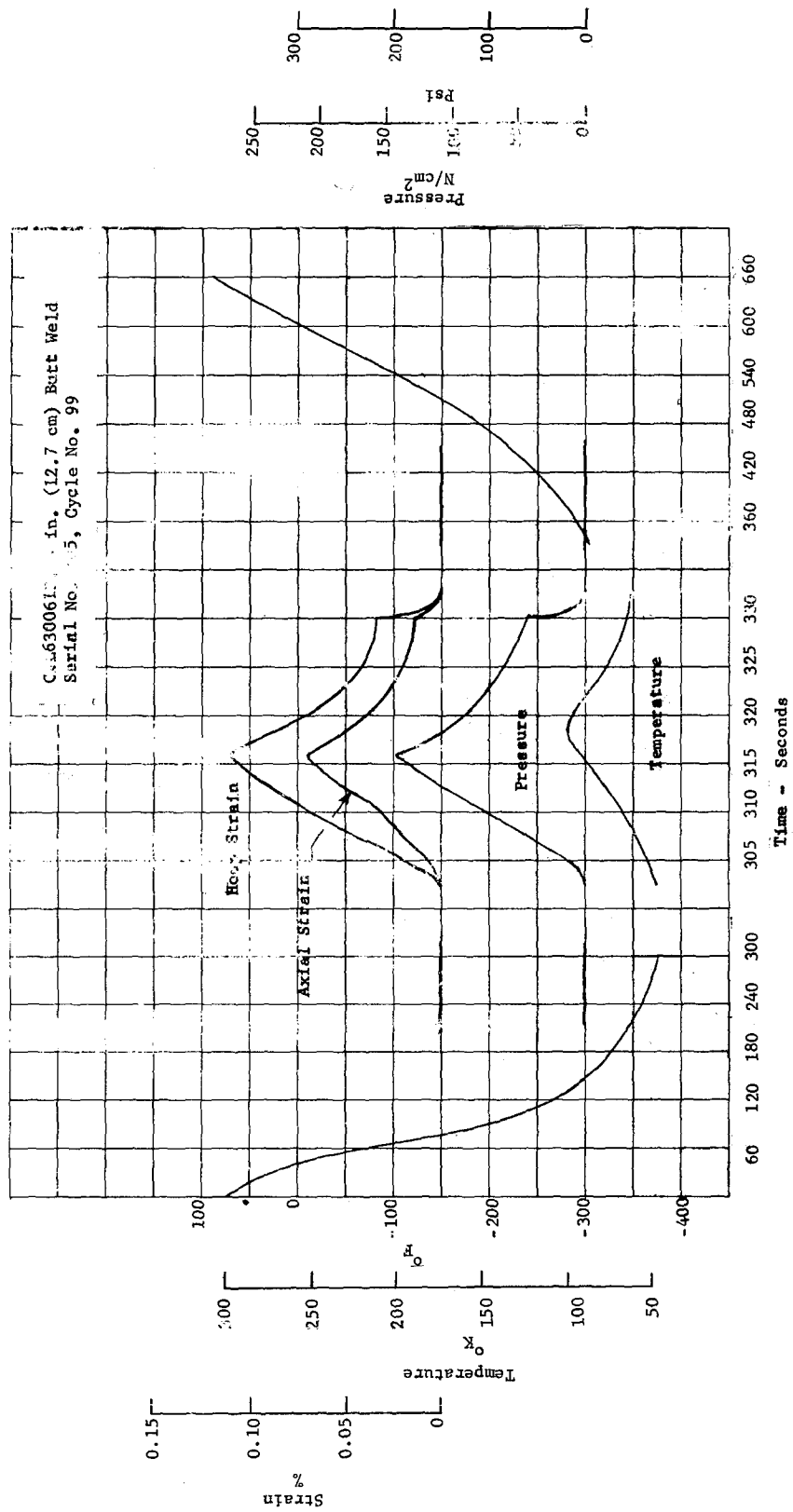
Fig. 88. - Strain, Pressure, and Temperature vs Time, Low Pressure Liquid Hydrogen Cycle
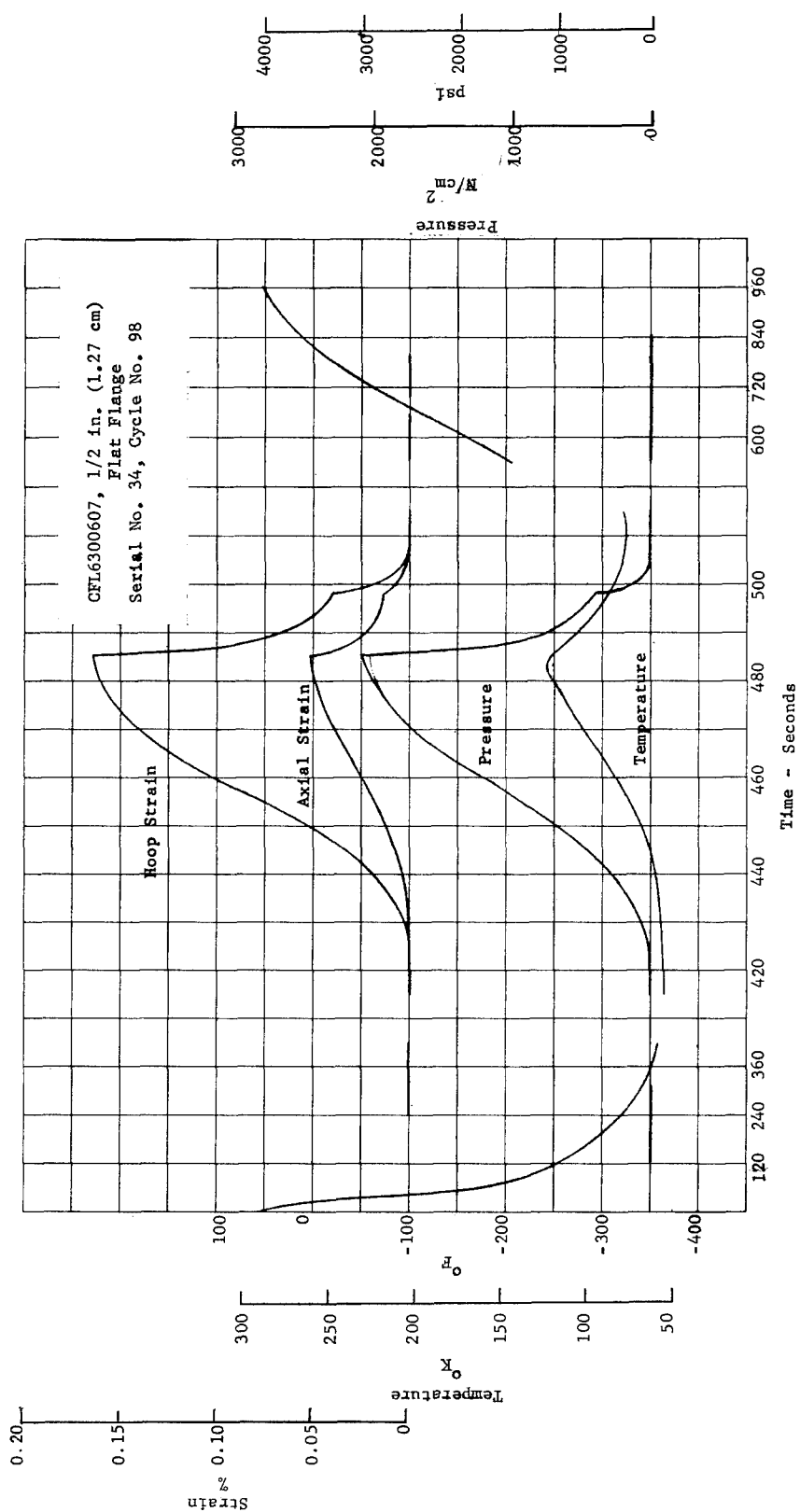
Fig. 89. - Strain, Pressure, and Temperature vs time, High Pressure Liquid Hydrogen Cycle

CFL6300607, 1/2 in. (1.27 cm)
Flat Flange
Serial No. 34, Cycle No. 98

Hoop Strain

Axial Strain

Pressure

Temperature

180
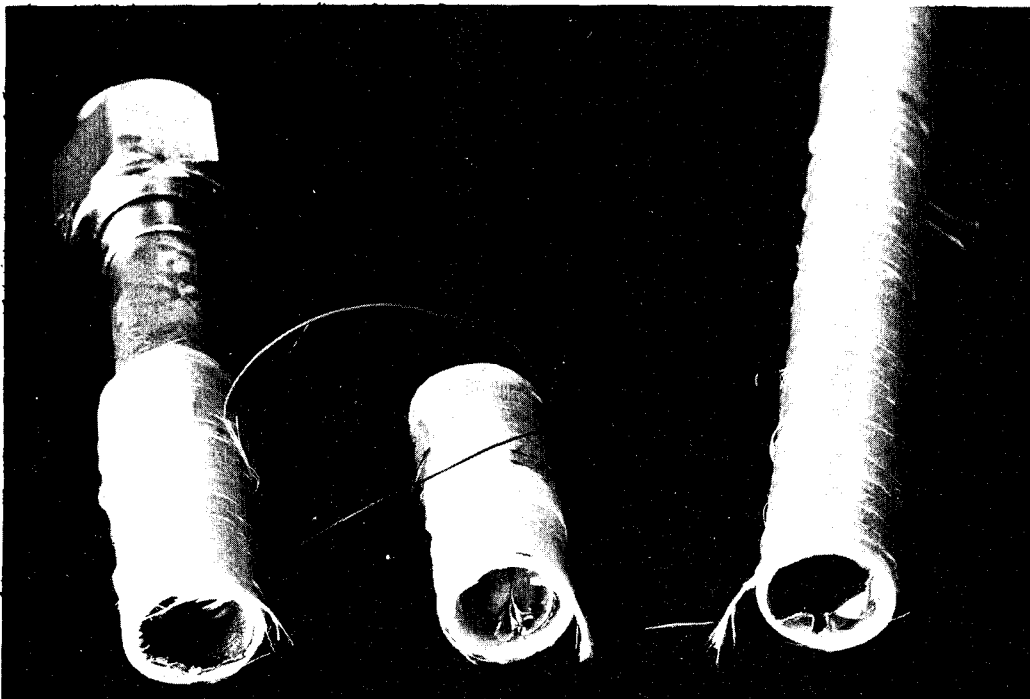
Fig. 90. - Torsion Failure Mode, 1/2 in. (1.27 cm) Diameter Tube
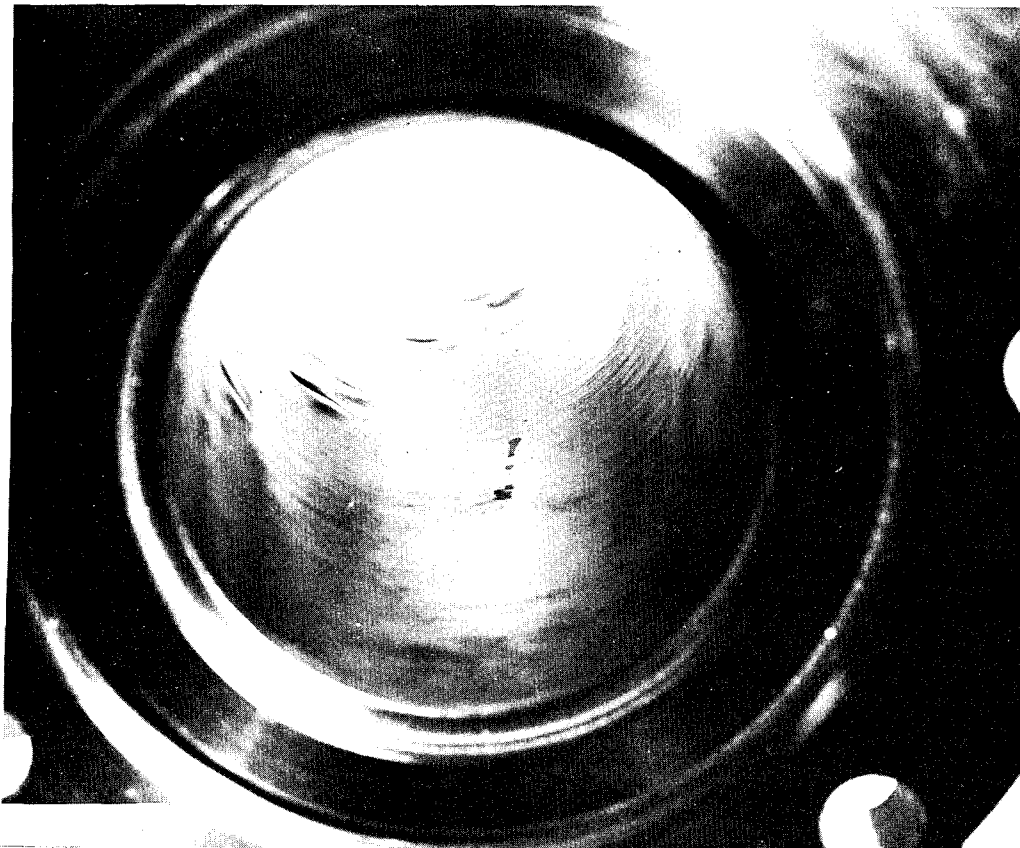
Fig. 91. - Torsion Failure Mode 2 in. (5.08 cm) Diameter Flat Flange

181

CFL6300612, 2 in. (5.08 cm) NASA flange: One specimen of this
design was subjected to the torsion test. The failure mode on this
specimen was a circumferential crack in the glass overwrap and a
subsequent buckling of the liner. This failure is shown in fig. 92.

Fig. 92 - Torsion Failure Mode 2 in. (5.08 cm) Diameter NASA Flange

CFL6300615, 5 in. (12.7 cm) NASA flange: Two specimens of
this design were subjected to the torsion test. There was no
failure in either of these test specimens as a result of the torsion
test. The applied torque, shown in table 38, was the maximum allow-
able for personnel safety.

TABLE 38

TORSION TEST RESULTS

| Test Specimen Description | | Torque at Failure | | | |
| | | Actual | | Predicted[a] | |
Part No.	S/N	in.-lbs.	N-m	in.-lbs.	N-m
CFL6300605	8	480	54	63	7
CFL6300605	12	400	45	63	7
CFL6300607	32	288	33	63	7
CFL6300607	36	400	45	63	7
CFL6300608	44	180	20	63	7
CFL6300611	80	840	95	525	60
CFL6300611	84	660	75	525	60
CFL6300612	92	2160	244	525	60
CFL6300615	128	4200[b]	475[b]	1236	140
CFL6300615	132	4200[b]	475[b]	1236	140

a. Predicted values were based on liner strength only. The higher actual values are due to the shear resistant bond between the glass overwrap and the end fitting.

b. Failure did not occur.

Thermal Testing

The thermal performances of tube specimens was experimentally evaluated in two series of thermal tests, consisting of (1) solid thermal conductivity determination of specimen segments at reduced temperatures and (2) thermal flux measurement for representative complete tube specimens.

Solid thermal conductivity testing.- A test series was conducted to measure the effective thermal conductivity of the walls of the composite tube for each of the three specimen diameters. The specimens consisted of short segments cut from representative completed test specimens, and are shown in figures 93 and 94.

Test Equipment: An existing test apparatus was used which had been successfully applied to measurement of thermal conductivity of similar composite tube specimens at cryogenic temperatures. The device is shown schematically in fig. 95. It consists of a vacuum chamber, a cryogen container which serves as a heat sink and a shroud enclosed test area. The specimen to be tested is mounted in thermal contact with the heat sink on one end and an electrical resistance heater on the other. The insulated shroud is physically mounted to the heat sink, and operates near the cold end temperature of the specimen. Instrumentation provides for measurement of heater power, temperatures at each end of the specimen and the shroud, and liquid level and pressure of the cryogen.

Because of the low expected thermal flux through the specimen, and its tubular configuration, care is required in the design of the test to achieve an acceptable accuracy. The approach taken was to control the expected specimen heat flux to a value such that the extraneous heat loss would be a reasonably small fraction of the total. When the predicted heat fluxes through paths other than the specimen are then subtracted out, a satisfactory accuracy is obtained even though the tare heat flux may deviate somewhat from its predicted value. This argument leads to the selection of a very short specimen. However, the effective length of the specimen is not the measured length of the tube segment. The effective length is dependent on the thermal contact between the specimen and the end fittings, and becomes more difficult to determine accurately as the length is decreased and temperature gradients in the vicinity of the end fittings increase. A specimen length of 1 in. (2.54 cm) has been found to provide a satisfactory compromise between the above considerations, and was selected for this program.

To attain a minimum heat flux through paths other than the specimen to be evaluated, the tube is insulated internally and externally as shown in fig. 95. The internal insulation is accomplished with
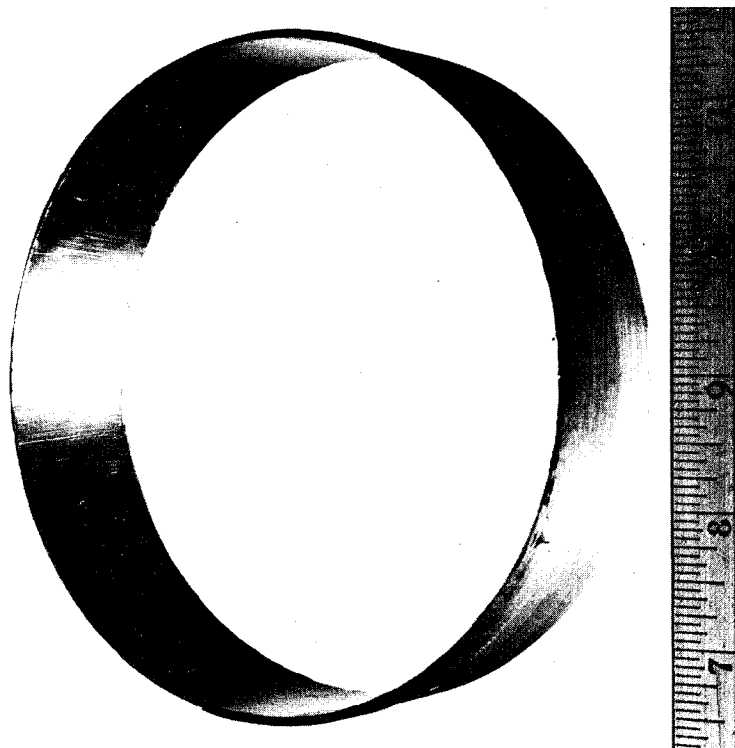
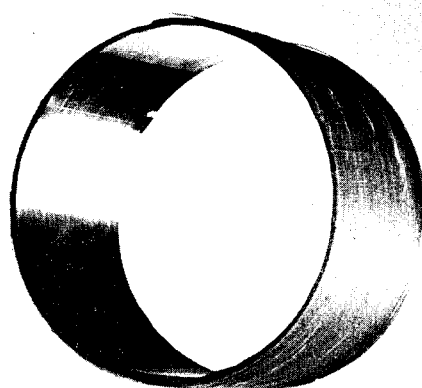Fig. 93. - Thermal Conductivity Test Specimens,
1/2 in. (1.27 cm) and 2 in. (5.08 cm)
Diameter.

Fig. 94. - Thermal Conductivity Test Specimen,
5 in. (12.7 cm) Diameter

185

carefully fitted disks of aluminized mylar separated with nylon net. The mylar disks are each perforated, and provision is made for evacuation of the tube interior. The outer insulation is accomplished by carefully fitting layers of aluminized nylon and net ove. the specimen and around the hot end to form a series of concentric enclosures. This configuration provides for reasonably constant temperature over each insulation layer and a minimum of heat transfer parallel to the layers. The necessity of feeding heater and thermocouple wires through the insulation increases the complexity of the insulation installation.

Because the heat leak into the insulated cryogen tank is very much greater than the heat flux through the specimen, boiloff measurement is not a practical means for determining heat flux. Rather, the heater power is measured. This is accomplished by measurement of voltage and current, with voltage taps located near the heater to avoid line loss errors. Constantan power leads through the specimen insulation minimize lead wire losses. Temperatures are measured with copper constantan thermocouples. Liquid level (hydrogen) is measured with carbon sensors, and pressure measurement is by bourdon tube gage.

Test item installation: The specimens were prepared for testing by installing internal radiation shields to reduce radiation heat transfer within the sample. The radiation shields used for this purpose are made up of 1/4-mil-thick (0.0006 cm) mylar aluminized on both sides. This material was cut into disks of a diameter that creates a slight contact between the wall of the sample and the disks. The radiation shield disks were separated by disks of nylon netting to minimize solid heat conduction through the radiation shielding. The disks were stacked inside the sample using two nylon net disks to separate each radiation shield from its adjacent shields. Care was taken to minimize the compaction of the shielding to further reduce solid conduction heat transfer. This method of assembly results in a density of approximately 35 radiation shields per in. (13.8 /cm).

Aluminum rings, machined to provide an interference fit, were pressed into each end of the sample. Aluminum end plates were then bonded to the sample with a thermally conductive epoxy adhesive. The end plates were counter bored so each end of the sample was in contact with aluminum for 0.125 in. (0.318 cm) along its length (i.e., the width of the internal ring and the depth of the counter bore). A typical specimen is shown before and after assembly in fig. 96.

Approximately 35 layers of multilayer insulation, of the type used inside the tubes, was used to insulate the specimen externally. This was accomplished by using oversize sheets of aluminized mylar and netting, each with a hole cut in its center to closely fit the outside diameter of the specimen. All of the mylar foils and spacers were assembled into the specimen, using a short radial slit from the hole to permit installation. Each layer of insulation was then care-
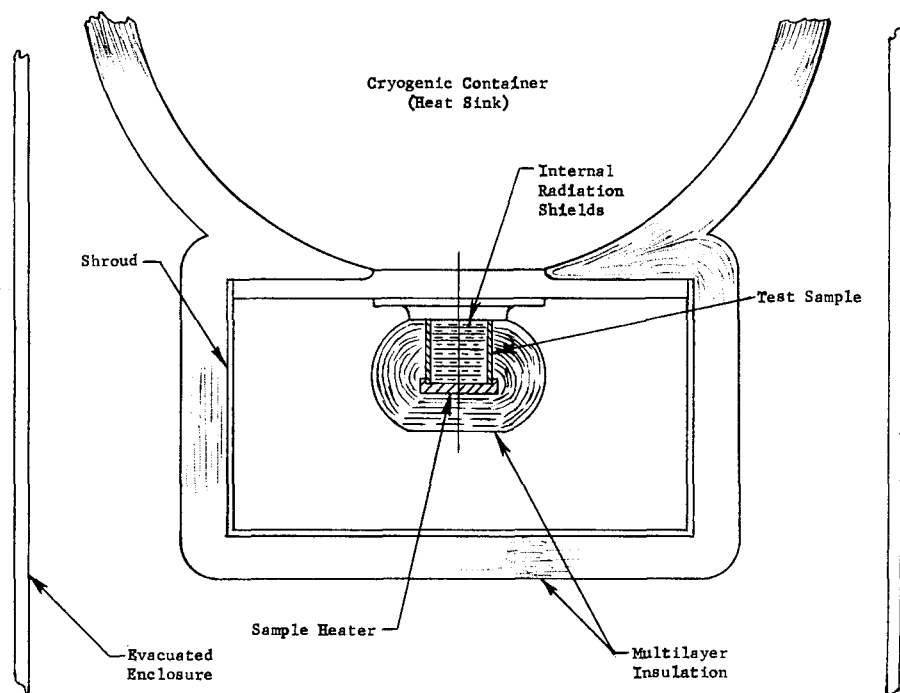
Fig. 95. - Thermal Conductivity Test Installation
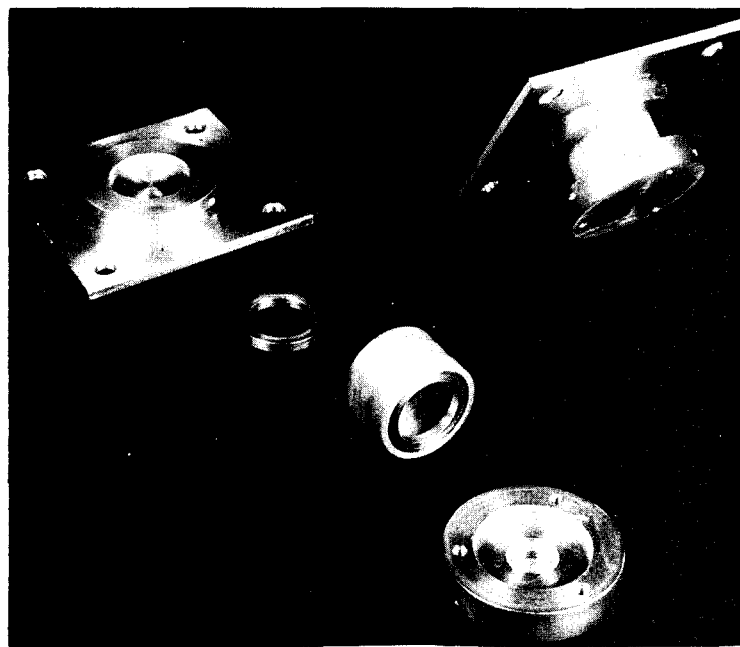
Fig. 96. - Thermal Test Sample Shown
Disassembled and Assembled

fully folded around the heater end of the specimen, trimmed, and closed
with mylar adhesive tape so as to make a bag like enclosure. Care was
taken to interweave the power and thermocouple lead wires through the
insulation layers so as to minimize overlapping gaps through the in-
sulation enclosure.

Test method: After the test chamber was evacuated and the heat
sink vessel was filled with liquid hydrogen, the assembly was allowed
to cool for 24-hr. At this time, temperatures were recorded and heater
power was adjusted to bring an increase in temperature difference along
the specimen of $15^{\circ}R$ $(8^{\circ}K)$. Temperatures and power were monitored for
3 to 6 hr to assure stabilization. Power was then increased to bring
the temperature difference along the specimen to $30^{\circ}R$ $(17^{\circ}K)$. After
temperatures were stabilized and recorded, the heat sink vessel was
emptied of liquid hydrogen.

As the cold end of the specimen slowly warmed, the heater power
was adjusted to maintain the temperature difference at the last
stabilization value. The warming required 36 to 48 hr with temperatures
and power being recorded every 30 minutes. Power adjustments were made
as required every 15 minutes. When the specimen warm end temperature
was near local ambient, the test was concluded. The specimens tested
are described in table 39.

Table 39.- Thermal Conductivity Test Results

Specimen diameter		Mean temperature		Measured thermal conductivity		Predicted thermal conductivity	
in.	cm	$^{\circ}R$	$^{\circ}K$	Btu/hr$^{\circ}$Rft	W/m$^{\circ}$K	Btu/hr$^{\circ}$Rft	W/m$^{\circ}$K
0.5[a]	1.27	100	56	0.46	0.005		
		300	167	1.51	0.018		
		500	278	2.11	0.025	1.78	0.021
2.0[b]	5.08	100	56	0.41	0.005		
		300	167	1.25	0.015		
		500	278	1.71	0.020	1.00	0.012
5.0[c]	12.7	100	56	0.45	0.005		
		300	167	0.73	0.009		
		500	278	0.93	0.011	0.96	0.011

a. Sample taken from CFL6300605, S/N 4 and included a 0.007 in. (0.018 cm)
thick Inconel 718 liner and three layers of overwrap (HLH).

b. Sample taken from CFL6300611 S/N 83 and included a 0.003 in. (0.008 cm)
thick Inconel 718 liner and three layers of overwrap (HLH).

c. Sample taken from CFL6300614, S/N 120 and included a 0.003 in. (0.008 cm)
thick Inconel 718 liner and four layers of overwrap (HLHH).

Generalized data presentation and test results: The thermal conductivity test results are presented in table 39 with a typical curve of the results shown in fig. 97.

Data reduction was accomplished by a thermal analysis program which accounts for all heat flows from the test heater, such as heat flow through the multilayer insulation covering the specimen and the radiation shields installed within the specimen. From the heat input data and the above analysis, the effective solid thermal conductivity of the specimen was determined. For data obtained under nonsteady conditions, an additional correction was made for the rate of heat gain or loss of the thermal mass involved. Because the actual effective thermal mass cannot be directly determined, a survey type analysis was conducted using a range of thermal masses based on the measured weight and material composition. The thermal mass giving the best curve fit through steady-state results was assumed to be appropriate. The measured values of thermal conductivity are compared in table 39 with those predicted from published data for the composite tube cross-section at 500°R (278°K).

Thermal flux testing.- A series of tests were conducted to evaluate the thermal performance of complete tube assemblies. Five specimens were tested representing the combinations of tube diameters and liner and overwrap configurations.

Test equipment and setup: The basic test fixture consisting of vacuum chamber and cryostat, used in the short specimen thermal conductivity tests was adapted for use in this test series. The specimens were of sufficient length to present a serious problem in insulating the tubes so as to isolate the heat flux transmitted by the tube from that entering through the side wall. Therefore, a thermal guard shroud was incorporated to minimize sidewall heat flux. This shroud consisted of a thin seamless steel cylinder, thermally connected to the heat sink (cryostat) and fitted with a heater on the opposite end.

The test specimen was installed inside the guard shroud and insulated from it with opacified fiberglass batting. The specimen was also thermally connected to the heat sink and fitted with a heater, and the entire assembly was insulated overall. By maintaining the hot end of the guard shroud at the same temperature as the hot end of the specimen, a temperature profile was established along the shield which approximated that along the specimens. Thereby, the radial heat flux into the specimen was kept to a very small value. The specimen tubes were not insulated internally and were exposed to the vacuum environment. Instrumentation was similar to that used for the short tube tests, but also included thermocouples at several points along the guard shield and along the specimen wall. Test specimens and apparatus at various stages of assembly are shown in figures 98 through 103. For small diameter specimens, two tests were accomplished simultaneously, using parallel installations. The test configuration is shown schematically in fig. 104.
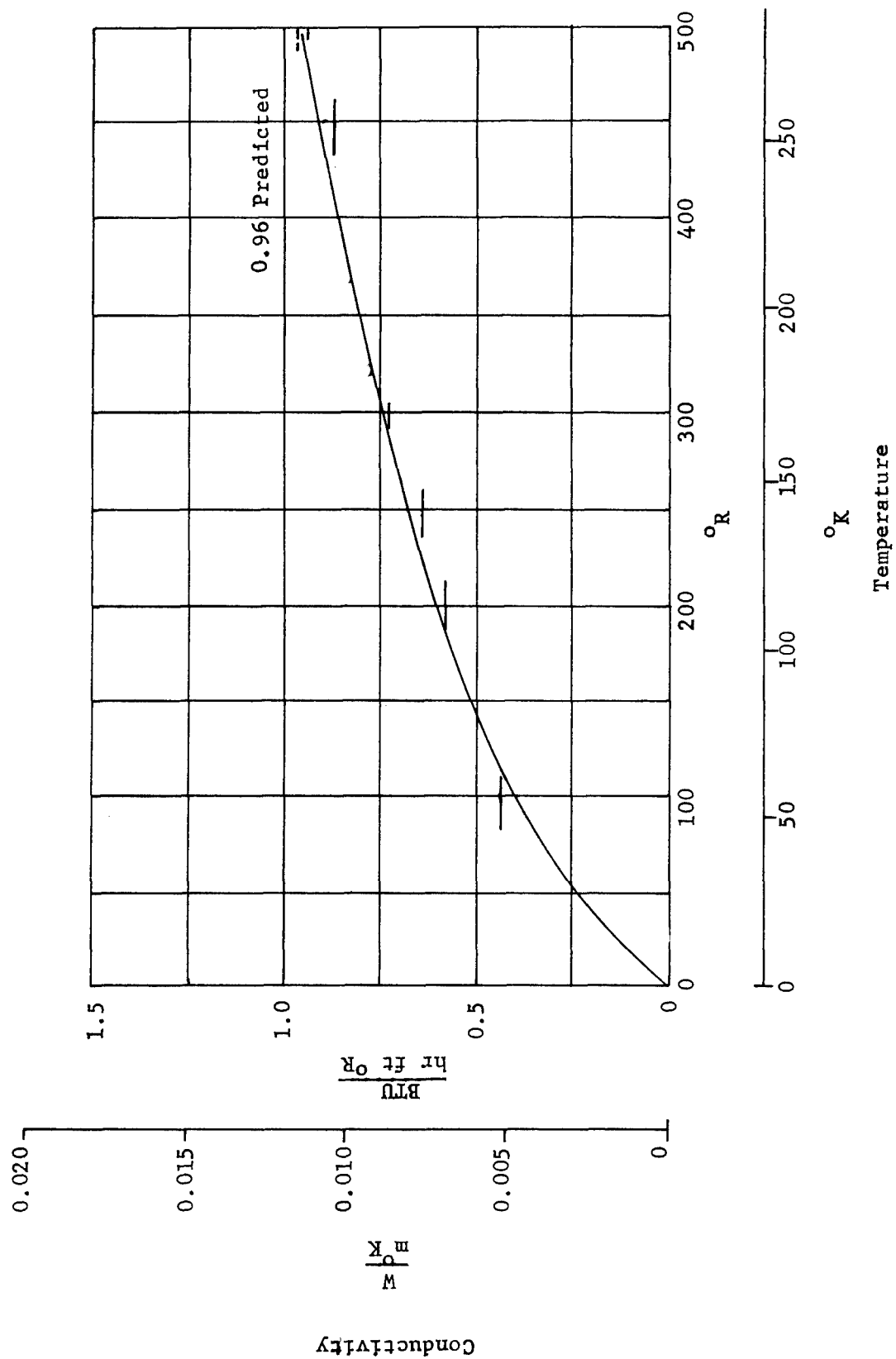
Fig. 97. — Thermal Conductivity of the 5 in. (12.7 cm) Diameter Specimen

190
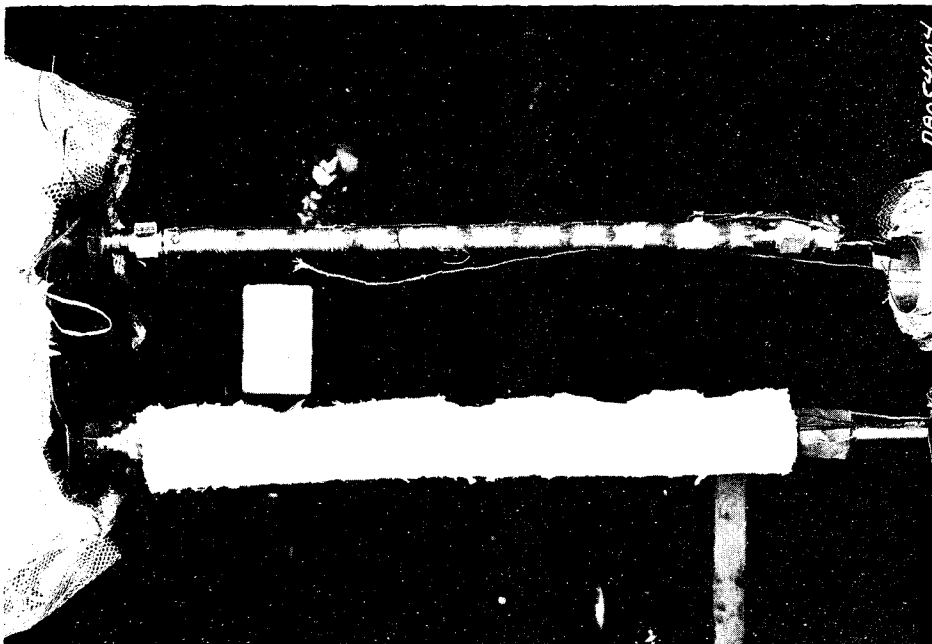
Fig. 98. - Thermal Flux Test Installation - 1/2 in. (1.27 cm) Diameter - Showing Test Item Insulation and Thermocouples.
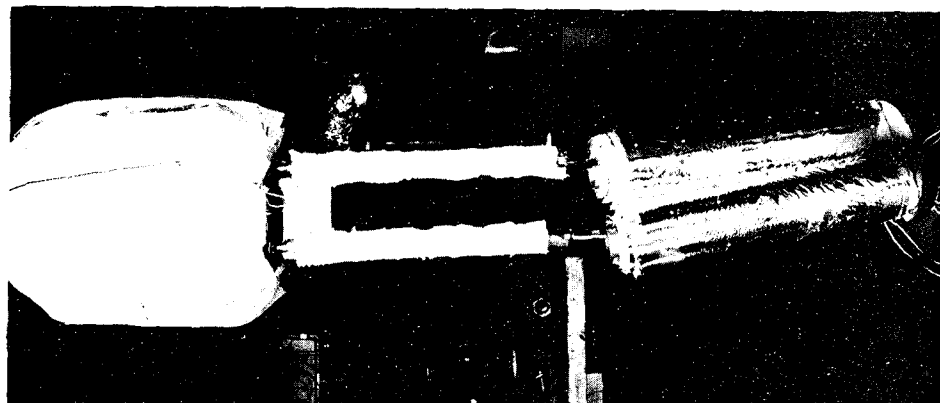
Fig. 99. - Thermal Flux Test Installation - 1/2 in. (1.27 cm) Diameter - Showing Guard Heater Installation.
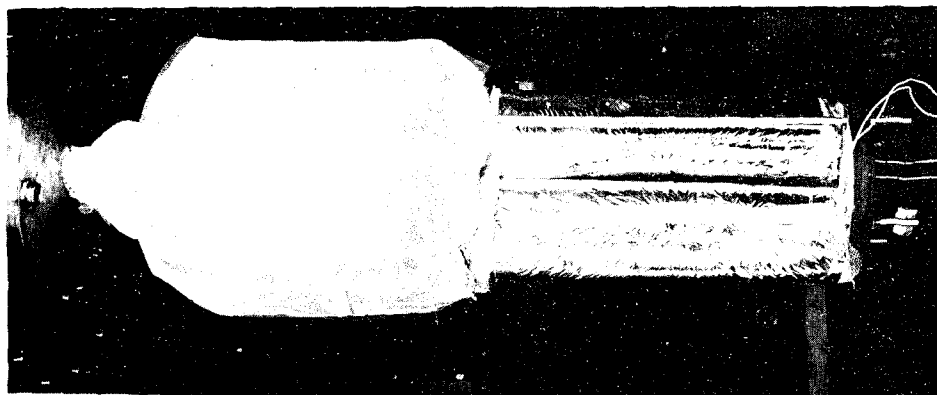
Fig. 100. - Thermal Flux Test Installation - 1/2 in. (1.27 cm) Diameter - Final Installation.

191

Fig. 101. - Thermal Flux Test Installation - Large Diameter - Showing Insulated Test Specimen.
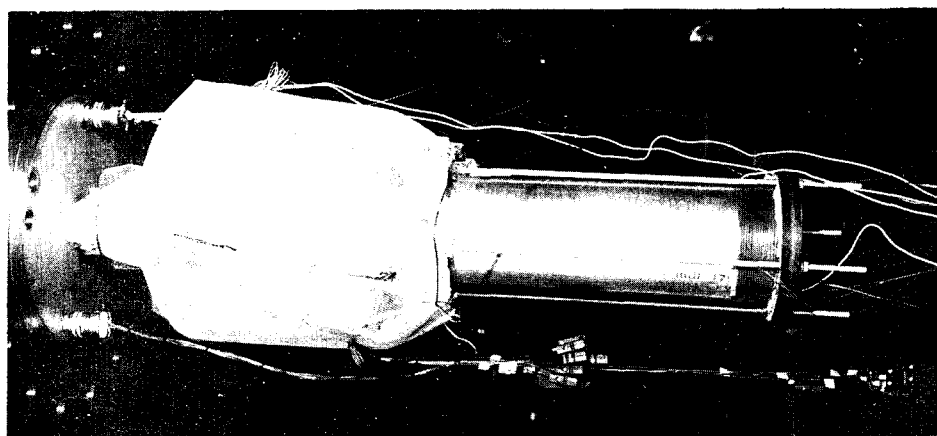
Fig. 102. - Thermal Flux Test Installation - Large Diameter - Showing Guard Heater Installation.
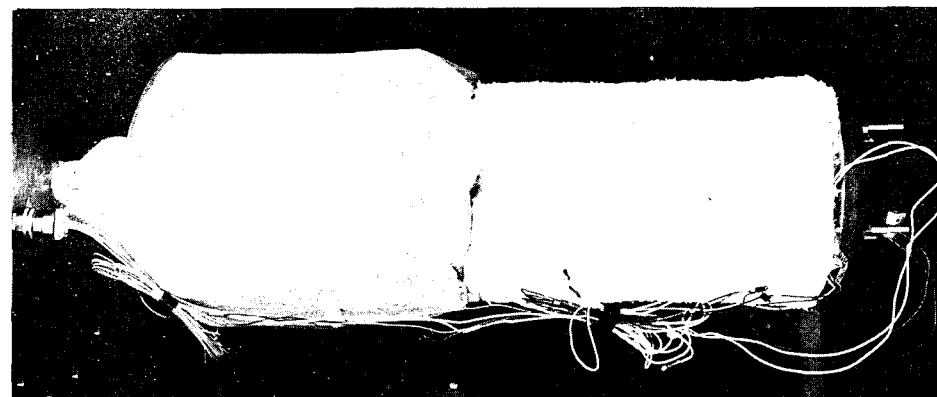
Fig. 103. - Thermal Flux Test Installation - Large Diameter - Showing Final Installation.

192
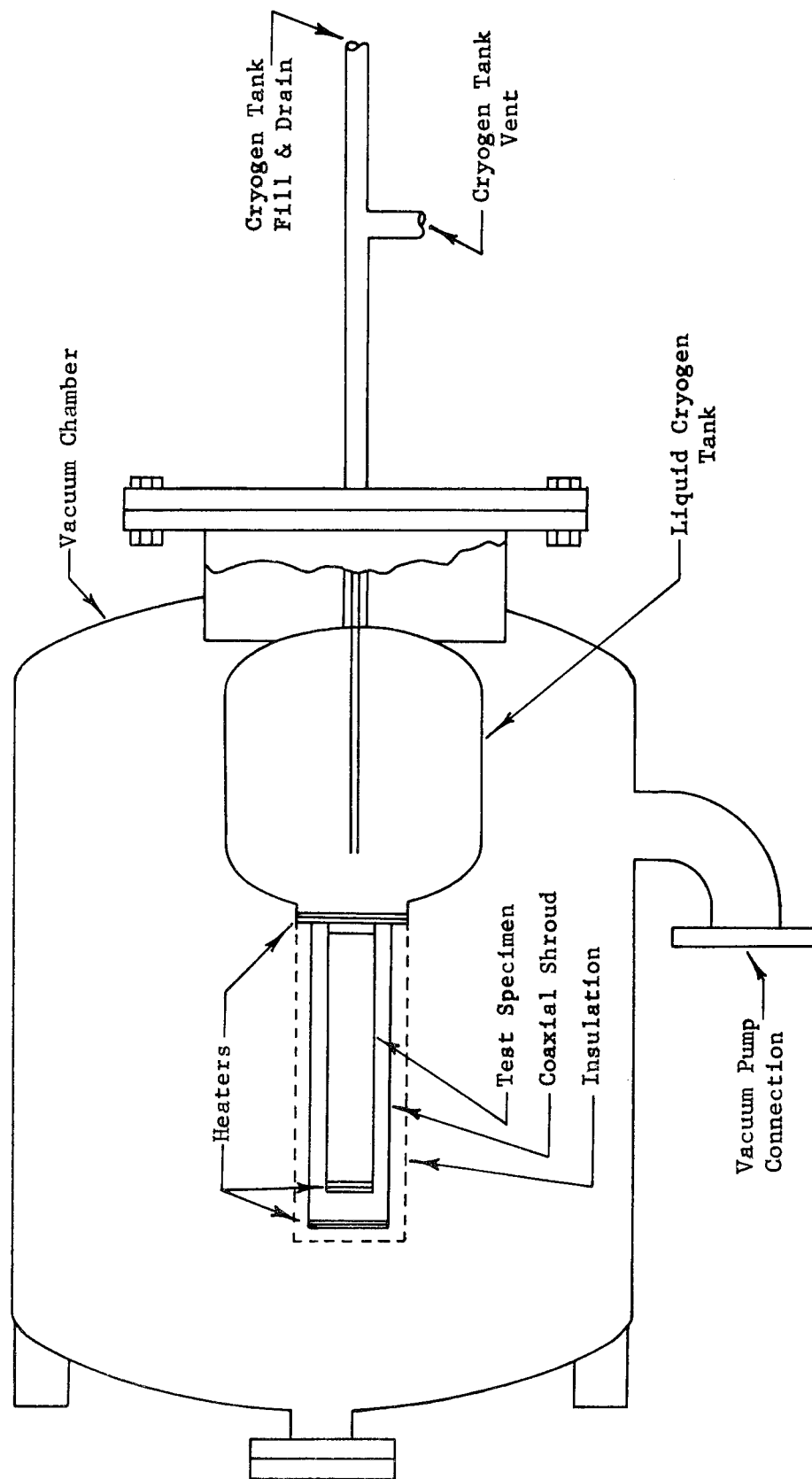
Fig. 104 - Assembly for Thermal Conductance Test

Test method: After evacuating the specimen and chamber, and introducing the liquid cryogen to the heat sink vessel, the tube-insulation-shroud assembly was allowed to cool until the tube mid-point temperature reached its expected final value. The tube heater power was then set at the predicted value required to maintain the hot end at approximately 530°R (295°K) and the shroud power was set to bring the tube and shroud warm ends to nearly the same temperature. The final power settings were maintained for 36 hr. Temperature along the tube end shroud and power to the two heaters was recorded at the end of this period. Each tube was tested at two cold end temperatures, using liquid nitrogen and liquid hydrogen in the heat sink. Typical pressure in the chamber during test was 2 x 10⁻⁵ mm Hg. Physical data of the tubes tested are shown in table 40.

TABLE 40. - THERMAL FLUX TEST SPECIMEN DATA

| Serial Number	Diameter		Liner			Overwrap			Length as tested	
			Thickness		Material	Emissivity	Thickness		Type		
	in.	cm	in.	cm			in.	cm		in.	cm
7	0.5	1.27	0.007	0.018	718 Inconel	0.1	0.030	0.08	HLH	18	46
43	0.5	1.27	0.009	0.023	304 Stainless	0.15	0.030	0.08	HLH	18	46
88	2.0	5.08	0.006	0.015	718 Inconel	0.1	0.030	0.08	HLH	18	46
83	2.0	5.08	0.003	0.008	718 Inconel	0.1	0.030	0.08	HLH	18	46
127	5.0	12.7	0.006	0.015	718 Inconel	0.1	0.040	0.10	HLHH	11	28

Generalized data presentation and computer simulation: In analyzing the thermal flux test data the computer program described in Task I was used to simulate each test. In addition to the thermal model, provision in the program was made for shroud node temperatures and conduction paths. The input data from the tests included tube end temperatures, shroud temperature distribution, tube and insulation physical dimensions, and material properties. Output included temperature distribution along the tube and thermal flux through the tube Figure 105 shows a typical comparison of calculated and measured temperature distribution along a tube. The discrepancy is acceptably small. Table 41 and 42 compare thermal flux measured and predicted in each of the 10 tests.

It is noted from tables 41 and 42 that total heat fluxes are generally greater than predicted. Two most likely sources of inaccuracy are undetected radiation leakage through the specimen insulation and radiation through the tube due to specular, rather than totally diffuse reflectivity of the inside surface of the liner. To assess the possible effect of the specular reflectivity, the maximum possible additional radient heat transfer was calculated and is presented in column 4 of tables 41 and 42. This calculation was based on an assumed inside emissivity of 0.05, with totally specular

reflectivity. Measured values of total hemispherical emissivity of the liner materials were found to lie between 0.05 and 0.20, depending on surface condition. The fraction of the additional radient transfer required to meet the deficit is given in column 5 of the table. From these values, it appears that a major part of the error could be attributed to this additional heat transfer path except for the serial no. 43 specimen.
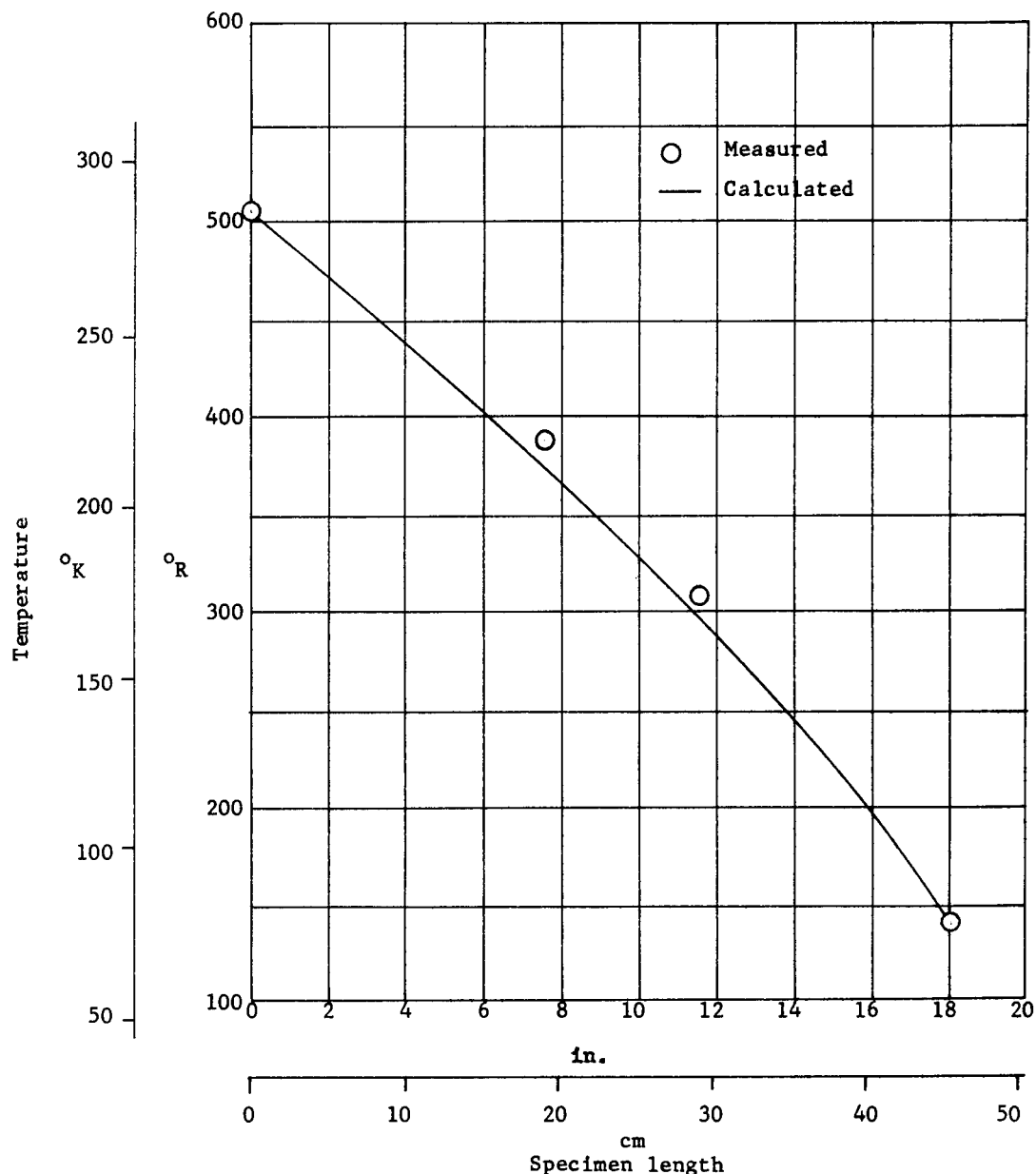
Fig. 105. - Temperature Distribution Along Specimen S/N 7 Found During The Liquid Nitrogen Thermal Flux Test As Measured and Calculated.

TABLE 41.- COMPARISON OF THERMAL FLUX TEST DATA AND COMPUTER PREDICTIONS

Test		Program Calculation of Heater Power, BTU/hr	Program Calculation of Radiation Heat Transfer BTU/hr	Measured Heater Power BTU/hr	Calculated Maximum Specular Radiation BTU/hr	Fraction of Specular Radiation to meet Deficit[a]	End Temperatures During Tests	
Spec. Serial No.	Cryogen	Column 1	Column 2	Column 3	Column 4	Column 5	Cold °R	Hot °R
43	N_2	0.316	0.026	0.937	0.306	2.11	148	536
43	H_2	0.343	0.027	1.17	0.304	2.81	57	535
7	N_2	0.263	0.022	0.343	0.248	0.407	141	510
7	H_2	0.262	0.025	0.437	0.252	0.794	44	511
83	N_2	1.222	0.527	3.08	2.28	1.109	163	525
83	H_2	1.389	0.525	3.39	2.36	1.072	98	528
88	N_2	1.183	0.475	2.66	2.28	0.856	137	533
88	H_2	0.971	0.480	2.86	2.44	0.972	122	533
127	N_2	7.399	4.412	6.62	11.56	0.314	285	517
127	H_2	8.190	4.668	6.62	12.41	0.249	260	518

a   Column 5 = $\dfrac{\text{column 3} - (\text{column 1} - \text{column 2})}{\text{column 4}}$

TABLE 42. - COMPARISON OF THERMAL FLUX TEST DATA AND COMPUTER PREDICTIONS

Test Spec. Serial No.	Cryogen	Program Calculation of Heater Power, Watt Column 1	Program Calculation of Radiation Heat Transfer Watt Column 2	Measured Heater Power Watt Column 3	Calculated Maximum Specular Radiation Watt Column 4	Fraction of Specular Radiation to meet Deficit[a] Column 5	End Temperatures During Tests Cold °K	End Temperatures During Tests Hot °K
43	N_2	0.093	0.008	0.275	0.090	2.11	82	298
43	H_2	0.100	0.008	0.343	0.089	2.81	32	297
7	N_2	0.077	0.006	0.100	0.073	0.407	79	283
7	H_2	0.077	0.007	0.128	0.074	0.794	24	284
83	N_2	0.358	0.154	0.904	0.668	1.109	91	292
83	H_2	0.407	0.154	0.99	0.691	1.072	54	293
88	N_2	0.347	0.139	0.78	0.668	0.856	76	296
88	H_2	0.285	0.141	0.84	0.715	0.972	68	296
127	N_2	2.168	1.293	1.94	3.387	0.314	158	287
127	H_2	2.400	1.368	1.94	3.636	0.249	144	288

a Column 5 = $\dfrac{\text{column 3} - (\text{column 1} - \text{column 2})}{\text{column 4}}$

TASK IV - ANALYSIS OF TEST RESULTS

For the purpose of clarity and continuity, all of the test results have been included and discussed in the applicable section of the fabrication and testing tasks.

SUMMARY OF RESULTS

The purpose of this test program was to investigate the feasibility of using metal lined glass-fiber tubing as tank pressurization and propellant outflow lines on upper-stage space vehicles using cryogenic propellants.

The concept of the composite tubes was to use extremely thin walled metal liners, to provide leak-free service and reduce conductive heat transfer, with an overwrap of glass fibers to provide structural integrity.

Results obtained during the course of the overall program include the following:

1) The most efficient use of the lines would be to locate the composite section as near the tank as possible and make them as long as is practical;

2) The composite tubes are lightweight and could provide a significant weight saving in space vehicles;

3) The composite tubes are sufficiently strong and rigid so that no special handling techniques, other than ordinary care, are required;

4) Some wrinkling or slight buckling of the liner during fabrication or assembly does not degrade the performance of the completed composite line.

Results obtained during the fabrication phase of the program:

1) Manufacturing methods required to fabricate the thin metal liners and apply the glass-fiber overwrap are available in the present state-of-the-art; however, further development of the solid-state bonding technique with respect to cleanliness requirements and size limitations may be warranted; and

2) All resistance welds made during fabrication of the liners or attaching the end fittings should be helium leak checked with a mass spectrometer leak detector.

Results obtained from the thermal testing phase of the program:

1) The three main mechanisms of heat transfer along the tubes in this test program are solid conduction, diffuse radiation, and specular radiation. Of these only the first two are

included in the computer program used in this analysis.
Calculated input energy therefore should fall below
measured and in fact it does in each test. The computer
calculations and test program results are compatible
when a maximum value of specular radiant transfer is
added to the calculations. Since specular and diffuse
radiant transfer are present to the same extent regardless
of wall thickness, and regardless of whether the tube is
a composite or completely metal, the program can show
the improvement in thermal performance of the thin-walled
tube over a similar thick-walled tube; and

2) The composite structure is clearly more efficient in con-
ductive heat transfer which satisfies the program objectives.

Results obtained during the structural testing phase of the
program:

1) The fusion weld method used to join the liner to the
end fitting on the CFL6300616 and original design of the
CFL6300612 proved to be unsatisfactory due to the
difference in the thickness of the welded members;

2) The high incidence of leakage failures in the CFL6300605,
CFL6300606, and CFL6300607 designs was attributed to
leakage at the resistance weld joining the liner to the
end fitting. The fact that some tubes of each design
were leak free indicates that close control of the fabri-
cation process is required to produce leak free joints;

3) The actual burst pressure of the test specimen final
designs was generally higher than predicted. These
higher burst pressures were attributed to friction
between the liner and the glass overwrap which allowed
the liner to transfer some axial load to the glass
overwrap. This friction was not accounted for during
the design analysis; and

4) The predicted gaps between the liners and the glass
overwrap at cryogenic temperatures were generally confirmed.

RECOMMENDATIONS

As a result of the knowledge and experience gained from this program, Martin Marietta Corporation makes the following recommendations:

1) Further development of solid-state bonding techniques as a method of attaching end fittings be accomplished.

2) Further development of resistance welding methods to join end fittings to small diameter, thin walled tubes be accomplished.

3) Develop liner materials that are not susceptible to hydrogen embrittlement.

4) Develop the fabrication techniques required to produce thin metal lined, glass overwrapped tubes of large diameter and/or long length, say 15 in. (38.1 cm) diameter and many feet long.

5) Develop methods of reducing losses due to specular radiation.

6) Update the existing feedline chilldown computer program to include composite tubing.

7) Develop a composite system with a low heat capacity.

8) Perform a test program to determine the capability of the composite tubes to withstand vibration levels encountered during launch and flight of space vehicles.

9) Use composite tubes to prevent heat soak back from rocket engines which results in damage to engine valves.

10) Use composite tubing for pressurization and propellant outflow lines in future designs of propulsion systems using cryogenic propellants.

11) Extend the use of composite tubing to commercial applications such as LNG tanker transfer lines and other cryogenic storage and transfer systems.

APPENDIX A

DATA ACQUISITION EQUIPMENT LIST

1. Recorders

    A. Sanborn 6 Channel

        Model: 156-100BW

        Chart Speeds: 0.25, 0.5, 1, 2.5, 5, 10, 25, 50, and 100 mm/sec.

        Frequency Response: DC to 100 Hz with 3dB down at 10 divisions P-P amplitude.

        Rise Time: 5 milliseconds

        Linearity: Essentially perfect over the middle 40 divisions of the 50 division chart. Maximum error over entire 50 divisions is less than 0.5 division.

        Sensitivity: Approximately 0.5 V/cm of deflection.

        Drift: Less than 0.5 division per hour.

    B. Honeywell 24 Channel, Multi-point

        Model: Electronik 153

        Chart Speed: 1 in./min (2.54 cm/min)

        Balance Speed: 4.5 seconds

        Printing Speed: 5.0 seconds

        Reference Junction: Copper-Constantan

    C. Beckman Instruments, Inc.

        Scanner: Model 4005

        Pre-amplifier: Model 4004-1

        Digital Voltmeter: Model 4011RVP

        Printer: Model 1453

2. Digital Instruments

    A. Dana Digital Voltmeter

        Model: 5740

Range: Ranges covering 10 millivolt DC to 1000.00 Volt DC

Resolution: From 0.1 micro volts DC to 10 millivolts DC

Short Term Accuracy: ± 0.001% of full scale on all ranges.

Digitizing Time: 13 ms constant range and polarity.

B. Honeywell DC Potentiometric

Model: 852

Range: 1KV, 100V, 10V and 1V

Resolution: 0.0001% of full scale on all ranges.

Short Term Stability: ± 0.005% per day, non-cumulative.

C. Beckman/Berkely Digital System

Range: 0.000 to 999.9 volts

Resolution: 0.01% of full scale

Linearity: 0.01%

Range Selection: Automatic

Sensitivity: 1 millivolt without pre-amplifier
1 microvolt with pre-amplifier

D. Leeds & Northrup Potentiometer

Model: 8686

Range: -10.100 to +1010.000 mv, +1010.000 to 1020.000 mv

Resolution: 1 microvolt

3. Signal Amplifiers

Dana Differential Amplifier
Model: 2860 (with filtering)
Linearity: DC to 2 KHZ ± 0.01%
Range: 1 to 2500 gain ± 0.01%

4. Leak Detector

Consolidated Electrodynamics, Helium Mass Spectrometer, Model
24-120.

INSTRUMENTATION LIST

1. Pressure Transducers

   A. Taber Instruments Corporation - Model 206

   B. Instrumented Pressure Gauge

      American Instrument Co., Inc.

      Model: 13399

      Range: 0 to 30,000 psi (0-20,700 N/cm^2)

2. Strain Gages

   A. Automation Industries

      Model C9-125-R2T Rosette

      Model S741-R2T-300 Rosette

   B. Balswin - Lima - Hamilton

      Type C-8

      Type DLB-MK35-4A-S13

REFERENCES

1. Alexander Mendelion: <u>Plasticity: Theory and Application</u>. MacMillan Co., N. Y., 1968.

2. F. R. Schwartzberg, et al.: <u>Cryogenic Materials Data Handbook</u>. Technical Documentary Report No. ML-TDR-64-280, Air Force Materials Laboratory, Revised 1968.

3. <u>Inconel Alloy 718</u>. Handbook. Huntington Alloy Products Division, The International Nickel Company Inc. February 1968.

4. J. M. Toth, Jr., and D. J. Soltysiak: <u>Investigation of Smooth-Bonded Metal Liners for Glass-Fiber Filament-Wound Pressure Vessels.</u> NASA CR-72165. Douglas Report DAC-60640, May 1967.

5. E. E. Morris, F. J. Darms, R. E. Landes, and J. W. Campbell: <u>Parametric Study of Glass-Filament - Reinforced Metal Pressure Vessels</u>. NASA CR-54-855, Aerojet Report 3184, April 1966.

6. R. H. Johns and A. Kaufman, <u>Filament-Overwrapped Metallic Cylindrical Pressure Vessels</u>, NASA TMX-52171, Lewis Research Center, 1966.

7. <u>Design Handbook for LF$_2$ Ground Handling Equipment</u>. Technical Report AFRPL-TR-65-133. Aerojet-General Corp., August 1965.

8. <u>Fluorine Systems Handbook.</u> Prepared by Douglas Missile & Space Systems Division for NASA Under Contract NASw-1351, July 1967.

9. <u>Leak Detection Manual.</u> Bell and Howell, Monrovia California, January 1969.

10. J. P. Gille: <u>Development of Advanced Materials for Integrated Tank Insulation System for The Long Term Storage of Cryogens in Space.</u> MMC Technical Report MCR-69-405. Prepared for NASA under Contract NAS8-21330, September 1969.

BIBLIOGRAPHY

Frederick D. Calfo: Effect of Residual Stress on Fracture Strength of AISI 301 Stainless-Steel and Ti-5Al-2.5Sn Eli Titanium Cracked Thin-Wall Cylinders. NASA Technical Note NASA TN D-4777. Lewis Research Center, September 1968.

D. L. Cheever, D. G. Howden, and R. E. Monroe: Feasibility Study of Resistance Welding of Aluminum Alloys, Stainless Steel, and Titanium in A Hard Vacuum. Technical Report NASA CR-61596. Battelle Memorial Institute, February 1968.

C. L. Estes: Resistance Spot Welding Stainless Steel Foil By The Expendable-Wire Technique. A technical report under AEC Contract W-7405-eng-26. Union Carbide Corporation, April 1968.

Raymond F. Girard: Automatic Pipe Welding Using A Magnetically-Driven Rotating ARC. Thesis GAW/EE/67A-2. Air Force Institute of Technology, May 1967.

A Holston, Jr., A. Feldman, and D. A. Stang: Stability of Filament Wound Cylinder, Under Combined Loading. Technical Report AFFDL-TR-67-SS. Martin Marietta Corp., May 1967.

Gerald Pickett and Millard W. Johnson, Jr.: Analytical Procedures for Predicting The Mechanical Properties of Fiber Reinforced Composites. Technical Report AFML-TR-65-220, Part III, University of Wisconsin, October 1967.

R. J. Roark: Formulas for Stress and Strain. 4th edition, McGraw-Hill, 1954.

F. R. Stuart, J. T. Goto, and E. E. Sechler: The Buckling of Thin-Walled Circular Cylinders Under Axial Compression and Bending. Technical Report NASA CR-1160. California Institute of Technology, September, 1968.

Preparation of Filament Wound Microtape Research Specimens. Technical Report NASA CR-72459. DeBell & Richardson, Inc., July 1968.

Structural Design with Fibrous Composites. Publication MAB-236. National Academy of Sciences - National Academy of Engineering, October 1968.

206

DISTRIBUTION LIST

Report Copies	Recipient	Designee
	National Aeronautics & Space Administration Lewis Research Center 21000 Brookpark Road Cleveland, Ohio 44135	
1	Attn: Contracting Officer, MS 500-313	
5	Liquid Rocket Technology Branch, MS 500-209	
1	Technical Report Control Office, MS 5-5	
1	Technology Utilization Office, MS 3-16	
2	AFSC Liaison Office, MS-4-1	
2	Library	
1	Office of Reliability & Quality Assurance, MS 500-111	
1	D. L. Nored, Chief, LRTB, MS 500-209	
3	J. R. Faddoul, Project Manager, MS 500-209	
1	E. W. Conrad, MS 500-204	
1	R. H. Kemp, MS 49-1	
2	Chief, Liquid Experimental Engineering, RPX Office of Advanced Research & Technology NASA Headquarters Washington, D.C. 20546	
2	Chief, Liquid Propulsion Technology, RPL Office of Advanced Research & Technology NASA Headquarters Washington, D.C. 20546	
1	Director, Launch Vehicles & Propulsion, SV Office of Space Science & Applications NASA Headquarters Washington, D.C. 20546	
1	Chief, Environmental Factors & Aerodynamics Code RV-1 Office of Advanced Research & Technology Washington, D.C. 20546	
1	Chief, Space Vehicles Structures Office of Advanced Research & Technology NASA Headquarters Washington, D.C. 20546	

Report Copies	Recipient	Designee
1	Director, Advanced Manned Missions, MT Office of Manned Space Flight NASA Headquarters Washington, D.C. 20546	
6	NASA Scientific & Technical Information Facility P. O. Box 33 College Park, Maryland 20740	
1	Director, Technology Utilization Division Office of Technology Utilization NASA Headquarters Washington, D.C. 20546	
1	National Aeronautics & Space Administration Ames Research Center Moffett Field, California 94035 Attn: Library	
1	National Aeronautics & Space Administration Ames Research Center Moffett Field, California 94035 Attn: C. A. Syvertson	
1	National Aeronautics & Space Administration Goddard Space Flight Center Greenbelt, Maryland 20771 Attn: Library	
1	National Aeronautics & Space Administration John F. Kennedy Space Center Cocoa Beach, Florida 32931 Attn: Library	
1	National Aeronautics & Space Administration Langley Research Center Langley Station Hampton, Virginia 23365 Attn: Library	
1	National Aeronautics & Space Administration Flight Research Center P. O. Box 273 Edwards, California 93523 Attn: Library	

Report Copies	Recipient	Designee
1	National Aeronautics & Space Administration Manned Spacecraft Center Houston, Texas 77001 Attn: Library	
1	National Aeronautics & Space Administration Manned Spacecraft Center Houston, Texas 77001 Attn: J. G. Thibodaux, Jr. Chief, Propulsion & Power Division	
1	National Aeronautics & Space Administration Georce C. Marshall Space Flight Center Huntsville, Alabama 35812 Attn: Library	
1	National Aeronautics & Space Administration George C. Marshall Space Flight Center Huntsville, Alabama 35812 Attn: J. Blumrich	
1	Jet Propulsion Laboratory 4800 Oak Grove Drive Pasadena, California 91103 Attn: Library	
1	Jet Propulsion Laboratory 4800 Oak Grove Drive Pasadena, California 91103 Attn: W. Jensen	
1	Defense Documentation Center Cameron Station Building 5 5010 Duke Street Alexandria, Virginia 22314 Attn: TISIA	
1	Office of the Director of Defense Research & Engineering Washington, D.C. 20301 Attn: Office of Asst. Dir. (Chem. Technology)	
1	RTD (RTNP) Bolling Air Force Base Washington, D.C. 20332	

Report Copies	Recipient	Designee
1	Arnold Engineering Development Center Air Force Systems Command Tullahoma, Tennessee 37389 Attn: Library	Dr. H. K. Doetsch
1	Advanced Research Projects Agency Washington, D.C. 20525 Attn: Library	D. E. Mock
1	Aeronautical Systems Division Air Force Systems Command Wright-Patterson Air Force Base Dayton, Ohio Attn: Library	D. L. Schmidt Code ARSCNC-2
1	Air Force Missile Test Center Patrick Air Force Base, Florida Attn: Library	L. J. Ullian
1	Air Force Systems Command Andrews Air Force Base Washington, D.C. 20332 Attn: Library	Capt. S.W. Bowen SCLT
1	Air Force Rocket Propulsion Laboratory (RPR) Edwards, California 93523 Attn: Library	
1	Air Force Rocket Propulsion Laboratory (RPM) Edwards, California 93523 Attn: Library	
1	Air Force FTC (FTAT-2) Edwards Air Force Base, California 93523 Attn: Library	Donald Ross
1	Air Force Office of Scientific Research Washington, D.C. 20333 Attn: Library	SREP, Dr. J. F. Masi
1	Space & Missile Systems Organization Air Force Unit Post Office Los Angeles, California 90045 Attn: Technical Data Center	
1	Office of Research Analyses (OAR) Holloman Air Force Base, New Mexico 88330 Attn: Library RRRD	

Report Copies	Recipient	Designee
1	U. S. Air Force Washington, D.C. Attn: Library	Col. C. K. Stambaugh Code AFRST
1	Commanding Officer U. S. Army Research Office (Durham) Box CM, Duke Station Durham, North Carolina 27706 Attn: Library	
1	U. S. Army Missile Command Redstone Scientific Information Center Redstone Arsenal, Alabama 35808 Attn: Document Section	Dr. W. Wharton
1	Bureau of Naval Weapons Department of the Navy Washington, D.C. Attn: Library	J. Kay, Code RTMS-41
1	Commander U. S. Naval Missile Center Point Mugu, California 93041 Attn: Technical Library	
1	Commander U. S. Naval Weapons Center China Lake, California 93557 Attn: Library	W. F. Thorm Code 4562
1	Commanding Officer Naval Research Branch Office 1030 E. Green Street Pasadena, California 91101 Attn: Library	
1	Director (Code 6T80) U. S. Naval Research Laboratory Washington, D. C. 20390 Attn: Library	H. W. Carhart J. M. Kralli
1	Picatinny Arsenal Dover, New Jersey 07801 Attn: Library	I. Forsten

Report Copies	Recipient	Designee
1	Air Force Aero Propulsion Laboratory Research & Technology Division Air Force Systems Command United States Air Force Wright-Patterson AFB, Ohio 45433 Attn: APRP (Library)	R. Quigley C. M. Donaldson
1	Space Division Aerojet-General Corporation 9200 East Flair Drive El Monte, California 91734 Attn: Library	S. Machlawski
1	Ordnance Division Aerojet-General Corporation 11711 South Woodruff Avenue Downey, California 90241 Attn: Library	
1	Ordnance Division Aerojet-General Corporation 11711 South Woodruff Avenue Downey, California 90241 Attn: W. L. Arter	
1	Propulsion Division Aerojet-General Corporation P. O. Box 15847 Sacramento, California 95803 Attn: Technical Library 2484-2015A	R. Stiff
1	Aerospace Corporation P. O. Box 95085 Los Angeles, California 90045 Attn: Library-Documents	
1	Air Products and Chemicals Company Allentown, Pennsylvania 18105 Attn: P. J. DeRea	
1	Electronics Division Aerojet-General Corporation Azusa, California 91702	

Report Copies	Recipient	Designee
1	Electronics Division Aerojet-General Corporation Azusa, California 91702 Attn: E. E. Morris	
1	ARO, Incorporated Arnold Engineering Development Center Arnold Air Force Station, Tennessee 37389 Attn: Dr. S. H. Goethert, Chief Scientist	
1	Atlantic Research Corporation Shirley Highway & Edsall Road Alexandria, Virginia 22314 Attn: Security Office for Library	
1	Battelle Memorial Institute 505 King Avenue Columbus, Ohio 43201 Attn: Defense Metals Information Center	
1	Bell Aerosystems Box 1, Buffalo, New York 14205 Attn: T. Rainhardt	
1	The Boeing Company Aero Space Division P. O. Box 3707 Seattle, Washington 98124 Attn: Ruth E. Peerenboom (1190)	
1	Brunswick Corporation Defense Products Division 1700 Messler Street Muskegon, Michigan 49441	
1	Western Division McDonnell Douglas Aircraft Company, Inc. 3000 Ocean Park Blvd. Santa Monica, California 90406 Attn: J. M. Toth	J. L. Waisman
1	Hercules Powder Company Chemical Propulsion Division 910 Market Street Wilmington, Delaware 19804	

Report Copies	Recipient	Designee
1	Narmco Research & Development Co. Whittaker Corporation 131 N. Ludlow Street Dayton, Ohio 45402	
1	Plastics Technical Evaluation Center Picatinny Arsenal Dover, New Jersey 07801	
1	Rocketdyne 6633 Canoga Avenue Canoga Park, California 91304 Attn: Library, Department 596-306	
1	Rohr Corporation Department 145 Chula Vista, California 91312	
1	TRW Systems 1 Space Park Redondo Beach, California 90200 Attn: Tech. Lib. Doc. Acquisitions	
1	Sandia Corporation Sandia Base Albuquerque, New Mexico 87115 Attn: H. E. Montgomery	
1	Swedlow, Incorporated 6986 Bandini Blvd. Los Angeles, California 90022	
1	Thiokol Chemical Corporation Wasatch Division P. O. Box 524, Brigham City, Utah 84302 Attn: Library Section	
1	Thiokol Chemical Corporation Wasatch Division P. O. Box 524, Brigham City, Utah 84302 Attn: D. Hess	
1	United Aircraft Corporation United Technology Center P. O. Box 358 Sunnyvale, California 94088 Attn: Librarian	

Report Copies	Recipient	Designee

1   Chemical Propulsion Information Agency
Applied Physics Laboratory
8621 Georgia Avenue
Silver Spring, Maryland 20910

1   The Garrett Corporation
20545 Center Ridge Road
Cleveland, Ohio 44116

1   Grumman Aircraft Engineering Corp.
Bethpage
Long Island, New York

1   General Dynamics/Convair
P. O. Box 1128
San Diego, California 92712
Attn: Library and Information Services (128-00)

1   B. F. Goodrich Company
Aerospace & Defense Products
500 South Main Street
Akron, Ohio 44311

1   Goodyear Aerospace Corporation
1210 Massilon Road
Akron, Ohio 44306

1   Hamilton Standard Corporation
Windsor Locks, Connecticut 06096
Attn: Library

1   ABL, Division of Hercules Powder Company
Cumberland, Maryland 21502
Attn: Thomas Bates

1   IIT Research Institute
Technology Center
Chicago, Illinois 60616
Attn: C. K. Hersh, Chemistry Division

1   Arde, Inc.
193 Route 17
Paramus, New Jersey 07652

1   North American Aviation, Inc.
Space & Information Systems Division
12214 Lakewood Blvd.
Downey, California 90242
Attn: Technical Information Center D/096-722 (A107)

Report Copies	Recipient	Designee
1	U. S. Rubber Company Mishawaka, Indiana 46544	
1	General Electric Company Apollo Support Dept., P. O. Box 2500 Daytona Beach, Florida 32015 Attn: C. Day	
1	Aerojet-General Corporation Park West Building - Suite 227 20545 Center Ridge Road Cleveland, Ohio 44116 Attn: W. Snapp	
1	Brunswick Corporation Defense Products Division P. O. Box 4594 43000 Industrial Avenue Lincoln, Nebraska 68504 Attn: J. Carter	
1	Marine Engineering Laboratory NSRDC ANNADIV Annapolis, Md. 21402 Attn: Karl H. Keller, Code 560	
1	Celanese Corp. Box 1000 Summit, New Jersey 07901 Attn: J. D. Lassiter	
1	Aeronutronic Division of Philco Ford Corp. Ford Road Newport Beach, California 92663 Attn: Technical Information Department	Dr. L. H. Linder
1	Aerojet Nuclear Systems Company P. O. Box 13070 Sacramento, California 95813	
1	Aerojet Nuclear Systems Company P. O. Box 13070 Sacramento, California 95813 Attn: G. L. Ryland	

Report Copies	Recipient	Designee
1	Alloy Spotwelders 2035 Granville Avenue Los Angeles, California 90025	
1	Metal Bellows Corp. 20977 Knapp Street Chatsworth, California 91311 Attn: H. Johnson	
1	Gardner Bellows Corp. 15934 Strathern Street Van Nuys, California 91406	
1	BV Machine Co., Inc. 2090 West Bates Avenue Englewood, Colorado 80110	